

# Effects of nano particles on alveolar macrophages

A thesis submitted for the degree of Doctor of  
Philosophy  
at the University of Leicester

By  
**Anantha Kalyan Tellabati MSc**  
Department of Infection Immunity and Inflammation  
University of Leicester

2013

---

**DEDICATION**

*I would like to dedicate my thesis to my father Tellabati Venkata Bhaskar Rao, to my mother Mani Kumari, to my wife Meenu, to my daughter Himanya and rest of my family for their love and support throughout my life.*

## **Statement of Originality**

The accompanying thesis submitted for the degree of Ph.D. entitled “Effects of nano particles on alveolar macrophages” is based on work conducted by the author in the Department of Infection Immunity and Inflammation of the University of Leicester mainly during the period between September 2005 and October 2010.

All the work recorded in this thesis is original unless otherwise acknowledged in the text or by references.

None of the work has been submitted for another degree in this or any other University.

Signed: \_\_\_\_\_

Date: \_\_\_\_\_

**Abstract:**

**Background:** Epidemiological studies suggest that inhalation of carbonaceous particulate matter from increases susceptibility to bacterial pneumonia. *In vitro* studies report that phagocytosis of carbon black by alveolar macrophages (AM) impairs killing of *Streptococcus pneumoniae*. We therefore aimed to use a mouse model to test the hypothesis that high levels of carbon loading of AM in vivo increases susceptibility to pneumococcal pneumonia. We also want to develop an air-tissue interface model to assess DNA damage to airway macrophages due to inhalation of manufactured nanoparticles.

**Methods:** Female outbred mice were treated with either intranasal phosphate buffered saline (PBS) or ultrafine carbon black (UF-CB in PBS; 500 µg on day 1 and day 4), and then infected with *S. pneumoniae* strain D39 on day 5. Survival was assessed over 72 h. The effect of UF-CB on AM carbon loading, airway inflammation, and a urinary marker of pulmonary oxidative stress was assessed in uninfected animals.

The human monocyte cell line Mono Mac 6 and primary alveolar macrophages were used to assess DNA damage. To measure DNA damage in macrophages, we used the alkaline Comet assay. After nanoparticle exposure, a total of 100 macrophages were analysed per sample, as  $n=50$  duplicate slides. Tail length, percentage of DNA in the tail of the comet (% tail DNA), tail extent moment and olive tail moment, were calculated for each cell using the Komet Analysis software.

**Results:** Instillation of UF-CB in mice resulted high levels of carbon loading in alveolar macrophages. In uninfected animals, UF-CB treated animals had increased urinary 8-oxodG ( $P = 0.055$ ), and an increased airway neutrophil differential count ( $P < 0.01$ ). All PBS-treated mice died within 72 h after infection with *S. pneumoniae*, whereas morbidity and mortality after infection was reduced in UF-CB treated animals (median survival 48 h vs. 30 h,  $P < 0.001$ ). At 24 hr post-infection, UF-CB treated mice had lower lung and the blood *S. pneumoniae* colony forming unit counts, and lower airway levels of keratinocyte-derived chemokine/growth-related oncogene (KC/GRO), interferon gamma( IFN- $\gamma$ ) and other inflammatory cytokines.

No increase in DNA damage was observed when cells were placed in the nitrogen gas flow for 10 mins compared with cells placed in air (insert control vs air control). Exposure to nanoparticles from all three metals for 10 min caused a significant increase in DNA damage in human Mono Mac 6 cells compared to insert control. There was no significant difference between DNA damage caused by gold (Au), silver (Ag) and Iron (Fe) nanoparticles.

**Conclusion:** Acute high level loading of AM with ultrafine carbon black particles per se does not increase the susceptibility of mice to pneumococcal infection in vivo.

We found significant DNA damage in macrophages cultured for 24 h with doses of up to 10 mg/cm<sup>2</sup> aerosolized iron, gold or silver nanoparticles.

## **Acknowledgments:**

I would like to acknowledge and extend my heartfelt gratitude to my supervisors Professor Jonathan Grigg, Professor Peter Andrew and Dr Paul Howes, who guided, taught and encouraged me through this project. Without their understanding and input this thesis would not have been possible. I would like to express my thanks to Dr G Don Jones for his enthusiastic, expert advice and input into the project.

Many people have provided me with help and support through my time as a PhD student and for that I am extremely grateful. I would like to thank all past and present members of Lab 227 and child health, who have in many ways helped me all the way through my PhD and that have become a very important part of my life.

Mum and Dad. You have always been supportive of me throughout my academic career. My mum, especially, has sacrificed a lot to allow me to have a good life and successful career and for that I will always be extremely thankful. I hope I've made her proud.

A special thanks to Dr Meenu Jassal, my wife. Meenu, you inspired and encouraged me to be the best I could, for which I am so grateful. I would not have got this far without your love, support, encouragement and enthusiasm, so thank you.

I would like to thank my family and friends for their support and encouragement. Thanks go to my brother Bharat and sister Sahithi for their love and encouragement. Special thanks go to Karthik for his continued support and always making the effort to understand my research.

## **List of abbreviations:**

µl -Micro litre

µm - Micro meter

8- oxodG - 8-oxo-7,8-dihydro-2'-deoxyguanosine

Ag - Silver

Al - Aluminium

Al<sub>2</sub>O<sub>3</sub> - Aluminium oxide

AM - Alveolar macrophages

ARDS - Acute respiratory distress syndrome

As - Arsenic

Au - Gold

BA - Blood Agar

Ba - Barium

BAB - Blood Agar Base

BALF - Bronchoalveolar lavage fluid

BER - Base excision repair pathway

BHI - Brain Heart Infusion

Br - Bromine

CAP - Concentrated ambient particles

CCD - Charge-coupled device

Cd - Cadmium

CFU - Colony-forming unit

CH<sub>2</sub>Cl<sub>2</sub> - Dichloromethane

CNG - Compressed natural gas

Co - Cobalt

COPD - Chronic obstructive pulmonary disease

Cr -Chromium

Cu - Copper  
DEP -Diesel exhaust particles  
DLS - Dynamic light scattering  
DMSO - Dimethyl sulfoxide  
ELISA - Enzyme-linked immunosorbent assay  
ESD - Electrostatic discharge  
EtOH- Ethanol  
FBS - Fetal bovine serum  
Fc region-Fragment crystallizable region  
FCS -Foetal Calf Serum  
Fe- Iron  
Fe<sub>2</sub>O<sub>3</sub> - Iron oxide or ferric oxide  
FPG - Formamido pyrimidine glycosylase  
Gy - Gray  
Hg - Mercury  
HMDS -Hexamethyldisilazane  
HPLC - High-performance liquid chromatography  
HRTEM -High resolution transmission electron microscopy  
ICAM-1 - Intercellular adhesion molecule 1  
IFN  $\alpha$ - Interferon alpha  
IgE -Immunoglobulin E  
IgG - Immunoglobulin G  
IL - 1  $\beta$  - Interleukin 1 beta  
IL - 12 - Interleukin 12  
IL - 6 -Interleukin 6  
IL-10 - Interleukin 10  
IL-8 - Interleukin 8  
IPD - Invasive pneumococcal diseases

kV - Kilo Volts

LCESI- MS/MS - Liquid chromatography- electrospray ionization-tandem mass spectrometry

LDH - Lactate dehydrogenase

LMPA - Low melting point agarose

MEMS - Micro electro mechanical systems

min- minutes

ml - milli litre

mm - milli molar

MM6 - Mono Mac 6 cells

Mn -Manganese

NEMS - Nano electromechanical systems

Ni -Nickel

NMPA - Normal melting point agarose

OD - Optical Density

PBS - Phosphate buffered saline

PEG - Poly ethylene glycol

pF - Pico farads

PM - Particulate matter

PM<sub>10</sub> - Particles measuring 10µm or less

PM<sub>2.5</sub> - Particles measuring 2.5µm or less

pmol - picomolar

PTFE - Poly tetra fluoro ethylene

QCM - Quartz Crystal Microbalance

ROI - Region of interest

ROS - Reactive oxygen species

Sb - Antimony

SCGE -Single cell gel electrophoresis

Se - Selenium  
SEM - Scanning electron microscope  
SiO<sub>2</sub> - Silicon dioxide  
SMPS - Scanning mobility particle sizer.  
SRM - Selected reaction monitoring  
TEM - Transmission electron microscopy  
TNF- $\alpha$  - Tumor necrosis factor alpha  
UF-CB - Ultra Fine Carbon Black  
UF-CB - Ultrafine carbon black  
UF-Co - Ultrafine Cobalt  
UF-Ni - Ultrafine Nickel  
UF-TiO<sub>2</sub> - Ultrafine Titanium dioxide  
V - Vanadium  
V/V - Volume / Volume  
VCAM-1 - Vascular adhesion molecule 1  
W/V - Weight / Volume  
Zn - Zinc  
ZnO - Zinc oxide

## List of Figures

<b>Figure 1.1:</b> A soot particle containing coagulated ultra-fine particles.....	6
<b>Figure 1.2:</b> Length scale showing the nanometre in context.....	7
<b>Figure 1.3:</b> Urban air particle number size distribution.....	11
<b>Figure 1.4:</b> Size distribution of environmental tobacco smoke, vegetation burning, petrol smoke and diesel smoke .....	13
<b>Figure 1.5:</b> Threshold of nanotechnology as basic sciences converge to the nanoscale.....	17
<b>Figure 1.6:</b> General effects of decreasing particle size.....	18
<b>Figure 1.7:</b> Clearance of particles.....	23
<b>Figure 1.8:</b> Lung deposition versus size of particles.....	25
<b>Figure 1.9:</b> The structure of <i>Streptococcus pneumoniae</i> .....	40
<b>Figure 1.10:</b> Age distribution of invasive pneumococcal isolates from Danish children.....	44
<b>Figure 2.1:</b> Sonication of ultra fine carbon black (UF-CB).....	69
<b>Figure 2.2:</b> Miles-Misra style of viable count.....	77
<b>Figure 2.3:</b> A schematic drawing of collection of BALF.....	82
<b>Figure 2.4:</b> MSD Mouse Pro-Inflammatory 7-Plex Cytokine Panel.....	73
<b>Figure 2.5:</b> A picture of Transwell-COL insert.....	89
<b>Figure 2.6:</b> A diagram of cell culture insert with Mono Mac 6 cells.....	89
<b>Figure 2.7:</b> A photograph of Spark discharge chamber.....	92
<b>Figure 2.8:</b> A schematic diagram of the system for cell exposure to manufactured metal nano particles.....	96
<b>Figure 2.9:</b> A photograph of small whole-body exposure chamber.....	97
<b>Figure 2.10:</b> A diagrammatic representation of the Comet assay methodology.....	100
<b>Figure 2.11:</b> Quartz crystal resonator.....	103

<b>Figure 2.12:</b> A Schematic diagram of quartz crystal microbalance (QCM)	104
<b>Figure 2.13:</b> A photograph of Scanning Mobility Particle Sizer	108
<b>Figure 2.14:</b> Outline of <i>in vitro</i> exposure studies	109
<b>Figure 3.1:</b> Images of heavily loaded (A) and medium loaded (B) macrophages.	115
<b>Figure 3.2:</b> Images of lightly loaded (C) and none loaded (D) macrophages.	116
<b>Figure 3.3:</b> Semi-quantitative analysis of carbon loading of alveolar macrophages (AM)	118
<b>Figure 3.4:</b> Whole lungs after two doses of 500 µg ultrafine-carbon black (UF-CB)	120
<b>Figure 3.5:</b> TEM image of mouse alveolar macrophage	122
<b>Figure 3.6:</b> Neutrophil differential count in bronchoalveolar lavage fluid	124
<b>Figure 3.7:</b> Representative fields of control cytopsin slide	125
<b>Figure 3.8:</b> Representative fields of BALF cytopsin slides	126
<b>Figure 3.9 A, B, C:</b> Lung histology of uninfected mice and infected mice	130
<b>Figure 3.10:</b> Lung haemorrhage was measured in lung tissue of control and exposed groups	132
<b>Figure 3.11:</b> Analysis of urinary 8-oxodG	133
<b>Figure 3.12:</b> Survival curves of mice infected with pneumococci and pre-treated UF-CB	135
<b>Figure 3.13:</b> Survival data shown for the mice infected with pneumococci and pre-treated UF-CB	135
<b>Figure 3.14:</b> Disease scores of mice infected with pneumococci	137
<b>Figure 3.15:</b> Lung CFU counts after 2 hours of infection	139
<b>Figure 3.16:</b> Lung CFU counts after 24 hours of infection	140
<b>Figure 3.17:</b> Post 24 hours blood CFU counts in mice	140
<b>Figure 3.18:</b> Lung CFU counts at different time points	142
<b>Figure 3.19:</b> Blood counts at different time points	143

**Figure 3.20:** Assessment of cellular content of the broncho alveolar lavage fluid.....146

**Figure 3.21:** Bronchoalveolar lavage (BAL) fluid cytokines.....154

**Figure 4.1:** Size distribution of metal nanoparticles generated by spark electrodes. ....157

**Figure 4.2:** TEM images of spark-derived metal nanoparticles.....158

**Figure 4.3:** An example of a DNA damage in control cell (A) and effected (particle exposed) cell (B) analysed by Komet Analysis software.....159

**Figure 4.4:** DNA damage (% tail DNA) caused by different grades of radiation. ....160

**Figure 4.5:** DNA damage (tail extent moment) caused by different grades of radiation.....161

**Figure 4.6:** DNA damage (olive tail moment) caused by different grades of radiation.....162

**Figure 4.7:** DNA damage (tail Length) caused by different grades of radiation. ....162

**Figure 4.8:** DNA damage caused by 10 min exposure of Mono Mac 6 cells to Fe, Au and Ag nanoparticles at an air-tissue interface.....164

**Figure 4.9:** Dose-dependent DNA damage in Mono Mac 6 cells caused by exposure to Fe nanoparticles.....166

**Figure 4.10:** DNA damage induced in rat alveolar macrophages after 10.2  $\mu\text{g}/\text{cm}^2$  exposure to Fe nanoparticles.....168

**Figure 4. 11:** Changes in cell proliferation in Mono Mac 6 cells after exposure to Au 5.4  $\text{mg}/\text{cm}^2$  (10 min).....169

**Figure 4.12:** TEM images of Mono Mac 6 cells that non- exposed to Gold (Au) nano particles.....172

**Figure 4.13:** TEM images of Mono Mac 6 cells that exposed to Gold (Au) nano particles.....174

**Figure 4.14:** SEM image of control alveolar macrophage.....176

**Figure 4.15:** SEM image of exposed alveolar macrophage.....177

## List of Tables

<b>Table 1.1:</b> Characteristic elements emitted from various combustion sources..	16
<b>Table 1.2:</b> Inflammatory cytokines selected in the work.....	27
<b>Table 1.3:</b> Summary of epidemiological, <i>in vivo</i> and <i>in vitro</i> studies on the health effects of ultrafine particles.....	35
<b>Table 1.4:</b> The Annual Incidence of Pneumococcal Disease.....	43
<b>Table 2.1:</b> Scoring of the signs of disease after infection.....	73
<b>Table 2.2:</b> Summary of MF1 mice groups and instillation days.....	75
<b>Table 2.3:</b> List of various Comet measurements calculated by the Komet image-analysis system.....	102
<b>Table 3.1:</b> Different groups of alveolar macrophages.....	114
<b>Table 3.2:</b> Histopathological examination of mice lung tissue.....	131

# Table of Contents

**Title**

**Dedication**

**Statement of Originality.....i**

**Abstract.....ii**

**Acknowledgements.....iii**

**List of abbreviations.....iv**

**List of figures.....viii**

**List of tables.....xi**

**Table of contents.....xii**

**Chapter 1: Introduction .....2**

1.1. Overview of ultrafine particles.....4

1.1.1. General characteristics of ambient particles.....8

1.1.2. Chemical composition.....14

1.2. Nanoparticles and their Applications .....16

1.3. Deposition, retention and clearance of inhaled particles.....21

1.3.1. Respiratory tract.....21

1.3.2. Inflammation.....25

1.3.3. Alveolar Macrophages.....27

1.4. Health impacts of ultrafine particles .....31

1.4.1. Nature of the effects.....32

1.5. *Streptococcus pneumoniae*: The pneumococcus .....38

1.5.1. Introduction .....38

1.5.2. Carriage .....40

1.5.3. Disease.....41

---

1.5.4. Age.....	42
1.5.5. Time.....	44
1.5.6. Geography .....	45
1.6. Pulmonary Defence Mechanisms.....	46
1.6.1. Physical or Anatomic factors .....	47
1.6.2. Antimicrobial peptides .....	49
1.6.3. Phagocytic and inflammatory cells .....	52
1.6.4. Adaptive immune responses .....	54
1.7. Ultrafine particles and vulnerability to infection.....	56
1.8. Thesis Aims .....	60

## **Chapter 2: Materials and Methods**

2.1. General Information.....	62
2.1.1. Solution.....	62
2.1.2. Suppliers.....	64
2.1.3. Preparation of blood agar plates.....	67
2.1.4. Culturing of <i>Streptococcus pneumoniae</i> .....	67
2.2. Particle preparation .....	67
2.3. Bacterial stock preparation .....	69
2.3.1. Dose confirmation.....	69
2.3.2. Animal passage .....	71
2.3.3. Virulence testing .....	71
2.4. Animal welfare .....	73
2.4.1. C57BL/6J mouse strain .....	73
2.4.2. MF1 mouse strain .....	74
2.5. Protocols for animal experiments .....	75
2.5.1. Intraperitoneal infections .....	75
2.5.2. Intranasal infections and instillations .....	76
2.5.3. Collection of blood- cardiac puncture .....	77
2.5.4. Collection of blood- tail bleeding .....	77

2.5.5. Calculation of CFU from blood .....	78
2.5.6. Calculation of CFU from lungs .....	78
2.5.7. Urine collection .....	79
2.5.8. Collection of broncho alveolar lavage fluid .....	79
2.5.9. Cytospin Preparation .....	81
2.5.10. BAL cytokines .....	81
2.6. Fixation and preparation of mice lung tissue .....	83
2.6.1. Deparaffinization .....	83
2.6.2. Hematoxylin and Eosin .....	83
2.6.3. Pathology score on lung histological sections.....	84
2.7. Urinary 8-oxodG assay .....	84
2.8. Mono Mac 6 cell culture.....	85
2.8.1. Passaging .....	86
2.8.2. Freezing .....	86
2.8.3. Thawing .....	87
2.8.4. Cell seeding on cell culture inserts .....	87
2.9. Rat alveolar macrophages .....	89
2.10. Generation of nanoparticles .....	89
2.11. Particle exposure to cells .....	92
2.12. Comet Assay .....	96
2.13. Quartz Crystal Microbalance .....	101
2.14. Cell viability Assay .....	103
2.15. X-ray irradiation .....	104
2.16. Characterization of nanoparticles .....	105
2.16.1. Scanning Mobility Particle Sizer .....	105
2.16.2. High resolution transmission electron microscopy .....	108
2.16.3. Scanning Electron microscope .....	108
2.17. Statistical analysis .....	109

---

**Chapter 3: Results one: Effect of instillation of ultrafine carbon black (UF-CB) into the lower airway of mice on mortality from *Streptococcus pneumoniae*.**

3.1. Analysis of carbon loading on alveolar macrophages .....	111
3.1.1. Particle distribution after intratracheal instillation .....	117
3.1.2. TEM investigation of particle engulfed alveolar macrophage	119
3.2. Analysis of broncho alveolar lavage fluid .....	121
3.3. Analysis of lung histopathology .....	125
3.4. Determination of 8-oxodG in mice urine samples .....	130
3.5. Disease and survival of mice after particle instillation and infection	131
3.6. Estimation of CFU from lungs and blood after intranasal infections at 2 hours and 24 hours .....	136
3.7. Comparison of bacterial growth in lungs and blood at different time points .....	139
3.8. Post infection Cellular analysis of bronchoalveolar lavage fluid ..	141
3.9. Pro-inflammatory cytokine levels in the presence and absence of UF-CB and/or infection in broncho alveolar lavage fluid .....	145

**Chapter 4: Results Two: DNA damage in macrophages caused by exposure nanoparticles at an air/tissue interface.**

4.1. Characterization of metal nanoparticles .....	154
4.2. Assessment of DNA damage by Comet assay after exposure of cells to different doses of radiation .....	157
4.3 Assessment of DNA damage in alveolar macrophages caused by metal nanoparticles exposure .....	162
4.4. Assessment of dose dependent DNA damage caused by iron nanoparticles exposure .....	164

4.5. Assessment of DNA damage in rat alveolar macrophages after exposure to iron nanoparticles .....165

4.6. Evaluation of cell viability in particle exposed cells .....166

4.7. TEM analysis of particles on alveolar macrophages .....168

4.8. SEM analysis of particles on alveolar macrophages .....173

**Chapter 5: Discussion and Future work**

5.1. Part A: *in vivo* study .....177

5.2. Part B: *in vitro* study .....191

**References** ..... 184

**Publications**



# Chapter 1

# Introduction

## 1. Introduction:

Pollution particles that released from industrial and indoor combustion process are hazardous to public health and are often linked to increased rate of mortality and morbidity during mid twentieth century time (Brimblecombe et al. 2001). Inhalation of suspended particulate matter, whether atmospheric or occupational, causes or aggravates inflammation in the respiratory tract, which can lead to or worsen inflammatory conditions like asthma and bronchitis (Davidson et al. 2005). In low-income countries, the burning of biomass fuels results in concentrations of inhalable carbonaceous particulate matter (PM) exceeding  $8000 \mu\text{g}/\text{m}^3$  (Colbeck et al. 2010), with young children and women differentially exposed (Bruce et al. 2000a). The Mechanism by which exposure to particles in urban air induces mortality and respiratory morbidity remains unclear.

The human body's defence system constantly guards against the entry of potential pathogens and particles. Primarily skin, the mucosal surfaces of the respiratory expose more, and then later gastrointestinal and urogenital tracts are slightly less expose to outer environment. But, they all maintain internal sterile environment and stand as a first line of defence against foreign particles (Valdivia-Arenas et al. 2007). Precisely, the lung and the intestine are the organs most exposed to the external environment. Infections of the lungs are one of the most frequent infections in humans with *Streptococcus pneumoniae*

being the most common (O'Brien et al. 2003). *Streptococcus pneumoniae* is responsible for a significant proportion of global pneumonia deaths (Wardlaw et al. 2006).

Surveillance data suggests that particle matter, which was generated by combustion process and biomass fuel, plays an important role in increased bacterial pneumonia in low-income countries. Reasons such as growing antibiotic resistance and lack of availability of antibiotics and vaccines also add to the increase of pneumococcal cases in those countries. Alveolar macrophages are the first line of pulmonary defence against pneumococcal pneumonia. First, Lundborg *et al* (Lundborg et al. 2007b) reported a dose-dependent increase in the survival of *S. pneumoniae* in rat alveolar macrophages (AMs) loaded with ultrafine carbon black *in vitro*. Second, Zhou and Kobzik (Zhou et al. 2007b) reported in a mouse model, that AM phagocytosis of carbonaceous urban PM *in vitro* impairs their ability to subsequently internalise *S. pneumoniae*. So, it is hypothesised that susceptibility to pneumococcal pneumonia is increased by carbon loading of AM *in vitro*. Using a mouse model, we sought to test this hypothesis by loading AM with ultrafine carbon black (UF-CB) *in vivo*, and then assessing morbidity and mortality to subsequent intranasal pneumococcal infection.

Nano particle size distributions are ranging from 1nm to 100 nanometers in two or three dimensions (European Commission 2001). Lately, there has been a

remarkable increase of handling of nanoparticles in research, technology, and also production different nanoparticles (Lewinski et al. 2008). Engineered nanoparticles offer a widespread usage in medicine, food, clothes, personal care products, information technology, and construction materials, resulting in a wide range of exposure conditions. As a result, it is very vital to evaluate the potential hazards of nanoparticles on human health (Nel et al. 2006b) (Maynard et al. 2006). So far, majority of studies (Bitterle, E. *et al.* 2006) have tried to assess the methodology that models toxicity of nanoparticle agglomerates in human cells. Like in majority of studies, Bitterle *et al.* used nanoparticles in aqueous suspension. However, inhaled particles (nanoparticles with an aerodynamic diameter of less than 100 nm) reaching the small airways will be in non-agglomerated and free form, which in turn may result in qualitative and quantitative differences in their ability to induce toxicity. In this study, we therefore sought to develop an air-tissue interface model to assess DNA damage to airway macrophages due to inhalation of iron (Fe), gold (Au), and silver (Ag) nanoparticles.

### **1.1. Overview of ultrafine particles:**

The prefix ‘nano’ is originated from the Greek word for ‘dwarf’. One nanometre (nm) is equal to one-billionth of a metre ( $10^{-9}$  m). To compare the size of ‘nano’, a human hair is approximately 80,000nm wide, and a red blood cell approximately 7000nm wide. Figure 1.2 shows the nanometre in context.

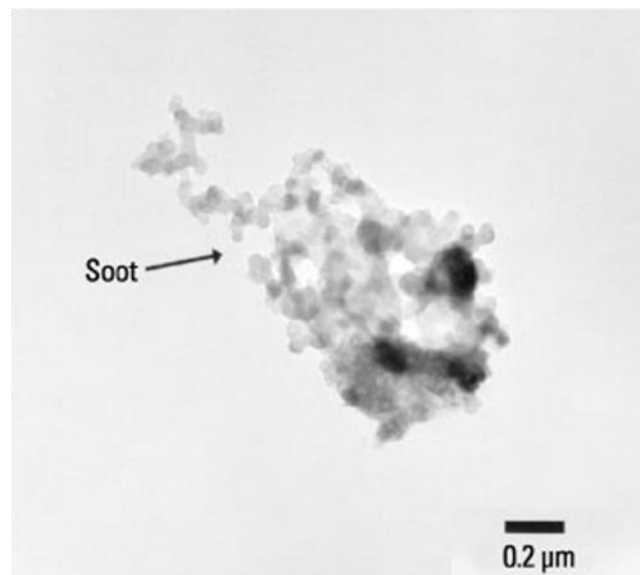
Only atoms and molecules such as proteins are below a nanometer in size (Sahoo et al. 2007).

Researchers use many different terms and classifications to define the word ‘particle size’. Most commonly used terminology is fine and coarse particles. Briefly, coarse particles are larger in size (more than 2.5  $\mu\text{m}$ ) compared to fine particles, which are less than 2.5  $\mu\text{m}$  (Oberdörster et al. 1994). Ultra fine particles, less than 100 nm, are sub-set of fine particle and used for research in this thesis (Jiang et al. 2008).

There has been different terminology used by ambient air quality standards to characterize indoor and outdoor particle mass concentrations. Mainly, particulate matter ( $\text{PM}_{10}$ ) is defined as the mass of particulate matter which passes through a size selective impactor inlet with a 50% efficiency cut-off at 10  $\mu\text{m}$  aerodynamic diameter. Mass concentrations of particles that are less than 2.5  $\mu\text{m}$  of their aerodynamic diameter are included in  $\text{PM}_{2.5}$  and mass concentrations of particles between 2.5  $\mu\text{m}$  and 10  $\mu\text{m}$  are included in  $\text{PM}_{10}$  fraction (Oberdörster et al. 2005a). Similarly,  $\text{PM}_1$  or  $\text{PM}_{0.1}$  particles which imply mass concentrations of particles smaller than 1 and 0.1  $\mu\text{m}$ , respectively (Vaattovaara et al. 2005). However, there is concern in referring  $\text{PM}_1$  or  $\text{PM}_{0.1}$  particles. Because, particles below 1  $\mu\text{m}$  and 0.1  $\mu\text{m}$  are more commonly measured in terms of their number rather than their mass concentrations.

Based on the sources and other atmospheric conditions, particle matter can be classified into three following modes (Harrison et al. 1996):

- **Nucleation mode:** particles categorised in this mode are produced by nucleation of atmospheric gases in a supersaturated atmosphere and they are in nanometre size.
- **Accumulation mode:** particles in this category derive from primary emissions as well as through gas to particle conversion, chemical reactions, condensation and coagulation (Figure 1.1).
- **Coarse mode:** particles in this category derived by mechanical processes.



---

**Figure 1.1:** A soot particle containing coagulated ultra-fine particles (Lioy et al. 2002).

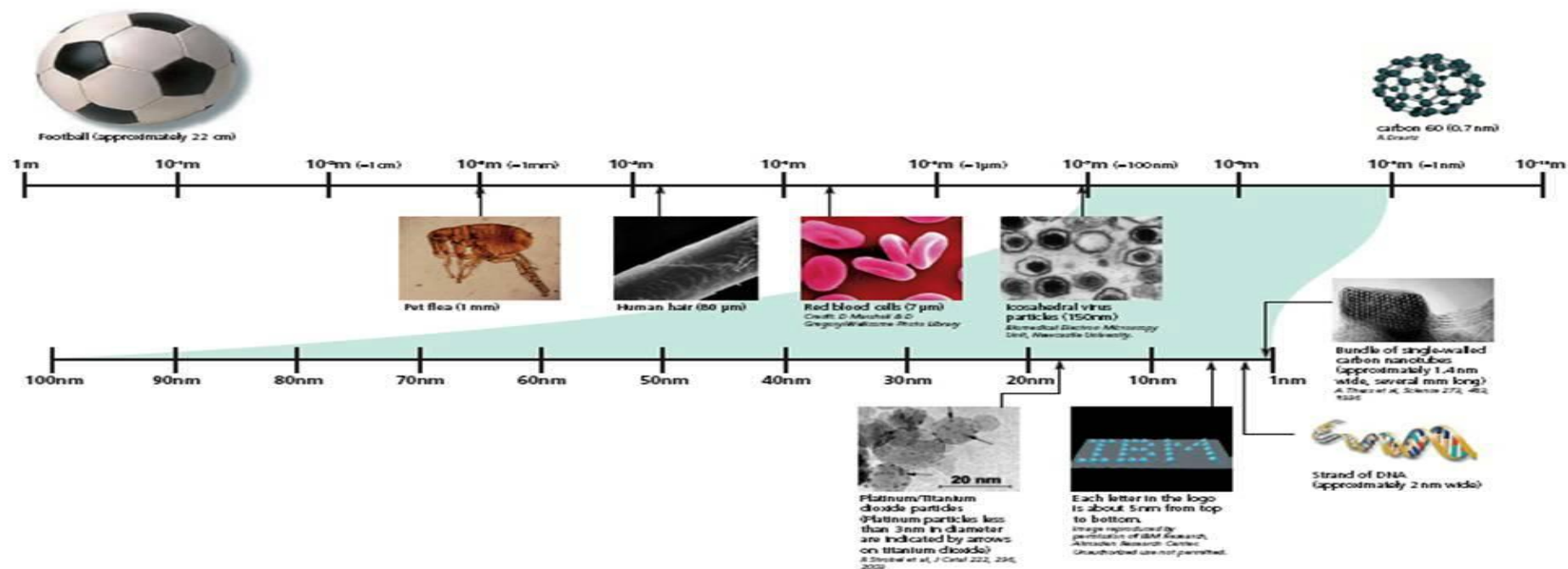


**Figure 1.2:** Length scale showing the nanometre in context This diagram places the nanoscale in context. One nanometre (nm) is equal to one-billionth (1,000,000,000) of a metre,  $10^{-9}$ m. Most structures of nanomaterials which are of interest are between 1nm and 100 nm in one or more dimensions. For example, carbon Buckyballs are about 1 nm in diameter. For comparison the world is approximately one hundred million times larger than a football, which is in turn one hundred million times larger than a buckyball. (Courtesy of the Royal Society&the Royal Academy of Engineering, 2004).

**1.1.1. General characteristics of ambient particles:**

Ambient air particle mixtures are generated by a great number of sources such as windblown dust, photochemical processes, cigarette smoking, motor vehicles, power plants etc. Particle conversion is the process where primary particle initially introduced into the air in either solid or liquid form and later secondary particle is developed in the air by gas (Morawska et al. 2002). Ultrafine particles are generated from various processing methods. Primarily, methods such as combustion, gas to particle conversion, nucleation processes or photochemical processes. Some of these methods could be primary source or secondary in particle conversion process. Particles that are in the range of micrometer size result mainly from mechanical way of particle conversion process and those particles are generated as primary emissions (Morawska et al. 1998).

Important physical characteristics of ambient particles include:

- Number concentration
- Number size distribution
- Mass concentration
- Mass size distribution
- Surface area, shape
- Electrical charge

Physical characteristics of ambient particles that are listed above play an important role in particle behaviour in the air and removal from atmospheric systems. Particle size is strongly linked with the health and environmental effect of air particles. Particle size determines the region in the lung where particles deposit and either indoors or outdoors locations that particles are able to reach or be accumulated (Areskoug et al. 2000).

Ambient particles that are suspended into the air, ranges in size from 0.001  $\mu\text{m}$  to about 100  $\mu\text{m}$  (Baron et al. 2005). Particles that exceed more than 100  $\mu\text{m}$  in size settle out rapidly due to gravity and as a result removed from the atmosphere. Majority of sources generate particles of various sizes instead of particles of a single size. The range of particle size distribution is characterised by an arithmetic or geometric (logarithmic) standard deviation (Friedlander et al. 2000). Different emission sources exhibit different size distributions (Morawska et al. 1998).

In general, the processes that generate particles produce same range of particle size distributions. Same source rarely generates particles covering both fine and course ranges (Djamarani et al. 1997). Some sources produce the particles within the sub micrometer range which generates high particle number in the air and some sources produce large particles which generates high particle mass. So, there is occasional correlation between either fine and coarse particles or particle number or particle mass (Zhu et al. 2002b).When reporting particle

distributions, particles are commonly referred to in terms of mass and number but rarely in terms of surface distributions (Pluschke 2004).

Particle size distributions are presented in a simple way in the left hand side of figure 1.3 (Morawska 2000), which does not reflect the logarithmic nature of the distribution. On the right hand side of the figure 1.3, particle size distributions plotted in a logarithmic scale  $dN/d\log DP$ ,  $dA/d\log DP$ , and  $dM/d\log DP$ , which represent particle number, surface and mass respectively, per logarithmic interval of size. In general, most of the air pollution particles fall in the range of ultra fine particles (Figure 1.3). However, when compared to the total mass of the ultrafine particles to the mass of larger particles, the mass of ultrafine particles is often very insignificant (Zhu et al. 2002b).

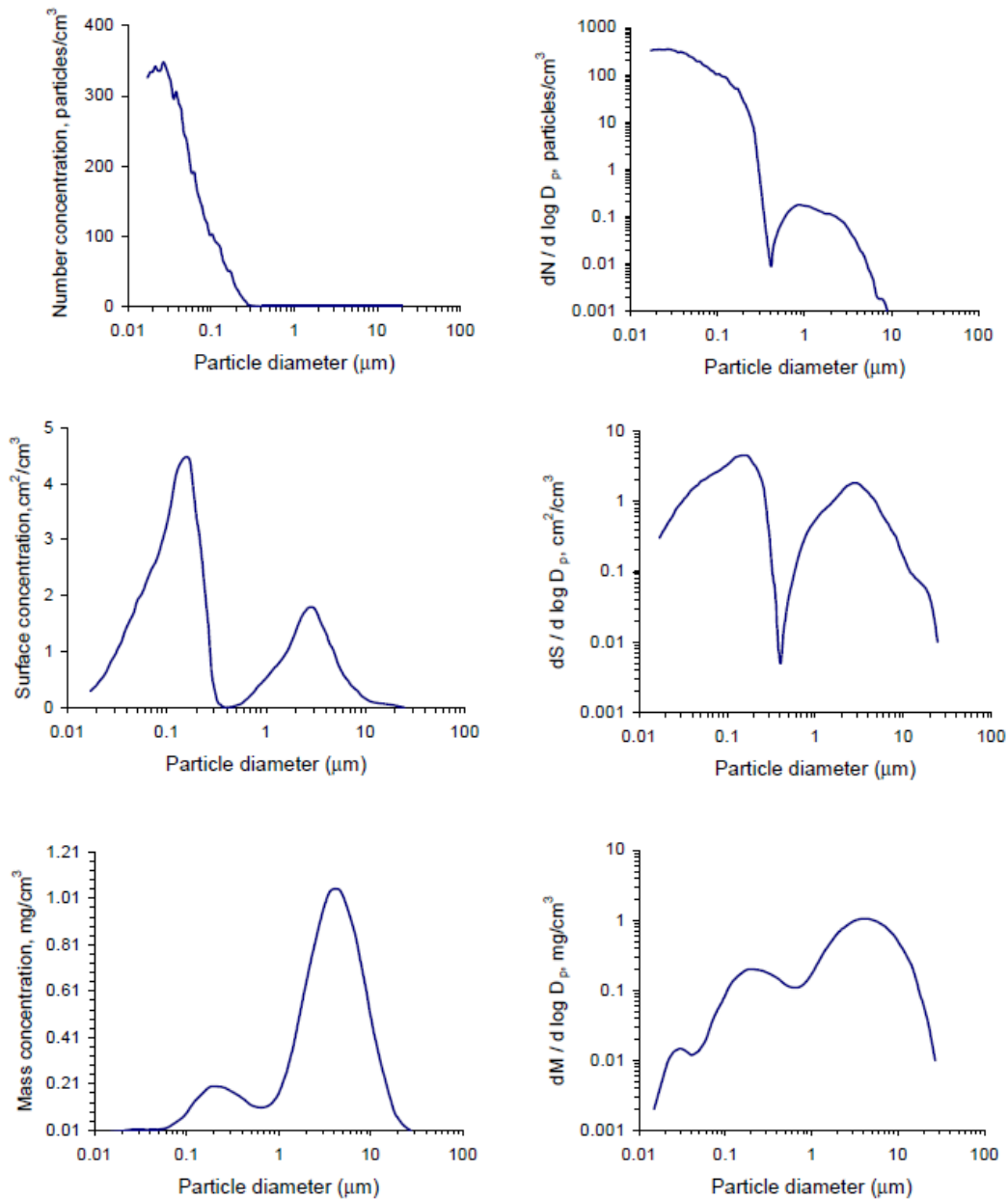


**Figure 1.3:** Top two graphs above showing urban air particle **number** size distribution, middle graphs showing particle **surface** distribution and bottom graphs showing particle **mass** distributions. Two different representations of vertical axis are used for each pair of size distributions. (Morawska 2000).

Size of particles generated by combustion sources is very small. The size of combustion generated particles; including vehicle emission have diameters smaller than 0.1  $\mu\text{m}$  (Morawska et al. 1998); (Ristovski et al. 1998). The size of gasoline generated particles is ranging from 0.01 – 0.08  $\mu\text{m}$ . Compressed natural gas (CNG) generated nanoparticles are ranging from 0.01-0.07  $\mu\text{m}$ . These particles are much smaller than particles (in between 0.020 and 0.060  $\mu\text{m}$ ) that emitted by diesel or even petrol engines (Ristovski et al. 2000). Biomass burning sources, either controlled house hold burning or uncontrolled fires, generates a great amount of ultrafine particles (particles less than 2.5  $\mu\text{m}$  in aerodynamic diameter) and very insignificant number of larger size particles (Schwela et al. 1999). Figure 1.4 illustrates that various particle size distributions from vegetation burning, tobacco smoke, petrol smoke and diesel smoke.

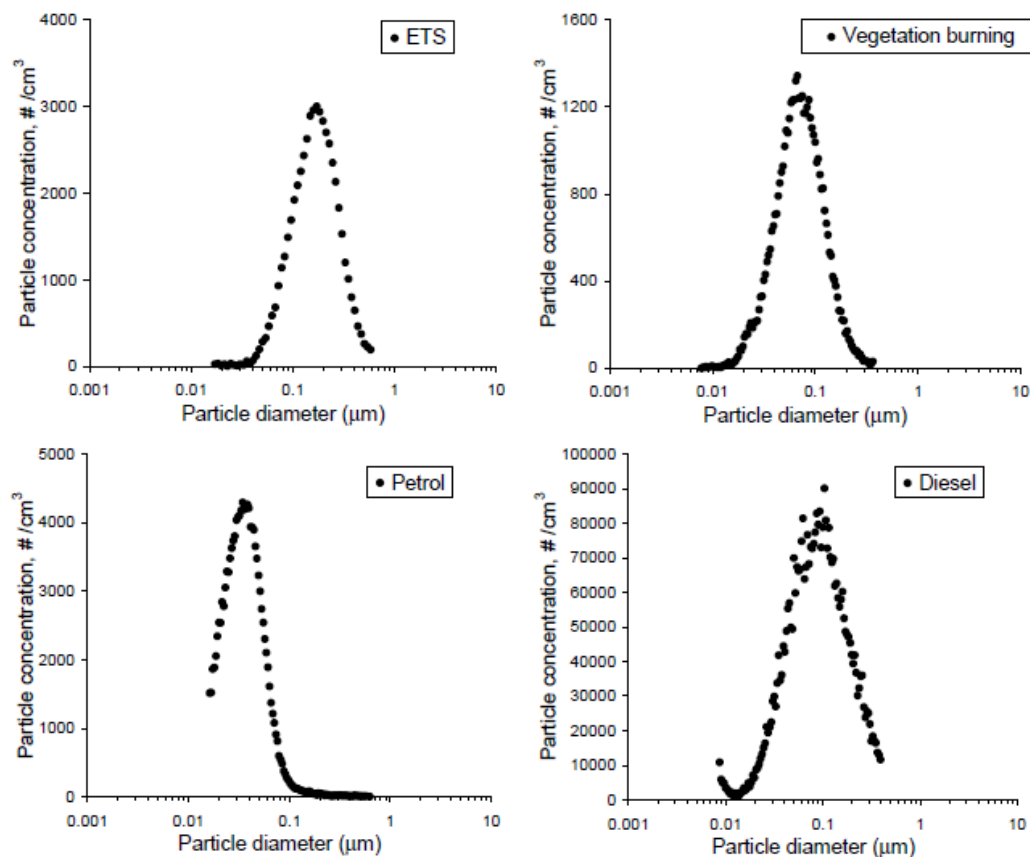


**Figure 1.4:** Diagram showing particle size distribution generated from various combustion sources such as environmental tobacco smoke, vegetation burning, petrol smoke and diesel smoke (Morawska 2000).

Nanoparticles show different physical properties by modifying the particle size. For instance, copper nanoparticles less than 50 nm size, do not display general characteristics such as malleability and ductility but rather very hard and durable (Khan 2007). Pellets made of small gold (Au) and palladium (Pd) nanocrystals exhibit non-metallic behaviour with specific conductivities in the range of  $10^{-6} \Omega^{-1} \text{ cm}^{-1}$ . An increase in the diameter of the nanocrystals, however, increases dramatically the conductivity (Norberg et al. 2004).

### 1.1.2. Chemical composition:

Particle generation source, post formation processes and various properties determine the chemical composition of particles (Morawska et al. 2003). The most important chemical compositions of particles include.

- Carbonaceous compounds
- Elemental composition
- Inorganic ions

Carbonaceous compounds, sometimes termed as “soot” or “black carbon”, are composed of organic and elemental carbon. Generally, soot particles are produced from combustion processes (Santoro et al. 1983). Soot particles, in general, appear as a group of ultrafine black particles. However, in terms of size of the particle agglomerates can measure up to a few hundred nanometres (Bockhorn 2000). The formation of soot particles is generally very complicated process, where a hydrocarbon fuel molecule that contains few carbon atoms converted into carbonaceous agglomerate which contains millions of carbon atoms. Soot formation goes through a gaseous-solid phase transition where the solid phase exhibits no unique chemical and physical structure. (Xi et al. 2006). Therefore, formation of soot particle occurs by entirely different conversion process, physically and chemically. Initially, primary particles agglomerate into larger aggregates, and reach a solid particle state by picking up growth components from the gas phase (Morjan et al. 2003).

Different fuel combustion emissions release various trace elements. It is mostly not just one specific element that released into the air from the combustion of a one particular fuel. Every fuel combustion process releases a wide variety of elements (Morawska et al. 2002). Examples of the most common source profiles of trace elements related to specific combustion sources are illustrated in table 1.1.

Apart from the main chemical composition of particles illustrated earlier, biological particulate matter play a crucial role in the incidences of allergies, allergic diseases and asthma are increasing worldwide. These airborne bioaerosols include fungi, bacteria, plant pollen, and spore material, all of which have been linked to allergic symptoms. Bioaerosols can induce irritational, allergic, infectious, and chemical responses in exposed individuals.

**Table 1.1:** Characteristic elements emitted from various combustion sources. (Morawska et al. 2002).

Emission Source	Characteristic Elements Emitted
Oil fired power plants	V, Ni
Motor vehicle emissions	Br, Ba, Zn, Fe, Pb (in countries where leaded petrol is used)
Refuse incineration	Zn, Sb, Cu, Cd, Hg
Coal combustion	Se, As, Cr, Co, Cu Al
Refineries	V
Nonferrous metal smelters	As, In (Ni smelting), Cu
Use of pesticides	As
Iron and steel mills	Mn
Plant producing Mn metal and Mn chemicals	Mn
Copper refinery	Cu

## 1.2. Nanoparticles and their Applications:

Great impacts of nanoscience on applied technology have resulted in intense interdisciplinary efforts (Figure 1.5). The dependence of properties on size on the nanoscale has been effectively utilized to control the chemical and physical properties of nanoparticles and to tailor them for specific applications (Figure 1.6).

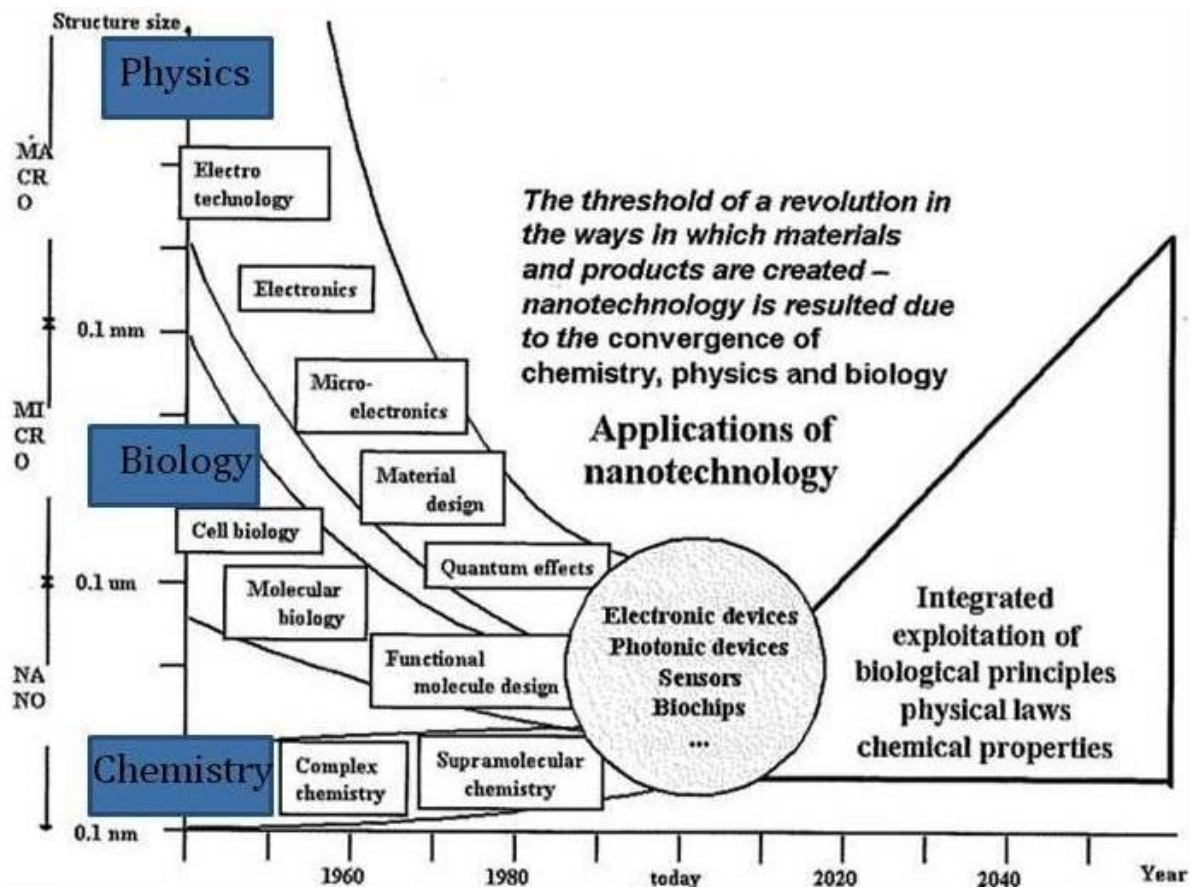


**Figure 1.5:** Threshold of nanotechnology as basic sciences converge to the nanoscale (Lu et al. 2010).

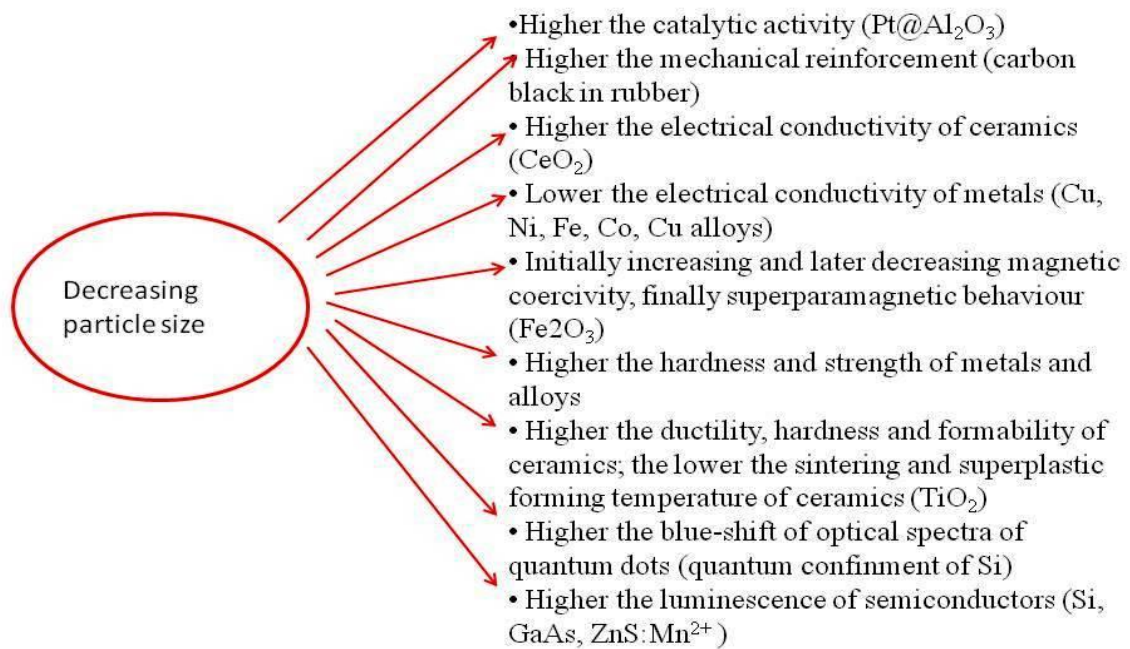


**Figure 1.6:** General effects of decreasing particle size (Gutsch et al. 2002)

Recent advances in nanotechnology enable biomaterials to have applications in (approximately 8000) different kinds of medical devices (Gogotsi 2006). Such as drug and gene delivery, molecular motors, repairing skeletal systems, returning cardiovascular functionality, replacing organs and monitoring living systems by nanosensors are nanostructure applications in biology (Han et al. 2007); (Feringa 2001)(Langer et al. 2003).

Biodegradable polymeric nanoparticles, which are coated with hydrophilic polymer such as poly ethylene glycol (PEG) known as long-circulating particles, have been used recently as potential drug delivery devices. Being able

to circulate for a prolonged period of time (increase of the molar mass leads to reduced kidney excretion) , able to target a particular organ as carriers of DNA in gene therapy, and their ability to deliver proteins, peptides and genes (Mohanraj et al. 2006) made these polymeric nanoparticles highly useful in drug delivery.

Nanoporous materials is also part of nano sized materials, have a distinctive properties that make them very useful in various fields such as biological molecular isolation, separation, catalysis, sensor and purifications. . Nanoporous materials are able to absorb and relate with atoms, ions, and molecules on their large interior surfaces and in the nanometer sized pore space (Lu et al. 2010).

Advances in energy and environmental applications of nanomaterials, enable nanomaterial-based membrane technologies, adsorbents, and catalysts to utilise and to advance in water pollution control, groundwater remediation, potable water treatment, and air quality control (Fryxell et al. 2007).

Quantum dots, are smaller nanoparticles (range from 2 to 10 nanometers in diameter), exhibit distinctive electrical properties that are different in character to those of the corresponding material that larger in size. Quantum dots can be used to produce light emitters of various colours by “band gap tuning” using particle size effects rather than the current complex techniques of synthesizing compound semiconductors (Kruis et al. 1998).

Nanostructured materials enhance the structural and the functional properties. These materials used in the making of ultrahigh strength, tough structural materials, strong ductile cements and novel magnets. Dirt-repellent materials, scratch-proof coatings, environmentally friendly fuel cells with highly effective catalysts are some utilities of nanostructured materials (Gutsch et al. 2002).

Nanostructured electrode materials are used in the process of making high-performance electrode materials. Research is underway in making single-electron electrode devices using gold particles (Nakaso et al. 2002). Typical capacitances of nanocrystals are in the range of 10-18 F (Farad)\*. At such low capacitances, successive charging events are discrete and no longer continuous charging. Using gold nanoparticles nanocrystals, single-electron devices such as supersensitive electrometers and memory devices could be fabricated in near future (Schwarz et al. 2004) .

Because Single-walled nano tubes can be good metallic and efficient semiconducting devices, they can be used as tips in scanning microscopes and also as efficient field emitters that are useful in display devices. Recently, scientists are managed to make a highly flexible and extremely strong (~100 times that of steel) single walled carbon nano tube (Mansoori 2005). Due to their surface plasmon resonance located within the visible domain of the electromagnetic spectrum, silver, gold and copper are essentially used for their color, yellow to red. Other group of metal nano particles such as Palladium, platinum, and ruthenium are used for heterogeneous catalysis (Wiesner et al. ).

\* The farad (F) is the Standard International (SI) unit of capacitance.

### **1.3. Deposition, retention and clearance of inhaled particles:**

PM<sub>10</sub>'s potential hazards after their inhalation mainly depends on their patterns of deposition inside the lung and pathways of their clearance from the deposition sites (Lippmann et al. 1980)(Kim et al. 1998)(Kim et al. 1998)(Kim et al. 1998) . Aerodynamic diameters of ambient air particle mixtures are play crucial role in particle deposition in lower lung airways. Particle clearance is generally considered difficult if they deposited in non-ciliated airway area of the lung. These particles can only be cleared as free particles in the form of phagocytosis by alveolar macrophages. If the particles penetrate the epithelium, either bare or within macrophages, they may be secluded within cells or enter the lymphatic circulation and be carried to distant lymph nodes (Zhu et al. 2002a).

#### **1.3.1. Respiratory tract:**

Human lungs regularly expose to various foreign particle matter and pathogens such as bacteria and viruses. Lung epithelial surface form a physical barrier that is very impermeable to most infectious agents and outside particle matter. Beyond the epithelial cell layers of lung, much evolved immune system that consists of innate (non-specific) and acquired (specific) immune system protect human body from foreign agents. The innate immune system is composed of

highly specialized and systemic cells such as alveolar macrophages, neutrophils etc., and also consists of surfactant proteins, defensins, antioxidants that provide immediate defense against infection (Oberdörster 2000).

Logically, when particle matter enters into the lung, the mucociliary escalator dominates the clearance of such particle matter in upper airways. Particles with an aerodynamic diameter of approximately 100 nm can manage to travel and deposited mainly in the alveolar part of lung, where alveolar macrophages plays a crucial role. Along with the direct involvement of macrophages, chemotactic signals (such as cytokines, reactive oxygen species, chemokines and other mediators) that are released to activate and attract neutrophils to help particle phagocytosis in alveolar region. In addition, particles can also be phagocytosised and cleared via the lymphatic system to the lymph nodes, or taken up by the epithelial cells lining the lungs. Physical characteristics such as size and aerodynamic efficiency as an advantage, nano sized particles (aerodynamic diameter is less than 50 nm) able to reach and deposit in the distal regions of the lungs during inhalation than larger and micro-meter sized particles (Oberdörster 2000); (Knaapen et al. 2009). Nanoparticles that were deposited in alveolar regions of lung, can escape through the clearance mechanisms such as mucociliary clearance and macrophage clearance. (Warheit et al. 2008) ( Figure 1.7).

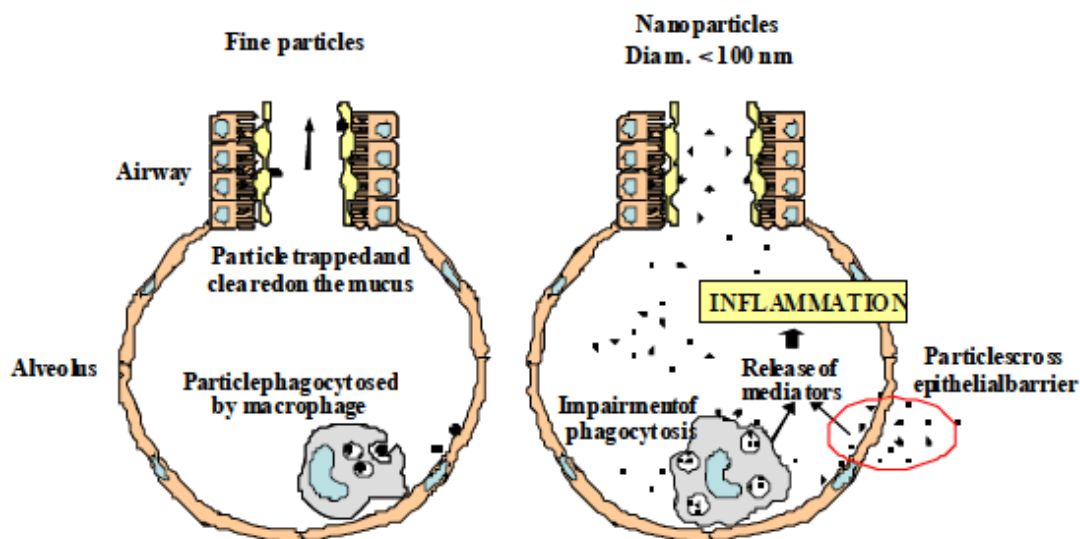


**Figure 1.7:** Schematic diagram of clearance of inhaled particles (fine and nanoparticles) from the alveolar region (Donaldson et al. 2001).

Particle deposition is the crucial first step toward in determining subsequent clearance mechanism. The respiratory tract is divided into three compartments depended on the clearance processes that associated with each region (Oberdörster et al. 2002). Fine particles that inhaled and deposited in the nostrils will be trapped in mucus and transported by mucociliary escalator through the nasopharynx, and into the gastrointestinal tract (Oberdörster et al. 2005b). Particles, which can pass through the airways and the larynx, will be deposited in terminal bronchioles, eventually will be cleared by mucus and suspended into the gastrointestinal tract. Smaller particles that are deposited, beyond layers of epithelium, on the alveolar region (consists of respiratory bronchioles, alveolar ducts, alveolar sacs and alveoli) will be removed by pulmonary macrophages through phagocytosis. The regions reached by the inhaled particles is affected

by the size as seen in figure 1.8, with large particles around 10  $\mu\text{m}$  depositing almost entirely in the upper airways, and smaller particles propelled deeper into the lungs. Once the particles have deposited in the lungs the particles will then initiate an inflammatory response by interacting with the cells of the immune system (Oberdörster et al. 2005b).

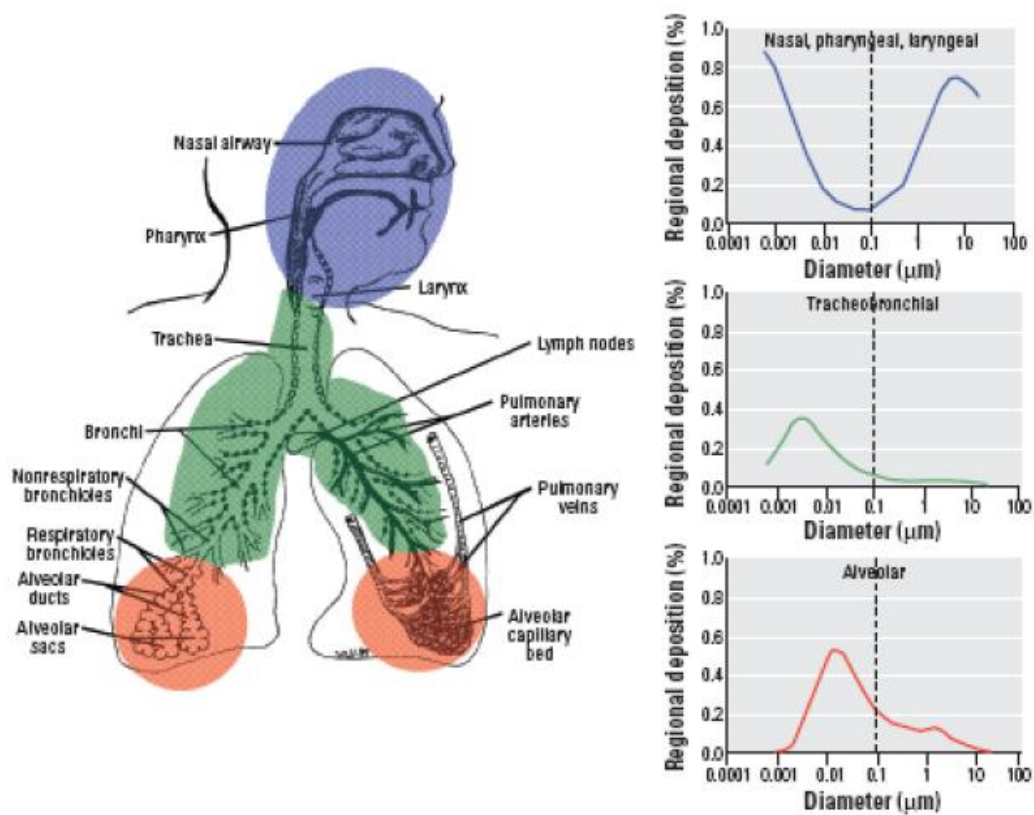


**Figure 1.8:** Diagram showing the relevance of particle size in different regions of the human lung and particle deposition (Oberdörster et al. 2005b).

### 1.3.2. Inflammation:

Inflammation is a protective mechanism by host organism to remove pathogens and support repair of tissue injury. Sometimes, chronic and persistent inflammation can also lead to inflammatory lung diseases, such as chronic obstructive pulmonary disease (Groneberg et al. 2004) and silicosis (Huaux 2007). Particle clearance at a small scale induces beneficial transient inflammation in lung. Chronic pulmonary inflammation, on the other hand, caused by inhaled, insoluble ambient particle mixture can damage to the lung tissue. polymorphonuclear leukocytes (PMNs), usually neutrophils, are consider important part of inflammation in diseases like chronic obstructive pulmonary disease (Groneberg et al. 2004); (Parr et al. 2006) and silicosis (Huaux 2007); (Gulumian et al. 2006). Kuempel *et al.* showed an increased neutrophil count found in coal miner's bronchoalveolar lavage fluid (BALF) (Kuempel et al. 2003).

The inflammation can be monitored by the influx of inflammatory cells, primarily macrophages and neutrophils, or by measuring markers such as proinflammatory cytokines (table 1.2) and total protein and LDH in the lung fluid after lavaging the lungs (Henderson et al. 1995).

**Table 1.2:** Inflammatory cytokines selected in the work

<b>Cytokine</b>	<b>Produced by</b>	<b>Actions/targets</b>
TNF- $\alpha$	Macrophages, NK cells, T cells, B cells, endothelial cells, astrocytes and smooth muscle cells	Local inflammation, macrophage activation, endothelial activation, vascular permeability
IL-1 $\beta$	Macrophages, epithelial cells, T cells and neutrophils	Fever, T-cell activation, macrophage activation, local tissue destruction
IL-6	T cells, macrophages, epithelial cells, monocytes and fibroblasts	T- and B-cell growth and differentiation, acute phase protein production, fever, immune response
IL-12	Dendritic cells and macrophages	T-cell activation, natural killer cell activation
IL-8	Macrophages, monocytes, T cells, neutrophils, fibroblasts, epithelial cells and endothelial cells	Neutrophil attractant
IFN- $\alpha$	Monocytes/ macrophages, lymphoblastoid cells and fibroblasts	Innate immune response against infection
IL-10	Monocytes and Lymphocytes	Inhibits the synthesis of pro-inflammatory cytokines

### **1.3.3. Alveolar Macrophages:**

Alveolar macrophages play a critical role in host immune system and unique among the pulmonary phagocytes. They constantly exposed to inhaled noxious particles and protect host organism. Alveolar macrophages defend the epithelial surface against outside environment (microbial and non-microbial particulates) (Kulkarni et al. 2006) and clear tissue debris/leukocytes and their products which could cause tissue damage (Sexton et al. 2004). Alveolar macrophages also actively participate in the initiation and regulation of innate and adaptive immune responses (Lohmann-Matthes et al. 1994) and produce enzymes involved in tissue remodelling and repair processes (Ding et al. 1988).

In 1905, Elie Metchnikoff reported about phagocytic mononuclear cells and their role in defence against certain bacterial infections (Metchnikoff 1905). Arguably, much earlier this same phenomenon (phagocytosis) was also observed by others, notably by Slavjansky in 1869 and William Osler, the latter looking at the pathology of miner's lung (Osler 1875). Later in the early 1960s, George Mackaness coined "macrophage activation" and reported that macrophages from mice infected with bacteria could initiate first line of defence against bacteria.(Mackaness 1962).

The macrophages exist throughout many of the tissue compartments of the major organs (Van Furth et al. 1972). For instance, alveolar macrophages in lungs, liver kuppfer cells, bone associated osteoclasts, nervous system microglia

and the peritoneal macrophages. The alveolar macrophages are typically large but can vary from 10-25  $\mu\text{m}$  in diameter (Van Furth et al. 1972) to anything upto 25-50  $\mu\text{m}$ . They have a nucleus that is round or kidney shaped, with a ruffled membrane and microvilli (Ross et al. 2002). The presence of large cytoplasmic vacuoles and large granules reflect their active phagocytic and metabolic activity (Ross et al. 2002).

The life span of lung macrophages has been estimated at approximately three months in humans and approximately 27 days in mice (Ross et al. 2002, van Oud Alblas et al. 1979). Alveolar macrophages continually replaced throughout adult life by the constitutive recruitment of macrophage precursors from the bone marrow via the blood stream (Van Furth et al. 1972, Ross et al. 2002, van Oud Alblas et al. 1979).

Surface area of human lung is very large and quantity of air breathed is approximately 15kg per day, on average, in a resting human. The lung is a very heterogeneous organ, consisting of 40 different cell types, each with unique morphological and functional characteristics (Crapo et al. 1982). Alveolar macrophage is one of the free cell populations which live on alveolar spaces and account for 5% of peripheral lung cells. During phagocytosis of nanoparticles, a number of active oxygen species are generated, which, can provoke harmful side effects and even cause injury to the lung (Timblin et al. 1999). The phagocytosis of nanoparticles can be affected by the physical-chemical

characteristics and source of the particle material. Inhaled nanoparticles can cause lung particle overload due to the inability of alveolar macrophages to recognize and/or clear particles of this size, leading to particle build up, chronic inflammation, fibrosis, and tumorigenesis (Borm et al. 2004). In rat model, chronic inhalation of poorly soluble nano particles can ultimately produced (Moore et al. 2000)lung tumours via an ‘overload’ mechanism (Moore et al. 2000).

Despite alveolar macrophages very slow in particle clearance, they are regarded as elite cells group in pulmonary immune system due to their effectiveness and high success rate in particle clearance. Macrophages represent a major share among all the other alveolar inflammatory cells. Microorganisms that were phagocytised, release vast number of toxic intracellular molecules, anti microbial proteins and peptides, lysozyme and also harmful chemically-reactive molecules such as hypochlorous acid, nitric oxide etc., (Reynolds et al. 1975). Pulmonary macrophages consist of receptors for antibodies and complement proteins role in defence against the bacterial insult.

Activated alveolar macrophage secrete pro inflammatory cytokines such as , interleukin (IL)-1 $\beta$ , tumor necrosis factor- $\alpha$  (TNF- $\alpha$ ) and interleukin (IL)- 6 and also release reactive oxygen species (Knaapen et al. 2009). Elevated levels of reactive oxygen species (ROS), lactate dehydrogenase (LDH), total protein, and albumin are observed in the lung after exposed to UF-CB and diesel exhaust

particles (DEP) (Iwai et al. 1997), (Ito et al. 2000), (Yang et al. 1999). Studies suggest that complex mixture of organic components on particles play a central role on alveolar macrophage activation (Castranova et al. 1985), (Jakab et al. 1990), (Hahon et al. 1982). For instance, diesel exhaust particles (DEP) induce macrophage respiratory burst and ultra fine carbon particles (UF-CB) triggers the release of tumor necrosis factor- $\alpha$  (TNF- $\alpha$ ) (Timblin et al. 2002). However, DEP have minimal effect on release of TNF- $\alpha$ , but, stimulate the release of other pro-inflammatory cytokines like interleukin (IL) -1 in both in *in vitro* and *in vivo* experiments (Yang et al. 1997), (Yang et al. 1999). Interestingly, when DEP was washed with methanol, diesel particles lost organic compounds and showed insignificant effect on interleukin (IL) -1 release (Yang et al. 1997).

Stimulated alveolar macrophages and the release of pro-inflammatory cytokines often seem to recruit neutrophils. At healthy conditions, neutrophils are almost absent in normal lung. In contrast, when particle or microbial load is high, alveolar macrophages activation occurs into alveolar spaces, following high levels of neutrophil infiltration (Delclaux et al. 2003). Studies suggested a close link between increased expression in alveolar macrophages of related cytokines and neutrophil recruitment (Bhatia et al. 2004). In addition, neutrophils itself actively involved in the inflammatory response via secretion of pro-inflammatory cytokines. In some cases, very high number of neutrophils and alveolar macrophages that are overloaded with insoluble so called nuisance

particles can lead to acute and chronic lung injury (Zhang et al. 1998). Sometimes, these persistent lung injuries and long term particle exposures may initiate lung tumours (Churg et al. 1999).

In summary, alveolar macrophages act in response to the usual day by day challenge of bacteria or particles entering the distant airways and are able to initiate an inflammatory response unless the microbial challenge is either too large or too virulent to be contained by the macrophages alone. Under such conditions, the alveolar macrophages stimulate pro inflammatory response (substances such as complement components, arachidonic acid metabolites such as leukotriene B<sub>4</sub>, and chemotactic peptides such as IL-8 and related chemokines) that trigger neutrophil infiltration into the alveolar spaces. (DiPersio et al. 1988).

#### **1.4. Health impacts of ultrafine particles:**

Epidemiological studies have provided the information regarding the potential health effects caused by particle matter. Animal toxicological studies, controlled human exposure studies, *in vitro* studies and epidemiological data identified various effects of particle matter and the effects varies in severity, duration and clinical significance of particle exposure to the individuals (Englert 2004);(Mage et al. 1999);(Costa et al. 1997). Identified and possible health effects of particle matter are mentioned on table 1.3.(Fullerton et al. 2009c)

#### 1.4.1. Nature of the effects:

The key health effects associated with PM include:

- Premature mortality.
- Prevalence of respiratory and cardiovascular disease (frequent hospital admissions and emergency room visits, school absences and work loss days).
- Altered in cardiovascular risk factors such as blood pressure, C-reactive protein or endothelial dysfunction.
- Altered in systemic blood markers.
- Altered in lung function and increased respiratory symptoms.
- Altered to lung tissues and structure.
- Altered respiratory defence mechanisms.

PM<sub>10</sub> associated health effects were confirmed in several epidemiological, *in vivo* and *in vitro* studies. Possible health effects are more severe and greater in subpopulations. Some of the studies that showed a definite association between particle matter and population groups are summarised in table 1.3. Some of these effects of particle matter are ranging from the the decreases in pulmonary function reported in children (Kulkarni et al. 2006); (Grigg 2009) to increased mortality reported in the elderly and in individuals with cardiopulmonary

disease (Pope III et al. 2004). High-risk subpopulations that may be affected by particle matter are listed below:

- Group of people suffering with respiratory disease such as COPD, acute bronchitis and cardiovascular disease such as ischemic heart disease (Chen et al. 2004).
- Group of people suffering with infectious respiratory disease such as pneumonia (Miller et al. 2000).
- Elderly people are also at high risk of premature mortality and hospitalisation for cardiopulmonary causes (Pekkanen et al. 2002).
- Children are at risk of increased respiratory symptoms and decreased lung function (Kaltoft et al. 2000a).
- Children and adults who are suffering from asthma are at risk of exacerbation of symptoms and increased need for medical attention (Rabe et al. 2004).

**Table 1.3:** Outline of epidemiological, *in vivo* and *in vitro* studies on the health effects of ultrafine particles:**Epidemiology:**

Study Description	Groups involved in the study	Possible Mechanisms	Particle used in study
Samet <i>et al.</i> , 2000 (Samet et al. 2000) found increased mortality and hospital admission are connected with increased PM <sub>10</sub> in majority of American cities and towns.	General population, Elderly	NA	PM <sub>10</sub>
Goldberg <i>et al.</i> , 2000 (Goldberg et al. 2000) assessed that PM <sub>2.5</sub> were linked with increased mortality from respiratory disease and diabetes. Individuals with no record of cardiovascular or pulmonary disease were at risk of mortality from particles.	General population to identify susceptible groups	NA	PM <sub>2.5</sub>
A Study conducted by Wichmann <i>et al.</i> , 2000 in Germany, found that ultrafine (< 0.1 µm) and fine particles (0.1–2.5 µm) were connected with high mortality.	General population	NA	ultrafine and fine particles

A study conducted on particulate matter and deaths and hospital admissions in elderly patients, revealed definite association was observed with fine particles. But no association found with the larger particles (Lippmann et al. 2000) .	General population, Elderly	NA	PM <sub>2.5</sub> , PM <sub>10</sub>
A study on the individuals with no known history of cardiac related disease, showed no effect of particle matter. This implies that normal healthy individuals are not at high risk (Pekkanen et al. 2002).	General population	NA	PM <sub>2.5</sub> , PM <sub>10</sub>

### Human Controlled Exposure:

Study Description	Groups Studied	Possible Mechanisms	Particle Aspects
Bronchial biopsy tissue that were taken from healthy and asthmatic individuals who are exposed to diesel exhaust particle and concentrated ambient particles (CAPs) showed the increased levels of inflammatory markers in healthy people and also in asthmatic patients (Holgate et al. 2003).	Healthy, asthma	Inflammation	Diesel, CAPs

***in Vivo and in Vitro Exposures:***

<b>Study Description</b>	<b>Groups Studied</b>	<b>Possible Mechanisms</b>	<b>Particle Aspects</b>
Short term inhalation of ultrafine carbon and platinum particles proved higher inflammatory response in the mice and rats suffering with respiratory diseases. No inflammatory response observed in healthy animals (Oberdörster 2000).	Rodents: Pulmonary disease, healthy young, healthy old	Inflammation	Ultrafine carbon, platinum
In healthy dogs, inhalation of concentrated ambient particles (CAPs) showed the association with temporary induced heat condition and increased levels of inflammatory markers (Godleski et al. 2000).	Dogs: Healthy, cardiac condition	Nervous system control of heart	CAPs
Inhalation of particle matter showed increased levels of blood pressure and vascular factors in healthy rats (Vincent et al. 2001).	Rats: Healthy	Vascular	Urban PM, washed PM, diesel exhaust, carbon
Concentrated ambient particles collected on filters induced alveolar macrophage cytokine production <i>in vitro</i> . Moderate levels of inflammation found in airways in healthy and asthmatic mice (Kobzik et al. 2001).	Mice: Healthy young, “asthmatic” young	Inflammation	CAPs

Prolonged inhalation of nickel particles involved in the coding of surfactant-associated protein B and transforming growth factors (Leikauf et al. 2001).	Mice: Susceptibility to death from continuously inhaled nickel	Lung injury or inflammation or both	Nickel
Healthy and hypertensive rats and guinea pigs with heart conditions didn't show any form of inflammatory changes after these animals exposed to concentrated ambient particles (Gordon et al. 2000).	Rats: Hypertensive; Guinea pigs: Cardiac condition	Cardiac	CAPs

## 1.5: *Streptococcus pneumoniae*: The pneumococcus

### 1.5.1. Introduction:

*Streptococcus pneumoniae* (the pneumococcus) is a Gram-positive, encapsulated, haemolytic, coccus of approximately 1 µm in length (Bannister et al. 2000); (Kaltoft et al. 2000a); (Kamerling 2000) (Figure 1.9). The *Streptococcus* genus comprises over 250 species, which include several known human pathogens. *S. pneumoniae* was first isolated more than 120 years ago (Sternberg et al. 1881), yet today *S. pneumoniae* remains a major cause of morbidity and mortality in both the developing and developed worlds (Lesinski et al. 2001). It is the causative agent of many types of infectious disease, including pneumonia, septicaemia, meningitis and otitis media (Magee et al. 2001). This important pathogen has a significant impact in public health, as cases of invasive pneumococcal diseases (IPD) are substantially high, especially in developing countries and in individuals predisposed to infection, e.g. elderly, young, diabetic, asplenic, immune compromised persons (i.e. those with impaired IgG synthesis, impaired phagocytosis, or defective clearance of pneumococci).

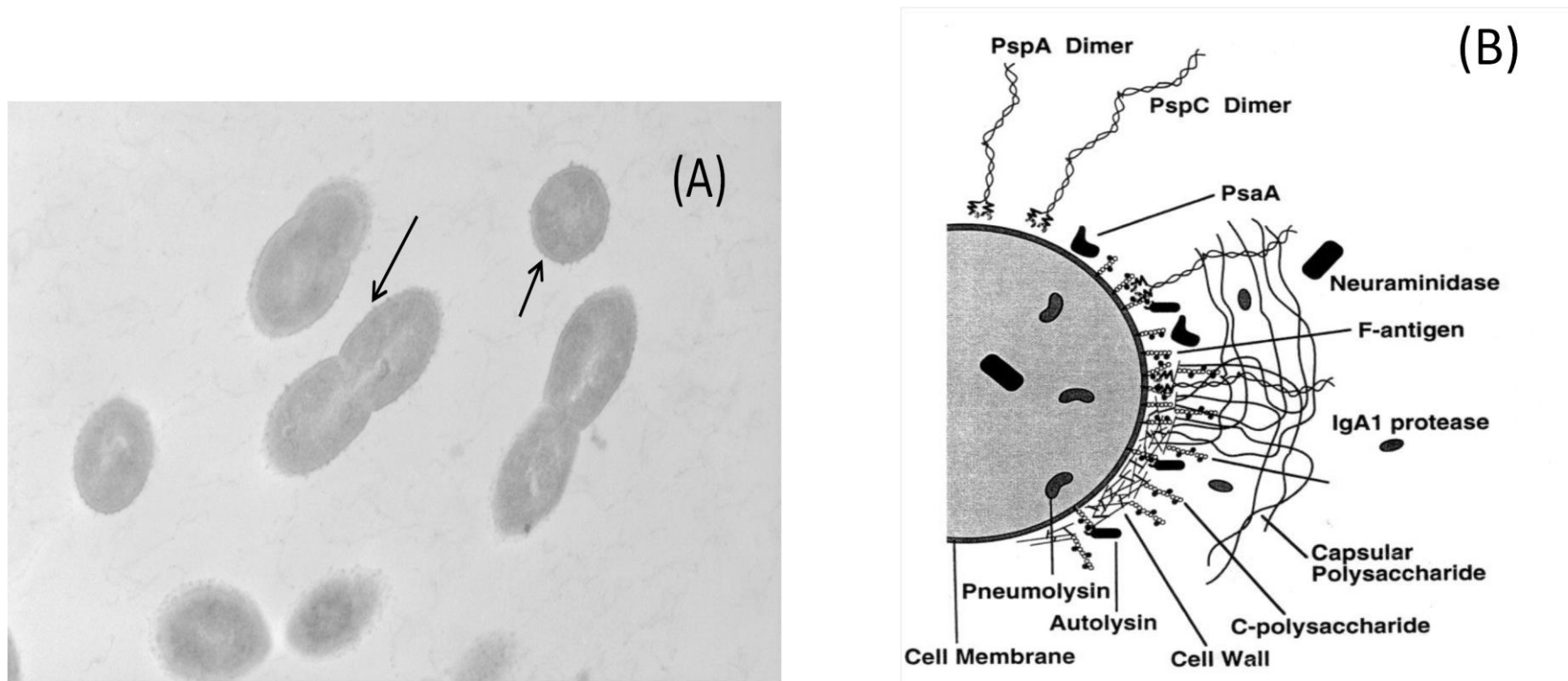


**Figure 1.9:** (A) The structure of *Streptococcus pneumoniae*. A chain of an encapsulated strain of *S. pneumoniae*. The arrow identifies the capsular polysaccharide (the low-density layer enveloping the bacterium). (B) The surface components and virulence factors of *S. pneumoniae*. A diagrammatic representation of *S. pneumoniae* depicting several surface components for which roles in virulence and/or elicitation of protection have been established (Briles et al. 2000).

There are currently over 90 chemically distinct capsular types (Henrichsen 1995), although not all of them cause severe infections. Differences in the composition of the capsular nature is thought to be accountable for the variation in virulence (Kamerling 2000) ( Figure 1.9).

There are two different nomenclature systems for the pneumococcal serotypes, one is the Danish system and other one is the American system (Kamerling 2000). In the American system serotypes are numbered sequentially, based on the order of discovery of pneumococcus. The alternative Danish system classifies serotypes based on cross-reaction between the serotypes, so that serologically cross-reactive types are assigned to a common serogroup (Kamerling 2000). For instance, *Streptococcus pneumoniae* D39 strain used mainly in this thesis, named according to the Danish system. The serotyping technique, known as the Quellung (Neufeld) reaction, causes pneumococci to appear to swell in the presence of specific antiserum (Heineman et al. 1973). The Quellung reaction can be used to conduct epidemiological studies to confirm certain serotypes to their diseases.

### **1.5.2. Colonisation:**

Like many microorganisms, carriage plays an important role in the pneumococcal disease. The nasopharynx is an ideal location for the pneumococcus to spread from one to another individuals (by droplet secretions) (Barthelson et al. 1998). The pneumococcus is commonly isolated from the human nasopharynx where asymptomatic colonisation can even occur

immediately after birth (Austrian 1986). The scale of colonisation can differ between individuals, although up to 40 % of the general population are thought to carry it in small numbers (Austrian 1997); (Tuomanen 1999). Studies have shown that as many as four different capsular serotypes may be carried simultaneously during childhood (Tuomanen 1999). Colonisation is therefore influenced by the individual's exposure to one or more of the 90 pneumococcal types. However, if an individual develops antibodies to a particular serotype after colonisation this does not eliminate the carrier state. In contrast, individuals that develop antibody to a given pneumococcal capsular type prior to colonisation are half as likely to be colonised with that serotype (MacLeod et al. 1945).

### **1.5.3: Disease:**

The diseases caused by *S. pneumoniae* are a major cause of morbidity and mortality throughout the world (Gilbert et al. 2000). Table 1.4 shows a summary of the incidence of IPD worldwide and in the United States.

**Table 1.4:** The Annual Incidence of Pneumococcal disease (KLEIN 1999)

---

**I. Worldwide**

## A. Pneumonia

1. Estimated number of cases: 20, 000, 000
2. Estimated number of deaths: 1, 050, 000

## B. Meningitis

1. Estimated number of deaths: 75, 000

## C. Total pneumococcal deaths: 1, 125, 000

(9 % of all childhood deaths)

**II. United States**

A. Pneumonia - estimated number of cases 500, 000

B. Meningitis - estimated number of cases 3, 000

C. Bacteraemia - estimated number of cases 50, 000

D. Otitis Media - estimated number of cases 7, 000, 000

---

**1.5.4: Age**

The World Health Organization estimates that at least 1.2 million children die of pneumococcal disease each year. In developing countries Pneumonia is the main cause of death in young children and overall diseases caused by *S. pneumoniae* account for 30 % of deaths in children less than 5 years old (Lesinski et al. 2001). In Europe, it is estimated that the pneumococcus is responsible for 25 % to 50 % of bacterial meningitis in children (Noah et al. 2001) and in the USA cases of invasive pneumococcal disease, including

meningitis and bacteraemia, are estimated to be as high as 160 cases per 100,000 in children less than two years of age (Advisory Committee on Immunization Practices 1997).

As shown in Figure 1.10, the number of IPD cases in infants can vary by age. A study performed on 806 invasive pneumococcal isolates from Danish children aged between 0 - 23 months during 1981 - 1999 showed that children were most at risk of developing pneumococcal meningitis at 10.2 months old, and bacteraemia at 15.9 months old (Kaltoft et al. 2000a). In the UK, epidemiological data during 1996 - 1998 showed that the incidence of invasive and other pneumococcal disease was highest among children during the first year of life (Sleeman et al. 2001).

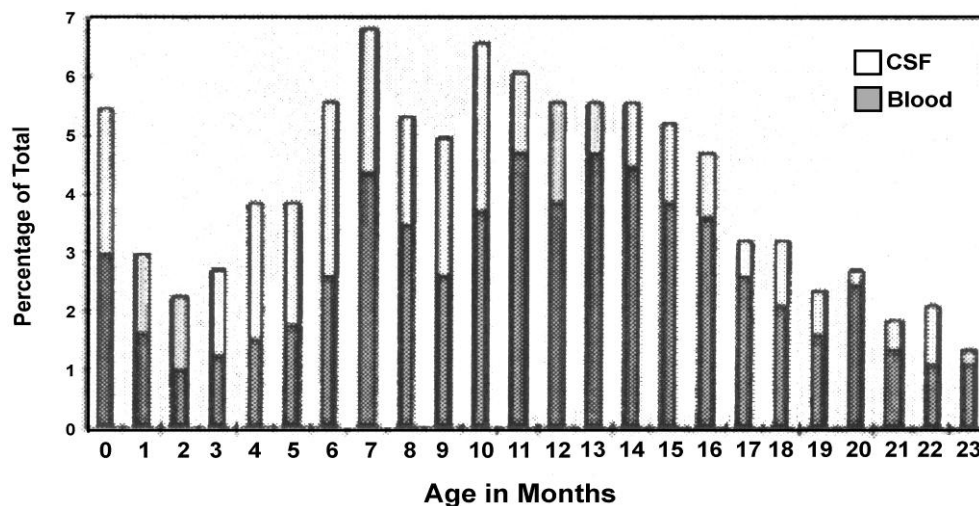


**Figure 1.10:** Age distribution of invasive pneumococcal isolates from Danish children ages 0-23 months during the period 1981-1999. (Kaltoft et al. 2000b).

High-risk subpopulations that may be affected by particle matter, also seems to correlate with age group that is affected by pneumococcal infections. Old age is also a risk factor for infection, although the reason for this is not as well understood as for infants (Artz et al. 2003). Reported annual incidences of IPD among the elderly in North America and Europe range from 25 to 90 cases/100 000 persons (Butler and Schuchat 1999). Mortality caused by pneumococcal infections is highest among those aged >65, with nearly 20 % cases resulting in death (Butler et al. 1999). This has been shown to rise to as much as 40 % for those aged 85 years or older (Artz et al. 2003). This threatens to become a critical public health issue, since the elderly population is expected to triple by 2050 (Artz et al. 2003).

#### **1.5.5: Time**

The distribution of specific serotypes implicated in disease can also vary with time. During the winter months the number of cases of pneumococcal disease has been shown to increase. This is thought to be because pneumococci are usually transmitted by droplet secretions, from person to person (O'BRIEN et al. 2003) and during these months the course of other respiratory infections and secretions, coughing and sneezing are increased (Kaltoft et al. 2000b). Kaltoft and colleagues investigated the seasonal distribution of 777 episodes of pneumococcal bacteraemia and 346 episodes of pneumococcal meningitis in Danish children aged 0 - 6 years old during 1981 – 1999. They found that there were significantly fewer episodes of invasive pneumococcal infections during

the summer months (June, July and August) when respiratory infections overall are low compared with the rest of the year (Kaltoft et al. 2000b).

### **1.5.6: Geography:**

The incidence of IPD can also vary geographically. There is an unequal distribution of pneumococcal serotypes causing disease throughout the world. For example, in Europe, the literature cited suggests that Italy has the lowest incidence with 1.1 reported cases per 100 000 population (Principi et al. 2000) and Greece has the highest incidence with 100/100 000 (Syriopoulou et al. 2000). Denmark and the UK have 16.8/100 000 (Kaltoft et al. 2000b) and 6.6/100 000 (Miller et al. 2000) reported cases of IPD respectively. The incidence and differences in the prominent serogroups isolated from children less than 5 years old are illustrated in Table 1.9.

These differences are thought to be due to the location of particular ethnic backgrounds. For example, persons in certain racial groups, including African-Americans, American Indians, Native Alaskans and Australian Aborigines, have all been shown to have an increased risk of disease (Butler et al. 1999). A person's socio-economic status is also said to be a risk factor (Butler et al. 1999). Alternatively, these differences could be due to the differences in carriage, and the virulence of the predominant serotypes, since different capsular serotypes are known to differ in virulence. Serotype 3, for example, requires  $10^5$  cfu to kill 50 % of mice and rats, whereas serotype 37, which

possesses a capsule composed of similar sugars and is the same size as serotype 3, requires  $10^7$  cfu to cause the same effect (Knecht et al. 1970). A 10-year (1952 - 1962) study at a New York medical centre showed that 56 % of all deaths due to pneumococcal pneumonia were only caused by six serotypes (Austrian et al. 1964).

## **1.6. Pulmonary Defence Mechanisms:**

Every day the pulmonary epithelial surface is exposed to thousands of litres of air for oxygen intake. In the process of the oxygen intake for the body, the lung is exposed to a multitude of foreign particles, toxic gases and microorganisms transported with the inhaled air (Areskoug et al. 2000). Some of these foreign particles are potentially injurious; others are relatively harmless. These unknown particles must be removed from the lung before they enter into the gas exchange region (Lohmann-Matthes et al. 1994).

Protection against the inhaled foreign material is a complex process. It involves a series of overlapping exclusion barriers that include filtration in the nose, the maintenance of tight junctions between epithelial cells, and the operation of the mucociliary system and phagocytic cells present in pulmonary epithelial lining. Several components are involved in this protective mechanisms (Nicod 1999). Each component of these protective mechanisms appears to have a distinct role as well as interacting with the other components. Schematically, the protective

mechanism of the lung defence can be divided into four different categories.

They are listed below:

1. Physical or Anatomic factors
2. Antimicrobial peptides
3. Phagocytic and inflammatory cells
4. Adaptive immune responses

### **1.6.1. Physical or Anatomic factors:**

Several factors may influence the deposition and the physical clearance of particles. Significant factors include particle size, cough and mucociliary transport.

#### **Particle size:**

Particle size plays an important role in particle deposition in the respiratory system and the likelihood of a particle access to the distal parenchyma. If the inhaled particle size is greater than 10  $\mu\text{m}$ , it is most likely to be deposited in the upper airway, for example, in the nose. Particles between 5 to 10  $\mu\text{m}$  tend to be deposited in the lower part of the upper airway, usually in the trachea or the bronchi (Lohmann-Matthes et al. 1994). Particles most likely to reach the distal lung parenchyma range in size from 0.5  $\mu\text{m}$  to 5  $\mu\text{m}$ . Many bacteria also fall within 0.5  $\mu\text{m}$  to 5  $\mu\text{m}$  size range. Smaller particles (between 10nm and 1  $\mu\text{m}$ )

are more likely to be deposited in the alveolar region of the lungs (respiratory bronchioles, alveolar ducts, alveolar sacs and alveoli)(Mohanraj et al. 2006).

**Cough:**

A cough is explained as a very deep breath, followed by a forced expiration against a closed glottis, which opens suddenly to produce the expulsive phase. This allows enough force to be produced in the major bronchi and trachea to expel material such as debris, infected mucus or products of epithelial damage. Cough is considered as an important protective mechanism and effectively clears irritating foreign material from the airways. Likewise, sneezing is an involuntary response to irritation of the nasal sinuses, which results in the forcible expulsion of air through the nostrils (Irwin et al. 1998).

**Mucociliary transport:**

Mucociliary transport or mucociliary clearance is classically explained as a wave pattern of beating cilia moving along with a layer of mucus (which traps foreign material) progressively upward along with the trachea-bronchial tree. Mucociliary epithelial cell lining is found from the trachea down to the respiratory bronchioles, projecting into the airway lumen. The structure of cilia is identical to that of cilia found elsewhere in the rest of the body. Interestingly, the cilia movement on a particular cell and the movement between cells are well coordinated, that produces actual “waves” of ciliary motion (estimated speed of 6 to 20 mm/min in the trachea)(Widdicombe et al. 1997).

There are two layers that make up the mucous blanket on the surface of these epithelial cells. One is known as the ‘sol’ layer and the other as the ‘gel’ layer’. The aqueous sol layer is in direct contact with the epithelial cells and contains a number of molecules that are part of the innate immune system. On the surface of the sol layer, there is the more viscous gel layer. Gel layer is formed by both submucosal mucous glands and goblet cells. Inhaled particles that are trapped in the mucous gel layer are escalated upward and eventually either expectorated or swallowed (Cross et al. 1994).

### **1.6.2. Antimicrobial peptides:**

Lung innate immune system is composed of small molecules and many proteins that protect the lungs from inhaled particles. These proteins provide an effective front-line defence through recognition structures and stimulate a further host immune response. Innate immune cells such as alveolar macrophages, neutrophils and dendritic cells, use pattern recognition molecules to bind microorganisms. Pattern-recognition molecules can be present in secretions and the circulation in soluble form, such as mannan-binding lectin (MBL), or they can be transmembrane molecules that mediate direct cellular responses to microbial exposure. Amongst these molecules are lysozyme, lactoferrin, defensins, and collectins (surfactant protein A [SP-A] and surfactant protein D [SP-D]) (Bals 2000).

**Lysozyme:**

(Ganz 2002) Lysozyme is an antimicrobial polypeptide that can be found in respiratory tract secretions. Lysozyme is secreted on to epithelial surfaces and is synthesised in the primary and secondary granules of neutrophils, as well as the granules of mononuclear phagocytes (Herbert et al. 2007). Lysozyme damages the cell walls of bacteria and fungi by hydrolyzing the  $\beta$ 1–4 glycosidic bonds between N-acetylmuramic acid and N-acetylglucosamine, which are structural components of bacterial peptidoglycan and fungal chitin, (Ganz 2002). The activity of lysozymal activity is more effective against gram-positive than gram-negative bacteria.

**Lactoferrin:**

Lactoferrin is mainly found in neutrophilic granules, serous cells and mammalian milk. It is also present in airway fluid. Lactoferrin plays an important role in producing neutrophil superoxide and increasing neutrophil adherence. Lactoferrin also has antimicrobial activity. It binds to bacteria through recognition of the carbohydrate portion of the microbial cell surface and blocks iron absorption (by the bacteria); as iron is essential for bacterial metabolism, this inhibits their growth and multiplication (Orsi 2004).

**Defensins:(Boyton et al. 2002)**

Defensins are small, arginine-rich cationic peptides that are found in stimulated pulmonary neutrophils. Defensins are divided into two important families, the  $\alpha$ -defensins and the  $\beta$ -defensins(Boyton et al. 2002). Neutrophil defensins are antimicrobial peptides and play a crucial role in the regulation of inflammatory and immunological processes. Unlike lysozyme, defensins show antimicrobial activity against both gram-positive and gram-negative organisms(Mizgerd 2008).

**Collectins:**

The collectin family of proteins include MBL, lung surfactant protein A (SP-A) and D (SP-D), bovine conglutinin and collectin-43 (CL-43). SP-A and SP-D initiate the first line of innate immune response (macrophages, neutrophils etc.) after recognising microorganisms and help to secrete pro-inflammatory mediators(Kingma et al. 2006). Since the lungs are repeatedly exposed to ambient air that contains significant numbers of microorganisms, the roles of SP-A and SP-D in the innate immune systems of the lung are crucial in lung defence (LeVine et al. 2000).

**1.6.3. Phagocytic and inflammatory cells:**

Pulmonary alveolar macrophages, dendritic cells, polymorphonuclear leukocytes and natural killer cells are the major phagocytic and resident inflammatory cells in the lung (Hance 1993).

**Pulmonary alveolar macrophages:**

Lung alveolar macrophages are large compared to other inflammatory cells (15-50  $\mu\text{m}$  in diameter). They derived from bone marrow progenitor cells and mostly live on the alveolar epithelium (Lambrecht 2006). Alveolar macrophages contain a wide variety of digestive enzymes that can organise the disposal of phagocytised foreign material. Pulmonary alveolar macrophages also play an important role in killing microorganisms that have reached the lower respiratory tract by releasing chemoattractant cytokines (chemokines) that recruit other inflammatory cells such as neutrophils and natural killer cells (Martin et al. 2005).

Particle size and composition of coating material play main role in the uptake of particles by alveolar macrophages. Particle of 1-3  $\mu\text{m}$  in diameter are more easily engulfed than those of 6  $\mu\text{m}$  by macrophages. However, very small particles with sizes of less than 0.26  $\mu\text{m}$  in diameter can escape macrophage phagocytosis. These small particles can reach deeper regions of alveoli and

translocated to in secondary organs such as liver, spleen, kidneys, brain and heart.(Chono et al. 2007).

**Dendritic cells:**

Like alveolar macrophages, dendritic cells are found throughout the lung (airways, lung interstitium etc.) and are derived from bone marrow cells. Dendritic cells can initiate the pulmonary immune response after they recognize inhaled particles through expression of ancient pattern-recognition receptors such as Toll-like receptors, NOD-like receptors, and C-type lectin receptors(Lambrecht et al. 2001). Dendritic cells are responsible for phagocytosis, processing of antigens, and then migrate to regional lymph nodes. In the lymph nodes, dendritic cells present antigen to T cells, an important step for the later immunologic defence provided by lymphocytes. In addition, lung dendritic cells have receptors for inflammatory mediators that are released upon damage to the tissues by pathogens or foreign particles (Geissmann et al. 2010).

**Polymorphonuclear leukocytes :**

Polymorphonuclear leukocytes (PMN) are very important in lung defence mechanism against microorganisms and particles present in inhaled air. In general, there are fewer PMNs resident in airways and alveoli when compared to other inflammatory cells (Sibille et al. 1990a). However, when bacteria overcome other defence mechanisms, PMNs play a prominent role by

colonising the alveolar spaces. These cells possibly are drawn to the lung by complement activation and chemotactic factors that are released by alveolar macrophages. Polymorphonuclear leukocyte granules have several antimicrobial substances, including defensins, lysozyme, and lactoferrin. Like other inflammatory cells, PMNs play an important role in killing microorganisms by phagocytosis (Zhang et al. 2000).

### **Natural killer cells:**

Natural killer (NK) cells are innate lymphocytes and provide a first line of defence against pathogens (mainly viruses). Natural killer (NK) cells are also able to detect and kill some cancer cells. NK cells make up 10% of resident lymphocytes in the lung and activate cytokines, particularly IFN- $\gamma$ . NK cells share the characteristic of lacking surface markers with T lymphocyte and B lymphocyte (Cooper et al. 2001).

### **1.6.4. Adaptive immune responses:**

The adaptive immune system, which is composed of T and B lymphocytes, is very specialized and antigen-dependent (Curtis 2005). The two major components of the adaptive immune system are B-lymphocytes (humoral immunity) and T-lymphocytes (cellular immunity) (Curtis 2005).

**T-lymphocytes:**

T cells (thymus-dependent) have an astonishing ability to initiate, amplify, and terminate antigen-specific immune responses. The important role of T cells is the ability to interact with populations of antigen-presenting cells and effector cells.

Depending on cell surface markers and functional characteristics, T cells are categorised into two different cell types. One type consists of cells that are positive for the CD4 surface marker, commonly called CD4<sup>+</sup> or helper T cells (Moore et al. 2001). CD4<sup>+</sup> cells are further divided into T<sub>H</sub>1 and T<sub>H</sub>2 subsets, which are important in cellular immune defence and allergic inflammation. The second type of T cells is positive for CD8 surface marker. In turn, CD8<sup>+</sup> cells include suppressor and cytotoxic T cells. Both cell types are able to release a variety of cytokines that interact with other components of the immune system, particularly B lymphocytes and macrophages (Kawakami 2004).

**B-Lymphocytes:**

B-Lymphocytes are the major components of humoral immunity and each B-lymphocyte recognizes specifically one particular antigen. Antigen-activated B-cells can multiply, and develop into plasma cells that secrete immunoglobulins,

and finally they convert into memory cells. Activated B-cells secrete two major types of immunoglobulins, which are IgA and IgG(LeBien et al. 2008).

IgA plays an important role in protection against viruses and bacteria and is present in the nasopharynx and upper airways. IgA bind to antigens of microorganisms and prevents their attachment to epithelial cells. IgA also has the ability of agglutinating microorganisms; the agglutinated microbes are more easily cleared by the mucociliary transport system (Monteiro 2010).

Unlike IgA, IgG is found in the lower respiratory tract. It has a number of defence properties such as neutralising viruses and bacterial toxins, agglutinating microorganisms, opsonising bacteria, causing lysis of gram-negative bacteria and activating the complement system(Sibille et al. 1990b).

In conclusion, the humoral immune system shows many important biological properties that include protecting the lung against a variety of bacterial and viral infections.

## **1.7. Association between ultrafine particles and vulnerability to infection:**

In developing countries, nearly 90 % of rural households, until today use biomass fuels such as firewood, animal dung and dry crop for cooking and heating (Bruce et al. 2000b). Though wood is regarded as most commonly used

for fuel, sources like animal dung and crop residues are also widely used in rural household areas (de Koning et al. 1985). On a typical day, in developing countries people exposed to as many as 3-7 hours of bio mass particles. In some cases, exposed times can reach up to 24 hours a day during winter months or in mountain areas (Chen et al. 1990). Traditionally, in developing countries, women involved majorly in cooking than men so that women exposed substantially higher to biomass particles. Also, mothers often carry young children less than five years on their back which cooking and therefore young children also quite often exposed to biomass smoke (Bruce et al. 2000b). Particles that released from indoor air pollution make young children more vulnerable to respiratory illness and bacterial pneumonia (Bruce et al. 2000b). Even though women rarely smoke cigarettes and outdoor pollution is limited to city environment, in rural areas women and children frequently admitted in the hospitals due to respiratory illness (World Health Organization 2000). Poor ventilation causes a rise in indoor air particulates between 500 to 100,000  $\mu\text{g}/\text{m}^3$ , which is 20 times greater than pollutant concentrations caused by cigarette smoking (Pandey et al. 1989). Acute respiratory infections (ARI) are accountable for nearly a third of all deaths in children under 5 years old. In worldwide, between 1997 and 1999, acute lower respiratory infections caused nearly up to 4 million deaths. Studies show that, infant girls in Gambia who been carried on back by their mothers suffered with more respiratory infections

(ARMSTRONG et al. 1991). In Zimbabwe, children admitted more frequently in hospitals from homes where wood was used for cooking fuel (Collings et al. 1990). Due to the high levels of indoor wood smoke pollutants, 18% of non-smoking women reported with chronic bronchitis and more than 30 % of women over 50 years of age reported with COPD in Kashmir (Chen et al. 1990).

Therefore there is a strong connection between pollution particle and respiratory infection. Individuals, who are already suffering with respiratory disease, will face a greater risk when they exposed to the particle matter. Recent investigations in asthma in younger children also concluded that air pollution can increase the morbidity in children with pre-existing asthma. Wordley *et al.* showed the association between particle matter and respiratory diseases in Birmingham, UK . Hospital admissions for asthma, bronchitis, all respiratory disease, and pneumonia all showed significant associations with PM<sub>10</sub> concentrations (Wordley et al. 1997). Same effect has found in hospitals in Rome that the cases connected with air pollution and respiratory illnesses rose over three years. Similarly, rise in carbon monoxide levels linked to rise in hospital admissions of asthma (5.5% increase) and COPD (4.3% increase) (Fusco et al. 2001).

In conclusion, it is confirmed that there is a relation between indoor or outdoor pollutions and respiratory diseases in younger children and adults. Most of the

studies mentioned earlier are concentrated mainly on clinical data that derived from their respective work. However, effects of particulate matter in the presence or absence of infection is little understood. Therefore, it is important to evaluate the role of infection model and asses the mechanism after exposed to particle matter.

## 1.8. Thesis Aims:

1. The lung response to inhaled particulates both *in vivo* and *in vitro*.
2. To assess the mechanism for an association between high levels of carbonaceous particulates and acute respiratory infection in animal model.
3. To develop an air-tissue interface model to assess DNA damage to airway macrophages due to inhalation of three (iron, gold, and silver) different engineered metal nanoparticles.





# Chapter 2 Methods and Materials

## 2.1 General Information:

### 2.1.1. Solutions

#### Blood Agar Base (BAB):

Blood Agar Base            4.0% (w/v)  
autoclaved

#### Blood Agar (BA):

Blood Agar Base was autoclaved\* and cooled down to ~48° C.  
Defibrinated horse blood (Oxoid) added 5% (v/v) to the warm BAB.

#### Serum broth:

BHI    80% (v/v)  
Foetal Calf Serum (filtered sterilised)    20% (v/v)

#### Brain Heart Infusion (BHI):

Brain Heart Infusion    3.7% (w/v)  
Autoclaved\*

#### PBS (pH 7.4):

137mM NaCl  
2.7mM KCl  
4.3mM Na<sub>2</sub>HPO<sub>4</sub>  
1.4mM KH<sub>2</sub>PO<sub>4</sub>  
Autoclaved\*

#### Lysis buffer (pH 10):

100 mM disodium EDTA  
2.5MNaCl  
10 mMTris-HCl  
1% triton X-100 (v/v) added fresh to the coplin jar.

**Alkaline buffer( pH  $\geq$  13):**

300 mM NaOH  
1mM disodium EDTA

**Neutralisation buffer (pH 7.5):**

0.4 M Tris-HCl

**RPMI (10% FCS):**

1% non-essential amino-acids  
1% Glutamine  
2% Penicillin and Streptomycin  
10% FCS  
1% Sodium pyruvate

**Freezing media:**

60% RPMI media  
10% DMSO  
30% FBS

\* Whenever autoclaving was required, this was performed at 121°C for 15 minutes at 1.5bar pressure.

## **2.1.2. Suppliers**

### **Andor Technology Plc**

Springvale Business Park  
7 Millennium Way, Belfast,  
County Antrim, BT12 7AL  
[www.andor.com](http://www.andor.com)

### **Becton Dickinson**

21 Between Towns Road, Cowley, Oxford,  
OX4 3LY, UK.  
[www.bdeurope.com](http://www.bdeurope.com)

### **Dako**

Denmark House,  
Angel Drive, Ely, CB7 4ET, UK.  
[www.dako.co.uk](http://www.dako.co.uk)

### **Elstree Ltd**

Borehamwood,  
Hertfordshire  
WD6 3SZ, UK

### **Fisher Scientific**

Bishop Meadow Rd,  
Loughborough, LE11 5RG, UK.  
[www.fisher.co.uk](http://www.fisher.co.uk)

### **GE Healthcare**

Amersham Place,  
Little Chalfont, HP7 9NA, UK.  
[www.amershambiosciences.com](http://www.amershambiosciences.com)

### **Invitrogen**

Inchinnan Business Park,  
3 Fountain Drive, Paisley,  
PA4 9RF, UK.  
[www.invitrogen.com](http://www.invitrogen.com)

### **Inficon Holding AG**

Two Technology Place  
East Syracuse, New York  
13057 USA  
[www.inficon.com](http://www.inficon.com)

### **Medion Diagnostics International Inc.**

7440 SW 50 Terrace  
Suite 110  
Miami, FL 33155  
[www.mediondiagnostics.us](http://www.mediondiagnostics.us)

### **Meso Scale Discovery**

9238 Gaither Road  
Gaithersburg, MD 20877 USA  
[www.mesoscale.com](http://www.mesoscale.com)

### **Nunc Brand**

Supplied by Fisher Scientific

### **Oxoid Limited**

Wade Road,  
Basingstoke  
Hampshire RG24 8PW.  
[www.oxoid.com](http://www.oxoid.com)

### **Reichert Analytical Instruments**

3362 Walden Ave.  
Depew, NY 14043 USA  
[www.reichertai.com](http://www.reichertai.com)

### **Sigma Aldrich**

The Old Brickyard,  
New Road, Gillingham,  
SP8 4XT, UK.  
[www.sigmaaldrich.com](http://www.sigmaaldrich.com)

### **Shandon Instruments**

Supplied by Fisher Scientific.

### **Vector Laboratories**

3 Accent Park,  
Bakewell Road, Peterborough  
PE2 6XS, UK.  
[www.vectorlabs.com](http://www.vectorlabs.com)

### **VWR International**

Hunter Boulevard,  
Magna Park, Lutterworth,  
LE17 4XN, UK.  
[uk.vwr.com](http://uk.vwr.com)

### **2.1.3. Preparation of Blood Agar (BA) plates:**

Single vent Petri dishes (90 mm) were used to prepare the blood agar plates (see section 2.1.1 for media composition). BA was melted and left to cool to ~48°C. The agar was poured into the Petri dishes (~15ml) and left to set at room temperature (Isenberg 1998).

### **2.1.4. Culturing *Streptococcus pneumoniae*:**

For pneumococci culture in broth, the container was tightly closed and incubated at 37°C for the required amount of time. For Anaerobic pneumococcal culture, BA plates or flasks inoculated with pneumococci were placed in anaerobic jars (BBL GasPack system) and a lighted candle was placed inside the jar before closing it tightly and incubating at 37°C overnight. This system produces ~5% CO<sub>2</sub> (Isenberg 1998).

## **2.2. Particle preparation:**

Ultrafine carbon black particles (UF-CB) (Printex 90, 14 nm diameter) (Degussa, Frankfurt, Germany), were obtained as a kind gift from Professor Ken Donaldson. Particles had been baked in a dry oven set at 160°C for 8 hours to avoid the possible endotoxin contamination (Wilson et al. 2001) .

To achieve high particle overloading in alveolar macrophages and homogeneous mixing of PBS and ultrafine particles, 500 µg/50 µl particles in sterile PBS was used in this study. In my preliminary experiments, less than 500

$\mu\text{g}$  of particles in  $50\ \mu\text{l}$  of sterile PBS didn't achieve particle overloading. Likewise, more than  $500\ \mu\text{g}$  of particles in  $50\ \mu\text{l}$  of sterile PBS made mice very difficult to breath. To make UF-CB solution, carbon black was added to sterile PBS at  $500\ \mu\text{g}/50\ \mu\text{l}$  concentration and sonicated 5 times (each time for 30s with 10 secs gap) using the sonication probe. Repeated vortexing was followed by sonication until the solution was used for the experiments *in vivo* (Li et al. 1999a) (Figure 2.1).

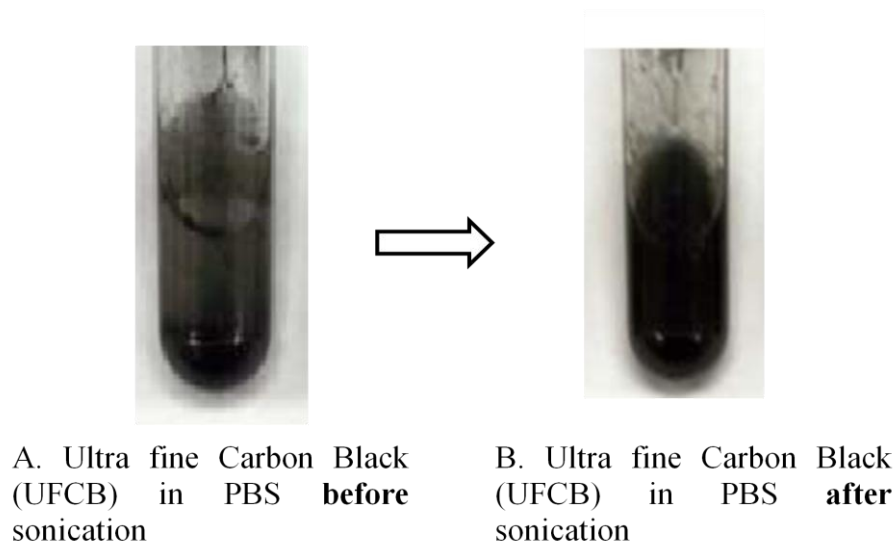


**Figure 2.1:** Ultra fine carbon black ( UF-CB) (  $500\ \mu\text{g}/50\ \mu\text{l}$ ) diluted in sterile PBS (A) and sonicated for 5 times (each time for 30s with 10 secs gap) to achieve good homogeneous mixing. This picture clearly illustrates that the particle aggregates were achieved good homogeneous mixing.

## 2.3. Bacterial stock preparation:

*Streptococcus pneumoniae* serotype D39 strain was received from the frozen stocks of Lab 227, Department of Infection, Immunity and Inflammation, University of Leicester, UK. *S.pneumoniae* was tested and confirmed with optochin sensitivity test. Sterile Optochins (ethyl hydrocuprein hydrochloride) inhibits the pneumococcal growth whereas other streptococci show good growth or a very small zone of inhibition.(Bowers et al. ).

*S. pneumoniae* was cultured overnight in 10 ml of Brain Heart Infusion (BHI) (Oxoid, Basingstoke, Hants, UK; product BO0366) broth at 37°C. On following day, the culture was centrifuged at 1500g for 15 mins and the pellet was suspended in BHI serum broth. A part of this (700 µl) was added to fresh BHI serum broth and the OD<sub>500</sub> was checked to confirm that it was 0.70. The cultures were incubated at 37°C for 5 hours. Subsequently the OD<sub>500</sub> was checked to see if it had reached 1.6, and 500 µl aliquots were prepared and frozen at -70° C.

### 2.3.1. Dose confirmation:

Dose was confirmed by counting colony forming units (cfu) formed from 30 µl (3 x 10 µl spots) in each sector on Blood Agar Base (BAB) with 5 % (v/v) defibrinated horse blood (Miles A A & Misra S S. ). Initially, 20 µl of bacteria culture was serially diluted in 180µL of sterile PBS. The BA plates were previously divided into 6 sections. Three drops of 10 µl each were then plated from each serial dilution in each one of these sections. The plates were allowed

to dry and incubated overnight in a CO<sub>2</sub> jar. In the following day the plates were counted. The counted sectors are the ones that have between 30-300 colonies. Calculation of cfu/ml was attained by the following equation;  $\text{cfu/ml} = y \times 10^d \times 100$ , where  $y$  is the average colony count in 10 $\mu\text{l}$  per dilution and  $d$  is the dilution factor.

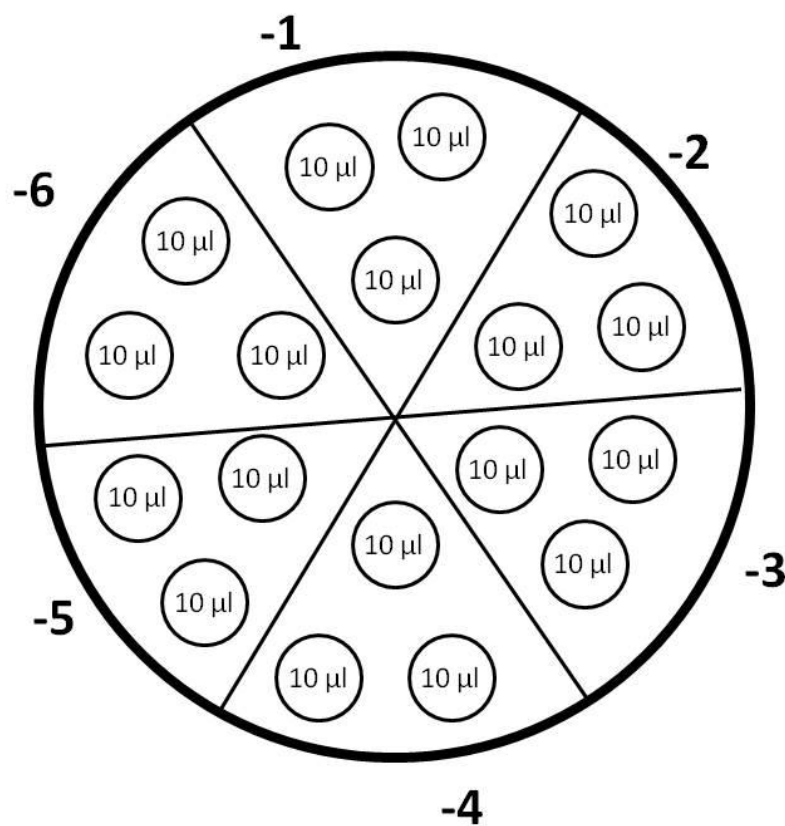


**Figure 2.2:** Miles-Misra style plating of diluted bacterial suspensions to achieve a viable count. Numbers (from <sup>-1</sup> to <sup>-6</sup>) outside the big circle represents the dilution factor ( $d$ ) performed, whereas small circles inside the each segment of dilution factor represents the placement of the triplicate 10 $\mu\text{l}$  spots for each dilution.

**2.3.2. Animal passage:**

The degree of virulence of pneumococci is enhanced by animal passage (Canvin et al. 1995). Cryotubes from  $-70^{\circ}\text{C}$  freezer were centrifuged at 1500g for 2 mins. Pellet was resuspended in sterile PBS (approx. 5 ml) at  $\text{OD}_{500}$  was about 1.6. 100  $\mu\text{l}$  of suspension was injected intraperitoneally using 0.5 ml fine insulin syringe to two female MFI mice. After 22-28 hrs, 50  $\mu\text{l}$  of blood was collected into 10ml of BHI broth and incubated at  $37^{\circ}\text{C}$ . Following day, cultures in BHI broth were spun at 1500g for 15 mins and the pellet was resuspended in 1ml serum broth. 700 $\mu\text{l}$  of suspension was taken and added to 10ml serum broth, which made  $\text{OD}_{500}$  was about 0.7. Tubes were incubated at  $37^{\circ}\text{C}$  for 5 hours to reach  $\text{OD}_{500}$  about 1.6. Bacterial cultures with appropriate  $\text{OD}_{500}$  were aliquoted into 500  $\mu\text{l}$  and stored at  $-70^{\circ}\text{C}$  in sterile cryotubes. After 24 hours of storing in  $-70^{\circ}\text{C}$ , tubes were centrifuged at 1500g for 2 mins and pellet was resuspended in 400 $\mu\text{l}$  sterile PBS. Colony forming units were confirmed as described earlier in the Miles and Misra method (See section 2.3.1).

**2.3.3. Virulence testing:**

To test the virulence of pneumococci, 10-fold dilutions of pneumococci were made and injected intraperitoneally to mice (Harlow et al. 1988). Cryotubes from  $-70^{\circ}\text{C}$  freezer were centrifuged at 1500g for 2 mins and the pellet was resuspended in 400 $\mu\text{l}$  sterile PBS. Each group (n=5) received the estimated dose between  $1 \times 10^4 - 1 \times 10^7$  cfu passaged bacteria diluted in 50  $\mu\text{l}$  sterile PBS. Colony forming units present in the suspension were determined by the method

described in see section 2.3.1. After the infection, mice were observed for next 10 days and disease signs were scored as shown in the table 2.1 (Morton et al. 1985). This dose was used in subsequent experiments.

For intranasal infections (see section 2.5.2) an infecting dose of  $1 \times 10^6$  in  $50 \mu\text{L}$  was used, whereas the dose used for intravenous infections (see section 2.5.1) was of  $1 \times 10^5$  in  $50 \mu\text{L}$ .

**Table 2.1:** Scoring of the signs of disease after infection (Morton et al. 1985).

Condition	Severity	Score
No sign		0
Hunched	+	1
Hunched	++	2
Starey/Piloerect	+	3
Starey/Piloerect	++	4
Lethargic	+	5
Lethargic	++	6
Moribund		Culled
Dead		Culled

## **2.4. Animal welfare:**

All animals were housed in pathogen free conditions within the Division of Biomedical Services at the University of Leicester. Animals had access to food and water *ad libitum*. All procedures were carried out in accordance with project licences approved by the United Kingdom Home Office and in accordance with the Animals (Scientific Procedures) Act 1986. All animal experimental procedures were carried out in accordance with UK Government legislation (Project Licence Number: PIL No 40/200 and Personal Licence Number: PPL No 80/1673).

### **2.4.1. C57BL/6J mouse strain:**

Female, aged 9 weeks, C57BL/6J mice (Harlan Olac, United Kingdom) were used to estimate the mortality caused by ultrafine carbon particles and pneumococci. To assess the survival caused by UFCB and *S. pneumoniae*, forty female outbred C57BL/6J mice (Harlan Olac, United Kingdom), were divided into four groups of ten to be used in the experiment shown in table 2.2.

On day one, two groups were instilled with 500 µg/ 50 µl of ultrafine carbon particles (UF-CB) and another two groups given sterile PBS. A second dose (500 µg/ 50 µl) of ultra fine carbon black (UF-CB) and PBS given to the respective groups on the fourth day of the experiment with a three day gap after the first dose. After 24 hours of the second dose of the ultra fine carbon particles (UF-CB), mice were infected with 1 x10<sup>6</sup> colony forming units of *S.*

*pneumoniae* in infection groups (see section 2.5.2). Throughout the study the animals were provided with water and food pellets *ad libitum*.

#### 2.4.2. MF1 mouse strain:

To assess the survival caused by UFCB and *S. pneumoniae*, forty female outbred\* MF1 mice (Harlan Olac, United Kingdom), aged 9 weeks, were divided into four groups of ten to be used in the experiment shown in table 2.2.

**Table 2.2:** Summary of MF1 mice groups and instillation days

	Day 1	Day 4	Day 5
Group A	UFCB	UFCB	<i>S. pneumoniae</i>
Group B	PBS	PBS	<i>S.pneumoniae</i>
Group C	PBS	PBS	PBS
Group D	UFCB	UFCB	PBS

Throughout the study the animals were provided with water and food pellets *ad libitum*. Initially, mice were transferred to an anaesthetic box and they were lightly anaesthetised with mixture of 2.5 % (v/v) fluothane (Zenca, Macclesfield) and oxygen (1.5-2 L/ minute). The mouse was held by the scruff of the neck in a vertical position with its nose upwards (see section 2.5.2). 50µl of PBS (136mM NaCl, 2.68mM KCL, 10.14 mM Na<sub>2</sub> HPO<sub>4</sub>, pH 7.4, autoclaved) containing 500 µg of UF-CB were given drop by drop into the nostrils of the mouse (Southam et al. 2002).

On day one, two groups were instilled with ultrafine carbon particles (UF-CB) and another two groups given sterile PBS. A second dose of ultra fine carbon black (UF-CB) and PBS given to the respective groups on the 4th day of the experiment with a three day gap after the first dose. After 24 hours of the second dose of the ultra fine carbon particles (UF-CB), mice were infected with  $1 \times 10^6$  colony forming units of *S. pneumoniae* in infection groups (see section 2.5.2). Bacteria were given drop by drop into the nostrils for the mouse to inhale. The clinical signs of disease and survival were recorded four times daily as described in table 2.1. (Morton et al. 1985).

*Description of Outbred mice:* Outbreds are intentionally not bred with siblings or close relatives, as the purpose of an outbred stock is to maintain maximum heterozygosity. One advantage of using outbred stocks is lower cost, because outbreds have relatively long lifespan, are resistant to disease, and have high fecundity (Harlan Laboratories).

## **2.5. Protocols for animal experiments:**

### **2.5.1. Intraperitoneal infections:**

For the intraperitoneal infections, 100  $\mu$ l of bacterial suspension was injected into mice intraperitoneally using a 0.5 ml fine insulin syringe. Each mouse was handled by grasping the scruff of the neck with the thumb and the index fingers to prevent it from biting. The tail was hold with the fourth and fifth fingers of

the same hand against the palm in order to stretch the mice gently. The hand was turned to show the ventral side of the mouse and dropped forward, so that the head of the mouse is at a lower level than the tail, this was done to slightly displace the organs forward and avoid their puncture. The infecting dose contained in an insulin syringe was injected by penetration of the needle into the lower right quadrant of the abdominal cavity at an approximate 45° angle (Lock et al. 1988) . After 22-28 hrs, when the animals were 2+ starry, they exsanguinated by cardio puncture with a 23G needle, followed by sacrifice of the animals by dislocation of the neck.

### **2.5.2. Intranasal infections and instillations:**

Mice were lightly anaesthetised with 2.5% (v/v) fluothane (Zenca, Macclesfield) over oxygen (1.5-2 L/minute). The mouse was hold by the scruff of the neck in a vertical position with its nose upward. 50µL of PBS containing  $1 \times 10^6$  bacteria (see 2.6.2) were given drop by drop through the nostrils for the mouse to inhale. After the whole dose was given, the mouse was placed inside a cage on its back to recover (Wu et al. 1997).

Intranasal instillation is an effective, noninvasive technique employed for the delivery of allergens, drugs or gene therapy, immunotherapy and pathogens to the upper and lower respiratory tracts (URT and LRT). Intranasal instillation provides a natural route of entry into mice, unlike intratracheal instillation, the introduction of the material is non-physiologic, involving invasive delivery,

usually dose rate is substantially greater than that which would have occurred during inhalation. In addition, intratracheal instillation is not a right technique to use for this study since first dose of carbon instillation followed by second dose of carbon and infection.

### **2.5.3. Collection of blood- cardiac puncture:**

The mice were deeply anaesthetised with 2.5% v/v fluothane (Zenca, Macclesfield) over oxygen (1.5-2 L/minute). When they were deeply anaesthetised, a mouse was placed on its back making sure it had a constant supply of anaesthetic. The base of the ribcage was compressed slightly on each side with the thumb and forefinger. The needle of a syringe was introduced parallel to the sternum through the diaphragm line, approximately 4mm below the sternum to penetrate the heart. Normally it was possible to obtain by this method 1ml of blood. The mouse was immediately culled by cervical dislocation after the blood was obtained (Lister et al. 1993).

### **2.5.4. Collection of blood – tail bleeding:**

To obtain small amount of blood, the mice were placed in an incubator at 37°C for 30 minutes to dilate their veins. The tail of a mouse was passed through a hole in the lid of a plastic cylinder, the mouse was then placed inside the cylinder and the lid closed, leaving the tail of the mouse exposed. The needle of a syringe was placed parallel to the tail vein and introduced with a very slight angle. Blood was obtained with a very gently vacuum. Alternatively, the vein

was punctured with the syringe needle and the blood collected from the bleeding (Schreiber et al. 1998).

### **2.5.5. Calculation of CFU from blood:**

Blood from mice was obtained as described in (see section 2.5.3 and 2.5.4). 20µL of blood were serially diluted in 180µL of PBS. Dilutions from  $10^{-1}$  to  $10^{-6}$  were done. Six 30 µL (3 x10µL) drops from each dilution were placed onto an agar plate, left to dry and incubated overnight on micro-aerobic conditions (see section 2.1.4 and figure 2.2). The next day, the number of colonies was counted on the appropriate dilution and the average number of colonies per 30µL spot was calculated. From this the CFU per millilitre of blood was calculated (Miles A A & Misra S S.).

### **2.5.6. Calculation of CFU from lungs:**

The mice were culled by using high dose of anaesthesia and the lungs aseptically removed and placed into pre-weighted universal tubes containing 10ml of PBS. The tubes containing the lungs were weighted again to determine the weight of the lungs. The lungs were homogenised with a tissue homogeniser (Ultra-Turrax T8 from IkaWerke) and 20µL of homogenate were serially diluted in 180µL of PBS. Dilutions of up to  $10^{-6}$  were done. Six 30µL (3 x10µL) drops from each dilution were placed onto an agar plate, left to dry and incubated overnight. The next day, the number of colonies was counted on the appropriate

dilution. From this value the number of cfu/mg of tissue was calculated (Miles A A & Misra S S. ).

### **2.5.7. Urine collection:**

Mice were placed in stainless steel metabolic cages soon after giving two doses of ultrafine carbon black for 12 hours with free access to water and food (Wagner et al. 1983). Urine was collected in sterile eppendorf tubes every 2 hours. Samples were stored in  $-70^{\circ}\text{C}$  for further analysis of 8-oxodG (8-oxo-7,8-dihydro-2'-deoxyguanosine).

### **2.5.8. Collection of bronchoalveolar lavage fluid (BALF):**

Mice were culled by using high dose of anaesthesia (pentobarbitone; 90 mg/kg) intraperitoneally, each mouse was placed in a ventral position and the skin of the neck was cut to expose the trachea. All of the tissue around the area of the trachea was removed and a small incision between two cartilage discs was made. A 18G catheter (without needle) was carefully inserted into the trachea through the incision and towards the lungs and secured with a nylon thread (Figure 2.3). 500 $\mu\text{L}$  of PBS (Invitrogen; Paisley, UK) were carefully injected inside the lungs with the use of a 1ml syringe without a needle (VWR international; Lutterworth, UK). The fluid was carefully aspirated and placed into a 15ml centrifuge tube on ice (van Rijt et al. 2004). The lavage was repeated three more times with 500 $\mu\text{L}$  of PBS and collected into the same microcentrifuge tube. Approximately 70–80% of the instilled volume was

consistently retrieved. All BAL samples were kept on ice until processed. The lavage fluid was pooled and centrifuged at 1200g for 5 mins. Supernatant was stored in  $-70^{\circ}\text{C}$  for cytokine analysis. Pellet was diluted in sterile PBS at  $\times 10^6$  cells/ml and cytopinned using cytocentrifuge slides and cuvettes (Shandon Instruments; Pittsburgh, PA). Slides were stained with Diff-Quick (Dade Behring; Deerfield, IL) for cell differential counting. Three hundred cells were counted at 400 x magnifications for the differential counting by light microscopy (van Rijt et al. 2004).

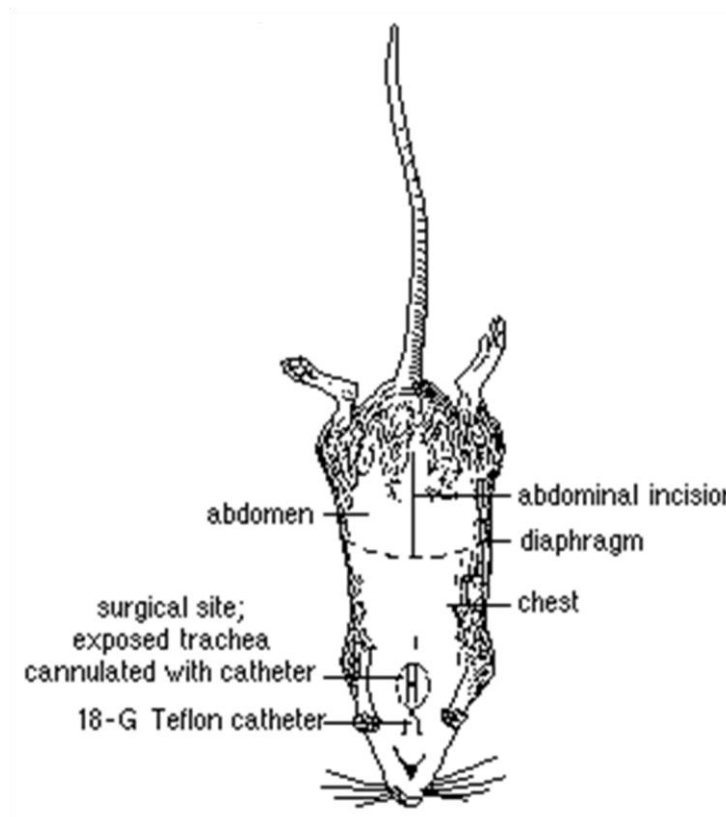


**Figure 2.3:** A schematic drawing of preparation of mouse for collection of broncho alveolar lavage fluid (Taken from Wiley's Current Protocols in Pharmacology).

### **2.5.9. Cytospin Preparation:**

A cell suspension in PBS (75  $\mu$ l) was loaded into a cyto-centrifuge cup and centrifuged using a cytocentrifuge (ThermoFisher Scientific, UK) on to a microscope slide at 25g for 6 min. The slide was allowed to air dry before being stained with 'Diff Quick' (Medion Diagnostics, Dürdingen, Germany). Each slide was immersed ten times in a fixative solution (Fast green in methanol) then blotted on tissue to remove excess fluid. This was repeated for Eosin G in PBS pH 6.6 (stain solution 1) and then finally for the Thiazine counterstain also in PBS pH 6.6 (stain solution 2). Slides were then washed with standard dH<sub>2</sub>O, blotted, and allowed to air dry, before microscopy examination (Takizawa et al. 2001). Thiazine is a cationic dye that binds negatively charged constituents such as nuclear material, whereas anionic dyes such as eosin bind to cytoplasmic proteins.

### **2.5.10. BAL cytokines:**

Concentrations of proinflammatory cytokines IL-6, IL-1 $\beta$ , IL-8\*, INF- $\alpha$  and TNF- $\alpha$  were determined by ELISA on BAL supernatant samples with Meso Scale Discovery (MSD) mouse Pro-Inflammatory 7-Plex Ultra-Sensitive

cytokine panel kit (MS2400; Meso Scale Discovery, Gaithersburg, MD) according to the manufacturer's protocol ( Figure 2.4). Samples were measured in triplicate and analysed with the SECTOR imager plate reader. Data analysis was performed using the discovery workbench software.

\* IL-8 is a potent proinflammatory chemokine that can stimulate the migration of neutrophils to sites of infection and inflammation. In general, mice do not have a gene that encodes IL-8 and instead express a variety of orthologs such as KC/GRO  $\alpha$ , MIP-2 and GRO  $\beta$ ,  $\gamma$ , all of which can bind to common receptors(Boisvert et al. 1998).

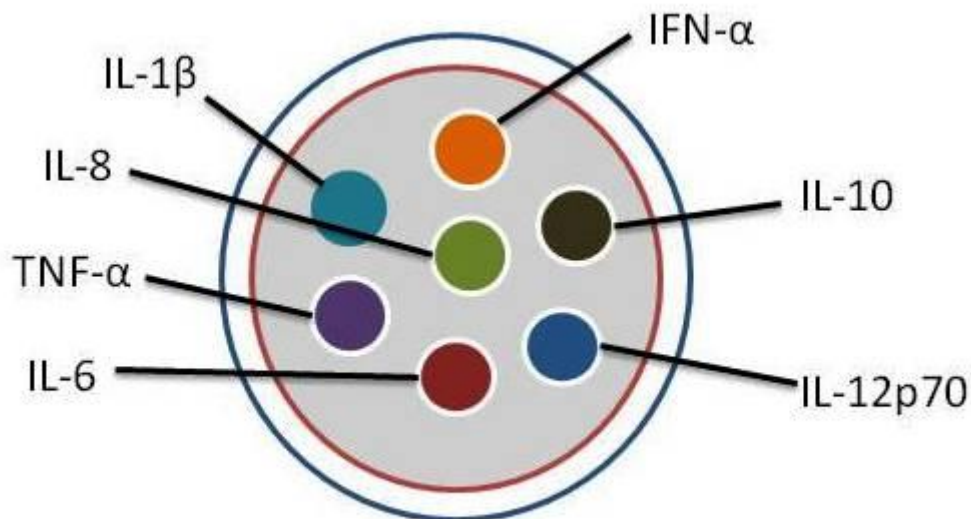


**Figure 2.4:** MSD Mouse Pro-Inflammatory 7-Plex Cytokine Panel. In multiplex assay, an array of capture antibodies against different targets is patterned on distinct spots on the same well. Colour map display demonstrates different

patterns of cytokine responses in different wells of a 96 well 7-spot ultra-sensitive cytokine plate. Spot diagram showing placement of analyte capture antibody.

## **2.6. Fixation and preparation of mice lung tissue:**

The mice were culled by using high dose of anaesthesia intraperitoneally (pentobarbitone; 90 mg/kg). The lungs were aseptically removed and placed into 4% paraformaldehyde. After fixation for 24 hours in 4% paraformaldehyde, lung tissues were processed for embedding in paraffin, slide preparation and sectioning (3  $\mu\text{m}$  – 6  $\mu\text{m}$ ) by Dept. of Pathology, University of Leicester.

### **2.6.1. Deparaffinization:**

Slides were placed in two successive washes of 5 minutes xylene, 5 minutes in 100% ethanol (EtOH), 5 minutes in 70% ethanol (EtOH), 5 minutes in 40% ethanol (EtOH) and washed for 5 minutes in bi-distilled water.

### **2.6.2. Hematoxylin and Eosin:**

Slides were incubated for one minute in filtered Harris Hematoxylin then rinsed in flowing water until the incubation chamber had been cleared of stain. Sections were then incubated one minute in 1.0% Eosin Y. Sections were dehydrated five minutes in ascending alcohol solutions of 70%, 80%, 95%, and twice in 100% ethanol (EtOH). Slides were cleared with two series of five minutes incubation in xylene (Sharplin et al. 1989).

### **2.6.3. Pathology score on lung histological sections:**

A pathology score of haemorrhage was measured on lung histological sections stained with hematoxylin-eosin. Two slides per mouse ( $n = 10$ ) were scored and averaged for control group and exposed group. Lung haemorrhage scored at low magnification  $\times 25$  and the following scoring scheme was used for scoring. 0= normal, 1=1% to 20%, 2=21% to 40%, 3=41% to 60 %, 4= 61% to 80% and 5= 81% to 100 %.

### **2.7. Urinary 8-oxodG assay:**

To collect urine, mice were placed in metabolism cages. Urine was pooled and frozen at  $- 80^{\circ}\text{C}$  prior to analysis. The experiment to measure the levels of 8-oxodG in urine was conducted by Dr.Raj singh, University of Leicester. For analysis of 8-oxo-7,8-dihydro-2'-deoxyguanosine (8-oxodG), a 100  $\mu\text{L}$  aliquot of mouse urine sample was diluted with 890  $\mu\text{L}$  of HPLC (High-performance liquid chromatography ) grade water and spiked with 10 pmol of the stable isotope internal standard [ $^{15}\text{N}_5$ ] 8-oxodG (1 pmol/ $\mu\text{L}$ ) (Gábelová et al. 2006). Urine samples were then subjected to solid phase extraction using Oasis HLB columns (1 mL, 30 mg, Waters Ltd., Elstree UK), evaporated to dryness and redissolved in 50  $\mu\text{L}$  of HPLC grade water. The purified urine samples were subjected to liquid chromatography-electrospray ionization-tandem mass spectrometry (LCESI- MS/MS) with selected reaction monitoring (SRM)

analysis by injecting a 10  $\mu\text{L}$  aliquot of each sample in triplicates ((Weimann et al. 2002)). Selected reaction monitoring analysis was performed for the  $[\text{M}+\text{H}]^+$  ion to oxidised base  $[\text{B}+\text{H}_2]^+$  transitions of 8-oxodG,  $m/z$  284 to 168 and the internal standard  $[\text{}^{15}\text{N}_5]$  8-oxodG,  $m/z$  289 to 173. The level of 8-oxodG in each urine sample was determined from the ratio of the peak area of 8-oxodG to that of the internal standard and normalized to the specific gravity which was determined using a Reichert TS 400 refractometer (Reichert Analytical Instruments, Depew, USA). The levels of 8-oxodG are expressed in pmol/mL relative to a specific gravity of 1.036 which is the average of all the samples.

## **2.8. Mono Mac 6 cell culture:**

The human monocyte cell line Mono Mac 6 was used as a model of exposure of human AM to nanoparticles (Wagner et al. 1983). Non- adhesive MM6 cells were cultured and maintained in cell culture flasks and removed by medium aspiration. Cells were cultured in 5%  $\text{CO}_2$  at  $37^\circ\text{C}$  in RPMI medium supplemented with 10% (v/v) heat inactivated fetal bovine serum (FBS), 2mM L-glutamine, 100  $\mu\text{g}/\text{ml}$  streptomycin, 100  $\mu\text{g}/\text{ml}$  penicillin and 1% (w/v) non essential amino acids. Prior to exposure to nanoparticles,  $1 \times 10^6$  Non- adhesive Mono Mac 6 cells were seeded onto each 24 mm diameter Transwell  $\text{\textcircled{R}}$ -COL insert (Fisher Scientific, Loughborough, UK) and incubated for 4hrs at  $37^\circ\text{C}$  with 5%  $\text{CO}_2$  at >95% humidity At 4 hr, medium was removed so that the fluid level fell below the insert membrane, leaving the cell layer exposed to air.

**2.8.1. Passaging:**

Cells were passaged once they had achieved 90 – 100% confluence. Media was removed by aspiration and cells washed with 10 milliliters of sterile PBS. 0.5 milliliter of 0.05% Trypsin/0.53 mM EDTA in PBS was added and the cells were incubated 5 minutes at 37°C until cells dissociated from the culture dish surface. Cells were diluted and stained with 0.5% trypan-blue in PBS and counted with a hemacytometer using the following formula:

$$\text{Cells/ml} = (\text{average number of cells per square}) (\text{dilution factor}) (10^4)$$

Where each square is 1 X 1 mm and the depth is 0.1 mm.

$5 \times 10^4$  cells/ml were then transferred to a fresh culture dish and pre-warmed media added to 10 ml (Ziegler-Heitbrock et al. 1994).

**2.8.2. Freezing:**

Media was removed from confluent cells by aspiration and washed with 10 ml of sterile PBS. 0.5 ml of 1X trypsin/EDTA (0.05% trypsin, 0.53 mM EDTA) in PBS was added and the cells were incubated 5 minutes at 37°C until cells dissociated from the culture dish surface. Cells were then collected in 5ml media and centrifuged 5 minutes at 600X g in a swing bucket rotor. Media was removed and cells were resuspended in 1 ml of freezing medium (60% media, 10% DMSO, 30% FBS). Cells were counted on a hemacytometer as previously described (See section 2.8.1), and the cells further diluted to a concentration of  $10^7$  cells/ml and frozen in 1 ml aliquots. Cells were then frozen at -80°C

overnight and then placed in liquid nitrogen for long term storage (Ziegler-Heitbrock et al. 1994).

### **2.8.3. Thawing:**

Frozen cells were removed from liquid nitrogen and placed directly in a 37°C water bath until thawed (~ 1 minute). Five ml of media were added to the cell suspension then centrifuged 5 minutes at 600X g and the supernatant removed by aspiration. The cell pellet was resuspended in 10 ml of media and placed in a 10 cm culture dish to grow to confluency.

### **2.8.4. Cell seeding on cell culture inserts:**

Collagen coated poly tetra fluoro ethylene (PTFE) Transwell-COL inserts (24 mm diameter; 3.0 µm pore size) (Corning Incorporated, NY) used to culture the Mono Mac 6 cells (Figure 2.5). Transwell-COL inserts were placed in 6-well plates (VWR, Leicester); 2.6ml of culture media added per plate well and 1.5 ml culture media with  $1 \times 10^6$  Mono Mac 6 cells were seeded onto each insert. Cells were incubated for 4 h at 37 °C with 5% CO<sub>2</sub> at >95% humidity At 4 hr, medium was removed so that the fluid level fell below the insert membrane, leaving the cell layer exposed to air (Phillips et al. 2003).



**Figure 2.5:** Transparent (when wet), collagen-treated PTFE membrane ( $3.0\mu\text{m}$ ), 6 well 24.5mm Transwell-COL insert are used for exposure studies. (Taken from Corning website).

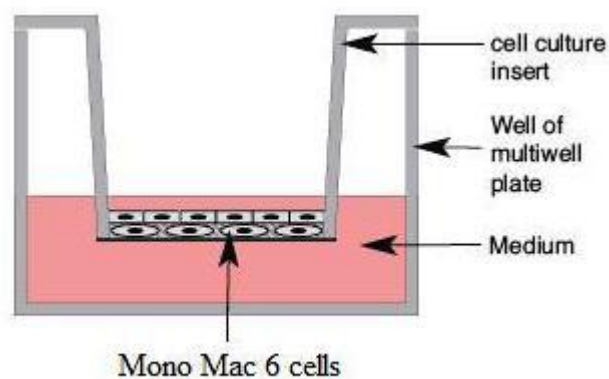


**Figure 2.6:** Diagram of cell culture insert with Mono Mac 6 cell suspension. Mono Mac 6 cells were plated on Transwell-Col supports (as above) incubated for 4 h at  $37^{\circ}\text{C}$  with 5%  $\text{CO}_2$  at  $\geq 95\%$  humidity.

## **2.9. Rat alveolar macrophages:**

Rats were euthanised by intra peritoneal injection of pentobarbitone (90 mg/kg). A cannula was fixed in the trachea, and lungs were lavaged gently with 3 mL sterile phosphate-buffered saline at 4 °C (Takano et al. 1997). The lavage was repeated 6 times and pooled bronchoalveolar lavage fluid (BALF) at 4 °C centrifuged at 1200g for 10 min. The cell pellet was washed with RPMI 1640 medium supplemented with 10% heat inactivated FBS, 2mM L-glutamine, 100 µg/ml streptomycin, 100 µg/ml penicillin and 1% non essential amino acids. In all the samples used in the experiments the alveolar macrophage count was > 98%. The total of the bronchoalveolar lavage fluid (BALF) cells was determined by haemocytometer, and  $1 \times 10^6$  AM in culture medium were transferred to each cell culture insert and then incubated for 4 hrs at 37 °C with 5% CO<sub>2</sub> at > 95% humidity. Adherent alveolar macrophages (AM) were washed gently twice with sterile PBS, and RPMI 1640 added to the lower part of the insert prior to exposure to nanoparticles.

## **2.10. Generation of nanoparticles:**

Gold (Au), silver (Ag), and iron (Fe) metal rods (2 mm diameter) used as sample electrodes were cut in approximately 7-10 cm lengths. Prior to measurement, the electrodes were cleaned and filed to give them a flat sparking surface. Once the spark ablation was complete, the electrodes were removed from the solution and rinsed with deionised water.

Spark ablation was used to produce nanoparticulate aerosols of gold (Au), Silver (Ag), and Iron (Fe). These three metal nanoparticles are chosen because of their wide range of applications in consumer products and medical devices, convenience as strong metal wires and readily available in lab.

Metal electrodes formed the spark gap, and sparks were produced by discharging a capacitor (Figure 2.7) through the surrounding gas (Kim et al. 2009). A spark source consisting of a 50 cm<sup>3</sup> chamber milled from a block of aluminium was constructed. In order to prevent the generation of ozone, we used oxygen-free nitrogen at ambient pressure was used as the aerosol gas. The flow rate of nitrogen was adjusted by Bronkhurst mass flow controllers and set to a constant 1.2 L/min. Nitrogen was first passed through a bubble flask to saturate the air to avoid drying of exposed cells and subsequently through a filter to prevent bacterial contamination. Interchangeable gold (Au), Silver (Ag), and Iron (Fe) electrodes were fabricated from 1 mm pure metal wire and mounted in the spark chamber. The spark gap was adjusted to 2 mm and a voltage of 6 kV applied from an external power supply in parallel with a 100 pF capacitor.

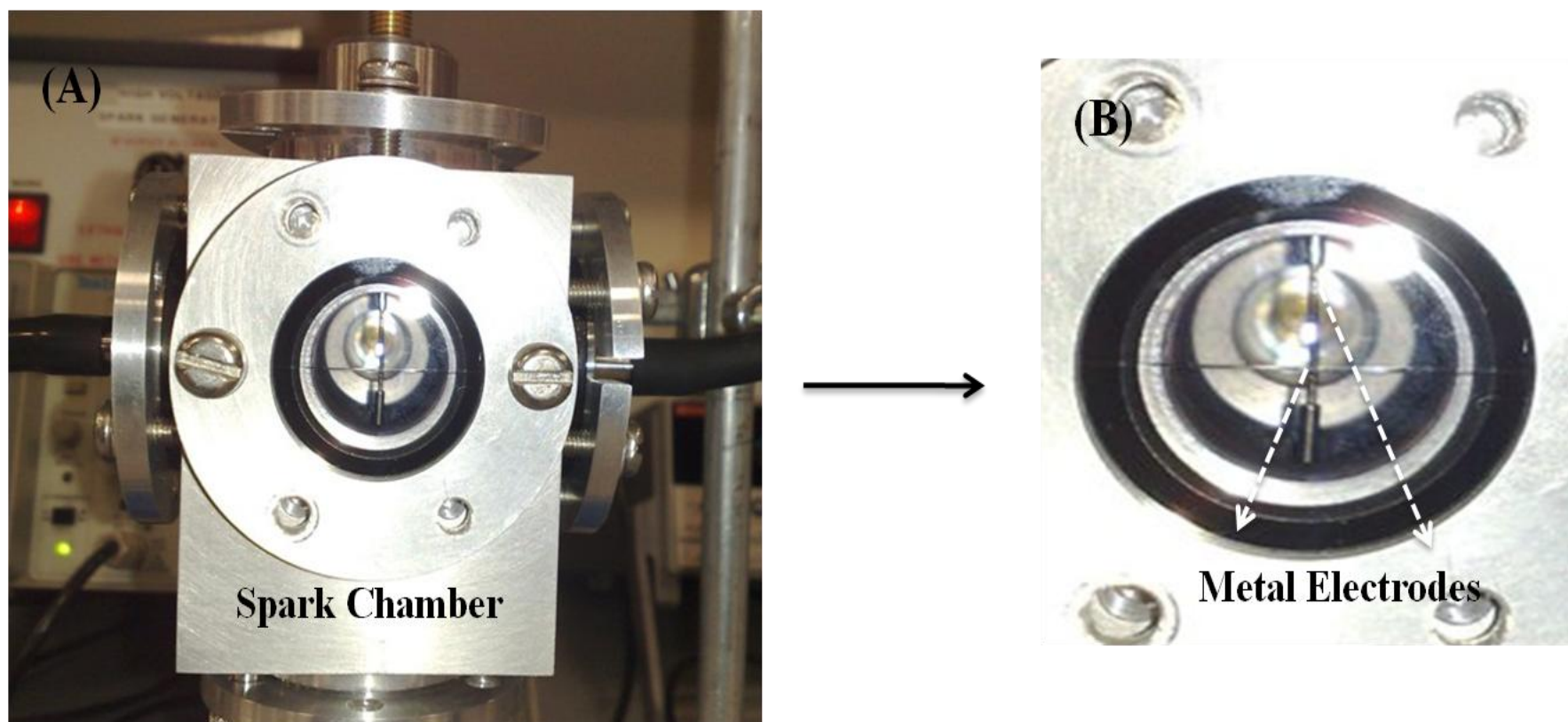


**Figure 2.7:** Photograph of Spark discharge chamber. Gold (Au), Silver (Ag), and Iron (Fe) nanoparticles generated from interchangeable pure metal electrodes placed in an electric spark discharge generator supplied with oxygen-free nitrogen in the discharge chamber (A). Close view of metal electrodes and spark shown in the picture B.

## 2.11. Particle exposure to cells:

The exposure chamber system was designed to accommodate the 24 mm diameter transwell inserts. The insert containing adherent cells was placed in a cylindrical glass dish with supernatant medium added below the porous membrane until the whole membrane was just in contact with the liquid. This ensured that the cells remained moist, but not submerged, during nanoparticle exposure (Sung et al. 2008). The glass dish was then placed in a sealed, stainless steel chamber. The nanoparticle aerosol flowed in and out through co-axial tubes attached to the lid. A Poly tetra fluoro ethylene (PTFE) cylinder accurately engaged the transwell insert to ensure that the geometry was constant for different exposures. Under normal conditions, only a small fraction of nanoparticles at the edge of the flow randomly collide with the walls of the membrane. In order to increase deposition, we used an electrostatic discharge (ESD) collector was used. A stainless steel needle was positioned 8 mm above the centre of the membrane, and the membrane was electrically earthed by means of a stainless steel wire dipped in the supernatant. A voltage of 3-6 kV was applied to the needle was sufficient to produce a corona discharge and the resulting stream of positive ions between the needle and the membrane, efficiently ionised the nanoparticles which were then electro statically attracted toward the earthed sample (Figure 2.8 and 2.9). Measurements with the

scanning mobility particle sizer showed that the corona discharge is about 80% efficient at ionizing the particles (Davoren et al. 2007). Initially, a non-uniform distribution of nanoparticles was observed on the inset membrane, with the majority of particles being delivered to a small area in the membrane centre. By replacing the nozzle with one that caused turbulent flow, it was possible to achieve a highly uniform coverage across the collagen-coated membrane. To compare DNA damage caused by different particles, monolayers of macrophages were exposed to the nanoparticulate stream for 10 min. Controls were cells placed in the nitrogen gas stream without particles, and cells placed in air for the same time period. After the experiment, medium was added to cover the macrophage layer, and the insert (i.e., cells and particles) transferred to an incubator for 24 h.

Spark ablation is well established technique to produce nanoparticles in Dr Paul Howes 's lab, University of Leicester. I have used his expertise to expose nanoparticles to MM6 cells and rat alveolar macrophages. I worked closely with Dr Paul Howes in generation of nanoparticles using metal electrodes, making changes in turbulent flow and particle exposure to cells.

Particle range was tested two separate individual experiments and iron, gold and silver particle exposure to MM6 cells was tested on three separate occasions.

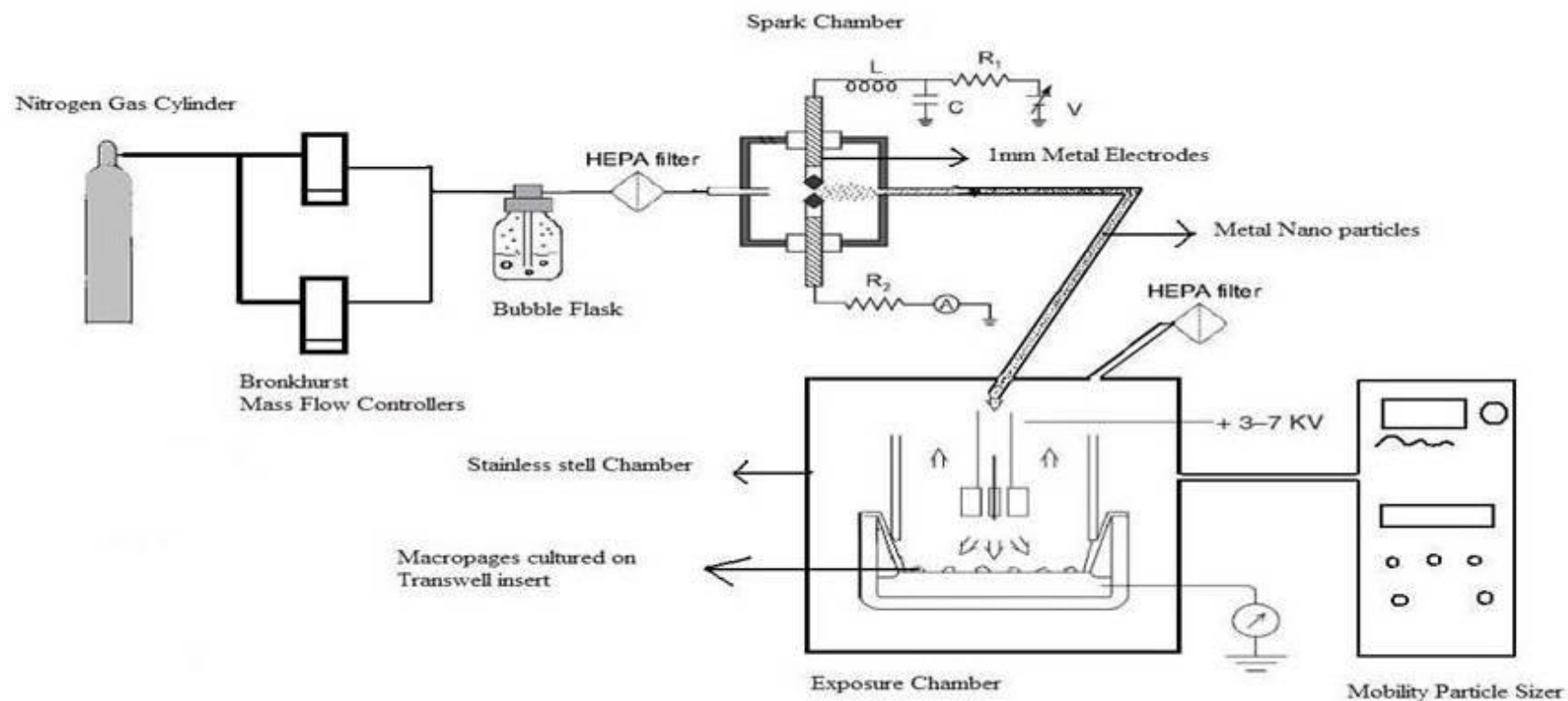


**Figure 2.8:** A schematic diagram of the system for cell exposure to manufactured metal nano particles. Metal nanoparticles in a nitrogen gas stream enter the chamber via a central tube. A voltage of 3–7 kV produces a corona discharge and the resulting stream of positive ions between the needle and the membrane efficiently ionized the nanoparticles which were then electro statically attracted toward the earthed cells adherent to a damped collagen membrane.

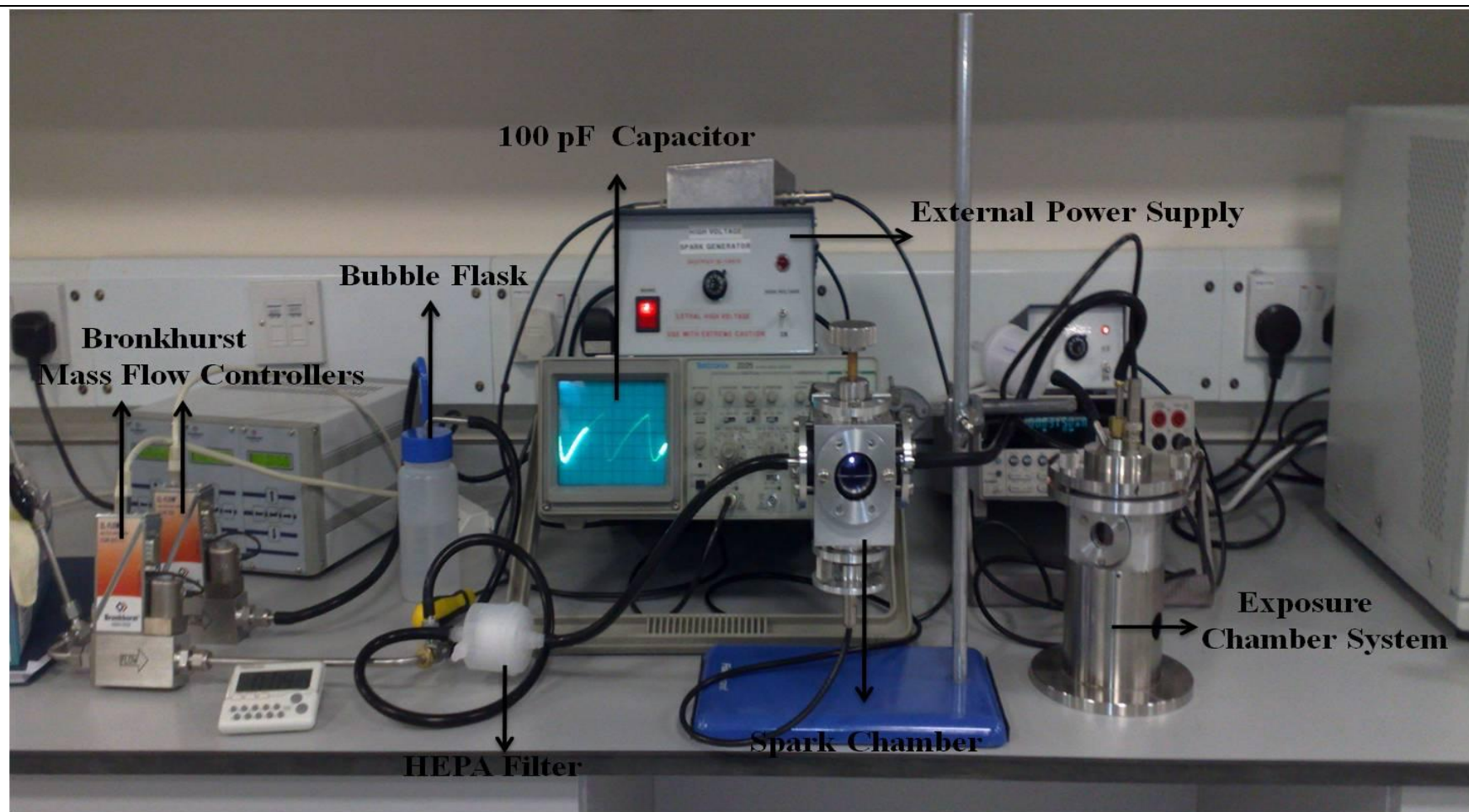


**Figure 2.9:** Photograph of small whole-body exposure chamber used in studies for nanoparticle exposure studies. Transwell inserts seeded with alveolar macrophages placed inside of the exposure chamber system for nanoparticle exposure.

## 2.12. Comet Assay:

Frosted microscope slides (VWR International, Leicester) were prepared in advance by coating with 1 % normal melting point agarose (NMPA) in phosphate buffered saline (PBS). Nanoparticle exposed cells and control cells were removed from the membrane of the transwell insert by trypsinization and suspended in 0.6% low melting point agarose (Singh et al. 1988). Eighty microliters of the agarose containing approximately  $3 \times 10^4$  macrophages were dispensed onto glass microscope slides previously coated with 1% normal melting point agarose. The solution was spread homogeneously on the slide with a glass cover slip. Slides were then held at 4°C for 30 minutes on a tray to allow the agarose to solidify, following which the cover slips were carefully removed. The slides were then submerged in ice-cold lysis buffer (100 mM disodium EDTA, 2.5M NaCl, 10 mM Tris-HCl, pH 10 containing 1% triton X-100 (v/v) added fresh) overnight in a coplin jar, in the dark, to lyse the cell and nuclear membranes. Slides were washed with distilled water and then placed in a horizontal electrophoresis tank containing ice-cold alkaline electrophoresis buffer (300 mM NaOH, 1 mM disodium EDTA, pH  $\geq 13$ ) for 20 min and electrophoresed at 30 V (0.7 V/cm) and 300 mA for 20 min. Slides were neutralized with 0.4 M Tris-HCl, pH 7.5 for 20 min and washed with double-distilled water, then allowed to dry (Collins 2004a). All procedures were carried out under subdued light to minimize background DNA damage. For staining,

slides were re-hydrated in distilled water, incubated with a freshly made solution of 2.5 mg/ml propidium iodide for 20 min, washed again for 30 min and allowed to dry. Comets were visualized in the fluorescence microscope at a magnification of 200 x. Images were captured by an on-line CCD camera and analyzed with the Komet Analysis software version 5.5 (Andor Technology, Belfast, UK). Two slides were used per sample in every experiment, and a total of 100 cells were scored for each dose (50 cells from each slide) for various parameters. Tail length, percentage of DNA in the tail of the comet (% tail DNA), tail extent moment and olive tail moment, were calculated for each cell/comet using the Komet Analysis software (Singh et al. 1988).

For consistency, the following principles were followed while scoring the slides: (a) Microscope optics and camera settings were kept constant throughout the experiment; (b) Default software settings were used; (c) The region of interest (ROI) was kept mostly constant throughout the experiment; (d) To minimize photo-bleaching of the fluorescent signal, the image was brought into focus and the image was quickly acquired for data analysis; (e) No interactive measurements were performed. (f) Measurements were not performed on highly diffused cells ('hedgehogs' or 'clouds', which may be identified by their specific microscopic image with a small or non-existent head and large, diffuse tails).

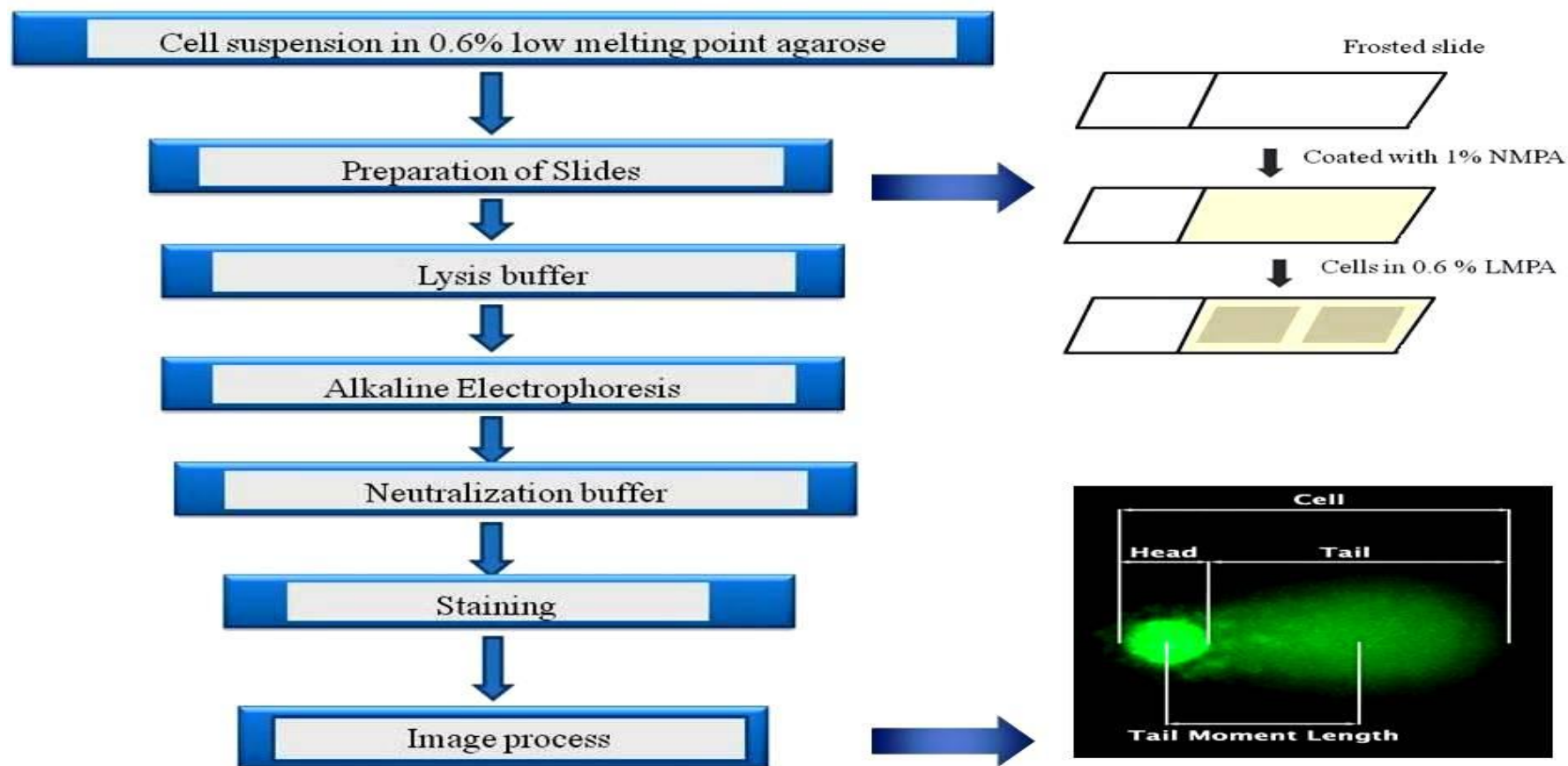


**Figure 2.10:** A Diagrammatic representation of the methodology for alkaline single cell gel electrophoresis (Comet assay). DNA damage caused by nanoparticle exposure to Mono Mac 6 cells was assessed by comet assay.

The various measurements were correlated with the dose of gamma irradiation and other particle exposure studies using a data-analysis package from Excel.

Means were calculated for all 34 measurements included in the Komet 5.0 image-analysis software (listed in table 4.1), and the final results were expressed as the mean of the means  $\pm$  SEM. Analysis was done for 50 comets (Figure 4.3) per experiment (duplicated) and only four excellent indicators of radiation-induced DNA damage (Tail length, percentage of DNA in the tail of the comet (% tail DNA), tail extent moment and olive tail moment) data were shown for each cell comet using the Komet Analysis software.

**Table 2.3 : List of various Comet measurements calculated by the Comet image-analysis system**

1. Cell area
2. Comet coefficient of variance
3. Comet distribution moment
4. Comet extent
5. Comet inertia
6. Comet mean
7. Comet mode
8. Comet optical intensity
9. Comet skew
10. Comet standard deviation
11. Head coefficient of variance
12. Head distribution moment
13. Head DNA
14. Head extent
15. Head inertia
16. Head mean
17. Head mode
18. Head optical intensity
19. Head skew
20. Head standard deviation
21. Length/height
22. Olive tail moment
23. Tail coefficient of variance
24. Tail distribution moment
25. Tail DNA
26. Tail extent
27. Tail extent moment
28. Tail inertia
29. Tail length
30. Tail mean
31. Tail mode
32. Tail optical intensity
33. Tail skew
34. Tail standard deviation

### 2.13. Quartz Crystal Microbalance (QCM):

The quartz crystal microbalance (QCM) is an extremely sensitive mass sensor, capable of measuring mass changes in the nanogram range. QCM measures a mass per unit area by measuring the change in frequency of a quartz crystal resonator (Figure 2.11). The surface of the acoustic resonator can able to detect the resonance disturbed by the addition or removal of small mass densities down to a level of below  $1 \mu\text{g}/\text{cm}^2$  ((Kurosawa et al. 2006)).

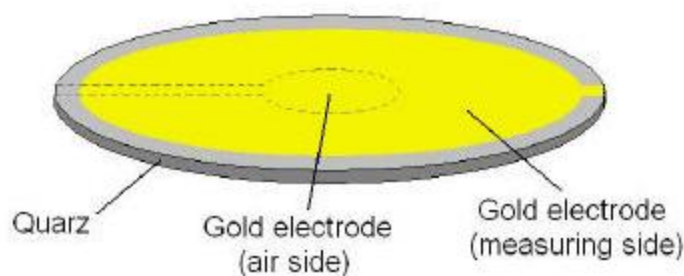
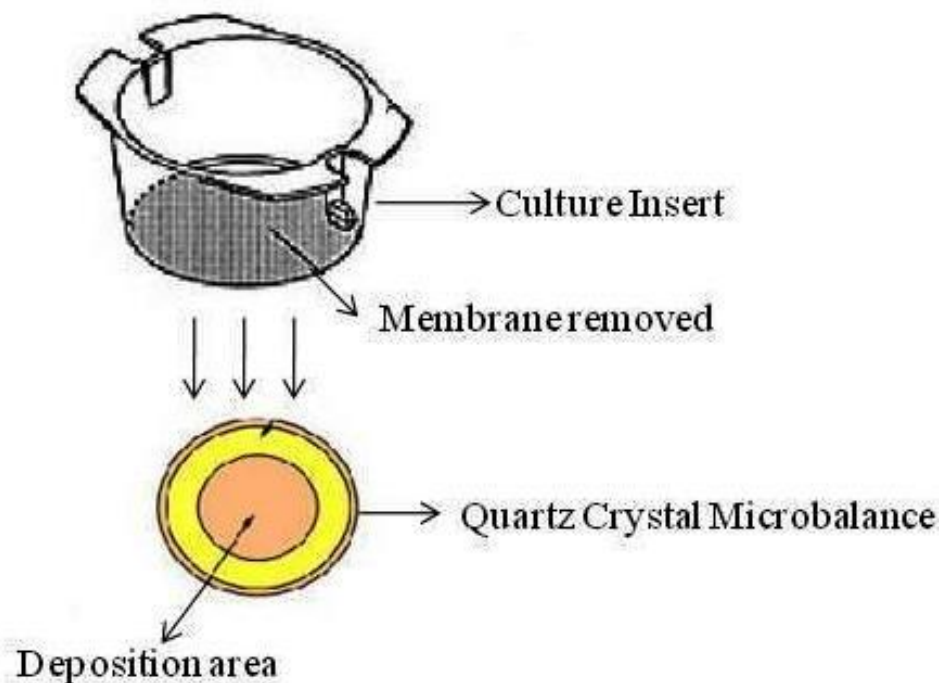


**Figure 2.11:** Quartz crystal resonator connected with gold electrode. The quartz crystal microbalance was used to measure the mass of the particle matter deposited on the insert membrane.

The balance measures the mass of particle material deposited on the surface of an oscillating quartz crystal by detecting the change in resonant frequency of the crystal (Leybold Inficon Sensor, XTC/2 Oscillator package, and XTM/2 Film Thickness Monitor; INFICON Holding AG, Bad Ragaz, Switzerland). The quartz crystal is a highly precise and stable oscillator. The quartz crystal is the crucial component of the quartz crystal microbalance because it registers and

reports the mass deposited on its electrodes quantitatively: the mass changes its oscillation frequency. To estimate the dose delivered to macrophages, the cell free - supporting membrane was replaced by a quartz crystal microbalance (Figure 2.12) ((Kurosawa et al. 2006)). The geometry in the deposition system was identical to that used for macrophage exposures.

---



---

**Figure 2.12:** A Schematic diagram of quartz crystal microbalance (QCM) measuring deposited particle mass.

## 2.14. Cell viability Assay:

Trypan blue exclusion test measures the viability of mono mac 6 (MM6) cells after the exposure to the particles and before the comet assay. Trypan blue test is used in my research to assess the cell death or cell damage caused by nanoparticles exposure. This method is quick, inexpensive, and requires only a small fraction of total cells from a cell population(Collins 2004b).

The human monocyte cell line Mono Mac 6 was used to measure the cell viability after exposing to nano particles (Altman et al. 1993). Cells were cultured in 5% CO<sub>2</sub> at 37 °C in RPMI medium supplemented with 10% heat inactivated fetal bovine serum (FBS), 2 mM L-glutamine, 100 µg/ml streptomycin, 100 µg/ml penicillin and 1% non essential amino acids. Prior to exposure to nanoparticles, 1 × 10<sup>6</sup> Mono Mac 6 were seeded onto each 24 mm diameter Transwell ®-COL inserts and incubated for 4 h at 37 °C with 5% CO<sub>2</sub> at >95% humidity ( see section 2.8 ). Cells were exposed to gold (Au) nanoparticulate stream for 10 min (see section 2.11). After exposing to nanoparticles, cell culture inserts were re- incubated in 5% CO<sub>2</sub> at 37 °C incubator. Duplicate culture inserts with and without nano particles were counted with trypan blue by using hemocytometer (section content 2.8.1) at 0 hours, 24 hours, 48 hours and 72 hours.

## 2.15. X-ray irradiation:

In order to observe the dose-response relationship and to compare the sensitivity of the comet assay, the applied doses at 0Gy\*, 2 Gy, 4 Gy, 6Gy and 10Gy were selected. The human monocyte cell line Mono Mac 6 was used ( See section 2.8) to measure the DNA damage caused by X-ray radiation .Cell-slides were irradiated on ice, using a Pantak DXT300 X-ray machine (Radiotherapy Unit, University of Leicester) operated at 300 kVp (HVL of 3.5mm Cu). Up to 12 slides were placed flat in a prescribed manner. On an aluminium sheet in thermal contact with ice, 0.8 cm from a 50 cm FSD, 20 cm square, normal therapy applicator. The dose rate (0.98 Gy/min) and uniformity of the field ( $\pm 10\%$ ). Duplicate slides were irradiated with a dose of different grays ( 0Gy, 2 Gy, 4 Gy, 6Gy and 10Gy) to generate an immediate damage dose response (He et al. 2000). A standard protocol of the comet assay was used according to the section 2.12 to measure the DNA damage.

\* Gray (symbol Gy) is referred as SI unit (International System of Units) for the quantity of adsorbed dose of ionizing radiation per unit mass of tissue. One Gray means one joule of energy from radiation deposited in 1 kilogram of material.

One Gray is equivalent to one joule/kilogram.

0 Gy, 2 Gy, 4 Gy, 6 Gy and 10 Gy were used (at the dose rate of 1 Gy = 0.98 Gy /min) to measure the DNA damage in human monocyte cell line.

## **2.16. Characterization of nanoparticles:**

### **2.16.1. Scanning Mobility Particle Sizer (SMPS):**

The scanning mobility particle sizer (SMPS) is frequently used to measure particle size distributions of combustion aerosols (Wang et al. 1990). Often, diesel soot emissions, and emission reduction systems, are examined with scanning mobility particle sizer. The aerodynamic diameter of a particle for a given sizing method is defined as the diameter of a sphere of unit density ( $1 \text{ g cm}^{-3}$ ). Interchangeable Au, Ag and Fe electrodes produced the spark by discharging a capacitor through the surrounding gas. Spark produced metal aerosols were characterised in real time by means of a Scanning Mobility Particle Sizer (model 3080N, TSI Instruments Ltd, High Wycombe) which produces spectra of particle number density versus size (total size range 3-1000nm). The Scanning Mobility Particle Sizer (Figure 2.12) is based on the principal of the mobility of a charged particle in an electric field.



**Figure 2.13:** Photograph of Scanning Mobility Particle Sizer. Particle size was measured in a nitrogen gas stream using a TSI Scanning Mobility Particle Sizer.

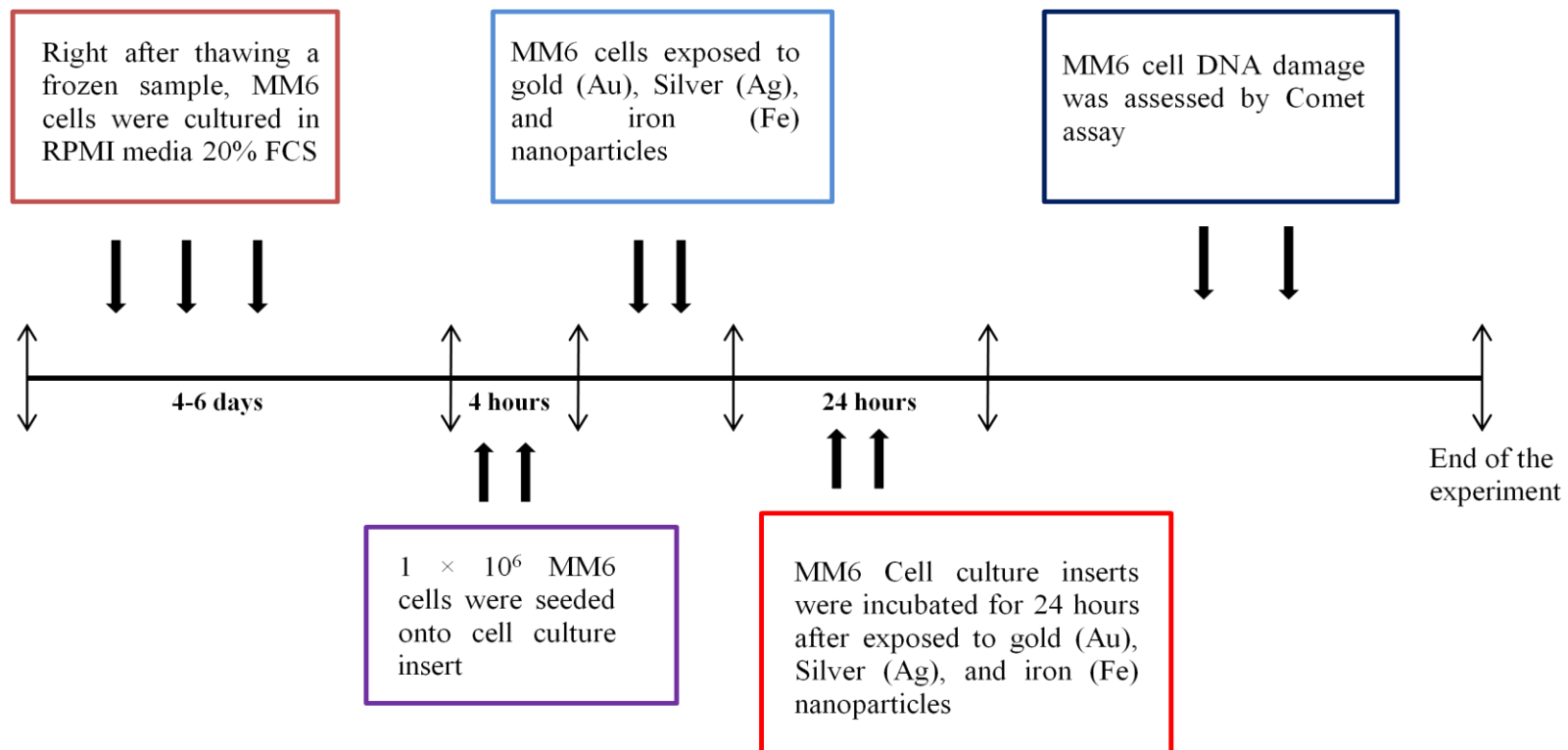


**Figure 2.14:** Mono Mac 6 cells and nanoparticles at an air/tissue interface experiments plan outline (*in vitro* study).

**2.16.2. High resolution transmission electron microscopy (HRTEM):**

Nanoparticles were also characterised by means of transmission electron microscopy (Wang 2000). Transmission electron microscope grids with carbon film supports were mounted at the centre of the deposition cell and exposed to Au, Ag or Fe nanoparticles for 10 min. Images were obtained using a high resolution TEM (JEOL 2100) and used to confirm the particle size distribution obtained from the scanning mobility particle sizer. Images were also used to determine the dose of particles.

**2.16.3. Scanning Electron microscope (SEM):**

All the transwell inserts (exposed to particles and controls) were washed gently with sterile PBS and fixed with 2.5% glutaraldehyde/PBS overnight at 4° C. After the fixation, inserts were processed with series of washing and dehydrating steps, which are detailed below:

1. PBS (x3)	15 mins
2. 70 % Ethanol	90 mins
3. 90 % Ethanol	20 mins
4. 100 % Ethanol	20 mins
5. 100 % Analytical grade Ethanol	20 mins
6. 2:1 Ethanol/Hexamethyldisilazane(HMDS)	20 mins
7. 1:2 Ethanol/Hexamethyldisilazane(HMDS)	20 mins
8. 100 % Hexamethyldisilazane(HMDS) (x2)	20 mins

Once the inserts were dehydrated with ethanol washes, sample wells were air dried in fume cupboard. After wells were dried, they mounted on SEM studs. Studs were immediately placed in sputter coater\* and later observed under the scanning electron microscope (Sondi et al. 2004).

\* The sputter coater uses an electric field and argon gas. The sample is placed in a small chamber that is at a vacuum. Argon gas and an electric field cause an electron to be removed from the argon, making the atoms positively charged. The argon ions then become attracted to a negatively charged gold foil. The argon ions knock gold atoms from the surface of the gold foil. These gold atoms fall and settle onto the surface of the sample producing a thin gold coating.

### **2.17. Statistical analysis:**

Statistical analysis was carried out using GraphPad Prism software (version 5.00, GraphPad Inc., California, USA). Survival results were validated by 4 separate experiments done at different times with  $n = 10$  in each group. Comparison of survival was done by log rank test. Data was validated by at least three separate experiments done at different time. Comet % tail DNA is expressed as mean  $\pm$  SEM. Data was analyzed using one-way ANOVA with the turkey's multiple comparison test. Comet results were validated by at least three separate experiments. Data were compared by the unpaired t test. P value of  $< 0.05$  was considered significant.

# Chapter 3

**Results: Effect of instillation of ultrafine carbon black (UF-CB) into the lower airway of mice on mortality from *Streptococcus pneumoniae*.**

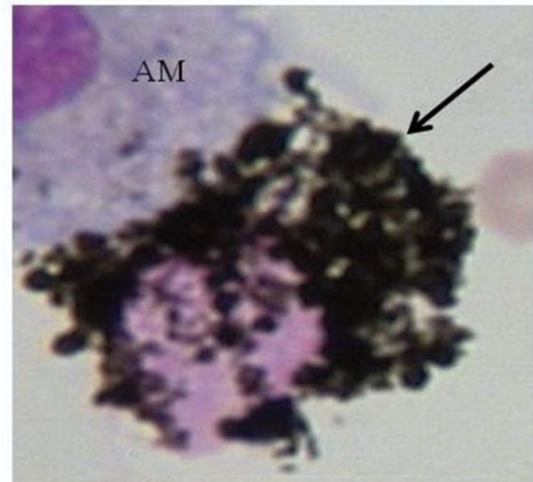
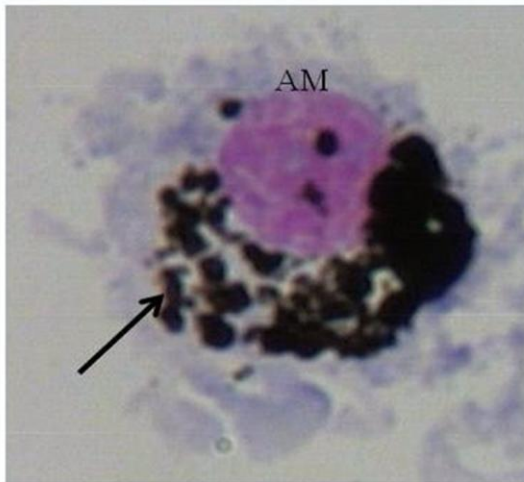
### **3.1. Analysis of ultrafine carbon loading on alveolar macrophages:**

In order to estimate the carbon black particle burden *in vivo*, MF1 female mice (n=10) aged 9 weeks obtained from Harlan Olac, United Kingdom were used to perform the experiment. Nanometer sized carbon black particle (UF-CB) burden was assessed on alveolar macrophages (AM) from bronchoalveolar lavage (BAL) fluid. Bronchoalveolar lavage (BAL) was obtained from mice by instilling 4 x 500 µl sterile PBS through a 25-gauge needle into the lungs, via the trachea, followed by aspiration of BAL fluid into the syringe. None of the animals in groups, UF-CB alone group and PBS control group, showed any short- or long-term morbidity after exposure with UF-CB alone and PBS control. Obtained BAL lavage fluid was cytocentrifuged (Shandon Instruments, Pittsburgh, PA), and afterwards cells were stained with Diff-Quik (Dade Behring; Deerfield, IL, USA). Carbon loading of AM was determined in 300 randomly selected AM using a semi-quantitative scale. Lung histology confirmed no inflammation and no AM carbon in mice exposed to PBS alone (See section 3.3). BAL obtained alveolar macrophages with carbon loading were categorized into four different groups (table 3.1) (fig 3.1 and 3.2).

**Table 3.1:** Four different groups of alveolar macrophages that explain the percentage of cytoplasm occupied by ultrafine carbon particles (UF-CB) were described below.

<b>Group</b>	<b>Discription</b>
<b>Heavily-laden Macrophages</b>	More than 50% of the Cytoplasm occupied by particles
<b>Moderately-laden Macrophages</b>	10 to 50% of the cytoplasm occupied by particles
<b>Lightly-laden Macrophages</b>	Less than 10% of the cytoplasm occupied by particles
<b>Carbon-free Macrophages</b>	No carbon black particles appeared in the cytoplasm

## A. Heavy loading

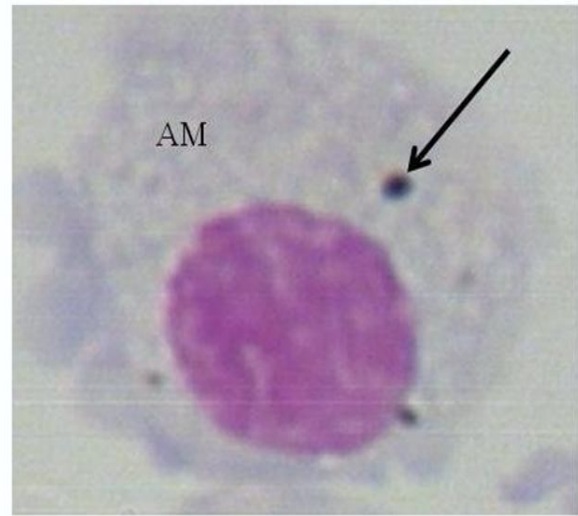
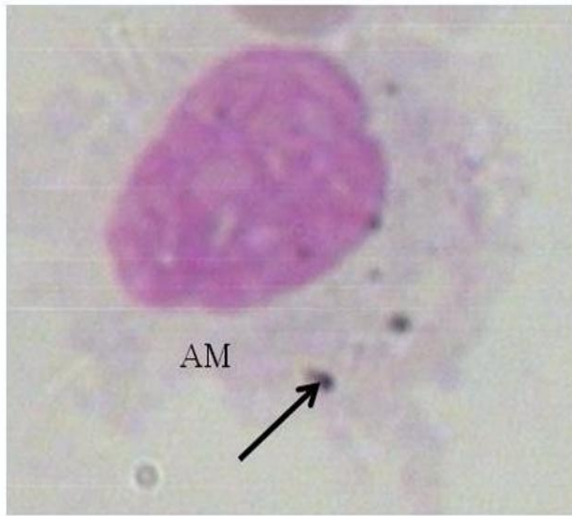


## B. Moderate loading



**Figure 3.1:** Images of ultrafine carbon black (arrowed) instilled alveolar macrophages (AMs) from mice. After 72 hrs of two doses of carbon, cells collected, stained with Diff-Quik and carbon loading measured in 300 randomly selected AMs. Heavily loaded (A) and moderately loaded (B) macrophages were counted more than 50% of the total macrophages.

### C. Light loading



### D. No loading

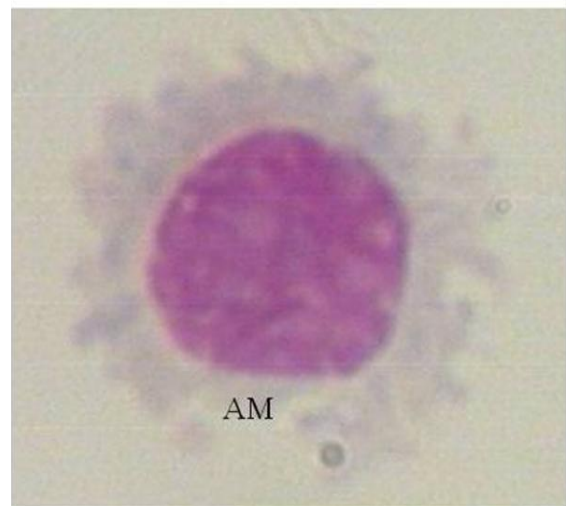
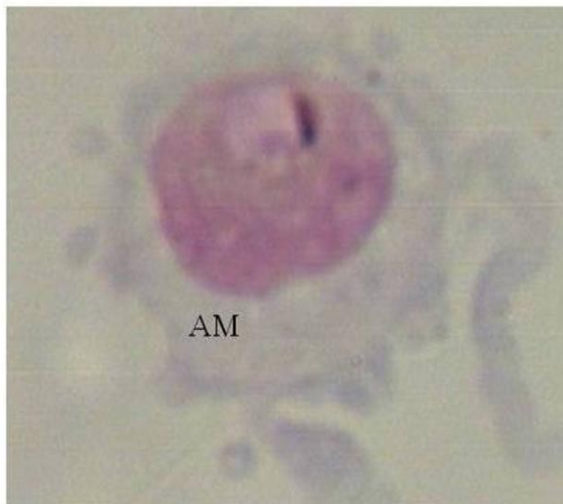


**Figure 3.2:** Images of ultrafine carbon black (arrowed) instilled alveolar macrophages (AMs) from mice. After 72 hrs of two doses of carbon, cells collected, stained with Diff-Quik and carbon loading measured in 300 randomly selected AMs. Lightly loaded (C) and none loaded (D) macrophages were accounted less than 40% of the total macrophages in the lungs.

Most of the macrophages, which were collected from exposed groups, were achieved particle loading inside their cytoplasm. Heavily-laden cells had more than 50% of their cytoplasm containing carbon black. Tightly packed and larger aggregates of carbon black particle clusters were found in the heavily-laden macrophages (Figure 3.1A). In moderately-laden macrophages, only 10 to 50% of the cytoplasm occupied by carbon particles (Figure 3.1B). They consisted of smaller aggregates and larger aggregates of particles in all over their cytoplasm. Lightly-laden alveolar macrophages (Figure 3.2C) had less than 10% cytoplasmic particle burden. Loosely packed smaller aggregates of carbon black particles incorporated in lightly-laden macrophages. Carbon loading was assessed semi-quantitatively as described in table 3.1 and macrophages were counted manually by eye under a light microscope. Particle aggregates of different sizes were often observed on nucleus in heavily-laden group, but not in moderately-laden or in lightly-laden group of macrophages. Figure 3.3 shows the percentage of different levels of carbon loaded macrophages. Significantly high numbers of highly loaded and moderate loaded macrophages were observed in BAL fluid.

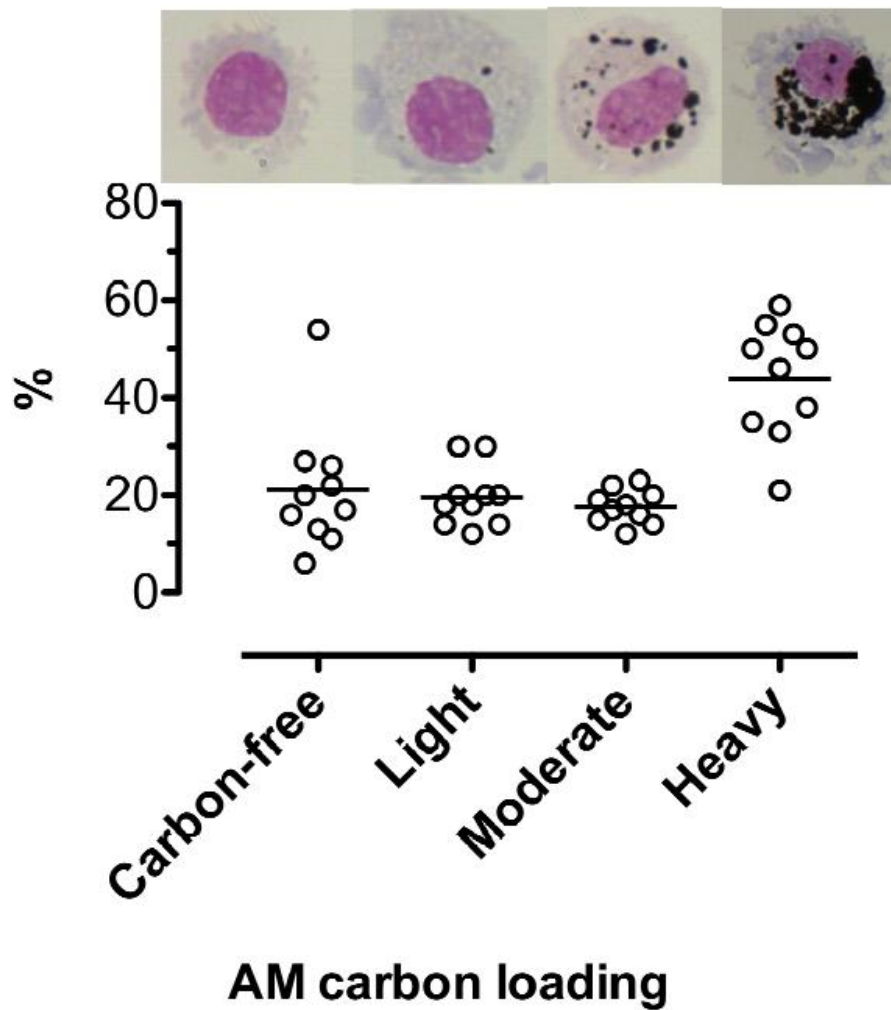


**Figure 3.3:** Carbon loading of alveolar macrophages (AM) from uninfected mice exposed to 2x doses of 500  $\mu\text{g}$  ultrafine-carbon black (UF-CB) in 50  $\mu\text{l}$  phosphate buffered saline (PBS). Bronchoalveolar lavage was performed 72 h after the second dose on day 4. Carbon loading was assessed semi-quantitatively as described in table 3.1. Data are from 10 animals. Bar represents mean. Representative images of BAL fluid AM loading are shown in the upper panel.

**3.1.1. Particle distribution after intratracheal instillation:**

Intratracheal instillation has frequently been used to expose animals to carbon particles. To ensure that UF-CB was properly intratracheally instilled into the lungs, the mice were killed by using high dose of anaesthesia .After 24 hrs of second instillation lungs were dissected and photographed. Lung particle distribution pictures suggested that intratracheal inhalation had evenly deposited the particles in lungs and that this method would not hinder our investigation of the effects of UF-CB. Lungs from two different groups were presented on figure 3.4. Inhalation of carbon particles caused slight increase in size in exposed lung. Carbon exposed lungs were showing progressive accumulation of carbon particles on surface. Analogous effects were observed with lung histological assessment (see section 3.3). As such accumulation particle matter in lungs resulted in the production of pro-inflammatory cytokines (see section 3.8), reactive species (see section 3.4) and in further lung injury and lung scarring (Castranova et al. 2000).

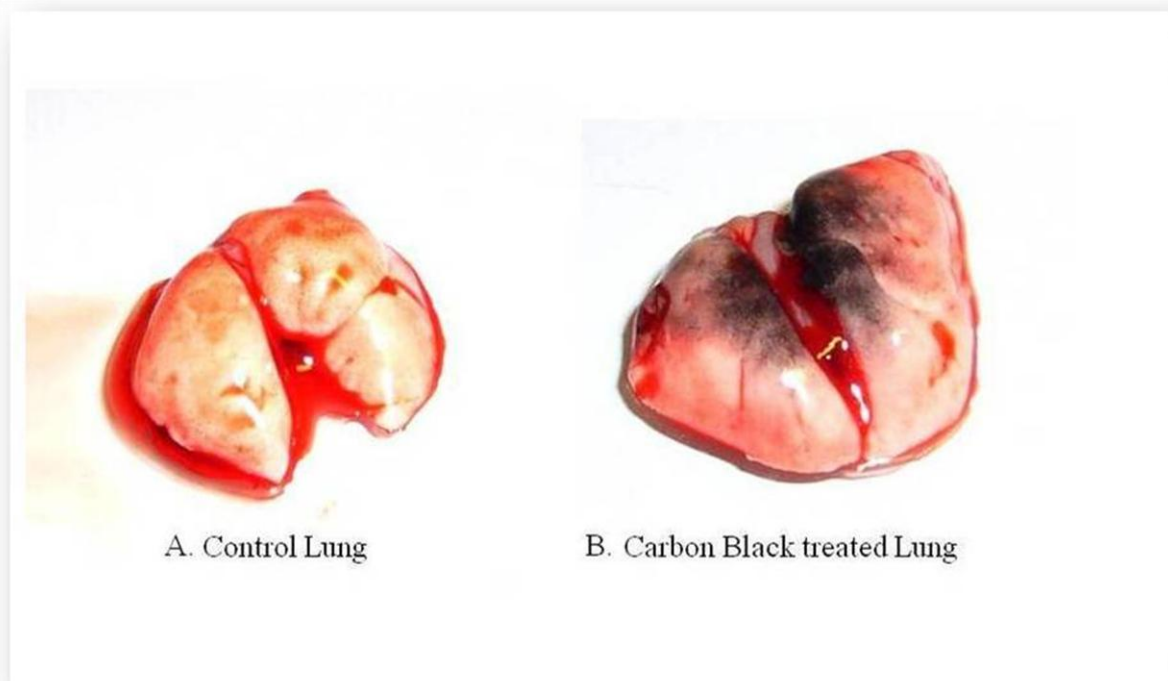


**Figure 3.4:** Examples of lung particle distribution. Lungs from mice instilled with 500  $\mu\text{g}$  of a test material ultrafine-carbon black (UF-CB) per mouse and euthanized 24hrs after the twice treatment. (A) PBS control lung. (B) Carbon black (Printex 90). Carbon can be seen on the lobes and bronchial area of the lung.

**3.1.2. TEM investigation of particle engulfed alveolar macrophage:**

The Transmission electron microscope (TEM) analysis demonstrated a rapid internalisation of the ultra fine carbon particles in the alveolar macrophages after two doses of instillation. The majority of the ultrafine particles were associated as aggregates and entered the cells by phagocytosis (Figure 3.5). Particles aggregates that entered into the cells were not limited to certain area on the macrophages. Smaller particle aggregates were appeared as well as larger aggregates inside alveolar macrophage. Loosely and highly packed particles appeared in all over the cytoplasm. Association of particles with lamellar bodies has been noticed in other studies (Castranova et al. 2000, Sorokin et al. 1989). It was assumed when macrophages observed under the TEM, that membrane enclosed particle aggregates of different size were often observed next to the nucleus but never inside the nucleus. Further studies would be necessary to confirm it.

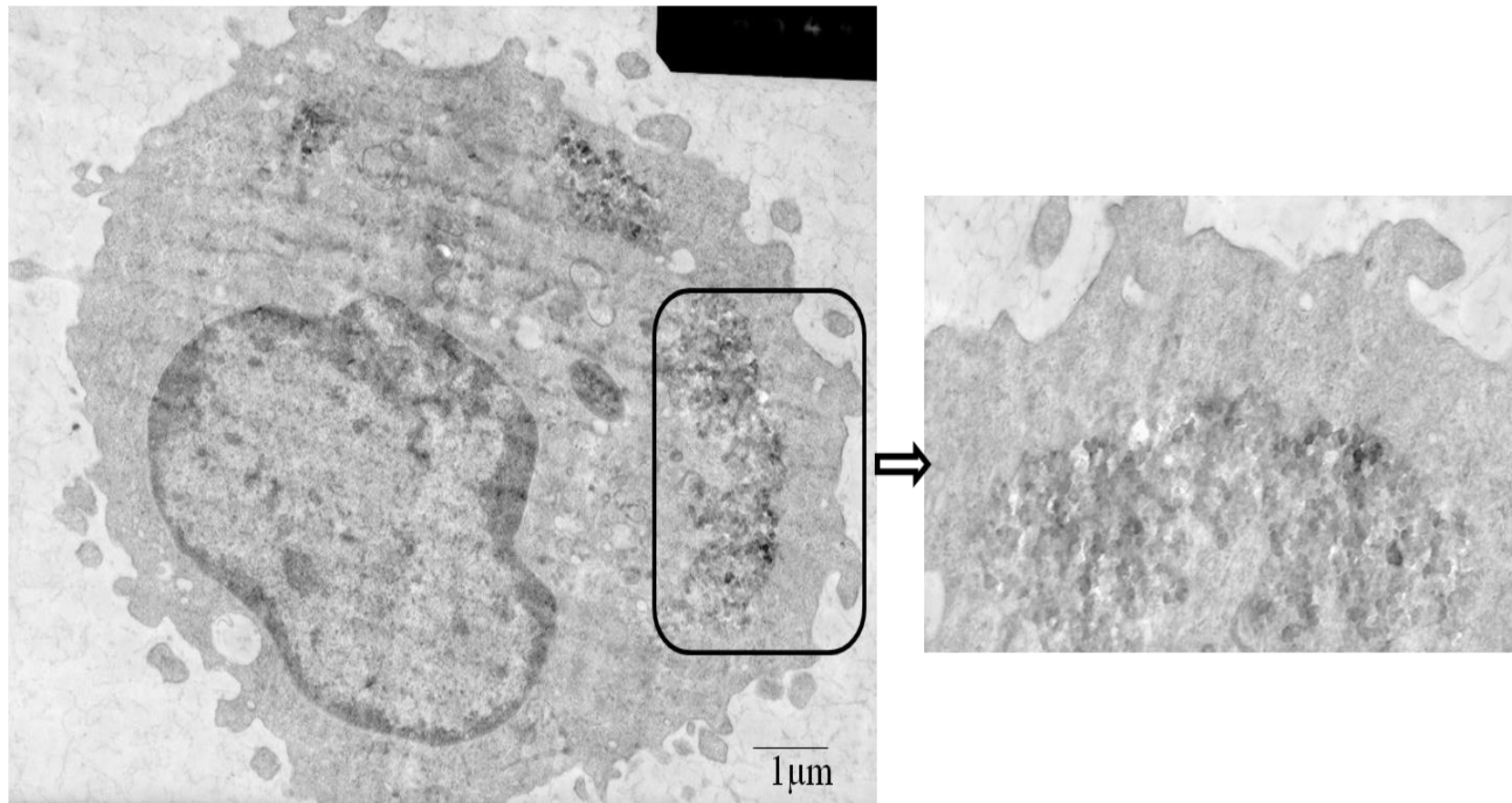


**Figure 3.5:** TEM image of mouse alveolar macrophage exposed to ultrafine carbon particles. Accumulation of the particles inside the macrophage shown clearly in the image (insert). Highly packed particles appeared in all over the cytoplasm of the macrophage.

### **3.2. Analysis of bronchoalveolar lavage fluid:**

Bronchoalveolar lavage is an invaluable means of accurately evaluating the inflammatory and immune processes of the human lung. Mice bronchoalveolar lavage (BAL) fluid obtained after two doses of ultra fine carbon black particle (UF-CB) instillation (see section 2.5.9). Bronchoalveolar lavage (BAL) was obtained from mice by instilling 4 x 500 µl sterile PBS through a 25-gauge needle into the lungs, via the trachea, followed by aspiration of BAL fluid into the syringe. Analysis of BAL cells showed the neutrophil increase in the fluid (Figure 3.6) in carbon black particle alone exposed group. Cytospin studies showed that particles were phagocytosized by pulmonary neutrophils (Figure 3.6). Nearly 80% of the neutrophils from the total cells were engulfed with carbon particles (Figure 3.8). The increase in BAL neutrophils may represent a normal physiological response of the lung to particles and activated neutrophils may release biochemical mediators. This mild inflammatory increase in neutrophils may have shown the protection from infection in our further studies.

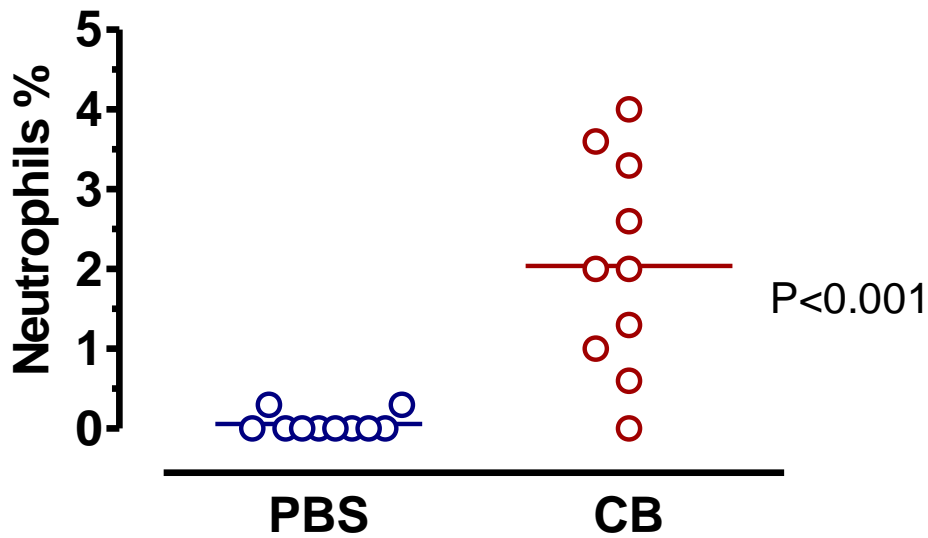
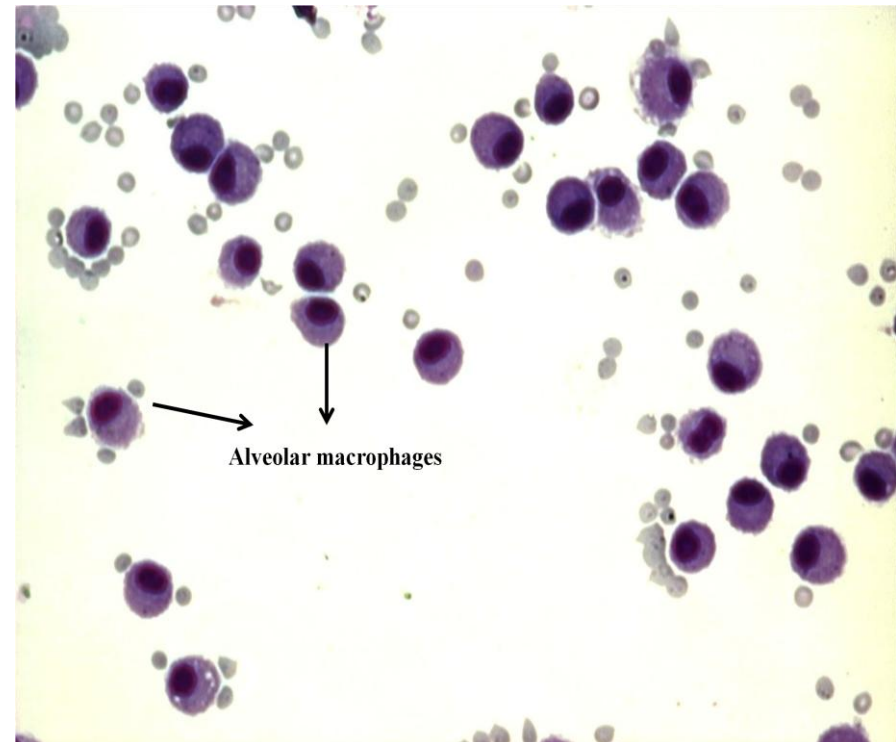
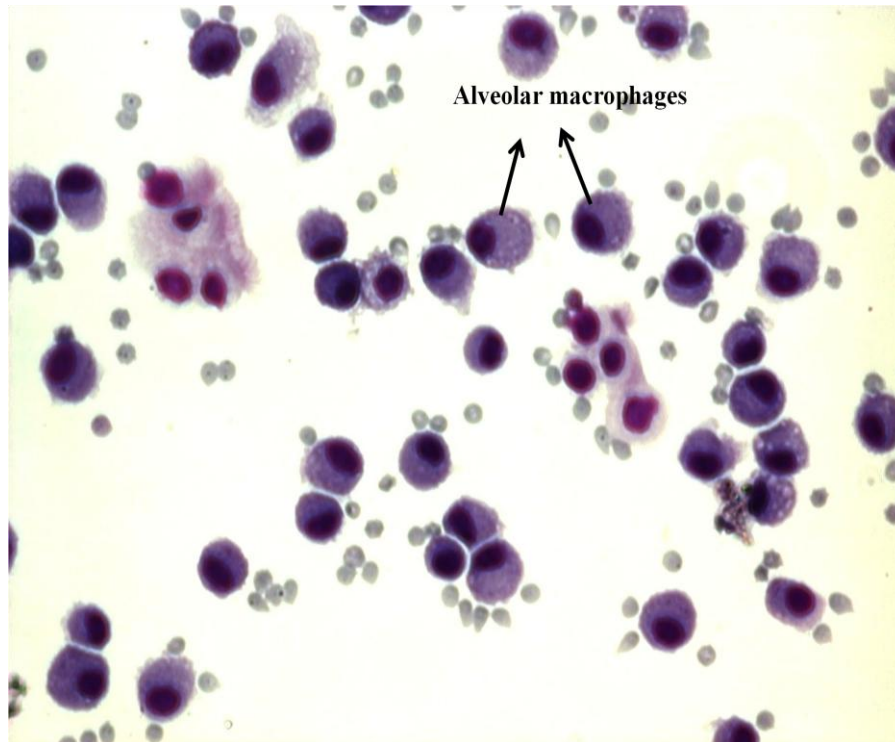


**Figure 3.6:** Neutrophil differential count in bronchoalveolar lavage fluid mice receiving either 2x doses on intranasal sterile PBS alone, or 2 doses of 500  $\mu\text{g}$  ultrafine-carbon black in 50 $\mu\text{L}$  PBS alone (UF-CB). BAL was done 72 h after the second intranasal dose. Each symbol represents an individual mouse. Bar represents mean,  $n=10$ ,  $P < 0.01$  by unpaired t test.

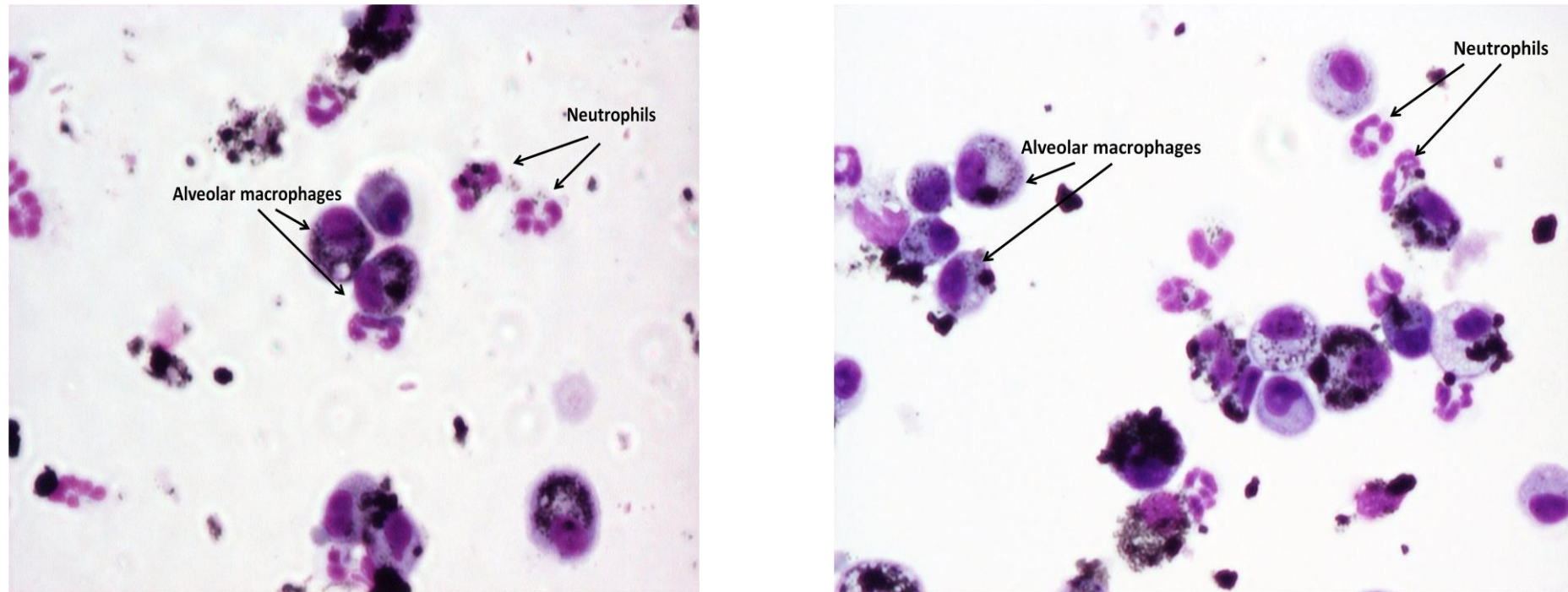
**A. Control group:**

---



---

**Figure 3.7:** Representative fields of control group cytospin slide. Approximately 98 % cells were macrophages of total cells in BALF fluid.

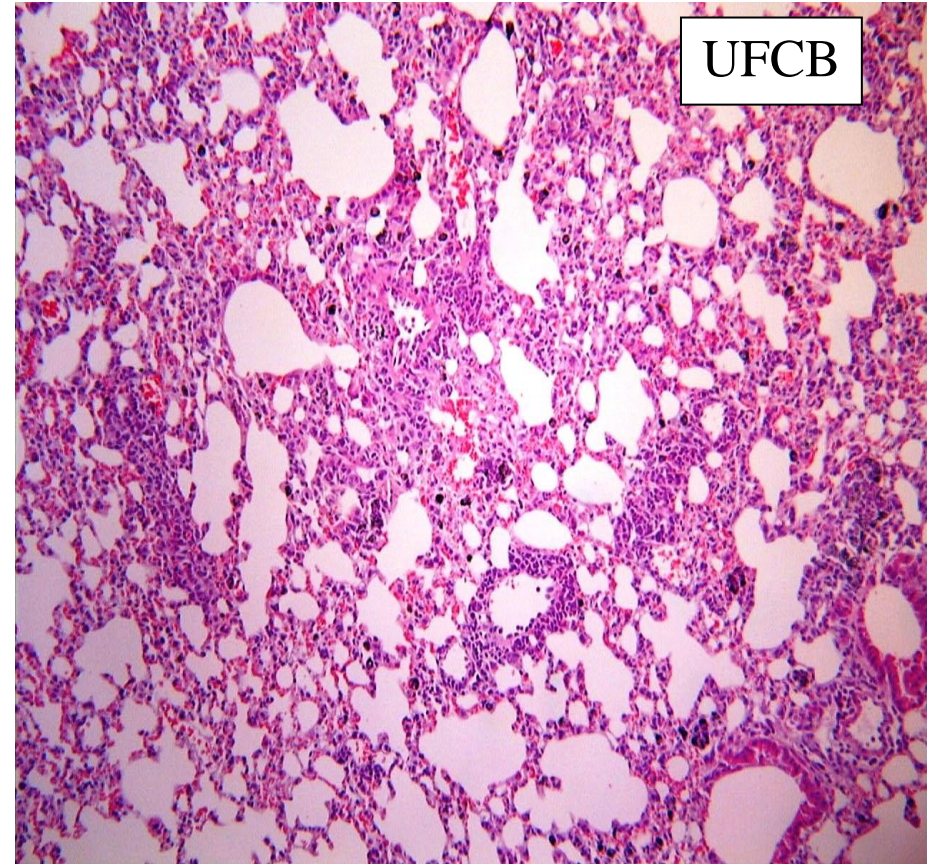
**B. Exposed group:**

**Figure 3.8:** Representative fields of BAL fluid cytospin slides made from ultrafine carbon particle exposed animals. Highly loaded alveolar macrophages and moderately loaded neutrophils were seen in BAL fluid. Significantly high number of neutrophils also appeared in bronchoalveolar lavage fluid (BALF) compared to control group.

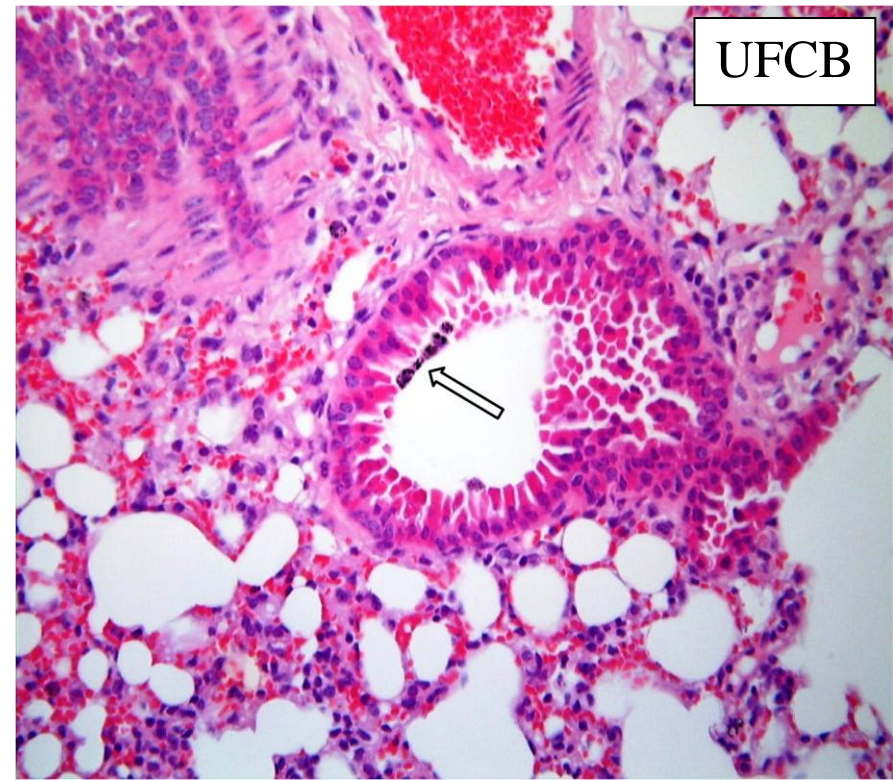
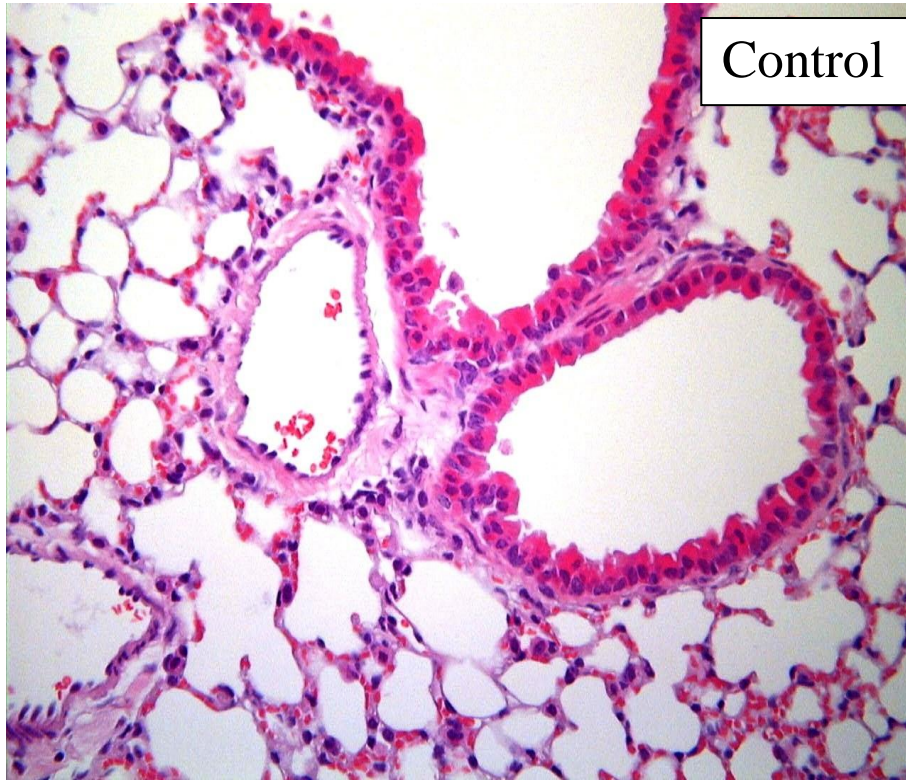
### **3.3. Analysis of lung histopathology:**

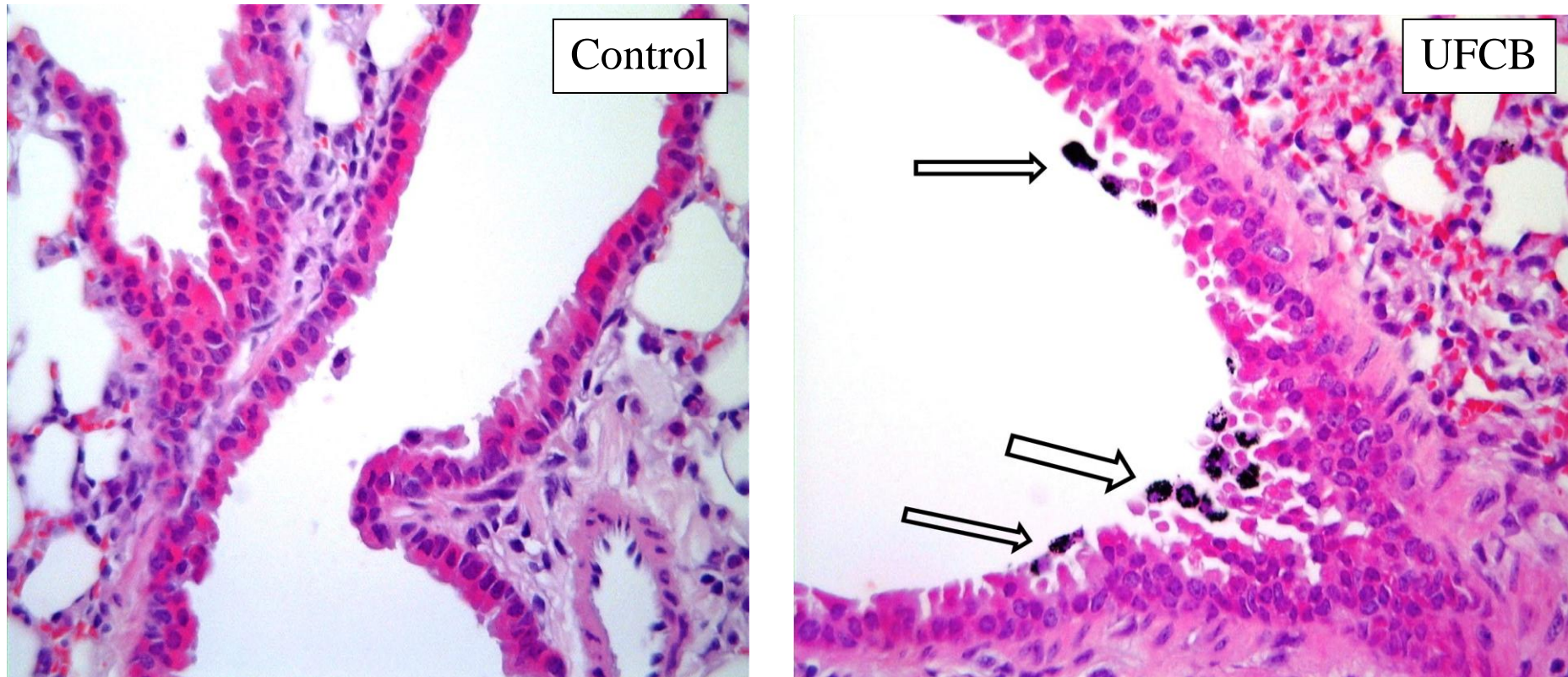
The results suggest that UFCB exposure can produce significant lung inflammation and possible increases in pro-inflammatory signals in the lung. Lung morphology studies after UFCB exposure revealed focal inflammatory responses, some epithelial hyperplasia, and fibrotic responses after acute exposure of MF1 mice ( $n=5$ ) to 500 ug/50 $\mu$ l UFCB. At low magnification (Figure 3.9a), carbon exposed lungs showed thicker walled alveoli and also the accumulation of fine particles of carbon in the lung. Increased PMNs (polymorphonuclear cells), macrophages and larger and more stretched alveoli were observed on the carbon exposed lung tissue. The airway inflammation was also confirmed by histological examination, showing perivascular and peribronchial infiltrates (Figure 3.9b and Figure 3.9c). Carbon loaded macrophages were clearly observed in the bronchial lumen (Figure 3.9b and Figure 3.9c). Full histo-pathological report was enclosed for the lung tissue of control and exposed groups (Table 3.2).

**A. Magnification 25x**



**B. Magnification 100x**



**C. Magnification 250x**

**Figure 3.9 A, B, C:** Lung histology of uninfected mice exposed to intranasal PBS (Control) and 2x doses of 500  $\mu\text{g}$  ultrafine-carbon black (UF-CB). Sections were imaged under light microscopy (A:50X, B:100X and C: 250x magnification). Changes induced by UF-CB are given in Table 3.2. The most distinctive feature is carbon-laden alveolar macrophages (arrow). There is no evidence of free carbon in the airway, or significant uptake of carbon by other airway cells.

**Table 3.2:** Histopathological examination of mice lung tissue

<b>PBS:</b>	
<b>Description</b>	<b>Severity</b>
Alveolar microvascular congestion	Minimal
Leucocyte infiltration	Minimal
<b>UFCB:</b>	
<b>Description</b>	<b>Severity</b>
Black particle inclusions mainly within alveolar macrophages	Moderate to marked
Alveolar microvascular congestion	Marked
Pneumonitis with consolidated microvascular leak	Marked
ATII hyperplasia	Marked
Alveolar wall fibroplasia	Moderate
Endothelial cell hypertrophy with leucocyte adhesion	Moderate to marked
Leucocyte infiltration of blood vessel walls	Moderate to marked
Bronchiolar epithelial hypertrophy	Marked
Black particle inclusions within bronchiolar epithelium	Moderate
Leucocyte infiltration of airway walls	Marked
Hypertrophy of transitional airway epithelium	Moderate
Hypertrophy of mesothelium	Moderate to marked

### 3.3.1. Assessment of haemorrhage on lung histological sections:

Mice group exposed to ultrafine carbon black had increased levels of haemorrhage after the intranasal instillation of 2x doses of UF-CB.

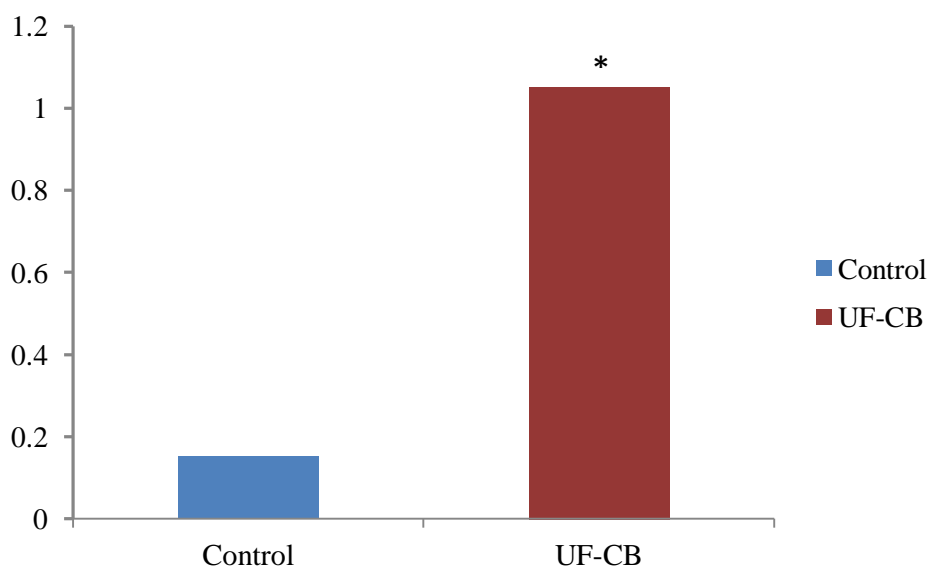


**Figure 3.10:** Lung haemorrhage was measured in lung tissue of control and exposed groups. A significant level of haemorrhage was found in carbon exposed groups.

### 3.4. Determination of 8-oxodG in mice urine samples:

Oxidative stress bio marker 8-oxo-7,8-dihydro-2'-deoxyguanosine (8-oxodG) was measured by liquid chromatography-electro spray ionization-tandem mass spectrometry (LC-ESI-MS/MS) as described in ( See section 2.7). Urine was collected 72 h after the second intranasal instillation of 2x intranasal doses of

500  $\mu\text{g}$  ultrafine-carbon black (UF-CB) in PBS or PBS alone. Increased urinary 8-oxodG was observed in UF-CB-exposed mice ( $n=6$ ) (Figure 3.10).

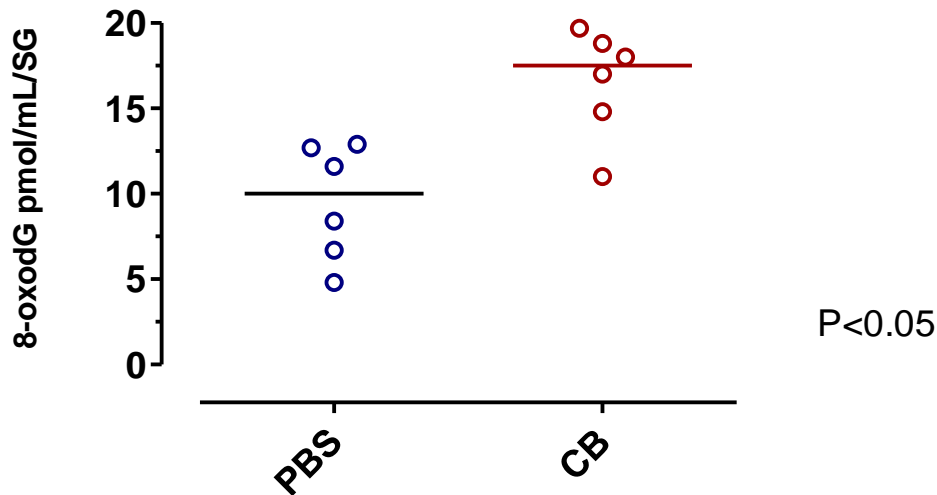


**Figure 3.11:** Urinary 8-oxodG in the urine of mice treated with i) 2x intranasal doses of PBS alone, and ii) 2x intranasal doses of 500  $\mu\text{g}$  ultrafine-carbon black (UF-CB) in PBS alone. Urine was collected 72 h after the second intranasal instillation. 8-oxodg was assayed by liquid chromatography-electro spray ionization-tandem mass spectrometry and results corrected for specific gravity. Bar represents mean,  $n=6$  per group, \*  $P<0.05$  by unpaired t test.

### 3.5. Disease and survival of mice after particle instillation and infection:

To assess the effect of exposure to UF-CB on susceptibility to pneumococcal infection, animals first received two doses of either intranasal sterile PBS or intranasal UF-CB (500  $\mu\text{g}$  UF-CB in 50  $\mu\text{l}$  sterile PBS) and later received either

intranasal 50 µl sterile PBS or  $1 \times 10^6$  colony forming units (CFU) *S. pneumoniae* in 50 µl sterile PBS. Mice were regularly monitored for signs of disease for up to 72 h after infection, or until they became severely lethargic, at which point animals were humanely sacrificed. After infection, the signs of disease of the mice were frequently evaluated and scored as explained in section 2.3.4. Briefly, a mouse was given a score of 0 if it showed no signs of disease; score of 2 if it was hunched, score of 4 if it had a starey coat and score of 6 if it was lethargic, at which point the mice was culled. For description purposes, if a mouse reached a score of 6 and was consequently culled before the end of the experiment (72 hours), this score continued to be used to represent the culled mouse.

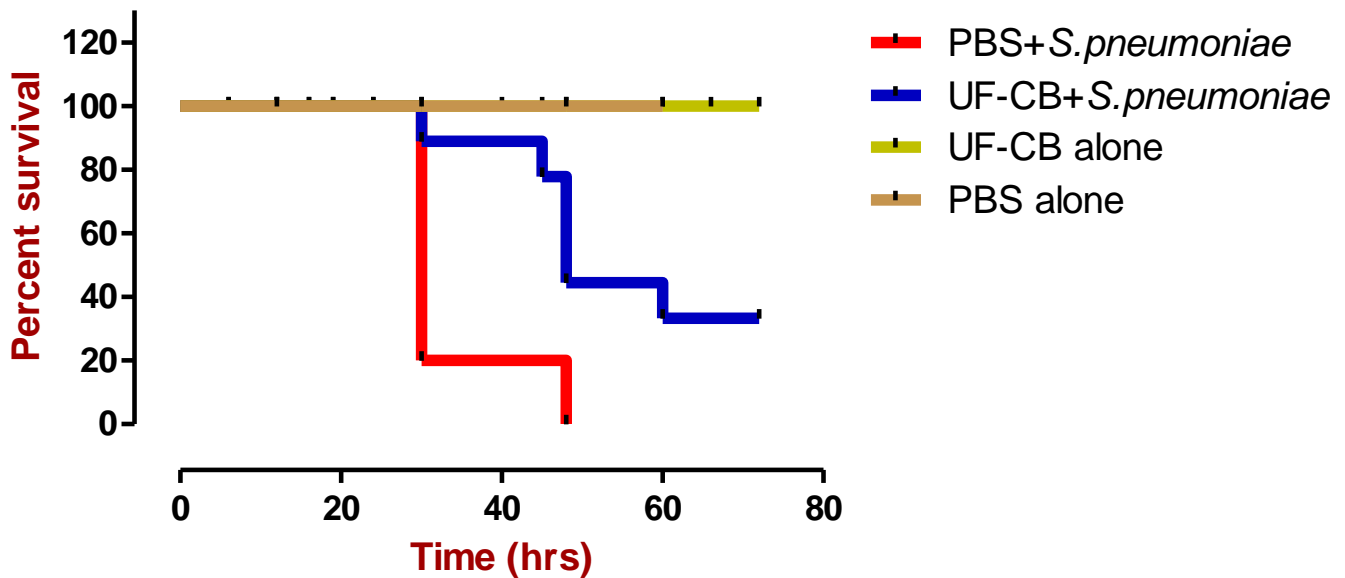


**Figure 3.12:** Survival curves of mice infected with pneumococci and pre-treated with; i) 2x intranasal doses of sterile PBS (PBS +infection) ii) 2x intranasal doses of 500  $\mu\text{g}$  ultrafine-carbon black (UF-CB +infection) iii) animals treated with PBS alone and iv) UF-CB alone had no morbidity. Data shown are representative of > 4 separate experiments done at different times each with 10 animals per group. In the data plotted, median survival of PBS treated mice was 30 h. In contrast, median survival in UF-CB treated mice was 48 h (hazard ratio 8.5 (95% CI 2.0 to 36),  $P < 0.001$  by log rank test).



**Figure 3.13:** Data shown are representative of four separate experiments done at different times each with 10 animals per group. All animals (ten out of ten) from the PBS+ *S. pneumoniae* group died within 3 days after the bacterial challenge (mean survival time=33.6 hours), whereas four animals out of ten animals from UFCB+ *S. pneumoniae* group were survived to the end of the experiment (mean survival time=56.7 hours).

Animal survival was analysed by a Kaplan-Meier curve (Figure 3.11). Survival after infection with *S. pneumoniae* was assessed up to 72 h. Initial experiments included uninfected (PBS alone and UF-CB alone) animals. However, no morbidity or mortality was observed in these uninfected groups. Additional survival experiments therefore used infected mice only (Figure 3.12 and Figure 3.13). All PBS-treated animals succumbed from pneumococcal infection by 72 hrs. In contrast, exposure to UF-CB consistently delayed time to death from

infection and increased morbidity-free survival at 72 h (Fig 6,  $P < 0.001$ , log rank test). Survival of UF-CB treated animals from pneumococcal infection at 72 h in over 4 separate experiments was between 40 % and 60 %, with surviving animals remaining disease-free for several days after the experiment. These results are reflected in the disease scores. Disease scores were significantly lower ( $P < 0.05$ ) in UF-CB exposed and infected group compared to infection alone group (Figure 3.13).

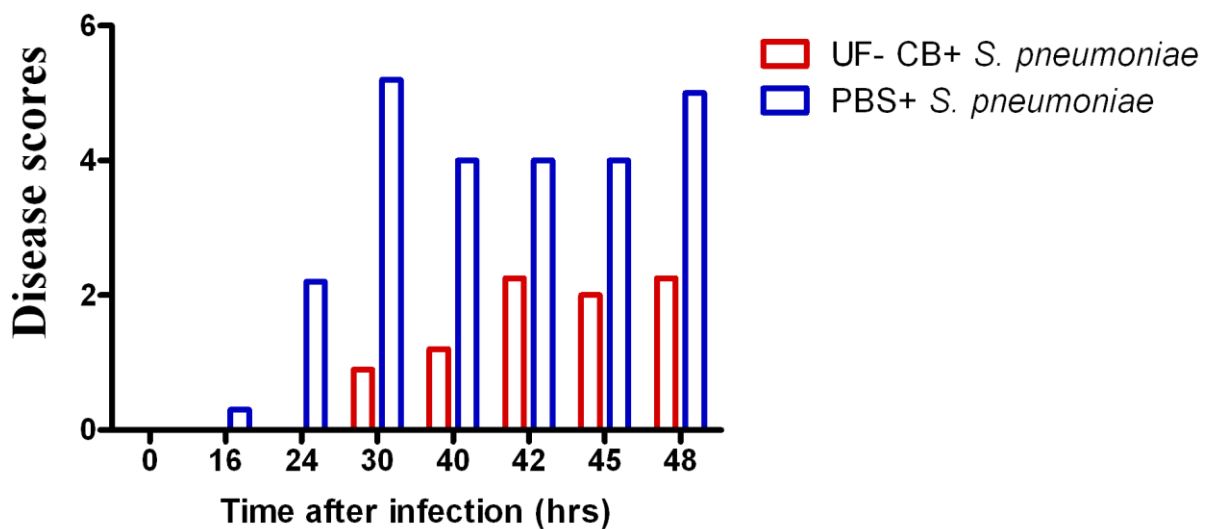


**Figure 3.14:** Disease scores of mice infected with pneumococci ( $1 \times 10^6$  cfu) and pre-treated with UF-CB. Data shown are representative of four separate experiments done at different times each with 10 animals per group. Disease scores from mice exposed to UF-CB were significantly lower ( $P < 0.05$ , T-test) than from mice that received infection alone.

### **3.6. Estimation of CFU from lungs and blood after intranasal infections at 2 hours and 24 hours:**

For 2 hours post infection experiment, three MF1 mice were used for both groups. To measure the morbidity caused by UF-CB, the number of bacteria from the lungs and blood of infected alone mice and UF-CB and infected groups were assessed at 2 hours post-infection. It is very unlikely to see changes in bacterial CFU counts at 2 hours post-infection. So, it is ethically acceptable to use the minimum number of animals for this experiment. Intranasal instillation of either PBS or UF-CB (500 µg/50 µl) and infection were administered the same way as described in 2.5.2. Figure 3.14 shows the number of bacteria in the lungs of mice after 2 hours of infection. No significant differences were observed in the lung tissue at 2 hour post-infection. As expected, no bacteria found in the blood of intranasally infected mice at 2 hour post-infection.

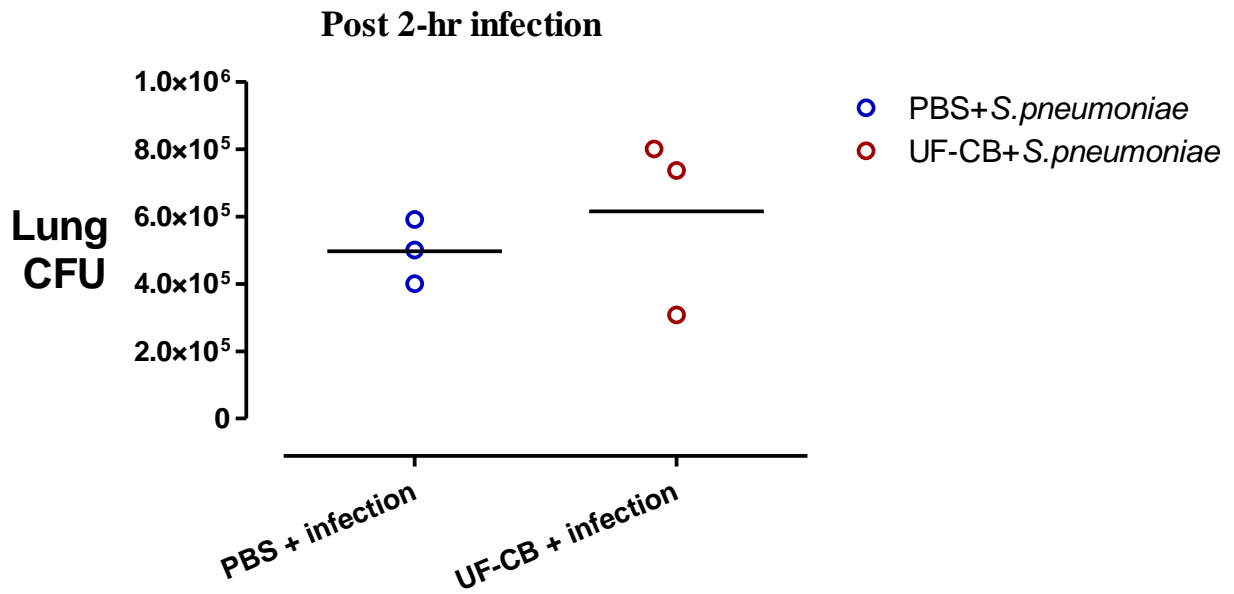


**Figure 3.15:** Lung CFU counts in mice treated with either 2x doses of sterile PBS or 2x doses of 500  $\mu\text{g}$  ultrafine-carbon black (UF-CB), then infected intranasally with pneumococci. Lung CFU count was assessed at 2 h post-infection.  $n=3$ , Bar represents mean.

For 24 hours post infection experiment, six MF1 mice were used at each point for both groups. Intranasal instillation of either PBS or UF-CB (500  $\mu\text{g}/50 \mu\text{l}$ ) and infection were administered the same way as described in 2.5.2. Figure 3.15 shows the number of bacteria in the lungs of mice after infection. As it can be seen from the figure 3.15 and figure 3.16, infection alone group showed higher levels of bacteria than group with UF-CB and infected with *S. pneumoniae* D39 in lungs and blood as well.

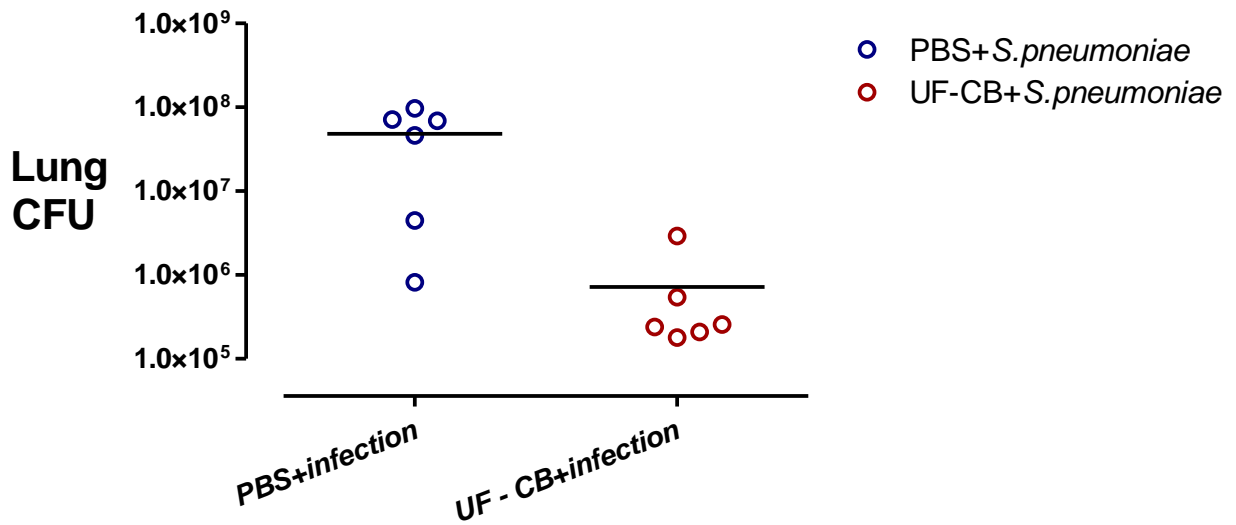


**Figure 3.16:** Post 24 hours lung CFU counts in mice treated with either 2x doses of sterile PBS or 2x doses of 500  $\mu$ g ultrafine-carbon black (UF-CB), then infected intranasally with pneumococci. Lung CFU count was assessed at 24 h post-infection.  $n=6$ , Bar represents mean.  $*P < 0.05$  by unpaired t test.

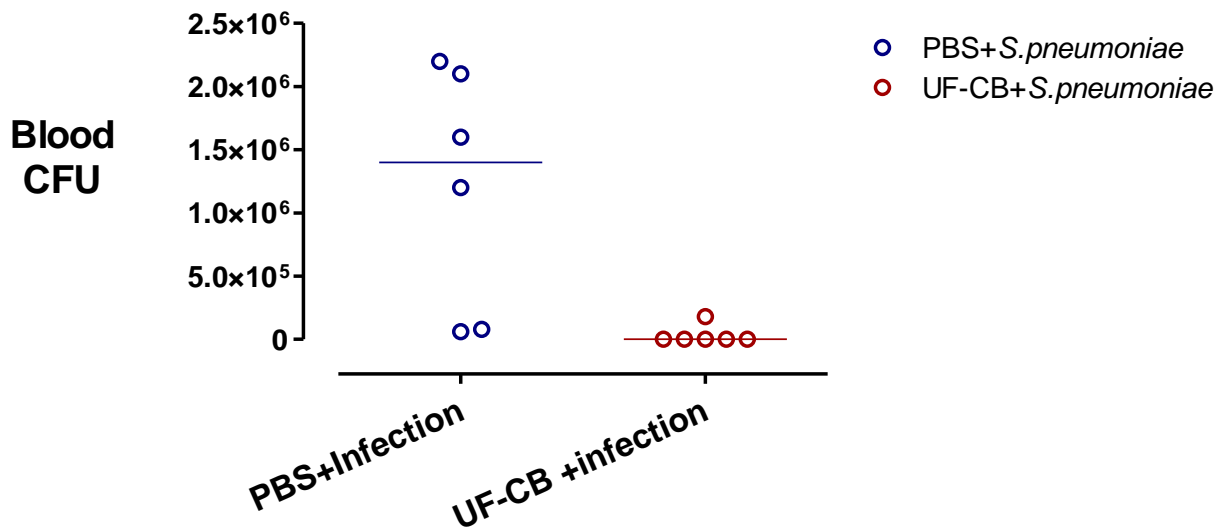


**Figure 3.17:** Post 24 hours blood CFU counts in mice treated with either 2x doses of sterile PBS or 2x doses of 500  $\mu$ g ultrafine-carbon black (UF-CB), then infected intranasally with pneumococci. Blood CFU count was assessed at 24 hours post-infection.  $n=6$ , Bar represents mean.  $*P < 0.05$  by unpaired t test.

### **3.7. Comparison of bacterial growth in lungs and blood at different time points:**

To determine whether increased survival after exposure to UF-CB was associated with decreased bacterial load in lung tissue and blood, pneumococcal CFU counts were measured at different time points up to 24 hours (4hours, 6 hours, 12 hours and 24hours). Five MF1 mice were used at each point for each group. As it can be seen from the figure 3.17 and figure 3.18, mice group infected with *S. pneumoniae* D39, showed higher levels of bacteria throughout than mice group with UF-CB and infected. Lung CFU counts were initially low in both PBS- and UF-CB-treated groups at 4 and 6 hrs after infection ( $P=NS$ , Figure 3.17). However by 12 h, lung CFU counts were lower in UF-CB treated animals, and by 24 h this decrease was significant ( $P<0.01$ ,  $n=5$ ).

As expected, blood CFU counts ( $P=NS$ , Figure 3.18) were very low until 12 hours. But, by 12 hours onwards bacterial growth was increased significantly in both groups. However, there was a significantly higher level of bacteria in infection alone group ( $P<0.01$ ,  $n=5$ ).

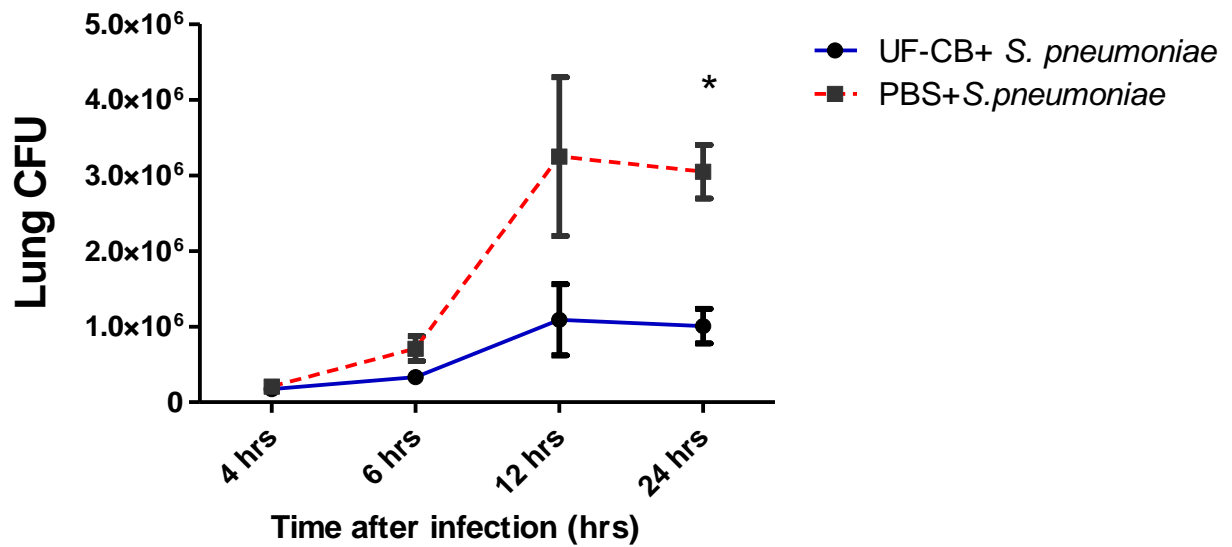


**Figure 3.18:** Lung CFU counts in mice treated with either 2x doses of sterile PBS or 2x doses of 500  $\mu\text{g}$  ultrafine-carbon black (UF-CB), then infected intranasally with pneumococci. Lung CFU count was assessed at different time points post-infection ( $n=5$ ), Data are described by mean +SEM,  $n=5$  for each time point for each group. \*  $P<0.01$  by unpaired t test.

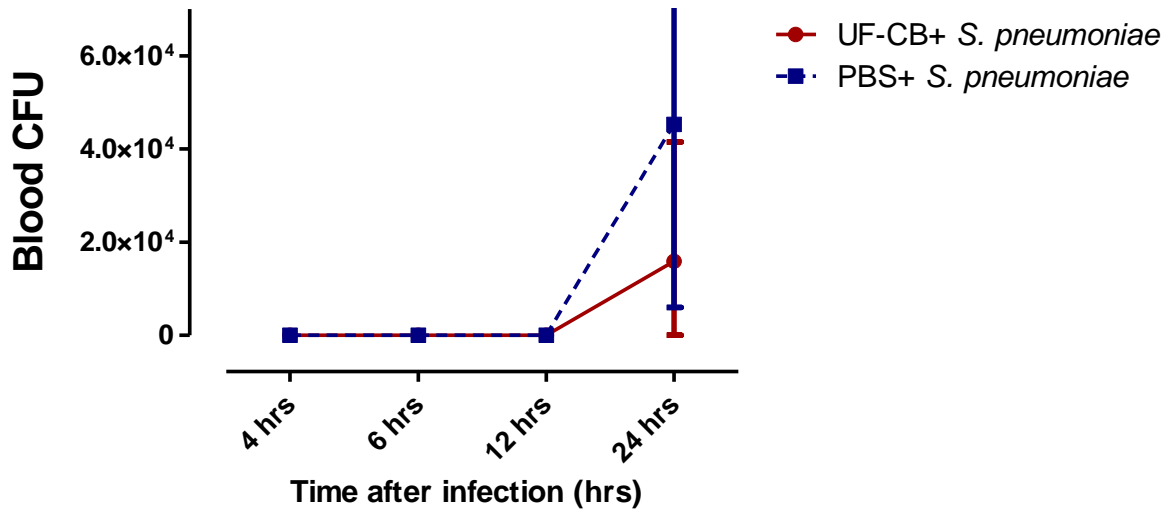


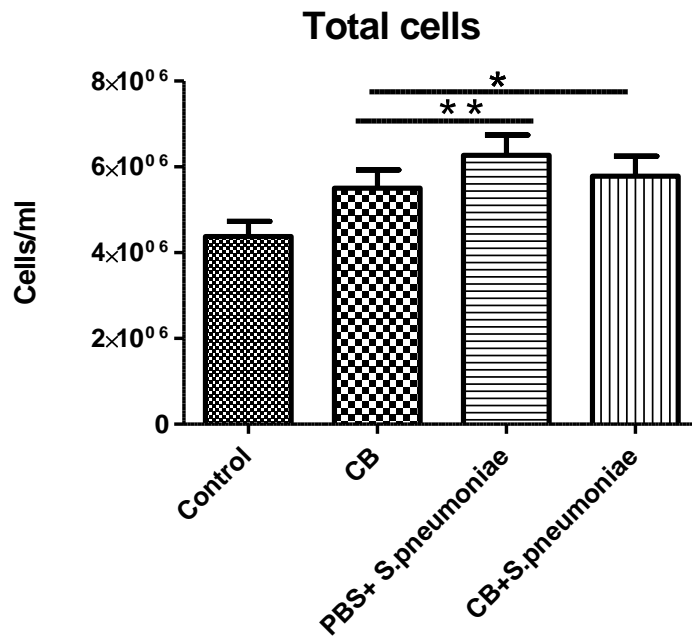
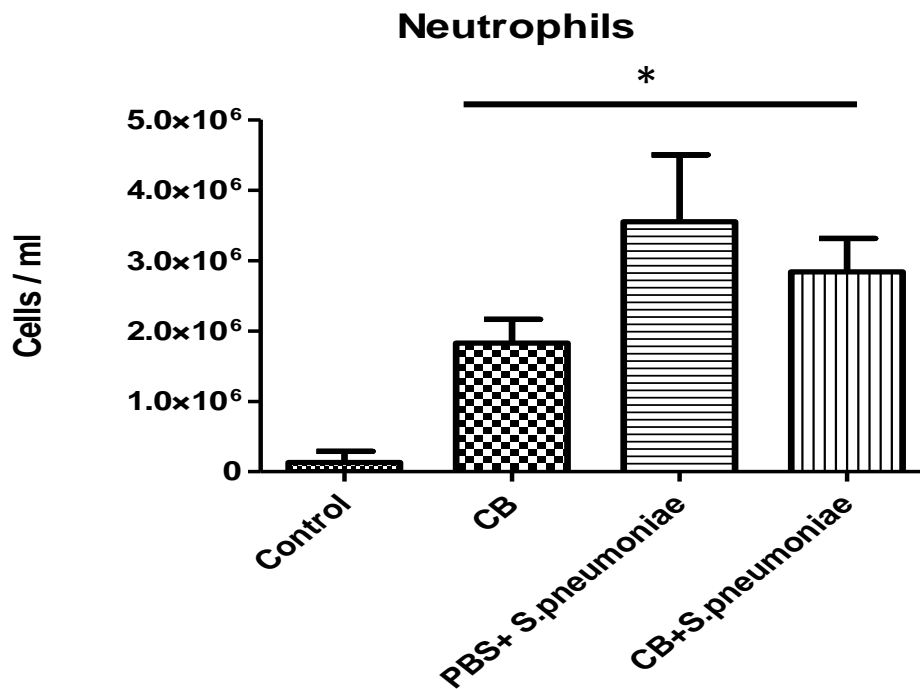
**Figure 3.19:** Blood counts in mice treated with either 2x doses of sterile PBS or 2x doses of 500  $\mu\text{g}$  ultrafine-carbon black (UF-CB), then infected intranasally with pneumococci. Blood CFU count was assessed at different time points post-infection ( $n=5$ ), Data are described by mean +SEM,  $n=5$  for each time point for each group. \*  $P<0.01$  by unpaired t test.

### 3.8. Post infection Cellular analysis of bronchoalveolar lavage fluid:

Bronchoalveolar lavage (BAL) was performed on animals ( $n=6$ ) 74 hours after the last challenge. Control group received two doses on intranasal sterile PBS alone and carbon black (CB) group received 2 doses of 500  $\mu\text{g}$  ultrafine-carbon black alone in 50  $\mu\text{L}$  PBS. For the Infection groups (PBS+ *S.pneumoniae* and UF-CB + *S.pneumoniae* groups), animals first received either intranasal sterile PBS or intranasal UF-CB (500  $\mu\text{g}$  UF-CB in 50  $\mu\text{l}$  sterile PBS) and later  $1 \times 10^6$  colony forming units (CFU) *S. pneumoniae* in 50  $\mu\text{l}$  sterile PBS. Total cell

counts were quantified by haemocytometer. BAL differential cell counts were performed on cytocentrifuge slides stained with Diff-Quick (Dade Behring; Deerfield, IL, USA). BAL sample analysis (total cell count, neutrophils and macrophages) of groups compared to control.

Alveolar macrophages, neutrophils and monocytes were counted from the BAL of all the groups. Data was calculated from 300 cells from each group. Airway inflammation was confirmed in BAL samples (Figure 3.19A) where total cell counts were significantly higher in UF-CB exposed and infected groups ( $P < 0.005$ ) in comparison to control group. Total cell were also significantly higher in BAL samples in infected groups compared to carbon treated group. Moreover, a prominent neutrophilia was present in BAL samples (Figure 3.19B). Significantly ( $p < 0.005$ ) increased numbers of neutrophils were found in exposed groups. There is also significant difference ( $p < 0.005$ ) between UFCB instilled and not instilled groups after infected with *Streptococcus pneumoniae*. Whereas the macrophage count was decreased in UF-CB exposed and infected groups compared to control group (Figure 3.19C) and did not differ significantly between the groups ( $p < 0.005$ ).

**A. Total cells:****B. Neutrophils:**

## C. Macrophages

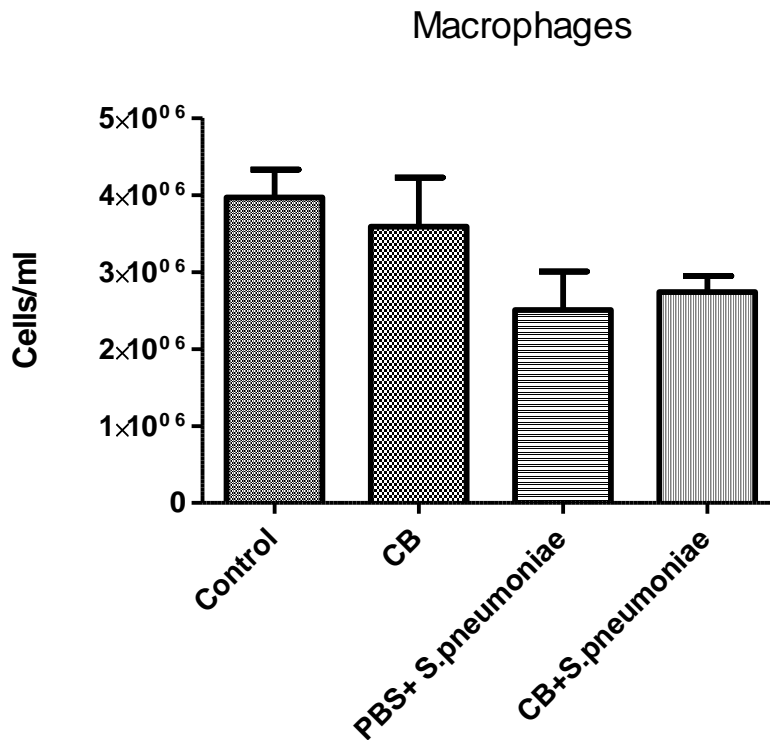


**Figure 3.20 A, B, C:** To observe inflammatory changes, animals ( $n=6$ ) were exposed to UF-CB followed by infection. Cellular content of the bronchoalveolar lavage fluid was assessed. Total cell counts were quantified by hemocytometer. BAL differential cell counts were performed on cytocentrifuge slides stained with Diff-Quick (Dade Behring; Deerfield, IL, USA). Data are calculated from 300 cells from each group. Significantly ( $p < 0.005$ ) increased numbers of total cells (A) neutrophils (B) were found in exposed groups. The macrophage (C) cell count was significantly decreased in other groups compared to control group.

### **3.9. Pro-inflammatory cytokine levels in the presence and absence of UF-CB and/or infection in bronchoalveolar lavage fluid:**

To determine the levels of inflammatory cytokines after exposure to UF-CB in association with or without infection in BAL fluids were measured by 96-well multi-spot plate (MSD, Gaithersburg, USA). BAL fluid was collected after 24 hours after pneumococcal infection in infected groups and after 24 hours of post second dose of UF-CB in exposed group. Control group of mice received sterile phosphate-buffered saline (PBS).

The concentration of inflammatory cytokines, namely interferon (IF)- $\gamma$  , interleukin (IL)-  $1\beta$ , interleukin (IL)-10, interleukin (IL)- 12, interleukin (IL)- 6, interleukin (IL)-8 and tumor necrosis factor (TNF)- $\alpha$  were measured in BAL fluid ( Figure 3.20 ,  $n=5$ ).

In contrast to interferon- $\alpha$  and interferon- $\beta$ , which can be expressed by all cells, IFN- $\gamma$  is secreted by T helper cells (specifically,  $T_h1$  cells), cytotoxic T cells ( $T_C$  cells) and NK cells. IFN- $\gamma$  increases lysosome activity of macrophages and activates plasma B cells. In this experiment, IFN- $\gamma$  levels were measured in response to UF-CB and pneumococcal infection. Although exposure to UF-CB alone or infection did not induce measurable enhancement of IFN- $\gamma$ , mice group infected with pneumococci resulted in significant enhancement of IFN- $\gamma$  (Figure 3.20A).

IL-1 $\beta$  is a member of the interleukin 1 cytokine family and produced by activated macrophages. This cytokine is an important mediator of the inflammatory response, and is involved in a variety of cellular activities, including cell proliferation, differentiation, and apoptosis. . In this experiment, IL-1 $\beta$  levels were measured in response to UF-CB and pneumococcal infection. Although exposure to UF-CB alone or infection did not induce measurable enhancement of IL-1 $\beta$ , mice group infected with pneumococci resulted in significant enhancement of IL-1 $\beta$  (Figure 3.20B).

Interleukin-10 (IL-10) is an anti-inflammatory cytokine and is produced primarily by monocytes and to a lesser extent by lymphocytes. In this experiment, IL-10 levels were measured in response to UF-CB and pneumococcal infection. Although a slight increase of IL-10 cytokine found in infected group, it is not significant compared to other groups (Figure 3.20C).

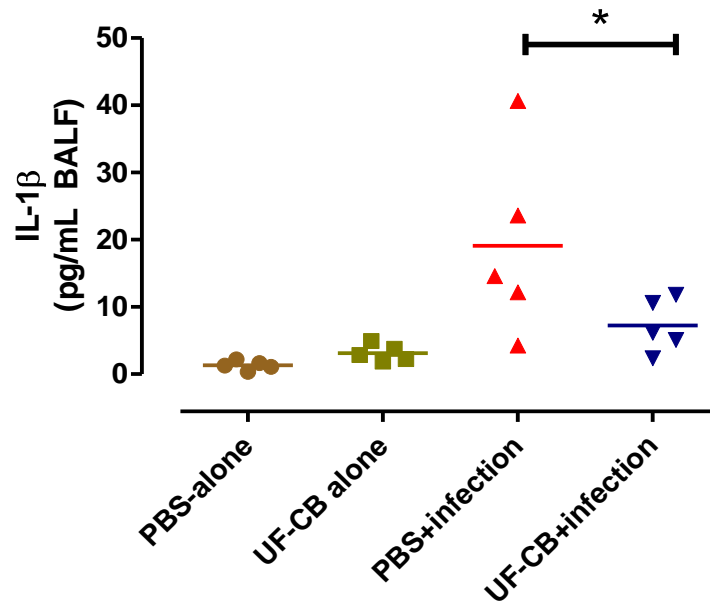
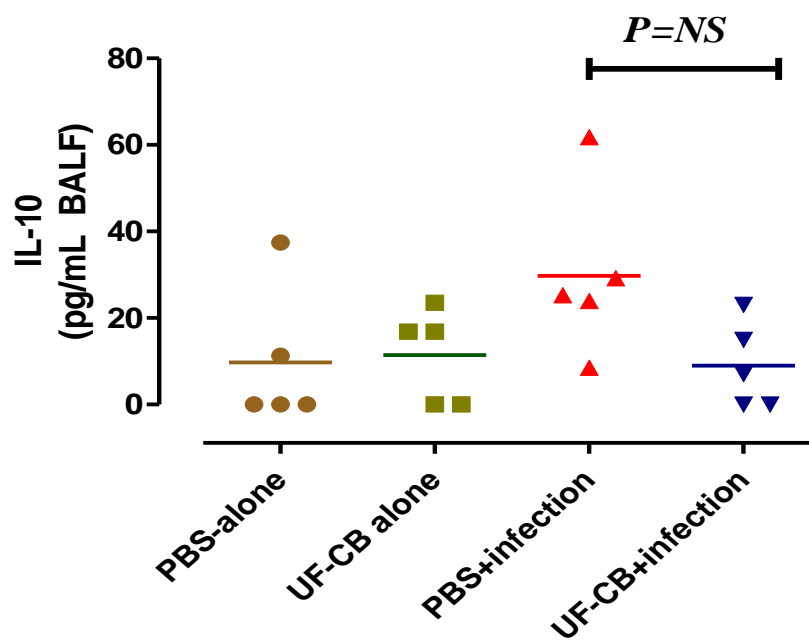
Interleukin 12 (IL-12) is produced by dendritic cells, macrophages and B cells in response to antigenic stimulation. In this experiment, IL-12 levels were measured in response to UF-CB and pneumococcal infection. Although exposure to UF-CB alone or infection did not induce measurable enhancement of IL-12, mice group infected with pneumococci resulted in significant enhancement of IL-12 (Figure 3.20D).

Interleukin-6 (IL-6) is an interleukin that acts as both a pro-inflammatory and anti-inflammatory cytokine. It is secreted by T cells and macrophages to stimulate immune response. In this experiment, IL-6 levels were measured in response to UF-CB and pneumococcal infection. Although exposure to UF-CB alone or infection did not induce measurable enhancement of IL-6, mice group infected with pneumococci resulted in significant enhancement of IL-6 (Figure 3.20E).

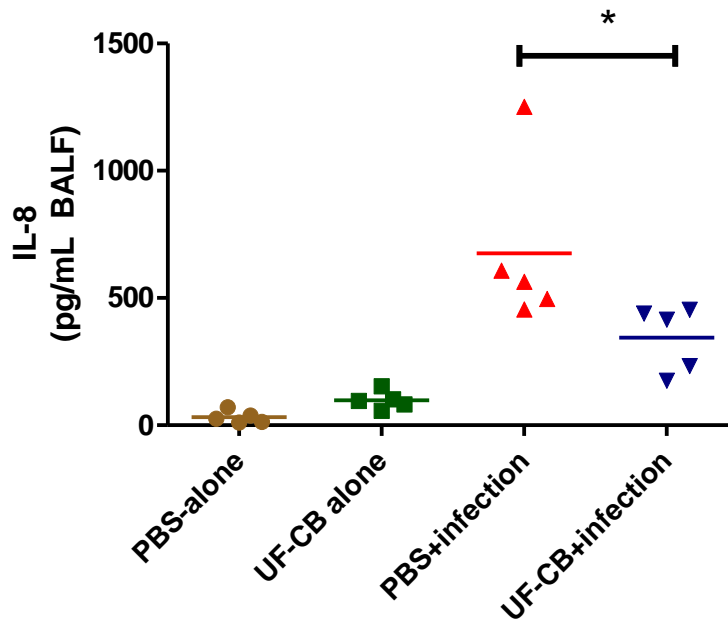
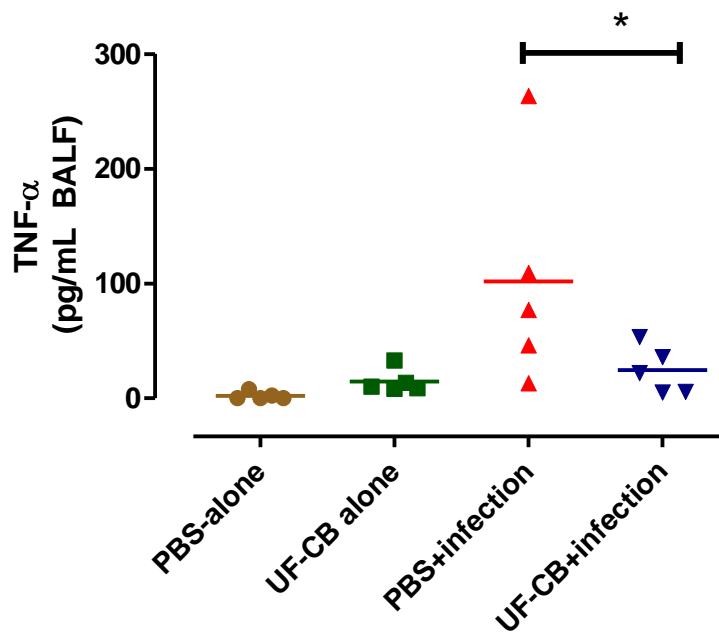
Interleukin-8 (IL-8) is a chemokine produced by macrophages and other cell types such as epithelial cells. In this experiment, IL-8 levels were measured in response to UF-CB and pneumococcal infection. Although exposure to UF-CB alone or infection did not induce measurable enhancement of IL-8, mice group infected with pneumococci resulted in significant enhancement of IL-8 (Figure 3.20F).

Tumor necrosis factor (TNF- $\alpha$ ) is a cytokine involved in systemic inflammation and is a member of a group of cytokines that stimulate the acute phase reaction. It is produced chiefly by activated macrophages, although it can be produced by other cell types as well. In this experiment, TNF- $\alpha$  levels were measured in response to UF-CB and pneumococcal infection. Although exposure to UF-CB alone or infection did not induce measurable enhancement of TNF- $\alpha$ , mice group infected with pneumococci resulted in significant enhancement of TNF- $\alpha$  (Figure 3.20G).



**B. Interleukin (IL)- 1 $\beta$  :****C. Interleukin (IL)-10:**



**F. Interleukin (IL)-8:****G. Tumor necrosis factor (TNF)- $\alpha$ :**

**Figure 3.21** : Bronchoalveolar lavage (BAL) fluid cytokines. BAL was done at the 24 hr post final exposure. Uninfected mice received; i) 2x doses of PBS alone, ii) 2x 500  $\mu$ g ultrafinecarbon black (UF-CB) alone. Infected mice received either 2x doses of PBS, or 2x 500  $\mu$ g ultrafine-carbon black (UF-CB), followed by instillation of pneumococci. Infection increased BAL fluid levels of interleukin (IL)-8, interleukin (IL)-1 $\beta$ , interleukin (IL)- 12, interleukin (IL)- 6 ,tumor necrosis factor (TNF)- $\alpha$ , and interferon (IF)- $\gamma$  ( $P<0.05$ , PBS alone vs. PBS+infection) and also ( $P<0.05$ , PBS+infection vs. UF-CB+infection) Bar represents mean,  $n=5$ . \*  $P<0.05$  by unpaired t test.

# Chapter 4

**Results: DNA damage in macrophages caused by exposure nanoparticles at an air/tissue interface.**

## 4.1. Characterisation of metal nanoparticles:

Prior to the particle exposure to the Mono Mac 6 cells, dose of the particles and particle characterization were thoroughly studied. To estimate the dose delivered to macrophages, a quartz crystal balance was used (see section 2.13). Quartz crystal balance analysis showed that the dose of metal nanoparticles deposited on cells increased linearly over time. The dose delivered varied with metal; iron (Fe) deposition was  $1.02 \mu\text{g}/\text{cm}^2/\text{min}$ , gold (Au)  $0.54 \mu\text{g}/\text{cm}^2/\text{min}$  and silver (Ag)  $0.34 \mu\text{g}/\text{cm}^2/\text{min}$ . The typical spectra for aerosols from the three metal electrodes produced under identical conditions are shown in figure 4.1. Gold (Au) and silver (Ag) spectra show a log-normal distribution compatible with non-agglomerated aerosols of primary nanoparticles with diameters of  $8 \pm 2 \text{ nm}$  and  $5.5 \pm 1.5 \text{ nm}$ , respectively. The Fe spectrum, in contrast, shows a broad asymmetrical distribution typical of a highly agglomerated aerosol (Figure 4.2). This was confirmed by measuring the distribution of iron (Fe) particles at higher flow rates when the aerosol is more dilute and has less time for the nanoparticles to agglomerate. At very high flow gas rates ( $\geq 15 \text{ l}/\text{min}$ ), particles become smaller than the 2 nm resolution of scanning mobility particle sizer analysis, and were not recorded. These data imply that the spark source produces a very high number density of Fe particles smaller than 2 nm which immediately agglomerate. TEM images of nanoparticle-exposed grids show that deposited particles of Ag and Au were approximately spherical with a distribution of sizes around 8 nm in diameter with a very low degree of

aggregation (Figure 4.2). In contrast, the TEM exposed to Fe, reveals an indistinct ‘film’ with texture on a length scale of less than 1 nm (Figure 4.2).

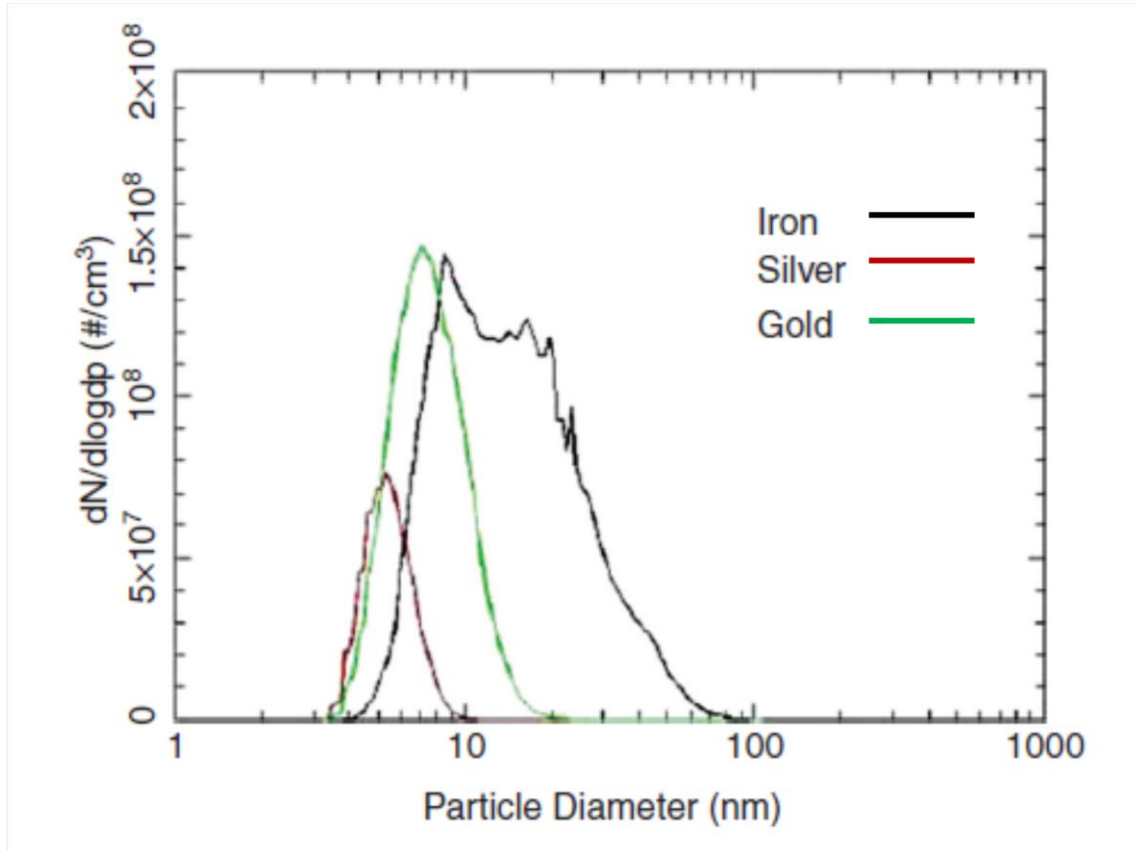


**Figure 4.1:** Size distribution of metal nanoparticles generated by spark electrodes. Particle size was measured in a nitrogen gas stream using a TSI Scanning Mobility Particle Sizer.

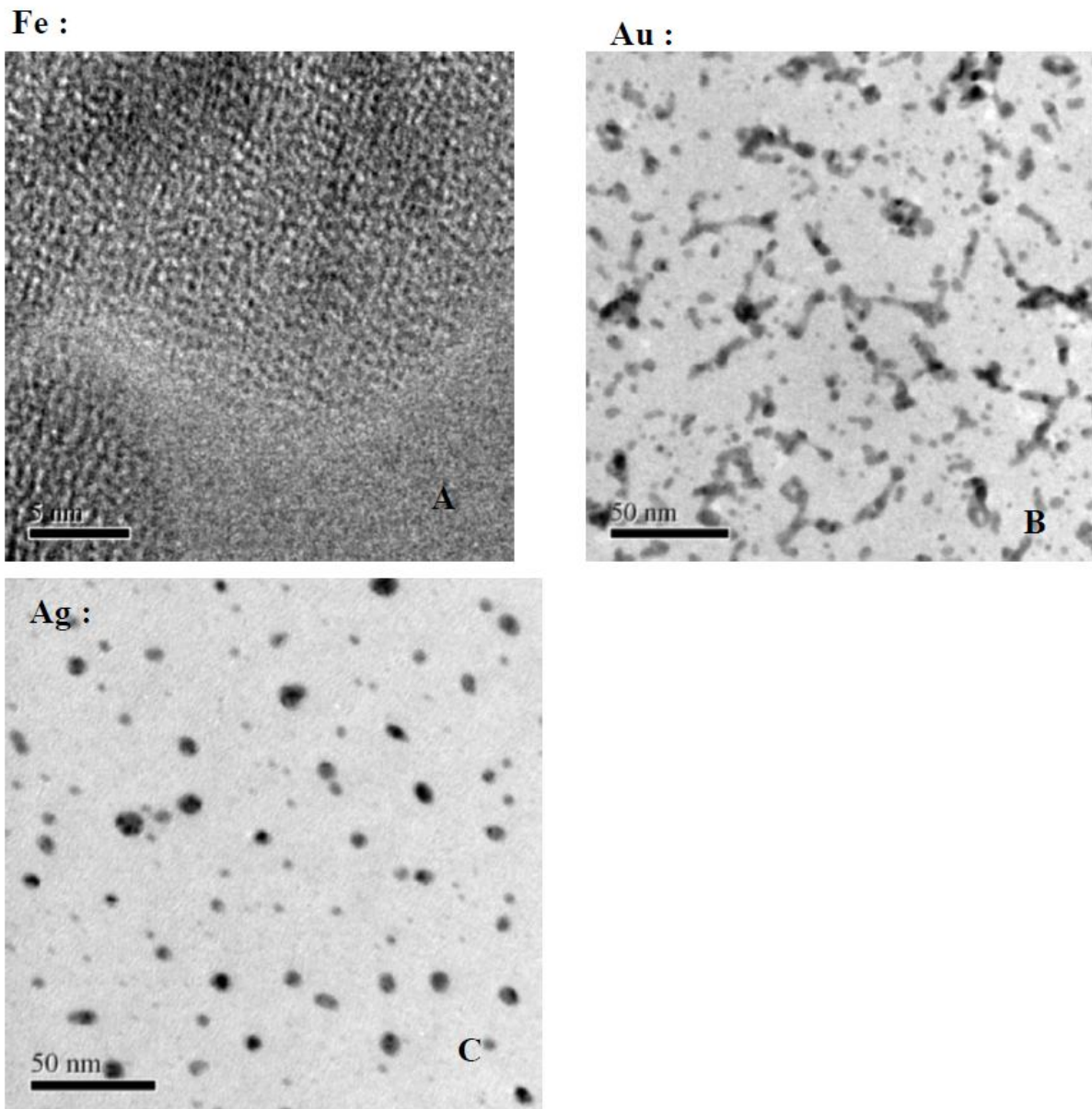


**Figure 4.2:** Transmission electron microscopy images of spark-derived metal nanoparticles. In each case the grid was exposed to the aerosol for 10 min with the electrostatic collector switched on. A) Fe nanoparticles were below the resolution of the TEM (note the length scale difference from B and C). In this case a holey carbon film TEM grid was used and the image shows the agglomerated Fe particles (top and left) overhanging the edge of a hole (bottom right). B) Au particles showing some degree of aggregation. C) Ag particles.

## 4.2. Assessment of DNA damage by Comet assay after exposure of cells to different doses of radiation:

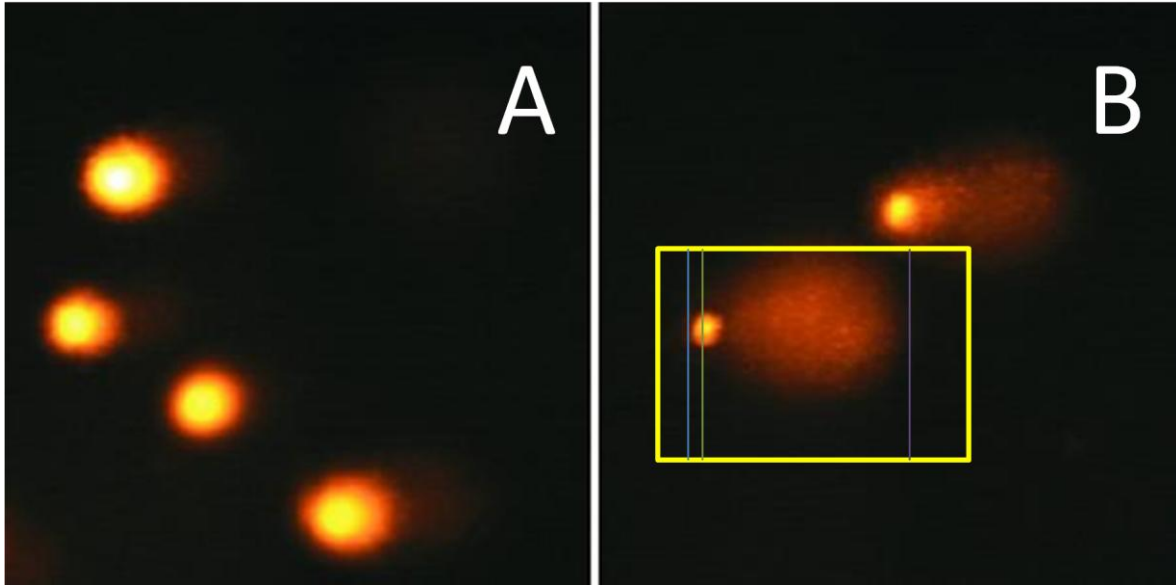


**Figure 4.3:** An example of a DNA damage in control cell (A) and effected (particle exposed) cell (B) analysed by Komet Analysis software. On picture B, blue line represents the start of the head, the green line is the middle of the head and the purple line is the end of the tail.

To interpret the DNA damage caused by nanoparticles, first mono mac 6 cells were initially exposed to different doses (i.e. 0, 1, 2, 4 and 8 Gy) of gamma radiation before the exposure studies. All irradiations were delivered using a Pantak DXT300 X-ray machine (Radiotherapy Unit, University of Leicester) operated at 300 kVp (HVL of 3.5mm Cu) and at the dose rate of 1.0 Gy/min. All irradiations were performed over ice to prevent immediate rejoining of strand breaks induced by the radiation.

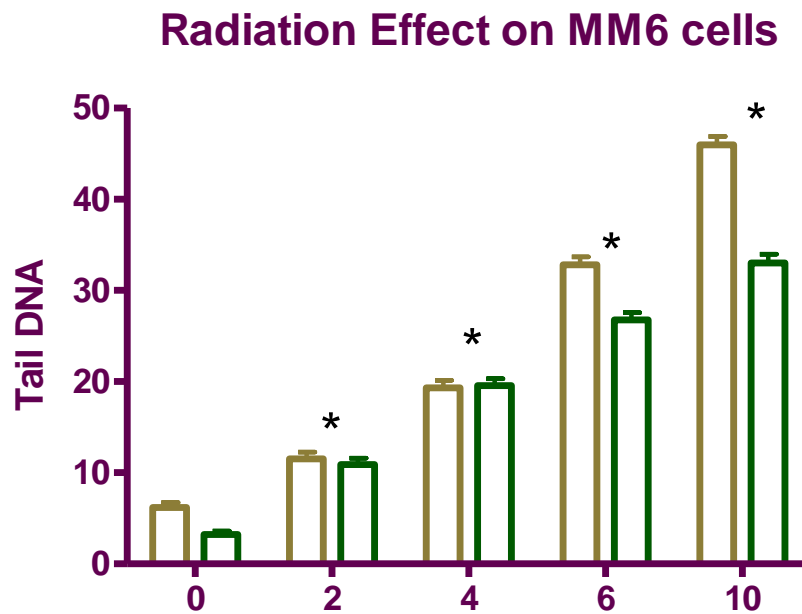


**Figure 4.4 :** DNA damage caused by different grades of radiation ( 0Gy, 2 Gy,4 Gy,6Gy and 10 Gy) and % tail DNA assessed in total of 100 cells per sample, as  $n = 50$  in duplicate slides. Each dose of radiation induced significant DNA damage compared with control ‘0’ grade ( $P < 0.005$ ). Data are representative of two separate experiments and are depicted as mean + SEM.

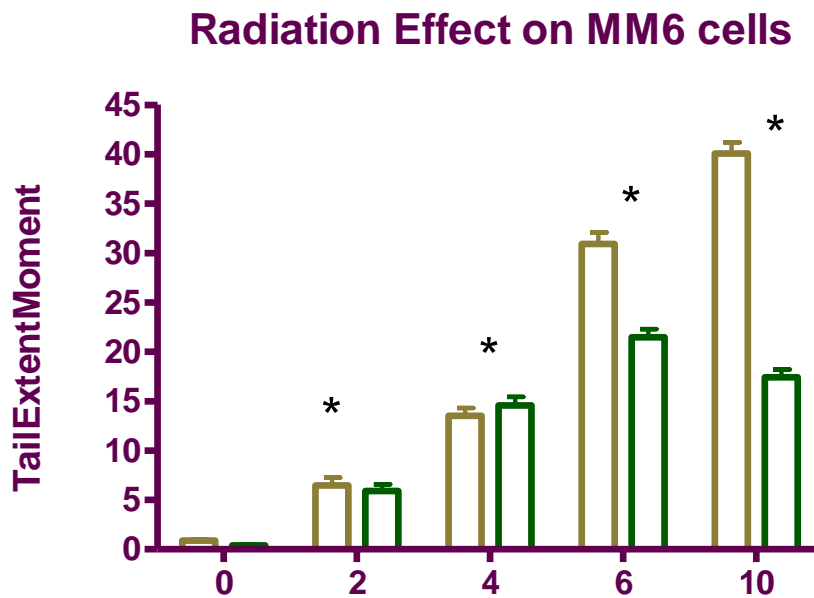


**Figure 4.5 :** DNA damage caused by different grades of radiation ( 0Gy, 2 Gy,4 Gy,6Gy and 10 Gy) and tail extent moment assessed in total of 100 cells per sample, as  $n = 50$  in duplicate slides. Each dose of radiation induced significant DNA damage compared with control '0' grade ( $P < 0.005$ ). Data are representative of two separate experiments and are depicted as mean + SEM.

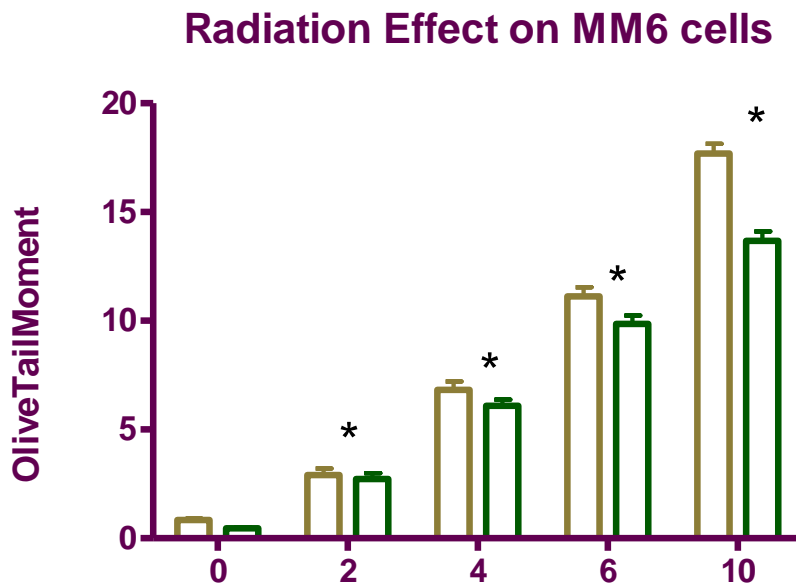


**Figure 4.6 :** DNA damage caused by different grades of radiation (0Gy, 2 Gy, 4 Gy,6Gy and 10 Gy) and olive tail moment assessed in total of 100 cells per sample, as  $n = 50$  in duplicate slides. Each dose of radiation induced significant DNA damage compared with control '0' grade ( $P < 0.005$ ). Data are representative of two separate experiments and are depicted as mean + SEM.

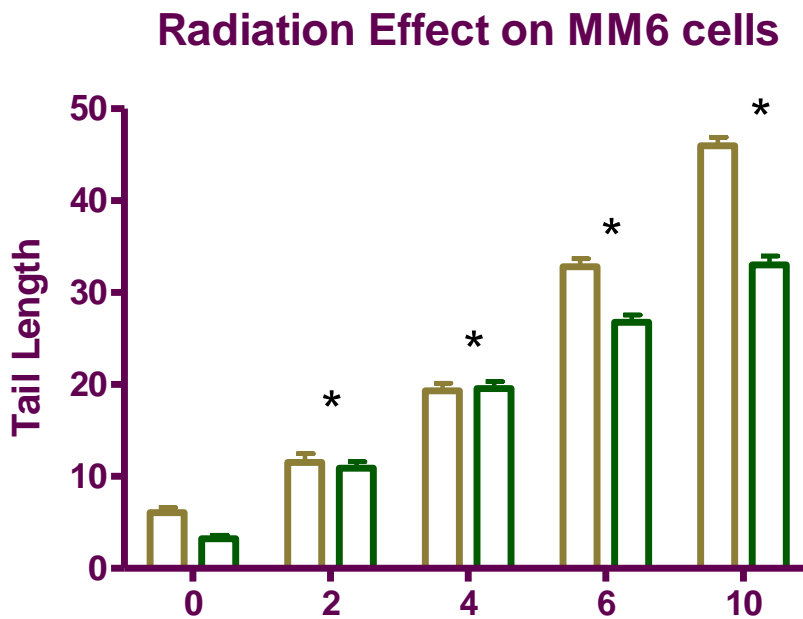


**Figure 4.7:** DNA damage caused by different grades of radiation (0Gy, 2 Gy, 4 Gy,6Gy and 10 Gy) and tail length assessed in total of 100 cells per sample, as  $n = 50$  in duplicate slides. Each dose of radiation induced significant DNA damage compared with control ‘0’ grade ( $P < 0.005$ ). Data are representative of two separate experiments and are depicted as mean + SEM.

DNA strand breaks formed in both control (0 Gy) and irradiated cells (2 Gy, 4 Gy, 6Gy and 10Gy) were calculated in total of 100 cells per sample. Changes in all comet parameters (tail length, tail extent moment, % tail DNA and olive tail moment) were highly correlated. When irradiated at different grades, cell line showed an increase in DNA damage as expected (Figure 4.4; 4.5; 4.6 and 4.7). All irradiated cells at all grades showed significant DNA damage ( $P < 0.005$ ) when compared to control cells in tail length, tail extent moment, % tail DNA and olive tail moment.

### **4.3 Assessment of DNA damage in alveolar macrophages caused by metal nano particles exposure:**

MonoMac 6 cells were used to measure DNA damage after exposure to nanoparticles and spark ablation was used to produce nanoparticle aerosols of gold (Au), silver (Ag), and iron (Fe). The alkaline version of single cell gel electrophoresis assay (i.e. Comet assay) used for detecting DNA damage at the level of individual cells. Two types of control cells were used in all the exposure experiments. (i) Macrophages placed in the nitrogen gas stream without particles (insert control), and (ii) macrophages placed in air for the same time period (air control).

Since changes in all Comet parameters (tail length, tail extent moment, % tail DNA and olive tail moment) were highly correlated in radiation experiment (see section 4.6), only % tail DNA is reported in thesis for further experiments. No increase in % tail DNA was observed when macrophages were placed in the nitrogen gas flow for up to 10 min compared with cells placed in air (insert control vs. air control). Exposure to all three metal nanoparticles for 10 min (i.e., a Fe dose of  $10.2 \mu\text{g}/\text{cm}^2$ , Au  $5.4 \mu\text{g}/\text{cm}^2$  and Ag  $3.4 \mu\text{g}/\text{cm}^2$ ) caused a significant increase in DNA damage in human Mono Mac 6 cells compared to insert control (Figure 4.8). All data were based on four separate experiments.

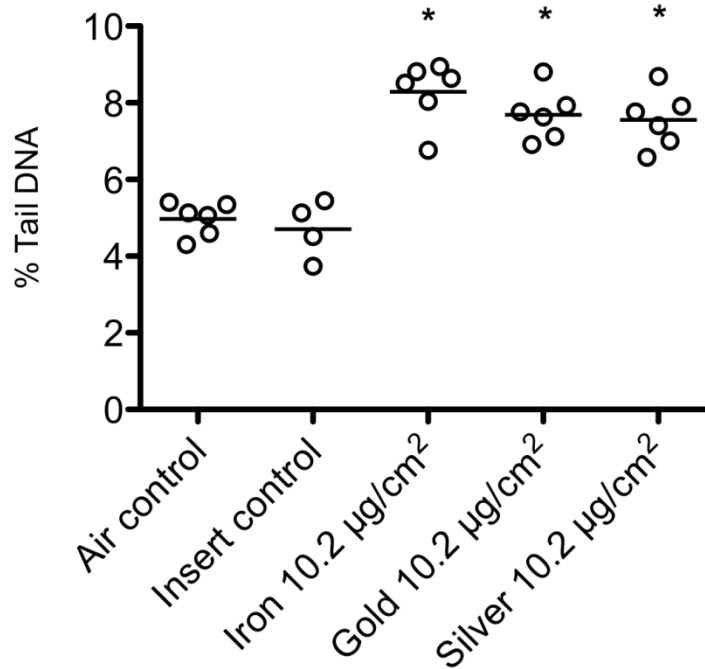


**Figure 4.8:** DNA damage (expressed as % tail DNA) caused by 10 min exposure of Mono Mac 6 cells to iron, gold and silver nanoparticles at an air-tissue interface, followed by 24 hr culture. The “air control” represents Mono Mac 6 cells cultured on the air-tissue insert and placed for 10 min in room air. The “insert control” represents Mono Mac 6 cells cultured on the insert and placed in the exposure chamber and exposed to the nitrogen gas flow without nanoparticles for 10 min. \* $P < 0.05$  vs either insert control or air control by Tukey’s multiple comparison test ( $P < 0.0001$  by ANOVA). There is no significant difference in DNA damage between the different metal nanoparticles, or between the air and insert control. Data are from  $\geq 4$  separate exposure experiments. Each data point is derived from 50 cells assays performed in duplicate. Bar represents mean.

#### 4.4. Assessment of dose dependent DNA damage caused by iron nanoparticles exposure:

MonoMac 6 cells were used to measure dose dependent DNA damage caused by iron (Fe) nanoparticles. Different doses of iron particles ( $0.51 \mu\text{g}/\text{cm}^2$ ,  $2.04 \mu\text{g}/\text{cm}^2$ ,  $5.1 \mu\text{g}/\text{cm}^2$  and  $10.2 \mu\text{g}/\text{cm}^2$ ) discharged on cells through the exposure system. Dose-response, assessed for Fe, showed significantly increased DNA damage at a does between 2.04 and  $5.1 \mu\text{g}/\text{cm}^2$  (Figure 4.9).

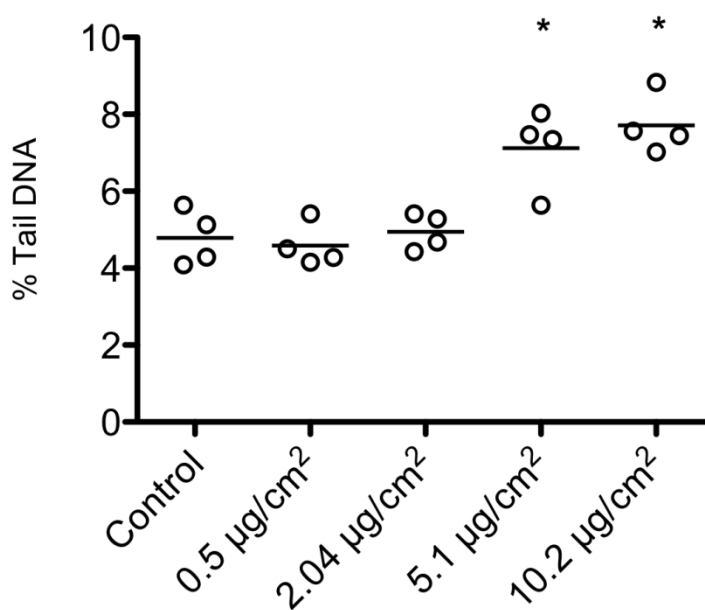


**Figure 4.9:** Dose-dependent DNA damage in Mono Mac 6 cells caused by exposure to iron nanoparticles. Dose was varied by changing the duration of exposure. Percent tail DNA is not significantly increased by 0.5 or  $2.04 \mu\text{g}/\text{cm}^2$  iron. Increased % tail DNA is induced by  $5.1$  and  $10.2 \mu\text{g}/\text{cm}^2$  iron ( $P < 0.0001$  ANOVA;  $*P < 0.05$  vs. either insert control or air control by Tukey's multiple

comparison test). Data are from 4 separate exposure experiments. Each data point is from 50 cells performed in duplicate. Bar represents mean.

#### **4.5. Assessment of DNA damage in rat alveolar macrophages after exposure to iron nanoparticles:**

Rat alveolar macrophages were collected by lavaging lungs gently with 3 ml sterile phosphate-buffered saline at 4°C.  $1 \times 10^6$  airway macrophages were transferred on 24 mm diameter Transwell®- COL inserts and incubated for 4 h at 37°C with 5% CO<sub>2</sub> at  $\geq 95\%$  humidity. Adherent macrophages were washed gently twice with sterile PBS, and RPMI 1640 added to the lower part of the insert prior to exposure to nanoparticles.  $10.2 \mu\text{g}/\text{cm}^2$  dose of iron nanoparticles were used to expose rat macrophages. A significant increase in % tail DNA was also observed in primary rat alveolar macrophages exposed to  $10.2 \mu\text{g}/\text{cm}^2$  Fe nanoparticles (Figure 4.10).

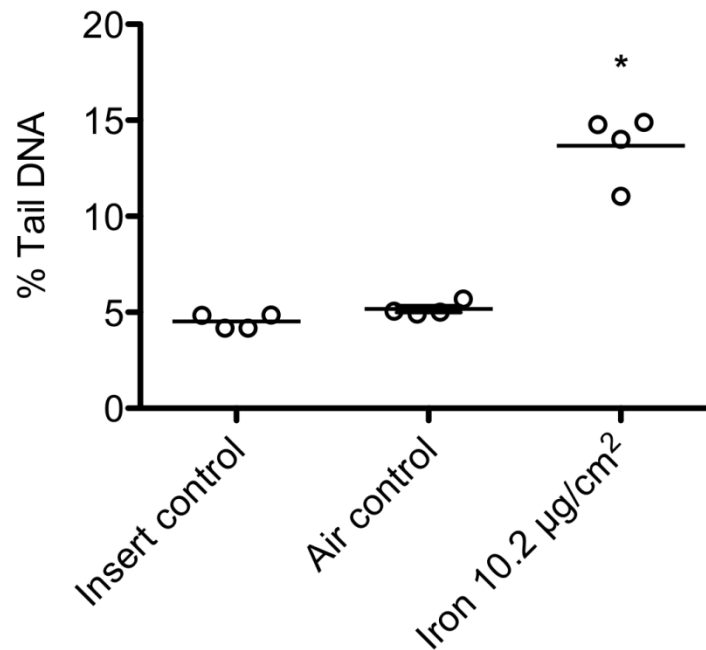


**Figure 4.10:** DNA damage induced in rat alveolar macrophages after exposure to iron nanoparticles ( $10.2 \mu\text{g}/\text{cm}^2$ ) at an air-tissue interface followed by 24 hr culture in medium. Controls are described in Figure 4.10.  $P < 0.0001$  by ANOVA. \* $P < 0.05$  vs control by Tukey's multiple comparison test. Data are from 4 separate exposure experiments. Each data point is derived from 50 cells assays performed in duplicate. Bar represents mean.

#### 4.6. Evaluation of cell viability in particle exposed cells:

Cell viability, assessed by trypan blue exclusion immediately after nanoparticle exposure was  $> 98\%$ . Concentrations of nanoparticles at doses that induced significant DNA damage (e.g., Au  $5.4 \mu\text{g}/\text{cm}^2$ ) did not reduce the proliferation of Mono Mac 6 cells at 24 h post-exposure (Figure 4.11). However, reduced

proliferation was found at 48 h post exposure, a finding compatible with cell-cycle arrest (Figure 4.11). A limitation of trypan blue is inaccuracy. While some cells are damaged, they may appear viable simply due to their intact membrane integrity. An alternative method for cell viability assessment is nuclear staining with propidium iodide or lactate dehydrogenase (LDH) activity assay.

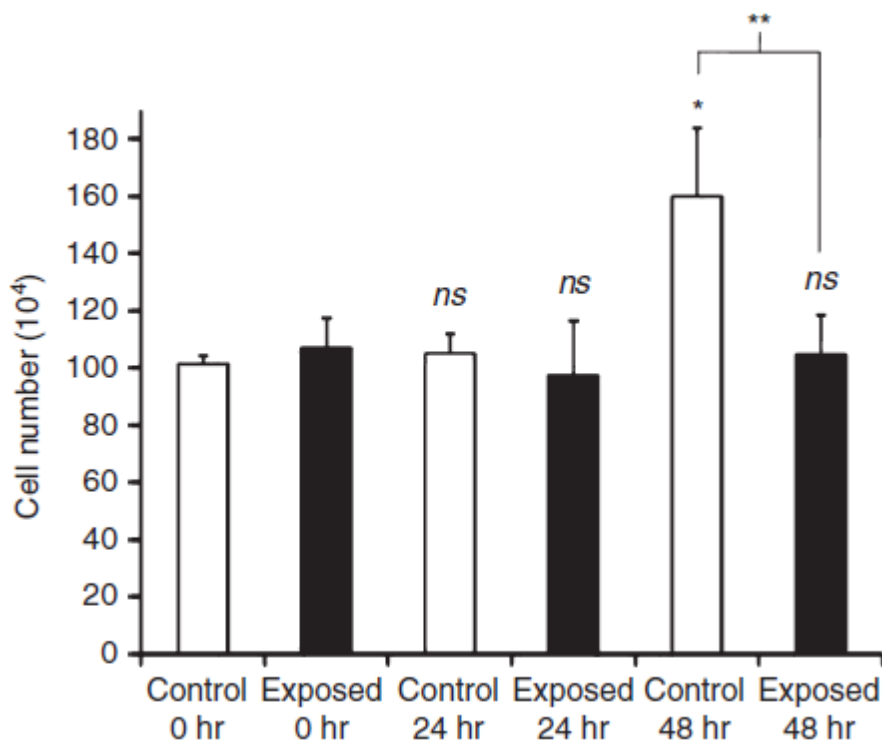


**Figure 4. 11 :** Changes in cell proliferation in Mono Mac 6 cells after exposure to Au 5.4 mg/cm<sup>2</sup> (10 min) followed by 24–48 hour culture in medium. Controls are cells exposed at an air/liquid interface to the nitrogen gas stream alone for 10 min. Cell viability was > 98% for all time points. There was no change in proliferation at 24 h. There was significant decrease in proliferation in Au exposed cells at 48 h (\*\*P < 0.01 vs. nanoparticle exposed cells; \* = P < 0.5 vs.

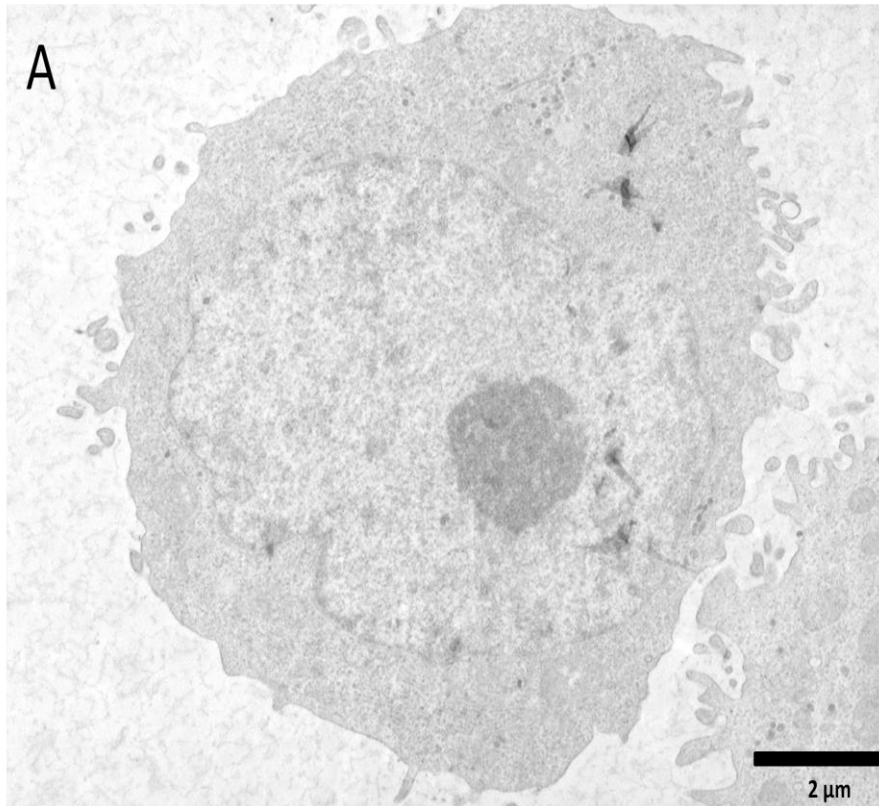
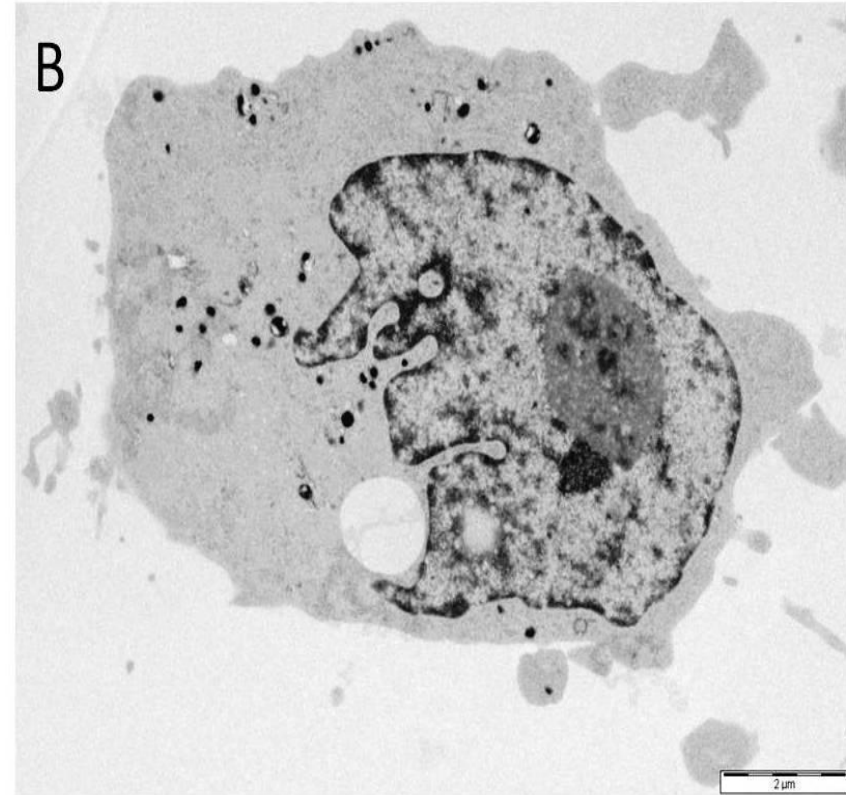
control 0 hr; ns = no significant difference vs. corresponding control or exposed 0 h). Data are representative of four separate experiments and are depicted as mean + SD.

#### **4.7. TEM analysis of particles on alveolar macrophages:**

Particle interactions with and uptake by cultured mono mac 6 cells were visualized using transmission electron microscopy (TEM). Figure 4.12 (A) shows the TEM image of macrophage cell that exposed to nitrogen flow in exposure chamber for 10 mins without gold particles. Fig (B) is the TEM image of gold particle exposed macrophage. On Fig 4.13 aggregates of gold (Au) particles could be seen in small vesicles in the immediate vicinity of the mono mac 6 cell membrane. The vesicles had variable diameters and enclosed moderate numbers of particles in the cytoplasm that were packed loosely together. Moving away from the cell membrane towards the nucleus, larger vesicles distributed in the cytoplasm contained increasing numbers of the distinct, identifiable particles. Particles were also observed within a cell nucleus.

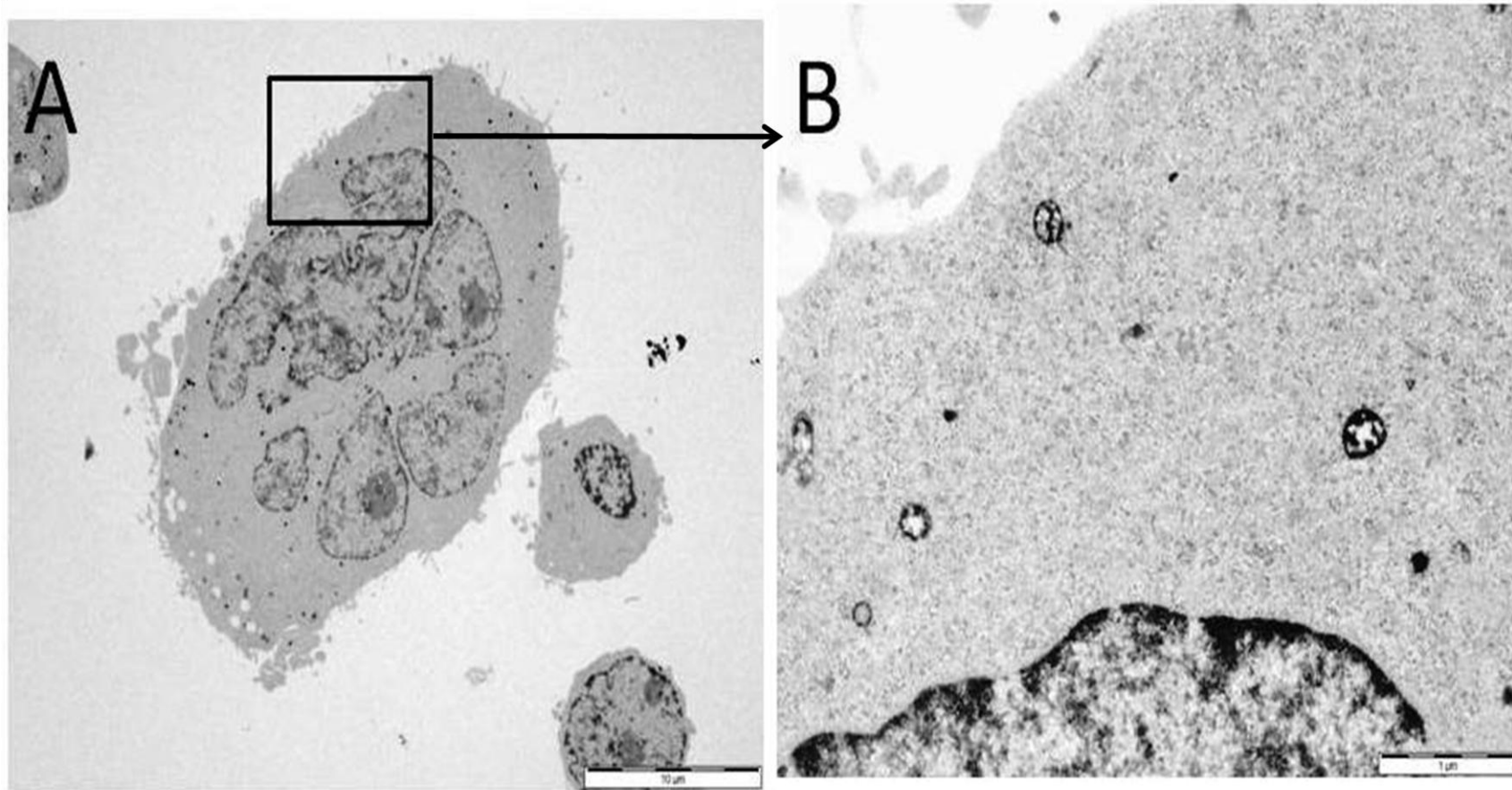
Aggregates of particles were found to be associated with cell surfaces and the cell membrane often appeared noticeably thicker and darker in the immediate proximity of the particle aggregates, a possible indication of clathrin accumulation on the cell membrane. Particles consistently appeared as discrete, individual particles roughly 20 – 50 nm in diameter. Individual particles could

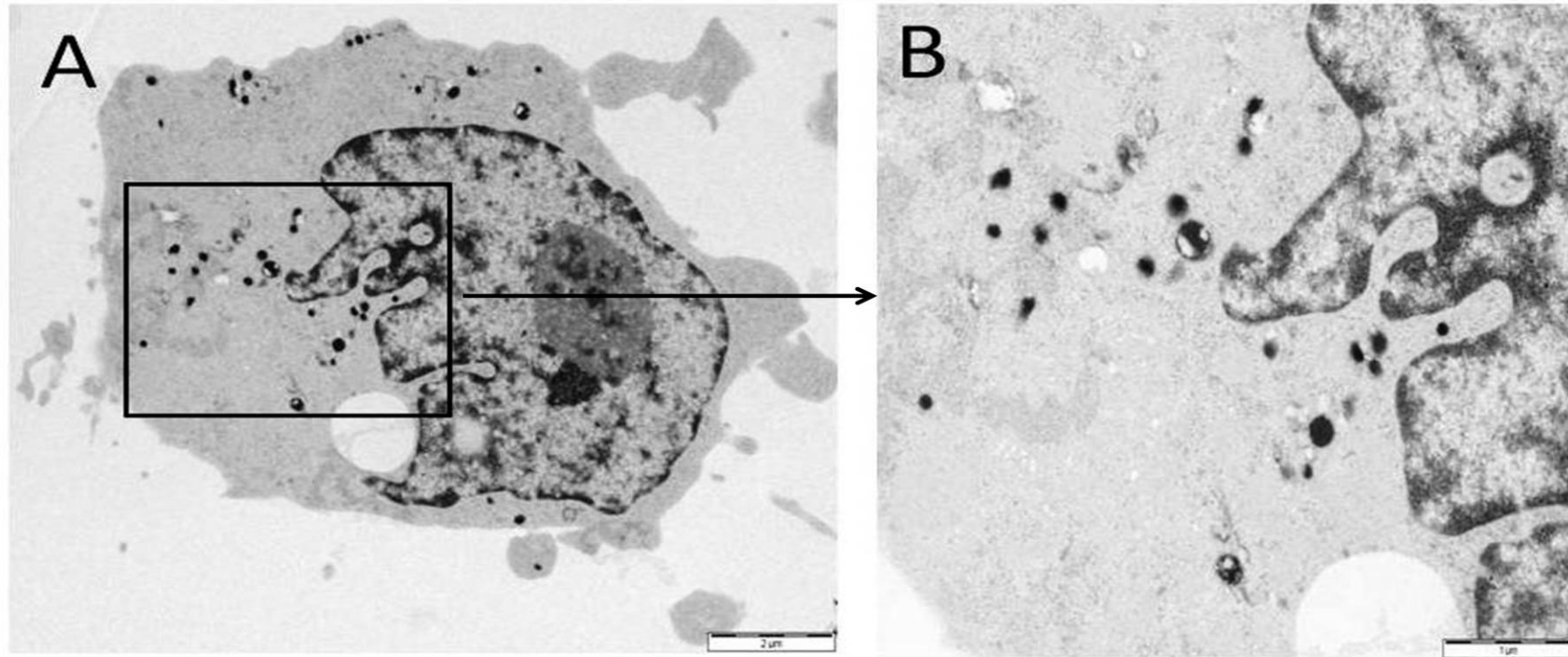
be seen in invaginations of the membrane or in small vesicles all over the cytoplasm.

**Control:****Exposed:**

**Figure 4.12:** TEM images of Mono Mac 6 cells that exposed to Gold ( Au) nano particles. (A) Cell with no exposure. (B) Cell exposed to particles. Aggregates of gold (Au) particles could be seen in small vesicles inside the cell and on the nucleus.

**Exposed:**

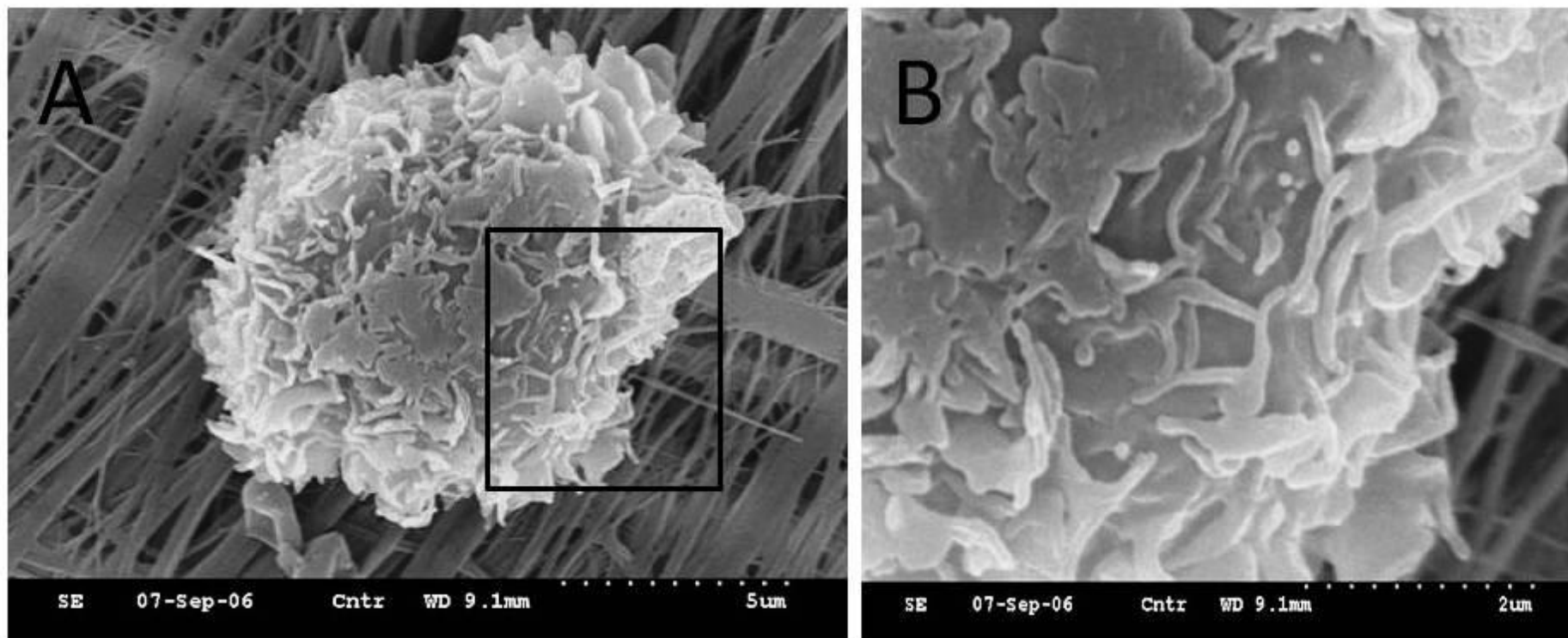


**Exposed:**

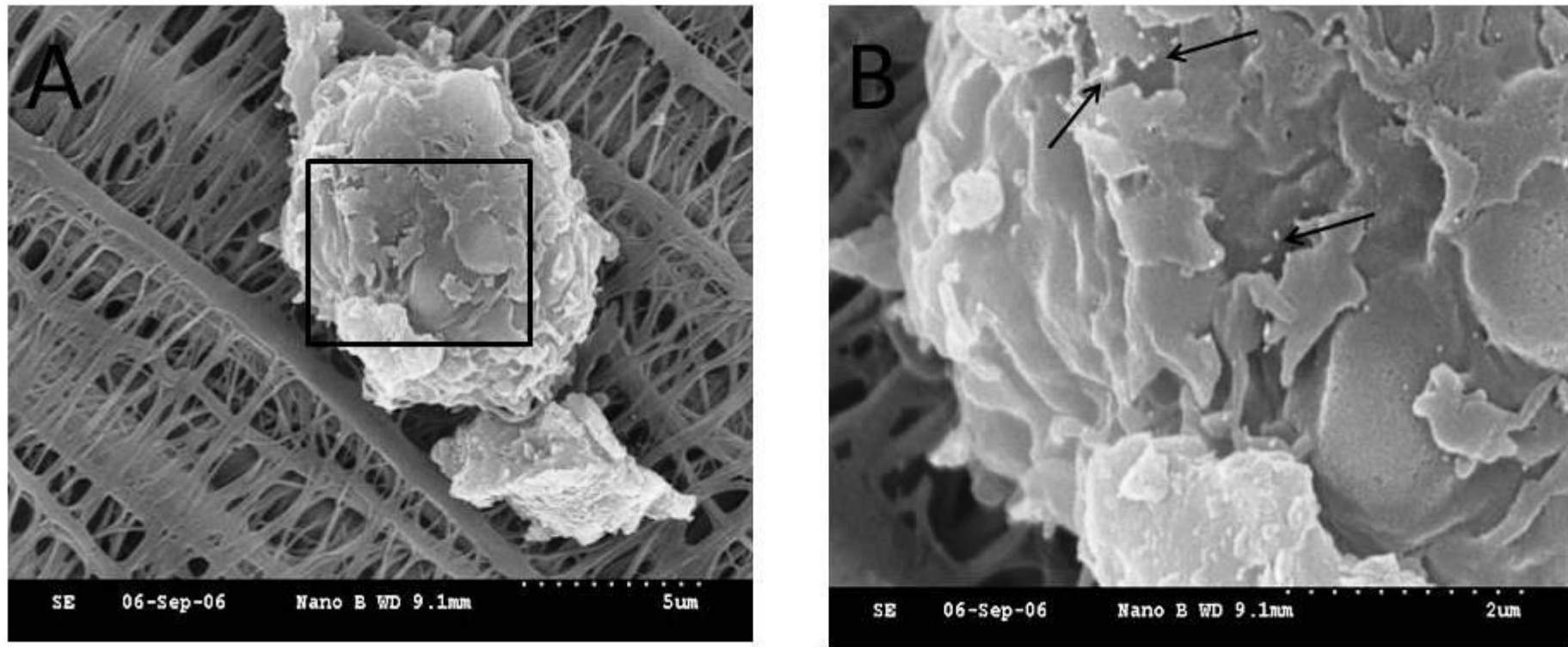
**Figure 4.13:** TEM images of Mono Mac 6 cells that exposed to Gold (Au) nano particles. (A) Gold particle exposed cells. (B) Close view of aggregates of gold particles inside the cell. Aggregates of gold (Au) particles could be seen in small vesicles inside the cell and on the nucleus.

#### **4.8. SEM analysis of particles on alveolar macrophages:**

Mono mac 6 cells challenged by gold particles, in vitro, by placing in the exposure chamber for 10 min. From scanning electron microscope images, it can be seen from that engulfing of the gold particles by macrophage cells. Figure 4.14 shows the control macrophage cell that exposed to nitrogen gas flow but without particles for 10 min in exposure chamber. Figure 4.15 (second SEM) shows exposed cell with particle coverage on cell membrane. Gold particles are in diameter of 40 - 10 nm. Exposed AM to particles showed many belts external to the body of the cell with some nanoparticle superficially attached to the cell surface, and several belts going through the body of the cell.

**Control:**

**Figure 4.14:** Scanning electron microscope image of alveolar macrophage . AMs were placed in the exposure chamber with the nitrogen gas flow but without particles for 10 min. (B) Close view of macrophage cell membrane (insert).

**Exposed:**

**Figure 4.15:** Scanning electron microscope image of alveolar macrophage . AMs were placed in the exposure chamber with the nitrogen gas flow and gold particles for 10 min. (B) In the close view of the macrophage cell membrane, gold nanoparticles can be seen on the surface (insert).



# Chapter 5

## Discussion and Future work

**Discussion: Part A:**

This study was designed to assess the hypothesis that loading of alveolar macrophages (AM) with particles of ultrafine elemental carbon particles (UF-CB) increases susceptibility to pneumococcal pneumonia. Previously, It was reported that high levels of carbon in AM associated from biomass-smoke exposed children and women living in Ethiopia (Kulkarni et al. 2005), and from adults living in Malawi (Fullerton et al. 2009a). Since elemental carbon nanoparticles are a major, and potentially toxic, component of biomass smoke PM (Kocbach et al. 2005), we hypothesised that susceptibility to pneumococcal pneumonia is increased by carbon loading of AM in vitro. In conflict with the hypothesis, using an established animal model of pneumococcal pneumonia, we found that mice exposed to ultra fine carbon black particles (UF-CB) were partially protected against the consequences of pneumococcal infection, with delayed morbidity and reduced mortality at 72 h - and no evidence of late-onset infection in the surviving animals.

In this study, ultrafine particles that are less than 100 nm in diameter were used as the particle model. They are extremely small compared with the cellular structures of the lungs and have a large surface area per unit mass compared with the classic toxic particles. Ultrafine particles may exist as singlet particles or as aggregates. In the form of aggregates their deposition characteristics can change as the aggregates will have a greater aerodynamic diameter than the

singlet particles. Peters *et al* (Peters et al. 1997) reported that decrement in evening peak flow in a group of asthmatic patients was best associated with the ultrafine component of the airborne particles during an episode of severe air pollution. This showed the best association with the ultrafine fraction, although there were associations with fractions of other sizes.

Understanding the importance of lung high particle burden is vital for the interpretation of inhalation studies with highly insoluble particles (Oberdorster 1995). In developing countries, the burning of biomass fuels such as wood, animal dung, and crop residues, results in high levels of exposure to inhalable carbonaceous particulate matter (Ezzati et al. 2001). The magnitude of these exposure levels are more than above the health-based guidelines of the developed world. This high level of particle exposure causes approximately two million deaths per year, a major proportion of these in young children (Bruce et al. 2000c). The phenomenon of particle aggregate “overload” occurs in rats when they are exposed to high concentrations of airborne particles which accumulate in the lungs to a point where there is failure of clearance, increased build up of dose, inflammation, proliferation, fibrosis, and tumour production (Borm et al. 2000). From the previous studies, it’s been summarized that even though they form aggregates but readily deposit in the lungs as singlets or aggregates and in the lungs the aggregates may disaggregate.

Ultrafine particles are generally made from combustion processes and are estimated to consist of 65% organic compounds, 7% elemental carbon, 7% sulphate, 4% trace elements, with very small quantities of sodium, chloride and nitrate (Cass et al. 2000). So, the components of PM<sub>10</sub> are not on the whole very toxic, comprising in large part sulphates, nitrates, chlorides, ammonium, carbonaceous material, metals, and wind blown crustal dust. Therefore attention has turned to the components that are most likely to have toxic potential which are the transition metals and endotoxin. In the rat, instillation of endotoxin results in recruitment of neutrophils into the lung and protection against subsequent death from *Pseudomonas aeruginosa* pneumonia (0% vs. 54% in controls) at 24 h (Jean et al. 1998). Similarly, we found in both BAL and lung tissue, that UF-CB induces a mild pulmonary neutrophilia. Endotoxin contamination of UF-CB is not a stimulus for the pulmonary neutrophilia observed in the present study, since particles were baked at high temperature for several hours before use. The ability of transition metals to have enhanced lung-injuring activity has shown in number of studies and in diverse materials such as TiO<sub>2</sub> (FERIN et al. 1991), carbon black (Li et al. 1996), cobalt (Zhang et al. 2003), and Al<sub>2</sub>O<sub>3</sub> (FERIN et al. 1991, Oberdörster et al. 1992). The mechanism underlying the effect is unknown, but data suggest that free-radical activity may be an important factor due to specific surface free-radical-generating activity of the metal compounds (Donaldson et al. 1996). *In vitro* studies on ultrafine

particles ( UF-Co, UF-Ni and UF-TiO<sub>2</sub> ) revealed that the ultrafines differed in their ability to generate free radicals, with UF-Co and UF-Ni having more free radical activity than UF-TiO<sub>2</sub> (Donaldson 1998). Similar to findings for other pathogenic dusts (Gilmour et al. 1997), hydroxyl radical was found to be the principal free radical mediating plasmid DNA breakage and depletion (Donaldson et al. 1996, Gilmour et al. 1997). Free radicals on the surface of particles may also stimulate inflammation via increased transcription of oxidative stress-responsive proinflammatory genes (Donaldson et al. 1996) such as the chemoattractant cytokine IL-8 (DeForge et al. 1993).

Airway macrophages are the primary phagocyte for inhaled particulate matter (PM), and in animal models, the amount of carbon-pigmented material in airway macrophages has been shown to reflect both the inhaled dose (Strom et al. 1990) and the total particulate burden in the lung (Brauer et al. 2001a). Since alveolar macrophages (AM) reside exclusively in the lower airway, and particles of carbon are not formed in vivo, black material within the cytoplasm of AM must be derived from inhaled PM. In previous studies, Bunn et al. (Bunn et al. 2001) explained alveolar macrophages engulf and retain inhaled material to prove that carbonaceous PM penetrate the lower airway of healthy UK infants exposed to low levels of fossil-fuel derived PM. In adults, the amount of carbonaceous particles extracted from the lung at autopsy reflects the long-term exposure to PM<sub>10</sub> (Brauer et al. 2001b), and PM in airway macrophages reflects

exposure to inhalable PM in an occupational settings (Fireman et al. 2004). Brauer et al. concluded from their research that long-term residence in an area of high ambient particle concentrations is associated with greater numbers of retained particles in the lung. To achieve a comparable degree of carbon loading in alveolar macrophages (AM), we used a high acute dose of ultrafine carbon black ( $2 \times 500 \mu\text{g}$  per animal). As a result, we found  $44 \pm 1.1\%$  of AM were heavily-laden with carbon and  $17.6 \pm 1.1$  moderately-laden macrophages in BAL fluid. The pattern of carbon in mouse AM after instillation of UF-CB was similar to that seen in AM from biomass-smoke exposed humans (Kulkarni et al. 2005, Fullerton et al. 2009b). Electronmicrograph images confirmed the carbonaceous ultrafine particles (UF-CB) within a phagosome of an alveolar macrophage (see section 3.1.2). Similarly, Bunn et al. showed the deposition and retention of carbonaceous particles in the lower airway of normal children (Bunn et al. 2001).

Pulmonary overload is characterized by the impairment of particle clearance resulting in persistent lung particle burdens. Previous studies with ultrafine particles have shown that pulmonary overload can be achieved with relatively insoluble, low toxicity particles, including UF-CB (Creutzenberg et al. 1990). Extended impairment of clearance has been shown to lead to the development of pulmonary tumors with ultrafine particles in rats but not in mice or hamsters

(Muhle et al. 1990, Heinrich et al. 1986). There were species differences in retained lung burdens. Lung burdens of UF-TiO<sub>2</sub> were increased in a concentration-dependent manner in rats, mice, and hamsters after 13 weeks of exposure. Initial lung burdens per gram of lung were similar in rats and mice; however, hamsters had approximately 23% of the rat and mouse burdens. The fact that hamsters had lower initial lung burdens is indicative of the ability of hamsters to efficiently clear particles from the lung during exposure (Bermudez et al. 2002, Creutzenberg et al. 1998). The retained lung burden in rats exposed to 10 mg/m<sup>3</sup> was 2.1 mg/lung and was comparable, adjusting for dose and daily length of exposure, to lung burdens found in other studies using this material (Ferin et al. 1992, Heinrich et al. 1995). Similarly, UF-TiO<sub>2</sub> lung burdens of 0.42 mg/lung in mice of the high-dose group were comparable to the mice in the study by Heinrich et al, when adjusted for dose and daily length of exposure.

Analysis of bronchoalveolar lavage fluid (BAL) is an effective method of detecting an inflammatory response in the lungs of animals in exposure studies. Increasing levels of lactate dehydrogenase (LDH),  $\beta$ -glucuronidase, hydroxyproline, content of serum proteins and an influx of neutrophils (PMNs) can be most sensitive indications of an inflammatory response in lungs. The present study investigated the effects of ultrafine particles on pulmonary cellular parameters using animal model. Increased neutrophils in BAL from animals

reported after exposure to ultrafine carbon black ( $2 \times 500 \mu\text{g}$  per animal). Similarly, high dose of particle exposure resulted significantly elevated (two- to three-fold) neutrophils in rat BAL fluid. This increased cell replication persisted through 13 weeks post-exposure and correlated well with proliferative lesions observed in these animals (Bermudez et al. 2004). Our results are also similar to the two- to three-fold elevations of alveolar cell replication noted in rats exposed to fine grade  $\text{TiO}_2$  (Bermudez et al. 2002, Warheit et al. 1997) (Bermudez et al. 2002)(Bermudez et al. 2002)(Bermudez et al. 2002)(Bermudez et al. 2002). In this study, we aimed to investigate the animal susceptibility to pneumococcal pneumonia after exposed to ultrafine particles. But, we observed a protective effect of carbonaceous PM on bacterial pneumonia which is against to our hypothesis.

Long-term high-dose inhalation studies have demonstrated that chronic effects such as inflammation, cytokine expression, epithelial hyperplasia, pulmonary fibrosis, and lung tumours can be produced by poorly soluble particles (i.e., CB,  $\text{TiO}_2$ , and crystalline silica) (Driscoll et al. 1996); (Kilpper et al. 1989); (Saffiotti et al. 1988). Only high-dose exposure to UF-CB resulted in an increased epithelial cell mutation frequency. Studies suggest that the mutations are the result of secondary events induced by chronic inhalation exposure to poorly soluble particles, lung particle overload-related particle persistence,

inflammation, and increased epithelial cell proliferation. It has been shown that cell proliferation increases the likelihood that oxidant-induced genetic damage becomes fixed in derived cells (Ames et al. 1990); (Cohen et al. 1991); (Butterworth 1990). To further investigate the oxidative stress-induced capabilities of air pollutants, it is important to characterize the events preceding fixation of genetic damage as measured by a well known and commonly used biomarker of free radical-induced oxidative DNA damage is the measurement of 8-oxo-dG, a mutagenic lesion of the C-8 position of 2'-deoxyguanosine (dG) residues in DNA (Kasai 1997). 8-oxo-dG induces G-T transversions, which are widely observed in mutated oncogenes and tumour suppressor genes (Feig et al. 1993, Fraga et al. 1990). In the present study, mice urine was collected and 8-oxo-dG was analysed by liquid chromatography- electrospray ionization-tandem mass spectrometry (LC-ESI-MS/MS). Increased levels of urinary 8-oxo-dG were observed in UF-CB alone treated animals. To support our studies, increased 8-oxodG levels were also found to be positively correlated with lung tumour incidence in mice that had been exposed to diesel exhaust particles (Ichinose et al. 1997). The monitoring of personal PM<sub>2.5</sub> exposure correlated with the level of 8-oxodG adducts in human lymphocytes (Sørensen et al. 2003). An increased urinary excretion of 8-oxodG adducts was observed in bus drivers from central Copenhagen compared to drivers from suburban areas of the city (Loft et al. 1999).

Lung effects of particle exposure have been studied by many research groups (Brown et al. 2001);(Gilmour et al. 2004);(Nilsen et al. 1997), only few studies showed a detailed histo-pathological response caused by carbon particles (UF-CB). To investigate particle-induced airway damage and inflammation, we used intranasal particle exposures ( $2 \times 500 \mu\text{g}$  per animal). One day after the second dose of particle treatment, results shows that carbon particle (UF-CB) induces an immediate inflammatory response. The airway inflammation was also confirmed by histological examination (see section 3.3), showing particle inclusions mainly within alveolar macrophages, bronchiolar epithelial hypertrophy, alveolar microvascular congestion, alveolar wall fibroplasias, particle inclusions within bronchiolar epithelium and leucocyte infiltration of airway walls in carbon particle (UF-CB) treated group, whereas the other control group showed no histological changes (Figure 3.9 A,B,C). Various rat studies have shown that carbon black particles induce acute airway inflammation early after intratracheal exposure (Gilmour et al. 2004, Brown et al. 2000). Based on present findings, we suggest that particles like ultrafine carbon black induce pulmonary inflammation in mice.

Enhanced inflammation, characterized by increased numbers of neutrophils and excessive cytokine production, provides a plausible explanation for the increased bacterial clearance and improved survival in the UF-CB treated animals. To determine whether an enhanced inflammatory response was present

in the UF-CB treated mice, lung lavage cells and levels of pulmonary cytokines were evaluated on days 1 to 4 following infection (Uninfected mice received; i. 2× doses of PBS alone, ii. 2× 500 µg ultrafine-carbon black alone. Infected mice received either 2× doses of PBS, or 2× 500 µg ultrafine-carbon black (UF-CB), followed by instillation of pneumococci). Given that, ultrafine carbon black (UF-CB) treated animals increased neutrophil count (see section 3.2), higher levels of inflammatory cytokine levels were expected. But, we were surprised to see lower cytokine levels in UF-CB alone treated animals. As expected, cytokine levels were higher after the infection. However, UF-CB treatment resulted in consistently lower levels of cytokine levels which correlate with the pulmonary pneumococcal CFU counts after infection. Our data suggest that the decreased levels of cytokines results a reduction in the ability of the bacteria to colonise or multiply in the respiratory tract in UF-CB and infected group. One possible explanation that could account for this is that instead of acting directly on the bacteria, our findings suggest that UF-CB alters the environment within the lung, rendering it less permissive to bacterial growth.

This is the first report of a protective effect of carbonaceous PM on bacterial pneumonia. To date, increased susceptibility to bacterial infection has been reported after exposure to environmental PM. For example in rats, inhalation of aerosolised diesel exhaust particles (20 mg/ m<sup>3</sup> for 4 h a day for 5 days)

followed by listeria infection, increased listeria lung CFU counts (Yin et al. 2004). In another example, a dose-dependent increase in *Staphylococcus aureus* CFU counts occurred in rabbits after inhalation of wood smoke for 1 h per day for 4 days (Zelikoff et al. 2002). One previous study has addressed the interaction between carbonaceous PM and susceptibility to pneumococcal pneumonia. Sigaud et al (Sigaud et al. 2007) exposed BALB/c mice to aerosolised interferon gamma, then instilled concentrated ambient particles intra-nasally, followed by infection with *S. pneumoniae*. In this model, all untreated mice survived and cleared instilled bacteria by 24 h. By contrast, mice exposed to concentrated ambient particles and interferon gamma, had increased BAL neutrophils and more severe pneumonia at 24 h. However, there are significant differences between our model and that of Sigaud et al (Sigaud et al. 2007), i.e. we used UF-CB as a surrogate for the carbonaceous fraction of biomass PM, and all untreated mice died from pneumococcal disease by 72 h. In general, the inflammatory response initiated by particle source or infection is host protective, although under certain circumstances it can be detrimental to the host. Inflammatory mediators triggered by the presence of pathogens activate the release of antimicrobial substances, recruit phagocytes that contribute to pathogen clearance, and aid in the priming of the adaptive immune response (Bals et al. 2004), (Janeway Jr et al. 2002). The protective effect of carbon black particles (UF-CB) reported here correlated with reduced bacterial

burden, neutrophil influx, and lower levels of cytokines in the lungs of *S.pneumoniae*-infected and UF-CB treated mice, suggesting that enhanced inflammation is an unlikely mechanism for the observed protection.

This raises an interesting question about the role of inflammation in host resistance to infection. Specifically, did the mice have a reduced bacterial burden and improved survival because of particle - activated inflammatory response to infection, or does carbon particles alter the environment in the lung such that it is more difficult for the bacteria to colonize? Taken together all the evidences we found in our research and it has been speculated that enhanced inflammatory response caused by carbon particles reflect a reduction in the ability of the bacteria to colonize or multiply in the respiratory tract.

Lung tissue injury, by damaging airway epithelial integrity would be expected to enhance susceptibility to bacterial infection. Indeed, we found changes in lung histology after UF-CB installation suggestive of mild tissue injury. However, UF-CB treatment resulted in consistently lower levels of pulmonary pneumococcal CFU counts after infection, and attenuated the induction of KC/GRO, and IF- $\gamma$ . Since there was no difference in lung CFU counts immediately after instillation of bacteria and at 4 h and 6 h after infection in UF-CB and PBS-treated groups, the possibility that UF-CB treated mice had lower number of instilled bacteria is excluded. Compatible with the reduced lung CFU counts up to 24 h in UF-CB exposed mice, and lower pro-

inflammatory cytokine levels, and fewer carbon-exposed animals developed pneumococcal bacteraemia at 24 h.

The mechanism whereby an acute dose of UF-CB protects mice against pneumococcal morbidity and mortality is unclear. Increased anti-pneumococcal function in carbon-laden AM is unlikely, since loading of AM with UF-CB *in vitro* significantly impairs pneumococcal killing (Lundborg et al. 2007a). Previous animal studies have shown UF-CB alone, via oxidative stress; induce a low grade airway neutrophilia (Li et al. 1999b). Increased urinary 8-oxodG in UF-CB-exposed mice in the present study is suggestive of increased pulmonary oxidative stress (Gallagher et al. 2003, Dick et al. 2003). We therefore speculate that partial protection against pneumonia in UF-CB exposed mice is due to oxidative stress stimulating the recruitment of neutrophils into the airway.

There are several limitations to our data. First, human AM acquire inhaled carbon over several days. To achieve a comparable degree of AM carbon loading requires a high acute dose of ultrafine carbon black ( $2 \times 500 \mu\text{g}$  per animal). The effect of chronic loading of murine AM with repeated low doses of UF-CB *in vivo* on vulnerability to pneumococcal pneumonia remains to be determined. Second, we have used lethal dose of pneumococci which does not model the effect of inhaled carbon on pneumococcal colonisation of the upper

airway. However, pneumococcal pneumonia is a leading cause of death in young children - and our results therefore model vulnerability to death in children with established infection. Third, biomass particulate matter (PM) consists not only of carbon nanoparticle aggregates (modeled in this study), but also adsorbed compounds such as metals. The potential importance of adsorbed compounds is suggested by Zhou and Kobzik (Zhou et al. 2007a), who reported decreased internalisation of *S. pneumoniae* and killing by a murine macrophage cell line loaded with concentrated ambient particles *in vitro*, but no impairment of internalisation when cells were loaded with carbon black. Organic components of particulate matter may also be critical in particle toxicity. The organic and metal PM components can induce pro-inflammatory effects in the lung due to their ability to cause oxidative stress (Kumagai et al. 1997) (Nel et al. 2001) .

**Discussion: Part B:**

The use of nanotechnology has led to great prospects for the development of new products and applications in various sectors. Particles in the nanoscale range, about 1–100 nm, may have impressive and useful characteristics, but the same properties can be problematic in a toxicological perspective. Therefore, increased focus on various toxicological issues related to nanoparticles is now critical. Many studies in the area of nanotoxicology have focused on cytotoxicity. One of the most important effects is damage to DNA, since an increased genetic instability is associated with cancer development. A number of mechanisms underlie the ability of nanoparticles to cause DNA damage. A key mechanism that is often described is the ability of the particles to cause oxidative stress (Nel et al. 2006a, Schins 2002). The oxidative pressure is generated by an increase in the number of reactive oxygen species (Knaapen et al. 2004). In this study, we therefore sought to develop an air-tissue interface model to assess DNA damage to airway macrophages due to inhalation of nanoparticulate iron (Fe), gold (Au), and silver (Ag). To measure DNA damage in macrophages, we used the alkaline Comet assay (also known as single cell gel electrophoresis) (Evans et al. 2004)(Ghosh et al. 2008) to measure DNA damage .

An air-liquid interface model was used to assess nanoparticulate-induced DNA damage to airway macrophages. The principle of the operation of the exposure chamber is schematically depicted in figure 2.8. Dense cloud of particles enters an exposure chamber in an air flow fitted on the top of the chamber. Previously described methods for deposition of micron-sized particles or droplets onto cells have relied on inertial impaction as the deposition mechanism. The use of impactors or impingers (Fiegel et al. 2003, Grainger et al. 2009, SCHREIER et al. 1998) requires high flow rates for effective particle deposition, which may impair cell viability (Mülhopt et al. 2008) and the deposition efficiency is also strongly dependent on particle size (Kennedy et al. 2002). The high flow speed in the device used by Grainger et al. (Grainger et al. 2009) may simulate *in vivo* conditions in the respiratory bronchioles after a sharp inspiration (Grainger et al. 2009). It exceeds typical flow speeds under normal breathing conditions and is completely unrealistic for the alveolar regime, where flow velocities are so small that deposition due to impaction can be disregarded (Heyder et al. 1986). A second type of cell exposure system for liquids utilizes high velocity sprays to deposit the liquid directly onto the cells via inertial impaction (Knebel et al. 2001). High-speed spray-deposition does not occur under *in vivo* conditions (except in the mouth after using a medical spray nebulizer), and both systems may induce cellular stress due to high speed droplet collisions. Again, none of the systems above provides information on the cell deposited dose.

The air-liquid interface cell exposure system, we used, utilises a completely different, more "gentle" technique of particle generation and deposition and it provides direct dose measurements. As discussed above, iron (Fe), gold (Au), and silver (Ag) nanoparticles are generated by spark ablation and are uniformly deposited via cloud and single particle settling onto cells at the air-liquid interface. Our method of particle exposure on Mono Mac6 cells and macrophages, is a relevant deposition process in the upper respiratory tract, gravimetric sedimentation simulates the *in vivo* conditions of super micron particle deposition in the alveolar region. The gentle form of particle deposition minimizes mechanical strain and subsequent stress for the exposed biological material, as was confirmed by the unaffected viability of Mono Mac6 cells (See section 4.6). Furthermore, nanoparticle doses applied here had any significant effect on cell viability, which is a pre-requisite for reliable measurements of particle-induced oxidative stress response, as performed in the current study.

Nanoparticle characteristics and concentrations were actively investigated by various nano-scale measurements (Size distribution - Scanning mobility particle sizer, Particle dose - Quartz crystal balance analysis (QCM) and degree of homogeneity - Transmission electron microscopy (TEM). The dry nanoparticle mass deposited on the cells determined from the dried deposit on the QCM. Quartz crystal balance analysis showed that the dose of metal nanoparticles

deposited on cells increased linearly over time. The dose delivered varied with metal; Iron (Fe) deposition was  $1.02 \mu\text{g}/\text{cm}^2/\text{min}$ , Gold (Au)  $0.54 \mu\text{g}/\text{cm}^2/\text{min}$  and Silver (Ag)  $0.34 \mu\text{g}/\text{cm}^2/\text{min}$ . We hypothesized that a 10 min exposure to metal particles would result in a similar nanoparticle dose to macrophages. However, quartz crystal balance analysis showed that the dose delivered was variable – with the dose highest for Fe ( $10.2 \mu\text{g}/\text{cm}^2$ ) and lowest for Ag ( $3.4 \mu\text{g}/\text{cm}^2$ ). A 10 min exposure did however result in similar levels of DNA damage to macrophages. These data suggest that, in an air-tissue exposure system, Ag nanoparticles are relatively more toxic to macrophage DNA. To date, there are no published data on the comparative toxicity of Ag, Au and Fe. A recent study of subchronic inhalation of 19 nm Ag particles in rats, found no major effects on lung histology at concentrations up to  $100 \text{ mg}/\text{m}^3$  over a 13-week period (Sung et al. 2009) – but this study did not measure DNA damage. In contrast, Tice et al. (Tice et al. 2000) found increased comet tail moment in human cancer cells and fibroblasts exposed to a suspension of 50 mg/ml Ag nanoparticles (6–20 nm) for 48 h.

This is the first study to assess DNA damage in macrophages exposed to either Fe, Ag or Au nanoparticles at an air-tissue interface. We found significant DNA damage to a human macrophage cell line exposed to 10 min of a spark-ablation generated nanoparticulate metal aerosol. These data are compatible to those

reported by Mroz et al. (Mroz et al. 2008), who found a three-fold increase in DNA damage in airway cells exposed to a 100  $\mu\text{g/ml}$  suspension of nanoparticles of carbon black for 3 h (where exposure to due to sedimentation). We speculate, however, that air-tissue exposure is a better model for the non-aggregated component of nanoparticulate aerosols. Technical difficulties prevented us from visualizing more closely the nanoparticles on the surface of macrophages using TEM, and we therefore cannot exclude the possibility that that DNA damage was due to uptake of metal nanoparticles that agglomerate on impacting on the macrophage surface. AshaRani et al. (AshaRani et al. 2008) showed positive effects in human lung fibroblast cells and human glioblastoma cells. Interestingly, their advanced TEM images (Figure 5.1) revealed nanoparticles not only within endosomes and lysosomes, but also free in the cytoplasm and in the nucleus. However, we consider this to be unlikely since TEM analysis of non-cellular grids placed in the exposure chamber showed a uniform deposition of discrete nanoparticles of Au and Ag. The deposition of Fe was more difficult to interpret since particles were below the resolution of the TEM. The size distribution spectrum for Fe suggests that agglomeration occurs in the gas phase, although these aggregates remain within the nanoparticle range.

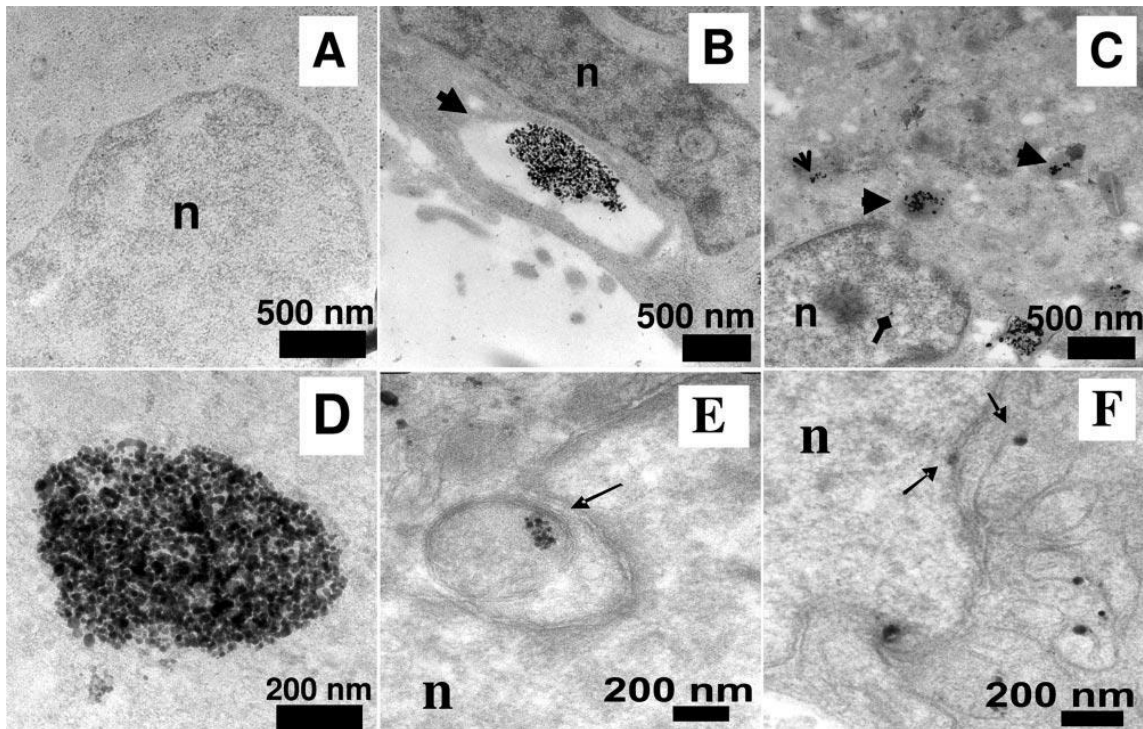


**Figure 5.1 :** TEM images of ultrathin sections of cells. Untreated cells showed no abnormalities (A), whereas cells treated with Ag-np showed large endosomes near the cell membrane with many nanoparticles inside (B). Electron micrographs showing lysosomes with nanoparticles inside (thick arrows) and scattered in cytoplasm (open arrow). Diamond arrow shows the presence of the nanoparticle in the nucleus (C). Magnified images of nanogroups showed that the cluster is composed of individual nanoparticles rather than clumps (D). Image shows endosomes in cytosol that are lodged in the nuclear membrane invaginations (E) and the presence of nanoparticles in mitochondria and on the nuclear membrane (F) (AshaRani et al. 2008).

We found that DNA damage to macrophages was robust and reproducible. We can exclude the confounding effect of Comet assay saturation, since measures of % tail DNA are within the accepted linear range of the assay (0–50%). Furthermore, we can exclude the possibility that DNA damage is due to a low level of nanoparticle-induced apoptosis. Apoptosis occurs with extensive DNA fragmentation leading to comets consisting of either nearly their entire DNA being in the tail (with the head dramatically reduced in size – yielding a ‘hedgehog’ comet) or ‘ghosts’ of comets, with a small percentage of normal DNA fluorescence, representing a residue of high-molecular-weight DNA in apoptotic cells. Analysis of the size distribution of the individual Comet measures reveals none of the 100 single measures recorded for the metal-exposed macrophages to be > 30% tail DNA i.e., well below the > 90% tail DNA expected for ‘hedgehog’ comets. We also found no evidence of ‘ghosts’. Additional support for a lack of cell death and apoptosis is provided by the absence of cell death after metal nanoparticle exposure by trypan blue exclusion and no change in proliferation of Mono Mac 6 cells at 24 h post exposure. This absence of apoptotic cell death may be important, since genotoxicity in the absence of cytotoxicity increases the potential for early transformation.

In contrast to our research, other studies on coated iron oxide nanoparticles have shown negative results in alkaline comet assay (Auffan et al. 2006) or in the neutral comet assay (Omidkhoda et al. 2007). Bhattacharya et al. (Bhattacharya

et al. 2009) and Karlsson et al. (Karlsson et al. 2009) used the same Fe<sub>2</sub>O<sub>3</sub> nanoparticle material as well as approximately the same doses on fibroblasts and lung epithelial cells, which allows a comparison between the studies. Karlsson et al. found negative results after 4 h exposure, whereas Bhattacharya et al. showed positive effects after 24 h exposure. Except for the obvious difference in exposure time, as well as a difference in the cells used, other factors may also explain the difference. Dynamic light scattering (DLS) revealed large agglomerates in the cell medium containing serum in the study by Karlsson et al., whereas the other study used a more dispersed solution in a medium without serum. Furthermore, the cell viability was somewhat reduced in the study by Bhattacharya et al. (Bhattacharya et al. 2009), a fact that could impact the results from the comet assay. In contrast to the studies discussed above, and similar to our study, almost all studies showed positive results from the comet assay (Barnes et al. 2008, Wang et al. 2007, Jin et al. 2007). In the studies where positive results were gained, the effects were considerable weaker when compared with those of other particles, such as ZnO (Gerloff et al. 2009), (Yang et al. 2009). The study by Gerloff et al. (Gerloff et al. 2009) detected no increase in DNA damage when using the alkaline version of the assay, but a slight increase in oxidatively produced lesions when using formamido pyrimidine glycosylase (FPG).

There are limitations to an air/tissue model. First, airway macrophages are specialized cells and may respond differently to macrophage cell lines. Although we did not assess DNA damage to human airway macrophages, we found a similar pattern of DNA damage in both rat airway macrophages and human Mono Mac 6 cells exposed to 10 mg/cm<sup>2</sup> Fe nanoparticles. Second, airway macrophages in vivo are in contact with both epithelial airway lining cells and epithelial lining fluid containing high levels of antioxidants (Zielinski et al. 1999). It should be feasible in future studies to include a combination of human alveolar macrophages (obtained by bronchoalveolar lavage or from tissue specimens), antioxidant rich fluid, and bronchial epithelial cell lines in the exposure chamber.

There are also few limitations with Trypan blue exclusion test used for a ‘viability check’. In this thesis, cell viability was determined by counting unstained cells. However, Trypan blue does not measure viability, but simply indicates whether cell membranes are intact. Few studies showed that cells with damaged membranes are trypan blue-positive, but they can recover and survive (Collins 2004b). Trypan blue cannot differentiate between the healthy cells and the cells that are alive but losing cell functions. In future studies, it is recommended to use enzyme activity assays like titanium – labelled thymidine uptake method, MTT assay and crystal violet method.

In summary, we found significant DNA damage in macrophages cultured for 24 h with doses of up to 10 mg/cm<sup>2</sup> aerosolized iron, gold or silver nanoparticles. We speculate that air/tissue exposure model is a valid way of assessing the toxic effects of non-agglomerated inhaled nanoparticles of Ag and Au. Studies are needed to further define the comparative toxicity of these metal nanoparticles to lower airway cells.

**Future Work:**

The results we achieved in this thesis didn't support the hypothesis that susceptibility to pneumococcal pneumonia is increased by carbon loading of AM *in vivo*. The mechanism for the protective effect is unknown, but may be due recruitment of low numbers of activated neutrophils into the lung prior to infection. It would be interesting to perform further experiments to assess pulmonary responses to chronic inhalation of ultra fine carbon particles and infection. However, due to time restrictions it was not possible to continue with these experiments. It could also be interesting approach to asses that biomass smoke involvement in susceptibility to infection in animal studies and *in vitro* cellular interactions.

In order to identify possible relationship of ultrafine carbon black particles with pulmonary cells, investigation of production of messenger molecules or expression of pro-inflammatory regulated cell adhesion molecules (such as vascular adhesion molecule 1 (VCAM-1) and intercellular adhesion molecule 1 (ICAM-1) would be an interesting analytical approach. Recently Mushtaq *et al.* (Mushtaq et al. 2011) reported that cigarette smoke upregulates the adhesion on *S. pneumoniae* to airway epithelial cells via upregulation of host-expressed receptors. It would be interesting to investigate that ultrafine carbon black particles share the common mechanism with lung epithelial cells.

In this thesis, we achieved good level of carbon loading in alveolar macrophages. In spite of assessing the cellular interactions with carbon particles in our work, fundamental studies to understand molecular interactions of nanoparticles with target cells remain largely unexplored. Such mechanism may be ionic interactions of the negative cellular membrane potential of alveolar macrophage with nanoparticle charge density, which will determine intracellular uptake and localization. Understanding such interactions is important not only for engineering of nanoparticles but also for determining nanoparticle cytotoxicity.

Our results suggested that nanoparticles play an important role in induction of inflammation and oxidative DNA damage. After particle exposure, levels of 8-OHdG was measured *in vivo* CB and DNA damage was measured in macrophages *in vitro*. To cope with DNA damage, cells are equipped with specific DNA repair enzymes. The oxidative DNA lesion 8-OHdG is specifically recognized and repaired by the base excision repair pathway (BER). DNA damage repair in exposure conditions are needed detailed investigation in future.

**References:**

ALTMAN, S.A., RANDERS, L. and RAO, G., 1993. Comparison of Trypan Blue Dye Exclusion and Fluorometric Assays for Mammalian Cell Viability Determinations. *Biotechnology Progress*, vol. 9, no. 6, pp. 671-674.

AMES, B.N. and GOLD, L.S., 1990. Too Many Rodent Carcinogens: Mitogenesis Increases Mutagenesis. *Science*, vol. 249, no. 4976, pp. 1487.

ARESKOUG, H., et al, 2000. Particles in Ambient Air- a Health Risk Assessment. *Scandinavian Journal of Work, Environment & Health*, vol. 26, pp. 1-96.

ARMSTRONG, J.R.M. and CAMPBELL, H., 1991. Indoor AirPollution Exposure and Lower Respiratory Infections in Young Gambian Children. *International Journal of Epidemiology*, vol. 20, no. 2, pp. 424.

ARTZ, A.S., ERSHLER, W.B. and LONGO, D.L., 2003. Pneumococcal Vaccination and Revaccination of Older Adults. *Clinical Microbiology Reviews*, vol. 16, no. 2, pp. 308.

ASHARANI, P., LOW KAH MUN, G., HANDE, M.P. and VALIYAVEETIL, S., 2008. Cytotoxicity and Genotoxicity of Silver Nanoparticles in Human Cells. *ACS Nano*, vol. 3, no. 2, pp. 279-290.

AUFFAN, M., et al, 2006. In Vitro Interactions between DMSA-Coated Maghemite Nanoparticles and Human Fibroblasts: A Physicochemical and Cyto-Genotoxic Study. *Environmental Science & Technology*, vol. 40, no. 14, pp. 4367-4373.

AUSTRIAN, R., 1997. The Enduring Pneumococcus: Unfinished Business and Opportunities for the Future. *Microbial Drug Resistance*, vol. 3, no. 2, pp. 111-115.

AUSTRIAN, R., 1986. Some Aspects of the Pneumococcal Carrier State. *Journal of Antimicrobial Chemotherapy*, vol. 18.

AUSTRIAN, R. and GOLD, J., 1964. Pneumococcal Bacteremia with Especial Reference to Bacteremic Pneumococcal Pneumonia. *Annals of Internal Medicine*, vol. 60, no. 5, pp. 759.

BALS, R., 2000. Epithelial Antimicrobial Peptides in Host Defense Against Infection. *Respiratory Research*, vol. 1, no. 3, pp. 141.

- BALS, R. and HIEMSTRA, P., 2004. Innate Immunity in the Lung: How Epithelial Cells Fight Against Respiratory Pathogens. *European Respiratory Journal*, vol. 23, no. 2, pp. 327.
- BANNISTER, B.A., BEGG, N.T. and GILLESPIE, S.H., 2000. *Infectious Disease*. Wiley-Blackwell.
- BARNES, C.A., et al, 2008. Reproducible Comet Assay of Amorphous Silica Nanoparticles Detects no Genotoxicity. *Nano Letters*, vol. 8, no. 9, pp. 3069-3074.
- BARON, P.A. and WILLEKE, K., 2005. *Aerosol Measurement: Principles, Techniques, and Applications*.
- BARTHELSON, R., MOBASSERI, A., ZOPF, D. and SIMON, P., 1998. Adherence of Streptococcus Pneumoniae to Respiratory Epithelial Cells is Inhibited by Sialylated Oligosaccharides. *Infection and Immunity*, vol. 66, no. 4, pp. 1439.
- BERMUDEZ, E., et al, 2002. Long-Term Pulmonary Responses of Three Laboratory Rodent Species to Subchronic Inhalation of Pigmentary Titanium Dioxide Particles. *Toxicological Sciences*, vol. 70, no. 1, pp. 86.
- BERMUDEZ, E., et al, 2004. Pulmonary Responses of Mice, Rats, and Hamsters to Subchronic Inhalation of Ultrafine Titanium Dioxide Particles. *Toxicological Sciences*, vol. 77, no. 2, pp. 347.
- BHATIA, M. and MOOCHHALA, S., 2004. Role of Inflammatory Mediators in the Pathophysiology of Acute Respiratory Distress Syndrome. *The Journal of Pathology*, vol. 202, no. 2, pp. 145-156.
- BHATTACHARYA, K., et al, 2009. Titanium Dioxide Nanoparticles Induce Oxidative Stress and DNA-Adduct Formation but Not DNA-Breakage in Human Lung Cells. *Part Fibre Toxicol*, vol. 6, pp. 17.
- BOCKHORN, H., 2000. Ultrafine Particles from Combustion Sources: Approaches to what we Want to Know. *Philosophical Transactions of the Royal Society of London. Series A: Mathematical, Physical and Engineering Sciences*, vol. 358, no. 1775, pp. 2659.
- BOISVERT, W.A., SANTIAGO, R., CURTISS, L.K. and TERKELTAUB, R.A., 1998. A Leukocyte Homologue of the IL-8 Receptor CXCR-2 Mediates the Accumulation of Macrophages in Atherosclerotic Lesions of LDL Receptor-Deficient Mice. *Journal of Clinical Investigation*, vol. 101, no. 2, pp. 353.

BORM, P.J.A. and KREYLING, W., 2004. Toxicological Hazards of Inhaled Nanoparticles-Potential Implications for Drug Delivery. *Journal of Nanoscience and Nanotechnology*, vol. 4, no. 5, pp. 521-531.

BORM, P., et al, 2000. The Relevance of the Rat Lung Response to Particle Overload for Human Risk Assessment: A Workshop Consensus Report. *Inhal.Toxicol*, vol. 12, pp. 1-17.

BOWERS, E. and JEFFRIES, L. Optochin in the Identification of Str. Pneumoniae. - *J Clin Pathol*.1955 Feb;8(1):58-60., no. 0021-9746 (Print).

BOYTON, R.J. and OPENSHAW, P.J., 2002. Pulmonary Defences to Acute Respiratory Infection. *British Medical Bulletin*, vol. 61, no. 1, pp. 1-12.

BRAUER, M., et al, 2001a. Air Pollution and Retained Particles in the Lung. *Environmental Health Perspectives*, vol. 109, no. 10, pp. 1039.

BRAUER, M., et al, 2001b. Air Pollution and Retained Particles in the Lung. *Environmental Health Perspectives*, vol. 109, no. 10, pp. 1039.

BRILES, D.E., et al, 2000. The Potential to use PspA and Other Pneumococcal Proteins to Elicit Protection Against Pneumococcal Infection. *Vaccine*, vol. 18, no. 16, pp. 1707-1711.

BRIMBLECOMBE, P. and MAYNARD, R.L., 2001. *The Urban Atmosphere and its Effects*. World Scientific Publishing Company.

BROWN, D.M., et al, 2000. Increased Inflammation and Intracellular Calcium Caused by Ultrafine Carbon Black is Independent of Transition Metals Or Other Soluble Components. *Occupational and Environmental Medicine*, vol. 57, no. 10, pp. 685.

BROWN, D.M., et al, 2001. Size-Dependent Proinflammatory Effects of Ultrafine Polystyrene Particles: A Role for Surface Area and Oxidative Stress in the Enhanced Activity of Ultrafines. *Toxicology and Applied Pharmacology*, vol. 175, no. 3, pp. 191-199.

BRUCE, N., PEREZ-PADILLA, R. and ALBALAK, R., 2000a. Indoor Air Pollution in Developing Countries: A Major Environmental and Public Health Challenge. *Bulletin of the World Health Organization*, vol. 78, no. 9, pp. 1078-1092.

BRUCE, N., PEREZ-PADILLA, R. and ALBALAK, R., 2000b. Indoor Air Pollution in Developing Countries: A Major Environmental and Public Health

Challenge. *Bulletin of the World Health Organization*, vol. 78, no. 9, pp. 1078-1092.

BRUCE, N., PEREZ-PADILLA, R. and ALBALAK, R., 2000c. Indoor Air Pollution in Developing Countries: A Major Environmental and Public Health Challenge. *Bulletin of the World Health Organization*, vol. 78, no. 9, pp. 1078-1092.

BUNN, H., DINSDALE, D., SMITH, T. and GRIGG, J., 2001. Ultrafine Particles in Alveolar Macrophages from Normal Children. *Thorax*, vol. 56, no. 12, pp. 932.

BUTLER, J.C. and SCHUCHAT, A., 1999. Epidemiology of Pneumococcal Infections in the Elderly. *Drugs & Aging*, vol. 15, no. Supplement 1, pp. 11-19.

BUTTERWORTH, B.E., 1990. Consideration of both Genotoxic and Nongenotoxic Mechanisms in Predicting Carcinogenic Potential. *Mutation Research/Reviews in Genetic Toxicology*, vol. 239, no. 2, pp. 117-132.

CANVIN, J.R., et al, 1995. The Role of Pneumolysin and Autolysin in the Pathology of Pneumonia and Septicemia in Mice Infected with a Type 2 Pneumococcus. *Journal of Infectious Diseases*, vol. 172, no. 1, pp. 119.

CASS, G.R., et al, 2000. The Chemical Composition of Atmospheric Ultrafine Particles. *Philosophical Transactions of the Royal Society of London. Series A: Mathematical, Physical and Engineering Sciences*, vol. 358, no. 1775, pp. 2581.

CASTRANOVA, V., et al, 1985. The Response of Rat Alveolar Macrophages to Chronic Inhalation of Coal Dust and/or Diesel Exhaust\* 1. *Environmental Research*, vol. 36, no. 2, pp. 405-419.

CASTRANOVA, V. and VALLYATHAN, V., 2000. Silicosis and Coal Workers' Pneumoconiosis. *Environmental Health Perspectives*, vol. 108, no. Suppl 4, pp. 675.

CHEN, Y., et al, 2004. Influence of Relatively Low Level of Particulate Air Pollution on Hospitalization for COPD in Elderly People. *Inhalation Toxicology*, vol. 16, no. 1, pp. 21-25.

CHEN, B.H., HONG, C.J., PANDEY, M.R. and SMITH, K.R., 1990. Indoor Air Pollution in Developing Countries. *World Health Statistics Quarterly. Rapport Trimestriel De Statistiques Sanitaires Mondiales*, vol. 43, no. 3, pp. 127-138 ISSN 0379-8070; 0379-8070.

- CHONO, S., TANINO, T., SEKI, T. and MORIMOTO, K., 2007. Uptake Characteristics of Liposomes by Rat Alveolar Macrophages: Influence of Particle Size and Surface Mannose Modification. *Journal of Pharmacy and Pharmacology*, vol. 59, no. 1, pp. 75-80.
- CHURG, A., GILKS, B. and DAI, J., 1999. Induction of Fibrogenic Mediators by Fine and Ultrafine Titanium Dioxide in Rat Tracheal Explants. *American Journal of Physiology-Lung Cellular and Molecular Physiology*, vol. 277, no. 5, pp. L975.
- COHEN, S.M. and ELLWEIN, L.B., 1991. Genetic Errors, Cell Proliferation, and Carcinogenesis. *Cancer Research*, vol. 51, no. 24, pp. 6493.
- COLBECK, I., NASIR, Z. and ALI, Z., 2010. Characteristics of indoor/outdoor Particulate Pollution in Urban and Rural Residential Environment of Pakistan. *Indoor Air*, vol. 20, no. 1, pp. 40-51.
- COLLINGS, D., SITHOLE, S. and MARTIN, K., 1990. Indoor Woodsmoke Pollution Causing Lower Respiratory Disease in Children. *Tropical Doctor*, vol. 20, no. 4, pp. 151.
- COLLINS, A.R., 2004a. The Comet Assay for DNA Damage and Repair. *Molecular Biotechnology*, vol. 26, no. 3, pp. 249-261.
- COLLINS, A.R., 2004b. The Comet Assay for DNA Damage and Repair. *Molecular Biotechnology*, vol. 26, no. 3, pp. 249-261.
- COOPER, M.A., FEHNIGER, T.A. and CALIGIURI, M.A., 2001. The Biology of Human Natural Killer-Cell Subsets. *Trends in Immunology*, vol. 22, no. 11, pp. 633-640.
- COSTA, D.L. and DREHER, K.L., 1997. Bioavailable Transition Metals in Particulate Matter Mediate Cardiopulmonary Injury in Healthy and Compromised Animal Models. *Environmental Health Perspectives*, vol. 105, no. Suppl 5, pp. 1053.
- CRAPO, J., et al, 1982. Cell Number and Cell Characteristics of the Normal Human Lung. *The American Review of Respiratory Disease*, vol. 126, no. 2, pp. 332.
- CREUTZENBERG, O., et al, 1990. Clearance and Retention of Inhaled Diesel Exhaust Particles, Carbon Black, and Titanium Dioxide in Rats at Lung Overload Conditions. *Journal of Aerosol Science*, vol. 21, pp. S455-S458.

- CREUTZENBERG, O., et al, 1998. Lung Clearance and Retention of Toner, TiO<sub>2</sub>, and Crystalline Silica, Utilizing a Tracer Technique during Chronic Inhalation Exposure in Syrian Golden Hamsters. *Inhalation Toxicology*, vol. 10, no. 7, pp. 731-751.
- CROSS, C.E., et al, 1994. Oxidants, Antioxidants, and Respiratory Tract Lining Fluids. *Environmental Health Perspectives*, vol. 102, no. Suppl 10, pp. 185.
- CURTIS, J.L., 2005. Cell-Mediated Adaptive Immune Defense of the Lungs. *Proceedings of the American Thoracic Society*, vol. 2, no. 5, pp. 412-416.
- DAVIDSON, C.I., PHALEN, R.F. and SOLOMON, P.A., 2005. Airborne Particulate Matter and Human Health: A Review. *Aerosol Science and Technology*, vol. 39, no. 8, pp. 737-749.
- DAVOREN, M., et al, 2007. In Vitro Toxicity Evaluation of Single Walled Carbon Nanotubes on Human A549 Lung Cells. *Toxicology in Vitro*, vol. 21, no. 3, pp. 438-448.
- DE KONING, H.W., SMITH, K. and LAST, J., 1985. Biomass Fuel Combustion and Health. *Bulletin of the World Health Organization*, vol. 63, no. 1, pp. 11.
- DEFORGE, L.E., et al, 1993. Regulation of Interleukin 8 Gene Expression by Oxidant Stress. *Journal of Biological Chemistry*, vol. 268, no. 34, pp. 25568.
- DELCLAUX, C. and AZOULAY, E., 2003. Inflammatory Response to Infectious Pulmonary Injury. *European Respiratory Journal*, vol. 22, no. 42 suppl, pp. 10s.
- DICK, C.A.J., BROWN, D.M., DONALDSON, K. and STONE, V., 2003. The Role of Free Radicals in the Toxic and Inflammatory Effects of Four Different Ultrafine Particle Types. *Inhalation Toxicology*, vol. 15, no. 1, pp. 39-52.
- DING, A.H., NATHAN, C.F. and STUEHR, D.J., 1988. Release of Reactive Nitrogen Intermediates and Reactive Oxygen Intermediates from Mouse Peritoneal Macrophages. Comparison of Activating Cytokines and Evidence for Independent Production. *The Journal of Immunology*, vol. 141, no. 7, pp. 2407.
- DIPERSIO, J., BILLING, P., WILLIAMS, R. and GASSON, J., 1988. Human Granulocyte-Macrophage Colony-Stimulating Factor and Other Cytokines Prime Human Neutrophils for Enhanced Arachidonic Acid Release and Leukotriene B<sub>4</sub> Synthesis. *The Journal of Immunology*, vol. 140, no. 12, pp. 4315.

- DJAMARANI, K. and CLARK, I.M., 1997. Characterization of Particle Size Based on Fine and Coarse Fractions. *Powder Technology*, vol. 93, no. 2, pp. 101-108.
- DONALDSON, K., BESWICK, P.H. and GILMOUR, P.S., 1996. Free Radical Activity Associated with the Surface of Particles: A Unifying Factor in Determining Biological Activity?. *Toxicology Letters*, vol. 88, no. 1-3, pp. 293-298.
- DONALDSON, K., et al, 2001. Ultrafine Particles. *Occupational and Environmental Medicine*, vol. 58, no. 3, pp. 211-216.
- DONALDSON, Q.Z.Y.K.K.S.K.N.N.K.K., 1998. Differences in the Extent of Inflammation Caused by Intratracheal Exposure to Three Ultrafine Metals: Role of Free Radicals. *Journal of Toxicology and Environmental Health, Part A*, vol. 53, no. 6, pp. 423-438.
- DRISCOLL, K.E., et al, 1996. Pulmonary Inflammatory, Chemokine, and Mutagenic Responses in Rats After Subchronic Inhalation of Carbon Black. *Toxicology and Applied Pharmacology*, vol. 136, no. 2, pp. 372-380.
- ENGLERT, N., 2004. Fine Particles and Human Health--a Review of Epidemiological Studies. *Toxicology Letters*, vol. 149, no. 1-3, pp. 235-242.
- EVANS, M.D., DIZDAROGLU, M. and COOKE, M.S., 2004. Oxidative DNA Damage and Disease: Induction, Repair and Significance. *Mutation Research/Reviews in Mutation Research*, vol. 567, no. 1, pp. 1-61.
- EZZATI, M. and KAMMEN, D.M., 2001. Quantifying the Effects of Exposure to Indoor Air Pollution from Biomass Combustion on Acute Respiratory Infections in Developing Countries. *Environmental Health Perspectives*, vol. 109, no. 5, pp. 481.
- FEIG, D.I. and LOEB, L.A., 1993. Mechanisms of Mutation by Oxidative DNA Damage: Reduced Fidelity of Mammalian DNA Polymerase. *Beta. Biochemistry*, vol. 32, no. 16, pp. 4466-4473.
- FERIN, J., OBERDÖRSTER, G., SODERHOLM, S.C. and GELEIN, R., 1991. Pulmonary Tissue Access of Ultrafine Particles. *Journal of Aerosol Medicine*, vol. 4, no. 1, pp. 57-68.
- FERIN, J., OBERDORSTER, G. and PENNEY, D.P., 1992. Pulmonary Retention of Ultrafine and Fine Particles in Rats. *American Journal of*

*Respiratory Cell and Molecular Biology*, May, vol. 6, no. 5, pp. 535-542 ISSN 1044-1549; 1044-1549.

FERINGA, B.L., 2001. In Control of Motion: From Molecular Switches to Molecular Motors. *Accounts of Chemical Research*, vol. 34, no. 6, pp. 504-513.

FIEGEL, J., et al, 2003. Large Porous Particle Impingement on Lung Epithelial Cell monolayers—toward Improved Particle Characterization in the Lung. *Pharmaceutical Research*, vol. 20, no. 5, pp. 788-796.

FIREMAN, E.M., et al, 2004. Induced Sputum Assessment in New York City Firefighters Exposed to World Trade Center Dust. *Environmental Health Perspectives*, vol. 112, no. 15, pp. 1564.

FRAGA, C.G., et al, 1990. Oxidative Damage to DNA during Aging: 8-Hydroxy-2'-Deoxyguanosine in Rat Organ DNA and Urine. *Proceedings of the National Academy of Sciences of the United States of America*, vol. 87, no. 12, pp. 4533.

FRIEDLANDER, S.K. and BOOKS24X7, I., 2000. *Smoke, Dust, and Haze: Fundamentals of Aerosol Dynamics*. Oxford University Press.

FRYXELL, G.E. and CAO, G., 2007. *Environmental Applications of Nanomaterials: Synthesis, Sorbents and Sensors*. World Scientific Pub Co Inc.

FULLERTON, D.G., et al, 2009a. Domestic Smoke Exposure is Associated with Alveolar Macrophage Particulate Load. *Tropical Medicine & International Health*, vol. 14, no. 3, pp. 349-354.

FULLERTON, D.G., et al, 2009b. Domestic Smoke Exposure is Associated with Alveolar Macrophage Particulate Load. *Tropical Medicine & International Health*, vol. 14, no. 3, pp. 349-354.

FULLERTON, D.G., et al, 2009c. Domestic Smoke Exposure is Associated with Alveolar Macrophage Particulate Load. *Tropical Medicine & International Health*, vol. 14, no. 3, pp. 349-354.

FUSCO, D., et al, 2001. Air Pollution and Hospital Admissions for Respiratory Conditions in Rome, Italy. *European Respiratory Journal*, vol. 17, no. 6, pp. 1143.

GÁBELOVÁ, A., et al, 2006. Genotoxic Activity of Ambient Air Pollution in Three European Cities: Prague, Košice and Sofia: An'in Vitro'Study. *Environmental Health in Central and Eastern Europe*, pp. 23-30.

GALLAGHER, J. and SAMS, R., 2003. Formation of 8-Oxo-7, 8-Dihydro-2'-Deoxyguanosine in Rat Lung DNA Following Subchronic Inhalation of Carbon Black. *Toxicology and Applied Pharmacology*, vol. 190, no. 3, pp. 224-231.

GANZ, T., 2002. Antimicrobial Polypeptides in Host Defense of the Respiratory Tract. *Journal of Clinical Investigation*, vol. 109, no. 6, pp. 693-698.

GEISSMANN, F., et al, 2010. Development of Monocytes, Macrophages, and Dendritic Cells. *Science*, vol. 327, no. 5966, pp. 656-661.

GERLOFF, K., et al, 2009. Cytotoxicity and Oxidative DNA Damage by Nanoparticles in Human Intestinal Caco-2 Cells. *Nanotoxicology*, vol. 3, no. 4, pp. 355-364.

GHOSH, P., et al, 2008. Gold Nanoparticles in Delivery Applications. *Advanced Drug Delivery Reviews*, vol. 60, no. 11, pp. 1307-1315.

GILBERT, C., ROBINSON, K., LE PAGE, R.W.F. and WELLS, J.M., 2000. Heterologous Expression of an Immunogenic Pneumococcal Type 3 Capsular Polysaccharide in *Lactococcus Lactis*. *Infection and Immunity*, vol. 68, no. 6, pp. 3251.

GILMOUR, P., et al, 1997. Surface Free Radical Activity of PM10 and Ultrafine Titanium Dioxide: A Unifying Factor in their Toxicity?. *Annals of Occupational Hygiene*, vol. 41, no. inhaled particles VIII, pp. 32.

GILMOUR, P.S., et al, 2004. Pulmonary and Systemic Effects of Short-Term Inhalation Exposure to Ultrafine Carbon Black Particles\* 1. *Toxicology and Applied Pharmacology*, vol. 195, no. 1, pp. 35-44.

GODLESKI, J.J., et al, 2000. Mechanisms of Morbidity and Mortality from Exposure to Ambient Air Particles. *Research Report (Health Effects Institute)*, Feb, vol. (91), no. 91, pp. 5-88; discussion 89-103 ISSN 1041-5505; 1041-5505.

GOGOTSI, Y., 2006. *Nanomaterials Handbook*. CRC Press.

GOLDBERG, M.S., et al, 2000. Identifying Subgroups of the General Population that may be Susceptible to Short-Term Increases in Particulate Air Pollution: A Time-Series Study in Montreal, Quebec. *Research Report (Health Effects Institute)*, no. 97, pp. 7.

- GORDON, T., NADZIEJKO, C., CHEN, L.C. and SCHLESINGER, R., 2000. Effects of Concentrated Ambient Particles in Rats and Hamsters: An Exploratory Study. *RESEARCH REPORT-HEALTH EFFECTS INSTITUTE*.
- GRAINGER, C., GREENWELL, L., MARTIN, G. and FORBES, B., 2009. The Permeability of Large Molecular Weight Solutes Following Particle Delivery to Air-Interfaced Cells that Model the Respiratory Mucosa. *European Journal of Pharmaceutics and Biopharmaceutics*, vol. 71, no. 2, pp. 318-324.
- GRIGG, J. Particulate matter exposure in children: relevance to chronic obstructive pulmonary disease Anonymous *Proceedings of the American Thoracic Society*, 2009.
- GRONEBERG, D.A. and CHUNG, K.F., 2004. Models of Chronic Obstructive Pulmonary Disease. *Respir Res*, vol. 5, no. 1, pp. 18.
- GULUMIAN, M., et al, 2006. Mechanistically Identified Suitable Biomarkers of Exposure, Effect, and Susceptibility for Silicosis and Coal-Worker's Pneumoconiosis: A Comprehensive Review. *Journal of Toxicology and Environmental Health-Part B-Critical Reviews*, vol. 9, no. 4-6, pp. 357-396.
- GUTSCH, A., et al, 2002. Gas-Phase Production of Nanoparticles. *Kona*, vol. 20, pp. 24-37.
- HAHON, N., BOOTH, J.A. and WHEELER, R., 1982. Activity of Diesel Engine Emission Particulates on the Interferon System. *Environmental Research*, vol. 28, no. 2, pp. 443-455.
- HAN, G., GHOSH, P., DE, M. and ROTELLO, V.M., 2007. Drug and Gene Delivery using Gold Nanoparticles. *Nanobiotechnology*, vol. 3, no. 1, pp. 40-45.
- HANCE, A., 1993. Pulmonary Immune Cells in Health and Disease: Dendritic Cells and Langerhans' Cells. *European Respiratory Journal*, vol. 6, no. 8, pp. 1213-1220.
- HARLOW, E., HARLOW, E. and LANE, D., 1988. *Antibodies: A Laboratory Manual*. CSHL press.
- HARRISON, R.M., SMITH, D. and LUHANA, L., 1996. Source Apportionment of Atmospheric Polycyclic Aromatic Hydrocarbons Collected from an Urban Location in Birmingham, UK. *Environmental Science & Technology*, vol. 30, no. 3, pp. 825-832.

- HE, J., CHEN, W., JIN, L. and JIN, H., 2000. Comparative Evaluation of the in Vitro Micronucleus Test and the Comet Assay for the Detection of Genotoxic Effects of X-Ray Radiation. *Mutation Research/Genetic Toxicology and Environmental Mutagenesis*, vol. 469, no. 2, pp. 223-231.
- HEINEMAN, H.S., et al, 1973. Quellung Test for Pneumonia. *New England Journal of Medicine*, vol. 288, no. 19, pp. 1027-1027.
- HEINRICH, U., et al, 1995. Chronic Inhalation Exposure of Wistar Rats and Two Different Strains of Mice to Diesel Engine Exhaust, Carbon Black, and Titanium Dioxide. *Inhalation Toxicology*, vol. 7, no. 4, pp. 533-556.
- HEINRICH, U., et al, 1986. Chronic Effects on the Respiratory Tract of Hamsters, Mice and Rats After long-term Inhalation of High Concentrations of Filtered and Unfiltered Diesel Engine Emissions. *Journal of Applied Toxicology*, vol. 6, no. 6, pp. 383-395.
- HENDERSON, R., et al, 1995. A Comparison of the Inflammatory Response of the Lung to Inhaled Versus Instilled Particles in F344 Rats. *Toxicological Sciences*, vol. 24, no. 2, pp. 183.
- HENRICHSEN, J., 1995. Six Newly Recognized Types of Streptococcus Pneumoniae. *Journal of Clinical Microbiology*, vol. 33, no. 10, pp. 2759.
- HERBERT, S., et al, 2007. Molecular Basis of Resistance to Muramidase and Cationic Antimicrobial Peptide Activity of Lysozyme in Staphylococci. *PLoS Pathogens*, vol. 3, no. 7, pp. e102.
- HEYDER, J., et al, 1986. Deposition of Particles in the Human Respiratory Tract in the Size Range 0.005-15 [Mu] m. *Journal of Aerosol Science*, vol. 17, no. 5, pp. 811-825.
- HOLGATE, S.T., et al, 2003. Health Effects of Acute Exposure to Air Pollution. Part I: Healthy and Asthmatic Subjects Exposed to Diesel Exhaust. *Research Report (Health Effects Institute)*, Dec, vol. (112), no. 112, pp. 1-30; discussion 51-67 ISSN 1041-5505; 1041-5505.
- HUAUX, F., 2007. New Developments in the Understanding of Immunology in Silicosis. *Current Opinion in Allergy and Clinical Immunology*, vol. 7, no. 2, pp. 168.
- ICHINOSE, T., et al, 1997. Lung Carcinogenesis and Formation of 8-Hydroxy-Deoxyguanosine in Mice by Diesel Exhaust Particles. *Carcinogenesis*, vol. 18, no. 1, pp. 185.

- IRWIN, R.S., et al, 1998. Managing Cough as a Defense Mechanism and as a Symptom. *Chest*, vol. 114, no. 2, pp. 133S-181S.
- ISENBERG, H.D., 1998. *Essential Procedures for Clinical Microbiology*. Amer Society for Microbiology.
- ITO, T., et al, 2000. Peroxynitrite Formation by Diesel Exhaust Particles in Alveolar Cells: Links to Pulmonary Inflammation. *Environmental Toxicology and Pharmacology*, vol. 9, no. 1-2, pp. 1-8.
- IWAI, K., et al, 1997. Lung Tumor Induced by Long-Term Inhalation Or Intratracheal Instillation of Diesel Exhaust Particles. *Experimental and Toxicologic Pathology: Official Journal of the Gesellschaft Fur Toxikologische Pathologie*, vol. 49, no. 5, pp. 393.
- JAKAB, G.J., et al, 1990. Suppression of Alveolar Macrophage Membrane-Receptor-Mediated Phagocytosis by Model Particle-Adsorbate Complexes: Physicochemical Moderators of Uptake. *Environmental Health Perspectives*, vol. 89, pp. 169.
- JANEWAY JR, C.A. and MEDZHITOV, R., 2002. Innate Immune Recognition. *Annual Review of Immunology*, vol. 20, no. 1, pp. 197-216.
- JEAN, D., et al, 1998. Protective Effect of Endotoxin Instillation on Subsequent Bacteria-Induced Acute Lung Injury in Rats. *American Journal of Respiratory and Critical Care Medicine*, vol. 158, no. 6, pp. 1702.
- JIANG, J., et al, 2008. Does Nanoparticle Activity Depend upon Size and Crystal Phase?. *Nanotoxicology*, vol. 2, no. 1, pp. 33-42.
- JIN, Y., KANNAN, S., WU, M. and ZHAO, J.X., 2007. Toxicity of Luminescent Silica Nanoparticles to Living Cells. *Chemical Research in Toxicology*, vol. 20, no. 8, pp. 1126-1133.
- KALTOFT, M., ZEUTHEN, N. and KONRADSEN, H., 2000a. Epidemiology of Invasive Pneumococcal Infections in Children Aged 0–6 Years in Denmark: A 19-year Nationwide Surveillance Study. *Acta Paediatrica*, vol. 89, pp. 3-10.
- KALTOFT, M., ZEUTHEN, N. and KONRADSEN, H., 2000b. Epidemiology of Invasive Pneumococcal Infections in Children Aged 0–6 Years in Denmark: A 19-year Nationwide Surveillance Study. *Acta Paediatrica*, vol. 89, pp. 3-10.

- KAMERLING, J.P., 2000. Pneumococcal Polysaccharides: A Chemical View. *Streptococcus Pneumoniae, Molecular Biology and Mechanisms of Disease*. New York: Rockefeller University, pp. 81-114.
- KARLSSON, H.L., GUSTAFSSON, J. and CRONHOLM, P., 2009. Size-Dependent Toxicity of Metal Oxide Particles--A Comparison between Nano- and Micrometer Size. *Toxicology Letters*, vol. 188, no. 2, pp. 112-118.
- KASAI, H., 1997. Analysis of a Form of Oxidative DNA Damage, 8-Hydroxy-2'-Deoxyguanosine, as a Marker of Cellular Oxidative Stress during Carcinogenesis. *Mutation Research/Reviews in Mutation Research*, vol. 387, no. 3, pp. 147-163.
- KAWAKAMI, K., 2004. Regulation by Innate Immune T Lymphocytes in the Host Defense Against Pulmonary Infection with *Cryptococcus Neoformans*. *Japanese Journal of Infectious Diseases*, vol. 57, no. 4, pp. 137-145.
- KENNEDY, N.J. and HINDS, W.C., 2002. Inhalability of Large Solid Particles. *Journal of Aerosol Science*, vol. 33, no. 2, pp. 237-255.
- KHAN, R.U., 2007. *WEAR REDUCTION IN FDB BY ENHANCING LUBRICANTS WITH NANOPARTICLES*.
- KILPPER, R., et al, 1989. Lung Response to Test Toner upon 2 Year Inhalation Exposure in Rats. *Experimental Pathology*, vol. 37, no. 1-4, pp. 239-242.
- KIM, C.S. and HU, S., 1998. Regional Deposition of Inhaled Particles in Human Lungs: Comparison between Men and Women. *Journal of Applied Physiology*, vol. 84, no. 6, pp. 1834.
- KIM, S., et al, 2009. Oxidative Stress-Dependent Toxicity of Silver Nanoparticles in Human Hepatoma Cells. *Toxicology in Vitro*, vol. 23, no. 6, pp. 1076-1084.
- KINGMA, P.S. and WHITSETT, J.A., 2006. In Defense of the Lung: Surfactant Protein A and Surfactant Protein D. *Current Opinion in Pharmacology*, vol. 6, no. 3, pp. 277-283.
- KLEIN, D.L., 1999. Pneumococcal Disease and the Role of Conjugate Vaccines. *Microbial Drug Resistance*, vol. 5, no. 2, pp. 147-157.
- KNAAPEN, A.M., BORM, P.J.A., ALBRECHT, C. and SCHINS, R.P.F., 2004. Inhaled Particles and Lung Cancer. Part A: Mechanisms. *International Journal of Cancer*, vol. 109, no. 6, pp. 799-809.

- KNAAPEN, A., GÜNGÖR, N., SCHINS, R. and BORM, P., 2009. Neutrophils and Respiratory Tract DNA Damage and Mutagenesis. *Role of Neutrophils in Pulmonary DNA Damage and Repair*, vol. 21, pp. 16.
- KNEBEL, J.W., et al, 2001. Development and Validation of a Semiautomatic System for Generation and Deposition of Sprays on Isolated Cells of the Respiratory Tract. *Toxicology Mechanisms and Methods*, vol. 11, no. 3, pp. 161-171.
- KNECHT, J.C., SCHIFFMAN, G. and AUSTRIAN, R., 1970. Some Biological Properties of Pneumococcus Type 37 and the Chemistry of its Capsular Polysaccharide. *The Journal of Experimental Medicine*, vol. 132, no. 3, pp. 475.
- KOBZIK, L., et al, 2001. Effects of Combined Ozone and Air Pollution Particle Exposure in Mice. *Research Report (Health Effects Institute)*, Dec, vol. (106), no. 106, pp. 5-29; discussion 31-8 ISSN 1041-5505; 1041-5505.
- KOCBACH, A., JOHANSEN, B., SCHWARZE, P. and NAMORK, E., 2005. Analytical Electron Microscopy of Combustion Particles: A Comparison of Vehicle Exhaust and Residential Wood Smoke. *Science of the Total Environment*, vol. 346, no. 1-3, pp. 231-243.
- KRUIS, F.E., FISSAN, H. and PELED, A., 1998. Synthesis of Nanoparticles in the Gas Phase for Electronic, Optical and Magnetic Applications--a Review. *Journal of Aerosol Science*, vol. 29, no. 5-6, pp. 511-535.
- KUEMPEL, E., et al, 2003. Pulmonary Inflammation and Crystalline Silica in Respirable Coal Mine Dust: Dose Response. *Journal of Biosciences*, vol. 28, no. 1, pp. 61-69.
- KULKARNI, N., PIERSE, N., RUSHTON, L. and GRIGG, J., 2006. Carbon in Airway Macrophages and Lung Function in Children. *New England Journal of Medicine*, vol. 355, no. 1, pp. 21-30.
- KULKARNI, N.S., et al, 2005. Carbon Loading of Alveolar Macrophages in Adults and Children Exposed to Biomass Smoke Particles. *Science of the Total Environment*, vol. 345, no. 1-3, pp. 23-30.
- KUMAGAI, Y., et al, 1997. Generation of Reactive Oxygen Species during Interaction of Diesel Exhaust Particle Components with NADPH-Cytochrome P450 Reductase and Involvement of the Bioactivation in the DNA Damage. *Free Radical Biology and Medicine*, vol. 22, no. 3, pp. 479-487.

- KUROSAWA, S., et al, 2006. Quartz Crystal Microbalance Immunosensors for Environmental Monitoring. *Biosensors and Bioelectronics*, vol. 22, no. 4, pp. 473-481.
- LAMBRECHT, B.N., 2006. Alveolar Macrophage in the Driver's Seat. *Immunity*, vol. 24, no. 4, pp. 366-368.
- LAMBRECHT, B., PRINS, B. and HOOGSTEDEN, H., 2001. Lung Dendritic Cells and Host Immunity to Infection. *European Respiratory Journal*, vol. 18, no. 4, pp. 692-704.
- LANGER, R. and PEPPAS, N.A., 2003. Advances in Biomaterials, Drug Delivery, and Bionanotechnology. *AIChE Journal*, vol. 49, no. 12, pp. 2990-3006.
- LEBIEN, T.W. and TEDDER, T.F., 2008. B Lymphocytes: How they Develop and Function. *Blood*, vol. 112, no. 5, pp. 1570-1580.
- LEIKAUF, G.D., et al, 2001. Pathogenomic Mechanisms for Particulate Matter Induction of Acute Lung Injury and Inflammation in Mice. *Research Report (Health Effects Institute)*, Dec, vol. (105), no. 105, pp. 5-58; discussion 59-71 ISSN 1041-5505; 1041-5505.
- LESINSKI, G.B. and WESTERINK, M., 2001. Novel Vaccine Strategies to T-Independent Antigens. *Journal of Microbiological Methods*, vol. 47, no. 2, pp. 135-149.
- LEVINE, A.M., et al, 2000. Distinct Effects of Surfactant Protein A Or D Deficiency during Bacterial Infection on the Lung. *The Journal of Immunology*, vol. 165, no. 7, pp. 3934.
- LEWINSKI, N., COLVIN, V. and DREZEK, R., 2008. Cytotoxicity of Nanoparticles. *Small*, vol. 4, no. 1, pp. 26-49.
- LI, X.Y., et al, 1999a. Short-Term Inflammatory Responses Following Intratracheal Instillation of Fine and Ultrafine Carbon Black in Rats. *Inhalation Toxicology*, vol. 11, no. 8, pp. 709-731.
- LI, X.Y., et al, 1999b. Short-Term Inflammatory Responses Following Intratracheal Instillation of Fine and Ultrafine Carbon Black in Rats. *Inhalation Toxicology*, vol. 11, no. 8, pp. 709-731.

- LI, X., GILMOUR, P., DONALDSON, K. and MACNEE, W., 1996. Free Radical Activity and Pro-Inflammatory Effects of Particulate Air Pollution (PM10) in Vivo and in Vitro. *Thorax*, vol. 51, no. 12, pp. 1216.
- LIOY, P.J., et al, 2002. Characterization of the dust/smoke Aerosol that Settled East of the World Trade Center (WTC) in Lower Manhattan After the Collapse of the WTC 11 September 2001. *Environmental Health Perspectives*, vol. 110, no. 7, pp. 703.
- LIPPMANN, M., YEATES, D. and ALBERT, R., 1980. Deposition, Retention, and Clearance of Inhaled Particles. *British Journal of Industrial Medicine*, vol. 37, no. 4, pp. 337.
- LIPPMANN, M., ITO, K., NADAS, A. and BURNETT, R.T., 2000. Association of Particulate Matter Components with Daily Mortality and Morbidity in Urban Populations. *Research Report (Health Effects Institute)*, Aug, vol. (95), no. 95, pp. 5-72, discussion 73-82 ISSN 1041-5505; 1041-5505.
- LISTER, P.D., GENTRY, M.J. and PREHEIM, L.C., 1993. Granulocyte Colony-Stimulating Factor Protects Control Rats but Not Ethanol-Fed Rats from Fatal Pneumococcal Pneumonia. *Journal of Infectious Diseases*, vol. 168, no. 4, pp. 922.
- LOCK, R.A., PATON, J.C. and HANSMAN, D., 1988. Comparative Efficacy of Pneumococcal Neuraminidase and Pneumolysin as Immunogens Protective Against Streptococcus Pneumoniae\* 1. *Microbial Pathogenesis*, vol. 5, no. 6, pp. 461-467.
- LOFT, S., POULSEN, H.E., VISTISEN, K. and KNUDSEN, L.E., 1999. Increased Urinary Excretion of 8-Oxo-2'-Deoxyguanosine, a Biomarker of Oxidative DNA Damage, in Urban Bus Drivers. *Mutation Research/Genetic Toxicology and Environmental Mutagenesis*, vol. 441, no. 1, pp. 11-19.
- LOHMANN-MATTHES, M., STEINMULLER, C. and FRANKE-ULLMANN, G., 1994. Pulmonary Macrophages. *European Respiratory Journal*, vol. 7, no. 9, pp. 1678.
- LU, M. and ZHAO, X.S., 2010. *Nanoporous Materials Science and Engineering*. Imperial College Press.
- LUNDBORG, M., et al, 2007a. Aggregates of Ultrafine Particles Modulate Lipid Peroxidation and Bacterial Killing by Alveolar Macrophages. *Environmental Research*, vol. 104, no. 2, pp. 250-257.

- LUNDBORG, M., et al, 2007b. Aggregates of Ultrafine Particles Modulate Lipid Peroxidation and Bacterial Killing by Alveolar Macrophages. *Environmental Research*, vol. 104, no. 2, pp. 250-257.
- MACKANESS, G., 1962. Cellular Resistance to Infection. *The Journal of Experimental Medicine*, vol. 116, no. 3, pp. 381.
- MACLEOD, C.M., HODGES, R.G., HEIDELBERGER, M. and BERNHARD, W.G., 1945. Prevention of Pneumococcal Pneumonia by Immunization with Specific Capsular Polysaccharides. *The Journal of Experimental Medicine*, vol. 82, no. 6, pp. 445.
- MAGE, D., WILSON, W., HASSELBLAD, V. and GRANT, L., 1999. Assessment of Human Exposure to Ambient Particulate Matter. *Journal of the Air & Waste Management Association*, vol. 49, no. 11, pp. 1280-1291.
- MAGEE, A.D. and YOTHER, J., 2001. Requirement for Capsule in Colonization by *Streptococcus Pneumoniae*. *Infection and Immunity*, vol. 69, no. 6, pp. 3755.
- MANSOORI, G.A., 2005. *Principles of Nanotechnology: Molecular-Based Study of Condensed Matter in Small Systems*. World Scientific Pub Co Inc.
- MARTIN, T.R. and FREVERT, C.W., 2005. Innate Immunity in the Lungs. *Proceedings of the American Thoracic Society*, vol. 2, no. 5, pp. 403-411.
- MAYNARD, A., et al, 2006. Safe Handling of Nanotechnology. *NATURE-LONDON-*, vol. 444, no. 7117, pp. 267.
- METCHNIKOFF, E., 1905. *Immunity in Infective Diseases*. University press.
- Miles A A & Misra S S.  
the Estimation of the Bactericidal Power of the Blood, no. 06 ISSN 0950-2688.
- MILLER, E., et al, 2000. Epidemiology of Invasive and Other Pneumococcal Disease in Children in England and Wales 1996–1998. *Acta Paediatrica*, vol. 89, pp. 11-16.
- MIZGERD, J.P., 2008. Acute Lower Respiratory Tract Infection. *New England Journal of Medicine*, vol. 358, no. 7, pp. 716-727.
- MOHANRAJ, V. and CHEN, Y., 2006. Nanoparticles—A Review. *Tropical Journal of Pharmaceutical Research*, vol. 5, no. 1, pp. 561-573.

- MONTEIRO, R.C., 2010. Role of IgA and IgA Fc Receptors in Inflammation. *Journal of Clinical Immunology*, vol. 30, no. 1, pp. 1-9.
- MOORE, A., MARECOS, E., BOGDANOV JR, A. and WEISSLEDER, R., 2000. Tumoral Distribution of Long-Circulating Dextran-Coated Iron Oxide Nanoparticles in a Rodent Model. *Radiology*, vol. 214, no. 2, pp. 568-574.
- MOORE, B., MOORE, T. and TOEWS, G., 2001. Role of T-and B-Lymphocytes in Pulmonary Host Defences. *The European Respiratory Journal: Official Journal of the European Society for Clinical Respiratory Physiology*, vol. 18, no. 5, pp. 846.
- MORAWSKA, L. Control of particles indoors—state of the art. *Anonymous Proceedings of Healthy Buildings*, 2000.
- MORAWSKA, L. and SALTHAMMER, T., 2003. *Fundamentals of Indoor Particles and Settled Dust*. Wiley, New York.
- MORAWSKA, L., et al, 1998. Comprehensive Characterization of Aerosols in a Subtropical Urban Atmosphere Particle Size Distribution and Correlation with Gaseous Pollutants. *Atmospheric Environment*, vol. 32, no. 14-15, pp. 2467-2478.
- MORAWSKA, L. and ZHANG, J., 2002. Combustion Sources of Particles. 1. Health Relevance and Source Signatures. *Chemosphere*, vol. 49, no. 9, pp. 1045-1058.
- MORJAN, I., et al, 2003. Carbon Nanopowders from the Continuous-Wave CO<sub>2</sub> Laser-Induced Pyrolysis of Ethylene. *Carbon*, vol. 41, no. 15, pp. 2913-2921.
- MORTON, D. and GRIFFITHS, P., 1985. Guidelines on the Recognition of Pain, Distress and Discomfort in Experimental Animals and an Hypothesis for Assessment. *Veterinary Record*, vol. 116, no. 16, pp. 431.
- MROZ, R., et al, 2008. Nanoparticle-Driven DNA Damage Mimics Irradiation-Related Carcinogenesis Pathways. *European Respiratory Journal*, vol. 31, no. 2, pp. 241.
- MUHLE, H., et al, 1990. Dust Overloading of Lungs: Investigations of various Materials, Species Differences, and Irreversibility of Effects. *Journal of Aerosol Medicine*, vol. 3, no. s1, pp. 111-128.

- MÜLHOPT, S., PAUR, H.R., DIABATÉ, S. and KRUG, H.F., 2008. In Vitro Testing of Inhalable Fly Ash at the Air Liquid Interface. *Advanced Environmental Monitoring*, pp. 402-414.
- MUSHTAQ, N., et al, 2011. Adhesion of Streptococcus Pneumoniae to Human Airway Epithelial Cells Exposed to Urban Particulate Matter. *Journal of Allergy and Clinical Immunology*.
- NAKASO, K., SHIMADA, M., OKUYAMA, K. and DEPPERT, K., 2002. Evaluation of the Change in the Morphology of Gold Nanoparticles during Sintering. *Journal of Aerosol Science*, vol. 33, no. 7, pp. 1061-1074.
- NEL, A., XIA, T., MÄDLER, L. and LI, N., 2006a. Toxic Potential of Materials at the Nanolevel. *Science*, vol. 311, no. 5761, pp. 622.
- NEL, A., XIA, T., MÄDLER, L. and LI, N., 2006b. Toxic Potential of Materials at the Nanolevel. *Science*, vol. 311, no. 5761, pp. 622.
- NEL, A.E., DIAZ-SANCHEZ, D. and LI, N., 2001. The Role of Particulate Pollutants in Pulmonary Inflammation and Asthma: Evidence for the Involvement of Organic Chemicals and Oxidative Stress. *Current Opinion in Pulmonary Medicine*, vol. 7, no. 1, pp. 20.
- NICOD, L.P., 1999. Pulmonary Defence Mechanisms. *Respiration*, vol. 66, no. 1, pp. 2-11.
- NILSEN, A., HAGEMANN, R. and EIDE, I., 1997. The Adjuvant Activity of Diesel Exhaust Particles and Carbon Black on Systemic IgE Production to Ovalbumin in Mice After Intranasal Instillation. *Toxicology*, vol. 124, no. 3, pp. 225-232.
- NOAH, N. and HENDERSON, B., 2001. Surveillance of Bacterial Meningitis in Europe 1999/2000. *PHLS, London, United Kingdom*.
- NORBERG, N.S., et al, 2004. Synthesis of Colloidal Mn<sup>2+</sup> : ZnO Quantum Dots and High-TC Ferromagnetic Nanocrystalline Thin Films. *Journal of the American Chemical Society*, vol. 126, no. 30, pp. 9387-9398.
- OBERDORSTER, G., 1995. Lung Particle Overload: Implications for Occupational Exposures to Particles. *Regulatory Toxicology and Pharmacology*, vol. 21, no. 1, pp. 123-135.

- OBERDÖRSTER, G., 2000. Pulmonary Effects of Inhaled Ultrafine Particles. *International Archives of Occupational and Environmental Health*, vol. 74, no. 1, pp. 1-8.
- OBERDÖRSTER, G., et al, 1992. Role of the Alveolar Macrophage in Lung Injury: Studies with Ultrafine Particles. *Environmental Health Perspectives*, vol. 97, pp. 193.
- OBERDÖRSTER, G., FERIN, J. and LEHNERT, B.E., 1994. Correlation between Particle Size, in Vivo Particle Persistence, and Lung Injury. *Environmental Health Perspectives*, vol. 102, no. Suppl 5, pp. 173.
- OBERDÖRSTER, G., et al, 2005a. Principles for Characterizing the Potential Human Health Effects from Exposure to Nanomaterials: Elements of a Screening Strategy. *Particle and Fibre Toxicology*, vol. 2, no. 1, pp. 8.
- OBERDÖRSTER, G., OBERDÖRSTER, E. and OBERDÖRSTER, J., 2005b. Nanotoxicology: An Emerging Discipline Evolving from Studies of Ultrafine Particles. *Environmental Health Perspectives*, vol. 113, no. 7, pp. 823.
- OBERDÖRSTER, G. and UTELL, M.J., 2002. Ultrafine Particles in the Urban Air: To the Respiratory Tract--and Beyond?. *Environmental Health Perspectives*, vol. 110, no. 8, pp. A440.
- O'BRIEN, K.L. and NOHYNEK, H., 2003. Report from a WHO Working Group: Standard Method for Detecting Upper Respiratory Carriage of Streptococcus Pneumoniae. *The Pediatric Infectious Disease Journal*, vol. 22, no. 2, pp. 133.
- OMIDKHODA, A., MOZDARANI, H., MOVASAGHPOOR, A. and FATHOLAH, A.A.P., 2007. Study of Apoptosis in Labeled Mesenchymal Stem Cells with Superparamagnetic Iron Oxide using Neutral Comet Assay. *Toxicology in Vitro*, vol. 21, no. 6, pp. 1191-1196.
- ORSI, N., 2004. The Antimicrobial Activity of Lactoferrin: Current Status and Perspectives. *Biometals*, vol. 17, no. 3, pp. 189-196.
- OSLER, S.W., 1875. *On the Pathology of Miner's Lung*.
- PANDEY, M., WAFULA, E., BOLEIJ, J. and SMITH, K.R., 1989. Indoor Air Pollution in Developing Countries and Acute Respiratory Infection in Children. *Environmental Health*, pp. 427-429.

PARR, D.G., et al, 2006. Inflammation in Sputum Relates to Progression of Disease in Subjects with COPD: A Prospective Descriptive Study. *Respiratory Research*, 20061118, Nov 18, vol. 7, pp. 136 ISSN 1465-993X; 1465-9921. DOI 10.1186/1465-9921-7-136.

PEKKANEN, J., et al, 2002. Particulate Air Pollution and Risk of ST-Segment Depression during Repeated Submaximal Exercise Tests among Subjects with Coronary Heart Disease the Exposure and Risk Assessment for Fine and Ultrafine Particles in Ambient Air (ULTRA) Study. *Circulation*, vol. 106, no. 8, pp. 933-938.

PETERS, A., et al, 1997. Respiratory Effects are Associated with the Number of III Traf Me Particles. *Am J Respir Crit Care Med*, vol. 155, pp. 1376-1383.

PHILLIPS, P., et al, 2003. Cell Migration: A Novel Aspect of Pancreatic Stellate Cell Biology. *Gut*, vol. 52, no. 5, pp. 677.

PLUSCHKE, P., 2004. *Indoor Air Pollution*. Springer Verlag.

POPE III, C.A., et al, 2004. Cardiovascular Mortality and Long-Term Exposure to Particulate Air Pollution: Epidemiological Evidence of General Pathophysiological Pathways of Disease. *Circulation*, vol. 109, no. 1, pp. 71.

PRINCIPI, N. and MARCHISIO, P., 2000. Epidemiology of Streptococcus Pneumoniae in Italian Children. *Acta Paediatrica*, vol. 89, pp. 40-43.

RABE, K.F., et al, 2004. Worldwide Severity and Control of Asthma in Children and Adults: The Global Asthma Insights and Reality Surveys. *Journal of Allergy and Clinical Immunology*, vol. 114, no. 1, pp. 40-47.

REYNOLDS, H.Y., ATKINSON, J.P., NEWBALL, H.H. and FRANK, M.M., 1975. Receptors for Immunoglobulin and Complement on Human Alveolar Macrophages. *The Journal of Immunology*, vol. 114, no. 6, pp. 1813.

RISTOVSKI, Z., et al, 2000. Particle Emissions from Compressed Natural Gas Engines. *Journal of Aerosol Science*, vol. 31, no. 4, pp. 403-413.

RISTOVSKI, Z., MORAWSKA, L., BOFINGER, N.D. and HITCHINS, J., 1998. Submicrometer and Supermicrometer Particulate Emission from Spark Ignition Vehicles. *Environmental Science & Technology*, vol. 32, no. 24, pp. 3845-3852.

ROSS, J., AUGER, M., BURKE, B. and LEWIS, C., 2002. The Biology of the Macrophage. *The Macrophage*, pp. 1-57.

- SAFFIOTTI, U. and STINSON, S.F., 1988. Lung Cancer Induction by Crystalline Silica: Relationships to Granulomatous Reactions and Host Factors. *J.ENVIRON.SCI.HEALTH, PART C.*, no. 2, pp. 197-222.
- SAHOO, S., PARVEEN, S. and PANDA, J., 2007. The Present and Future of Nanotechnology in Human Health Care. *Nanomedicine: Nanotechnology, Biology and Medicine*, vol. 3, no. 1, pp. 20-31.
- SAMET, J.M., et al, 2000. The National Morbidity, Mortality, and Air Pollution Study. *Part II: Morbidity and Mortality from Air Pollution in the United States Res Rep Health Eff Inst*, vol. 94, no. pt 2, pp. 5-70.
- SANTORO, R., SEMERJIAN, H. and DOBBINS, R., 1983. Soot Particle Measurements in Diffusion Flames. *Combustion and Flame*, vol. 51, pp. 203-218.
- SCHINS, R.P.F., 2002. Mechanisms of Genotoxicity of Particles and Fibers. *Inhalation Toxicology*, vol. 14, no. 1, pp. 57-78.
- SCHREIBER, M.A., et al, 1998. Timing of Vaccination does Not Affect Antibody Response Or Survival After Pneumococcal Challenge in Splenectomized Rats. *The Journal of Trauma*, vol. 45, no. 4, pp. 692.
- SCHREIER, H., GAGNÉ, L., CONARY, J.O.N.T. and LAURIAN, G., 1998. Simulated Lung Transfection by Nebulization of Liposome cDNA Complexes using a Cascade Impactor Seeded with 2-CFSMEo-Cells. *Journal of Aerosol Medicine*, vol. 11, no. 1, pp. 1-13.
- SCHWARZ, J.A., CONTESCU, C.I. and PUTYERA, K., 2004. *Dekker Encyclopedia of Nanoscience and Nanotechnology*. CRC.
- SCHWELA, D.H., GOLDAMMER, J.G., MORAWSKA, L.H. and SIMPSON, O., 1999. Health Guidelines for Vegetation Fire Events. *Guideline Document. Published on Behalf of UNEP, WHO, and WMO. Institute of Environmental Epidemiology, Ministry of the Environment Singapore*.
- SEXTON, D., AL-RABIA, M., BLAYLOCK, M. and WALSH, G., 2004. Phagocytosis of Apoptotic Eosinophils but Not Neutrophils by Bronchial Epithelial Cells. *Clinical & Experimental Allergy*, vol. 34, no. 10, pp. 1514-1524.
- SHARPLIN, J. and FRANKO, A.J., 1989. A Quantitative Histological Study of Strain-Dependent Differences in the Effects of Irradiation on Mouse Lung during the Early Phase. *Radiation Research*, vol. 119, no. 1, pp. 1-14.

- SIBILLE, Y. and REYNOLDS, H.Y., 1990a. Macrophages and Polymorphonuclear Neutrophils in Lung Defense and Injury. *The American Review of Respiratory Disease*, vol. 141, no. 2, pp. 471.
- SIBILLE, Y. and REYNOLDS, H.Y., 1990b. Macrophages and Polymorphonuclear Neutrophils in Lung Defense and Injury. *The American Review of Respiratory Disease*, vol. 141, no. 2, pp. 471.
- SIGAUD, S., et al, 2007. Air Pollution Particles Diminish Bacterial Clearance in the Primed Lungs of Mice. *Toxicology and Applied Pharmacology*, vol. 223, no. 1, pp. 1-9.
- SINGH, N.P., MCCOY, M.T., TICE, R.R. and SCHNEIDER, E.L., 1988. A Simple Technique for Quantitation of Low Levels of DNA Damage in Individual Cells. *Experimental Cell Research*, vol. 175, no. 1, pp. 184-191.
- SLEEMAN, K., et al, 2001. Invasive Pneumococcal Disease in England and Wales: Vaccination Implications. *Journal of Infectious Diseases*, vol. 183, no. 2, pp. 239.
- SONDI, I. and SALOPEK-SONDI, B., 2004. Silver Nanoparticles as Antimicrobial Agent: A Case Study on E. Coli as a Model for Gram-Negative Bacteria. *Journal of Colloid and Interface Science*, vol. 275, no. 1, pp. 177-182.
- SØRENSEN, M., et al, 2003. Personal Exposure to PM<sub>2.5</sub> and Biomarkers of DNA Damage. *Cancer Epidemiology Biomarkers & Prevention*, vol. 12, no. 3, pp. 191.
- SOROKIN, S., KOBZIK, L., HOYT, R. and GODLESKI, J., 1989. Development of Surface Membrane Characteristics of "Premedullary" Macrophages in Organ Cultures of Embryonic Rat and Hamster Lungs. *Journal of Histochemistry & Cytochemistry*, vol. 37, no. 3, pp. 365.
- SOUTHAM, D., DOLOVICH, M., O'BYRNE, P. and INMAN, M., 2002. Distribution of Intranasal Instillations in Mice: Effects of Volume, Time, Body Position, and Anesthesia. *American Journal of Physiology-Lung Cellular and Molecular Physiology*, vol. 282, no. 4, pp. L833.
- STERNBERG, G.M., Joseph Meredith Toner Collection (Library of Congress) and National Board of Health (US)., 1881. *A Fatal Form of Septicaemia in the Rabbit Produced by the Subcutaneous Injection of Human Saliva: An Experimental Research*. Printed by John Murphy & Co.

- STROM, K.A., et al, 1990. Inhaled Particle Retention in Rats Receiving Low Exposures of Diesel Exhaust. *Journal of Toxicology and Environmental Health, Part A*, vol. 29, no. 4, pp. 377-398.
- SUNG, J.H., et al, 2009. Subchronic Inhalation Toxicity of Silver Nanoparticles. *Toxicological Sciences*, vol. 108, no. 2, pp. 452.
- SUNG, J.H., et al, 2008. Lung Function Changes in Sprague-Dawley Rats After Prolonged Inhalation Exposure to Silver Nanoparticles. *Inhalation Toxicology*, vol. 20, no. 6, pp. 567-574.
- SYRIOPOULOU, V., et al, 2000. Epidemiology of Invasive Childhood Pneumococcal Infections in Greece. *Acta Paediatrica*, vol. 89, pp. 30-34.
- TAKANO, H., et al, 1997. Diesel Exhaust Particles Enhance Antigen-Induced Airway Inflammation and Local Cytokine Expression in Mice. *American Journal of Respiratory and Critical Care Medicine*, vol. 156, no. 1, pp. 36.
- TAKIZAWA, H., et al, 2001. Increased Expression of Transforming Growth Factor- $\beta$  1 in Small Airway Epithelium from Tobacco Smokers and Patients with Chronic Obstructive Pulmonary Disease (COPD). *American Journal of Respiratory and Critical Care Medicine*, vol. 163, no. 6, pp. 1476.
- TICE, R., et al, 2000. Single Cell gel/comet Assay: Guidelines for in Vitro and in Vivo Genetic Toxicology Testing. *Environmental and Molecular Mutagenesis*, vol. 35, no. 3, pp. 206-221.
- TIMBLIN, C., JANSSEN-HEININGER, Y. and MOSSMANN, B., 1999. Pulmonary Reactions and Mechanisms of Toxicity of Inhaled Fibers. *Toxicology of the Lung, 3d Ed.* Philadelphia: Taylor & Francis, pp. 221-240.
- TIMBLIN, C.R., et al, 2002. Ultrafine Airborne Particles Cause Increases in Protooncogene Expression and Proliferation in Alveolar Epithelial Cells\* 1. *Toxicology and Applied Pharmacology*, vol. 179, no. 2, pp. 98-104.
- TUOMANEN, E., 1999. Molecular and Cellular Biology of Pneumococcal Infection. *Current Opinion in Microbiology*, vol. 2, no. 1, pp. 35-39.
- VAATTOVAARA, P., et al, 2005. A Method for Detecting the Presence of Organic Fraction in Nucleation Mode Sized Particles. *Atmospheric Chemistry and Physics*, vol. 5, no. 12, pp. 3277-3287.
- VALDIVIA-ARENAS, M.A., et al, 2007. Lung Infections and Innate Host Defense. *Drug Discovery Today: Disease Mechanisms*, 0, vol. 4, no. 2, pp. 73-

81. Available from: <http://www.sciencedirect.com/science/article/B75D7-4RCW585-1/2/81eba78e08630f22d3fbffa9cb6d3388> ISSN 1740-6765. DOI DOI: 10.1016/j.ddmec.2007.10.003.

VAN FURTH, R., et al, 1972. The Mononuclear Phagocyte System: A New Classification of Macrophages, Monocytes, and their Precursor Cells. *Bulletin of the World Health Organization*, vol. 46, no. 6, pp. 845.

VAN OUD ALBLAS, A.B. and VAN FURTH, R., 1979. Origin, Kinetics, and Characteristics of Pulmonary Macrophages in the Normal Steady State. *The Journal of Experimental Medicine*, vol. 149, no. 6, pp. 1504.

VAN RIJT, L.S., et al, 2004. A Rapid Flow Cytometric Method for Determining the Cellular Composition of Bronchoalveolar Lavage Fluid Cells in Mouse Models of Asthma. *Journal of Immunological Methods*, vol. 288, no. 1-2, pp. 111-121.

VINCENT, R., et al, 2001. Inhalation Toxicology of Urban Ambient Particulate Matter: Acute Cardiovascular Effects in Rats. *Research Report (Health Effects Institute)*, Oct, vol. (104), no. 104, pp. 5-54; discussion 55-62 ISSN 1041-5505; 1041-5505.

WAGNER, D.A., YOUNG, V.R. and TANNENBAUM, S.R., 1983. Mammalian Nitrate Biosynthesis: Incorporation of  $^{15}\text{NH}_3$  into Nitrate is Enhanced by Endotoxin Treatment. *Proceedings of the National Academy of Sciences of the United States of America*, vol. 80, no. 14, pp. 4518.

WANG, J.J., SANDERSON, B.J.S. and WANG, H., 2007. Cyto-and Genotoxicity of Ultrafine  $\text{TiO}_2$  Particles in Cultured Human Lymphoblastoid Cells. *Mutation Research/Genetic Toxicology and Environmental Mutagenesis*, vol. 628, no. 2, pp. 99-106.

WANG, S.C. and FLAGAN, R.C., 1990. Scanning Electrical Mobility Spectrometer. *Aerosol Science and Technology*, vol. 13, no. 2, pp. 230-240.

WANG, Z., 2000. Transmission Electron Microscopy of Shape-Controlled Nanocrystals and their Assemblies. *The Journal of Physical Chemistry B*, vol. 104, no. 6, pp. 1153-1175.

WARDLAW, T., SALAMA, P., JOHANSSON, E.W. and MASON, E., 2006. Pneumonia: The Leading Killer of Children. *The Lancet*.

WARHEIT, D.B., SAYES, C.M., REED, K.L. and SWAIN, K.A., 2008. Health Effects Related to Nanoparticle Exposures: Environmental, Health and Safety

Considerations for Assessing Hazards and Risks. *Pharmacology & Therapeutics*, vol. 120, no. 1, pp. 35-42.

WARHEIT, D., et al, 1997. Inhalation of High Concentrations of Low Toxicity Dusts in Rats Results in Impaired Pulmonary Clearance Mechanisms and Persistent Inflammation\* 1. *Toxicology and Applied Pharmacology*, vol. 145, no. 1, pp. 10-22.

WEIMANN, A., BELLING, D. and POULSEN, H.E., 2002. Quantification of 8-Oxo-Guanine and Guanine as the Nucleobase, Nucleoside and Deoxynucleoside Forms in Human Urine by High-Performance Liquid chromatography–electrospray Tandem Mass Spectrometry. *Nucleic Acids Research*, vol. 30, no. 2, pp. e7.

WIDDICOMBE, J., BASTACKY, S., WU, D. and LEE, C., 1997. Regulation of Depth and Composition of Airway Surface Liquid. *European Respiratory Journal*, vol. 10, no. 12, pp. 2892-2897.

WIESNER, M.R. and Jean-Yves. Bottero. *Environmental Nanotechnology*. McGraw-Hill Professional.

WILSON, M.J., HAGGART, C.L., GALLAGHER, S.P. and WALSH, D., 2001. Removal of Tightly Bound Endotoxin from Biological Products. *Journal of Biotechnology*, vol. 88, no. 1, pp. 67-75.

WORDLEY, J., WALTERS, S. and AYRES, J.G., 1997. Short Term Variations in Hospital Admissions and Mortality and Particulate Air Pollution. *Occupational and Environmental Medicine*, vol. 54, no. 2, pp. 108.

World Health Organization., 2000. *The World Health Report 2000: Health Systems: Improving Performance*. World Health Organization.

WU, H.Y., et al, 1997. Intranasal Immunization of Mice with PspA (Pneumococcal Surface Protein A) can Prevent Intranasal Carriage, Pulmonary Infection, and Sepsis with Streptococcus Pneumoniae. *Journal of Infectious Diseases*, vol. 175, no. 4, pp. 839.

XI, J. and ZHONG, B.J., 2006. Soot in Diesel Combustion Systems. *Chemical Engineering & Technology*, vol. 29, no. 6, pp. 665-673.

YANG, H., et al, 2009. Comparative Study of Cytotoxicity, Oxidative Stress and Genotoxicity Induced by Four Typical Nanomaterials: The Role of Particle Size, Shape and Composition. *Journal of Applied Toxicology*, vol. 29, no. 1, pp. 69-78.

- YANG, H.M., et al, 1999. Effects of Diesel Exhaust Particles (DEP), Carbon Black, and Silica on Macrophage Responses to Lipopolysaccharide: Evidence of DEP Suppression of Macrophage Activity. *Journal of Toxicology and Environmental Health Part A*, vol. 58, no. 5, pp. 261-278.
- YANG, H.M., MA, J.Y.C., CASTRANOVA, V. and MA, J.K.H., 1997. Effects of Diesel Exhaust Particles on the Release of Interleukin-1 and Tumor Necrosis Factor-Alpha from Rat Alveolar Macrophages. *Experimental Lung Research*, vol. 23, no. 3, pp. 269-284.
- YIN, X.J., et al, 2004. Suppression of Cell-Mediated Immune Responses to Listeria Infection by Repeated Exposure to Diesel Exhaust Particles in Brown Norway Rats. *Toxicological Sciences*, vol. 77, no. 2, pp. 263.
- ZELIKOFF, J.T., CHEN, L.C., COHEN, M.D. and SCHLESINGER, R.B., 2002. The Toxicology of Inhaled Woodsmoke. *Journal of Toxicology and Environmental Health, Part B*, vol. 5, no. 3, pp. 269-282.
- ZHANG, P., SUMMER, W.R., BAGBY, G.J. and NELSON, S., 2000. Innate Immunity and Pulmonary Host Defense. *Immunological Reviews*, vol. 173, no. 1, pp. 39-51.
- ZHANG, Q., et al, 1998. Differences in the Extent of Inflammation Caused by Intratracheal Exposure to Three Ultrafine Metals: Role of Free Radicals. *Journal of Toxicology and Environmental Health Part A*, vol. 53, no. 6, pp. 423-438.
- ZHANG, Q., et al, 2003. Comparative Toxicity of Standard Nickel and Ultrafine Nickel in Lung After Intratracheal Instillation. *Journal of Occupational Health*, vol. 45, no. 1, pp. 23-30.
- ZHOU, H. and KOBZIK, L., 2007a. Effect of Concentrated Ambient Particles on Macrophage Phagocytosis and Killing of Streptococcus Pneumoniae. *American Journal of Respiratory Cell and Molecular Biology*, vol. 36, no. 4, pp. 460.
- ZHOU, H. and KOBZIK, L., 2007b. Effect of Concentrated Ambient Particles on Macrophage Phagocytosis and Killing of Streptococcus Pneumoniae. *American Journal of Respiratory Cell and Molecular Biology*, vol. 36, no. 4, pp. 460.
- ZHU, Y., et al, 2002a. Study of Ultrafine Particles Near a Major Highway with Heavy-Duty Diesel Traffic. *Atmospheric Environment*, vol. 36, no. 27, pp. 4323-4335.

ZHU, Y., HINDS, W.C., KIM, S. and SIOUTAS, C., 2002b. Concentration and Size Distribution of Ultrafine Particles Near a Major Highway. *Journal of the Air & Waste Management Association*, vol. 52, no. 9, pp. 1032-1042.

ZIEGLER-HEITBROCK, H., et al, 1994. Tolerance to Lipopolysaccharide Involves Mobilization of Nuclear Factor Kappa B with Predominance of p50 Homodimers. *Journal of Biological Chemistry*, vol. 269, no. 25, pp. 17001.